



1st National Conference on Chemical Technology

NCCT 2017

BOOK OF PROCEEDINGS

THEME:

**The Role of Chemical
Technology In a
Diversifying Economy**

DATE: 7th - 10th August, 2017

VENUE: National Research Institute for Chemical
Technology (NARICT), Basawa - Zaria.



2017 NCCT NARICT, ZARIA CONFERENCE SCHEDULE

**1st National Conference on Chemical
Technology (NCCT)**

August, 7th – 10th 2017

**National Research Institute for Chemical
Technology (NARICT), Zaria, Nigeria.**

BOOK OF PROCEEDINGS

©



Waste conversion, Energy & Catalysis

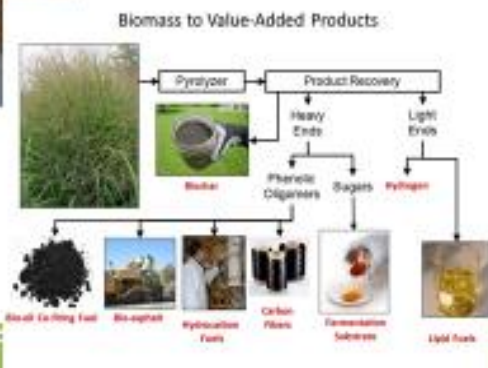




Table of Content

PAPER ID	TITLE	AUTHOR	PAGES
CCT-: 005	Some preliminary physicochemical investigation and acute toxicity study of methanol leaf extract of ginger lily (<i>Costus afer</i> ker gawl.) and giant African land (<i>Archachatina marginata</i>) snail slime on swiss albino mice	Barminas et al.,	006 – 008
CCT-: 011	Effects of the presence of oil well in South- East Nigeria on quality of cassava (<i>Manihot esculenta crantz</i>): a case study of Anambra West Local Government Area	Patrick et al.,	009 – 010
CCT-: 015	Synthesis, characterization and antibacterial activity of some mixed drug metal (ii) complexes of sulfamethoxazole and ampicillin trihydrate	Abubakar et al.,	011 – 013
CCT-: 024	Empirical optimization of ultrasound-assisted alkaline catalysed transesterification of <i>Lannea acida</i> seed oil to biodiesel	Lubabatu et al.,	014 – 015
CCT-: 037	Optimizing Deproteinization of Chitin using response surface methodology	Abubakar et al.,	016 – 019
CCT-: 025	Assessment and optimization of biodiesel production from neem seed oil using sulfated zirconia catalyst	Muhammad et al.,	020 – 022
CCT-: 028	Influence of increasing skirt height on quantity of wood and time consumed for cooking on a wood stove	Ajunwa et al.,	023 – 025
CCT-: 029	The challenges and prospects of using biomass energy in Nigeria	Suleiman I. L.	026 – 028
CCT-:038	An assessment of the potash biocatalyst potential of plantain peel residues for reducing sugar production from <i>Phoenix dactylifera</i> seed pit	Yusuf O. et al	029 – 032
CCT-: 044	Extraction and some characteristics of tamarind seed starch as a biopolymer	Musa et al.,	033 – 035
CCT-: 045	A bench scale laboratory production of brown sugar from sugarcane	Abdullahi et al.,	036 – 038
CCT-: 048	Design, construction and testing of solar still having submerged flat absorber plate	Ibrahim et al.,	039 – 041
CCT-: 049	Performance comparison of a submerged v-pattern absorber still and the conventional basin still	Ibrahim et al	042 – 044
CCT-: 057	MFI-type zeolite membranes for the separation of CO ₂ /N ₂ mixtures	Dahiru et al.,	045 – 047
CCT-: 008	Determination of heavy metals in locally processed meat sold in Sokoto metropolis, Sokoto State	Liman M. G. & D. Umar	048 – 050
CCT-: 062	Key components of catalysts for methanol steam reforming: a short review	Fasanya et al.,	051 – 054
CCT-: 040	Assessment of heavy metals contamination of brassica oleracea l. cultivated on farmlands along Hunkuyi-Zaria road, Nigeria	Anyim et al.,	055 – 058
CCT-: 067	Aromatization of liquefied petroleum gas over ZnO/ZSM-5 catalysts	Gbadamasi et al.,	059 – 063
CCT-: 042	Hydrothermal liquefaction of <i>Jatropha curcas</i> : energy evaluation and recovery	Alhassan Y. & Kumar N.	064 – 066
CCT-: 032	Phytochemical screening and spectroscopic study of the leaves of <i>Adina microcephala</i>	Audu et al.,	067 – 070
CCT-: 041	Properties of chemically modified baobab pod/sisal fibre reinforced low density polyethylene hybrid composite	Shehu et al.,	071 – 073
CCT-: 063	The study of the rheology and properties of corn starch dyed with reactive dye	Suleiman et al.,	074 – 077
CCT-: 003	Antimicrobial properties of <i>Nauclea diderrichii</i> (rubiaceae) leaf extracts	Katsayal et al.,	078 – 081
CCT-: 050	Effects of different drying methods on some proximate properties of onion powder: A comparative study	Okoduwa et al.,	082 – 084
CCT-:010	Effect of soaking and fermentation on the proximate composition and anti-nutritional properties of seeds of <i>Senna occidentalis</i>	Feka et al.,	085 – 087
CCT-: 030	Low cost biodegradable adsorbent material for the removal of methylene blue from aqueous solutions: a review	Ozogu et al.,	088 – 091
CCT-: 053	Application of cryogenics as an engineering tool for textile and apparels; a review	Ozogu et al.,	092 – 095
CCT-: 027	Catalytic alkene epoxidation using continuous flow reactor	Mohammed et al.,	096 – 098
CCT-: 055	Propane aromatization over hierarchical Zn/ZSM5 catalysts	Bashir et al.,	099 – 102
CCT-: 061	Effect of molecular weight and concentration on plasticizing efficiency of some trimellitates in poly (vinyl chloride) (PVC)	Abbas et al.,	103 – 105
CCT-: 070	Nutraceutical evaluation of the aerial part of <i>Daucus carota</i> LINN. (apiaceae)	Ayeni et al.,	106 – 109
CCT-: 068	Antimicrobial investigation of Eucalyptus essential oil on some selected bacteria	Nwobi et al.,	110 – 112
CCT-: 065	Aromatization of LPG over ZnO/ZSM-5 catalysts: a statistical optimization of process variables	Isa et al.,	113 – 117
CCT-: 004	Exosome-loaded plant extract as an anti-ovarian cancer drug delivery system	Ukwubile C. A. & Nettey H.	118 – 121
CCT-: 009	Removal of oil from crude oil polluted water using mango seed bark as sorbent in a packed column	Lawal et al.,	122 – 124



CCT-: 043	Process modelling and economic analysis for cellulosic bioethanol production in Nigeria	Oyegoke et al.,	125 – 128
CCT-: 056	Methylene blue removal from wastewater using orange peel adsorbent	Usman et al.,	129 – 130
CCT-: 046	reduce, reuse and recycling of waste for sustainable economy: A case of alum from aluminum cans.	Apampa S. A.	131 – 132
CCT-: 059	A promising concept of waste management through pyrolysis of low density polyethylene	Osigbesan et al.,	133 – 135
CCT-: 069	Adsorption of methylene blue from a synthesized industrial wastewater in a batch system using activated carbon from coconut shell	Edokpayi et al.,	136 – 138
CCT-: 039	Optimization of <i>in situ</i> transesterification of oil from mixed-feedstock of rubber, cassava, and jatropha oil seeds	Muibat et al	139 – 141
CCT-: 075	Ionic liquid based deep eutectic solvent for the removal of aromatics from aliphatic hydrocarbons	Muhmmada et al	142 – 144
CCT-: 079	Comparative study of biogas production from selected agrowastes	Dangoggo S.M. & Yusuf A.U.	145 – 147
CCT-: 078	Treatment of tannery effluent with <i>Chlorella vulgaris</i>	Gauje et al.,	148 – 151
CCT-: 019	Studying the optimal conditions for the production of glucose from hydrolysis of <i>Spirogyra africana</i>	Egere et al.,	152 – 155
CCT-: 077	Preliminary studies of pectin from <i>Adansonia digitata L.</i> pulp	Ibraheem et al.,	156 – 157
CCT-: 054	Catalytic reforming of gaseous product from pyrolysis of low density polyethylene: catalysts preparation and characterization	Waziri et al.,	158 – 161
CCT-: 047	Development of biomass briquettes from tannery solid waste: characterization of briquettes	Onukak et al.,	162 – 165
CCT-: 014	Iron (II) metal-organic framework for sustainable energy storage application	Mbonu I.J. & Mebitaghan B.	166 – 168
CCT-: 020	Influence of thermal and chemical pre-treatment on <i>Spirogyra africana</i> biomass for glucose production	Egere et al.,	169 – 173
CCT-: 060	Effect of natural zeolite on intumescent ammonium polyphosphate-pentaerythritol-melamine system in flame retardation of poly (vinyl chloride) (PVC)	Abba et al.,	174 – 176
CCT-: 076	Improving the stability of propane aromatization catalyst via isomorphous substitution of zinc in ZSM-5	Yusuf et al.,	177 – 180
CCT-: 034	Bioremediation potential of heavy metals resistant <i>Aspergillus versicolor</i> isolated from tannery effluent, Challawa Industrial Estate, Kano State, Nigeria.	Sule et al.,	181 – 184
CCT-: 071	Exploring <i>Gmelina arborea</i> leaves for biofuels, petrochemical and pharmaceutical feedstocks	Ibrahim et al.,	185 – 189
CCT-: 074	Synthesis and characterization of environmentally safe soapy and soap-less detergents from pure caraway	Muktari et al.,	190 – 193
CCT-: 023	Comparative antioxidant effect of cucumber and carrot using different methods	Aliyu et al.,	194 – 195
CCT-: 072	A survey of aflatoxins contamination in sorghum and millet marketed in zaria metropolis	Shitu et al.,	196 – 197
CCT-: 021	Esterification of carboxylic acid with alcohol in ZnCl ₂ /urea deep eutectic solvent	Sani et al.,	198 – 200
CCT-: 066	Analysis of atmospheric aerosols: aerosol optical depth and its impact on climate and visibility	Bello et al.,	201 – 203

**ABSTRACT CCT-: 005**Barminas Jeff Tsware², Agu Matthew Onyema¹, Abubakar Bawa³, Jude Chinedu Onwuka⁴

1. Department of Science Laboratory Technology, Federal Polytechnic Bali, Taraba State, Nigeria.
2. Dept of Chemistry, Modibbo Adama University of Technology Yola, Adamawa State, Nigeria.
3. Dept of Science Laboratory Technology, Federal Polytechnic Mubi, Adamawa State, Nigeria
4. Department of Chemistry, Federal University Lafia, Nasarawa State, Nigeria.

Email: mataguonyema@gmail.com**SOME PRELIMINARY PHYSICOCHEMICAL INVESTIGATION AND ACUTE TOXICITY STUDY OF METHANOL LEAF EXTRACT OF GINGER LILY (*COSTUS AFER* KER GAWL.) AND GIANT AFRICAN LAND (*Archachatina marginata*) SNAIL SLIME ON SWISS ALBINO MICE**

ABSTRACT: The study was carried out to determine the level of toxicity of *Costus afer* leaves and snail slime using different amount of the extract. The solubility status of the snail slime was evaluated using different organic solvents, mineral acids and alkalis. The snail slime was found to be slightly soluble in concentrated HCl, dil. NaOH at temperature other than room temperature. Some preliminary physicochemical composition of the snail slime was also determined. Protein, carbohydrate and fat were found to be qualitatively present at high, moderate and low amount respectively. The percentage of extract yield for the plant was also determined using petroleum ether, methanol, acetone, and water with their results as: 0.85 %, 6.27 %, 1.75 % and 2.06 % respectively. The preliminary phytochemical screening of the methanol, acetone, and water extracts of the bioactive component of the *Costus afer* leaves was conducted. The result indicated the presence of alkaloid, phenol, flavonoid and cardenoloids in the methanol extract; carbohydrate and saponin were present in the acetone extract; carbohydrate, glycosides, cardiac glycosides and saponin were present in the aqueous extract. The result obtained shows that the bioactive components from *Costus afer* leaf extract and snail slime were non-toxic to mice in sub-acute and acute dose of 5000 mg/kg. Our preliminary findings may lend support that the snail slime in both acid and alkaline medium which proves slightly soluble, may go a long way to act as a carrier of chemical and biological materials for use as nanoparticles in medical and pharmaceutical formulated drugs.

Keywords: *Costus afer*, Snail slime, Glycosides, Physicochemical, Phytochemical, Sub-acute dose, Toxicity

1. Introduction

In most African country and Nigeria for instance, traditional medicine has become art of the people's culture with the advent of the development of traditional health care delivery system and training of traditional healthcare attendants which has been formalized to avoid degeneration of the knowledge of traditional healing.

According to [10] *Costus afer* is commonly called ginger, bush sugar cane or Monkey sugar cane. The Ibos call it "Okpete" or "Okpote Ohia", Hausas called it Kakizawa, Yorubas called it "Tete - ogun" [5], [13]. It's a monocot, herbaceous, unbranched tropical plant that is relatively tall. It is commonly found in moist or shady forest of west and tropical Africa [10]. It may grow up to 3 m high and belong to the family Costaceae [7]. *Costus afer* is a useful medicinal plant that is highly valued for its manifold of uses in anti-diabetic, anti-inflammatory and anti-atheistic properties in South East and South West of Nigeria. In Nigeria, Giant African Land Snails are called different names with respect to the geographical location. In Northern Nigeria, among the Hausa community it is called Dodon Kodi while in the Eastern Nigeria (Ibo) and Western Nigeria (Yoruba) it is called Ejula and Igbi respectively. Snail has a lot of slimy substances known as snail slime which it drops along its path as it moves. It also uses this slime to regenerate its shell and skin when damaged. The group of snails commonly referred to as Giant African Land Snails belong to Phylum Mollusca, the mucus is produced by the glands

of the Snails foot especially a large gland located below the mouth [8].

The aim of the study is to extract and investigate the physicochemical analysis, toxicity effect and level of active crude *Costus afer* methanol leaf extract and giant African land snail slime on Swiss Albino Mice.

The objectives of the study are as follows:

- a) To extract some bioactive components from the leaf of *Costus afer* with solvents of different polarity such as Petroleum ether, Acetone, Methanol and Water.
- b) To determine the solubility profile of the snail slime with mineral acids, bases and solvents like acetone, ethanol, water, sodium hydroxide, hydrochloric acid etc.
- c) To determine the preliminary physicochemical analysis of snail slime (i.e. the presence of carbohydrate, protein, sugar, fats and oils).
- d) To determine acute toxicity profile of *Costus afer* and the Snail slime in a normal Swiss Albino Mice.

2. Materials and methods

2.1. Collection of plant materials and African giant land snail

The *Costus afer* was collected from Umuewi village in Njaba Local Government Area of Imo State. The African giant land Snail was purchased from Afor Awo-Omamma Market of Oru-East Local Government Area of Imo State.

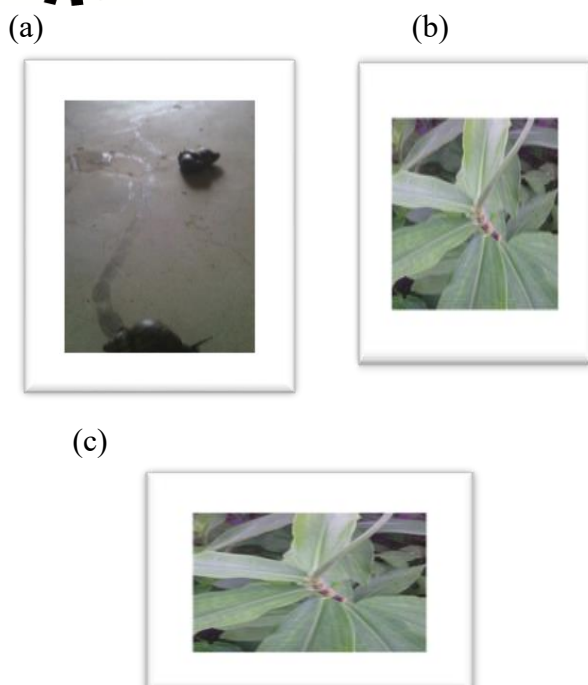


Fig. 1. (a-c): Shows Giant African Land Snail, trail of the snail slime and *Costus afer* leaf, respectively

2.2 Animal materials

Twenty-four Swiss Albino Mice of both sexes weighing about (21 - 30g) were purchased from animal house, Department of Zoology University of Jos. The animals were kept in a separate animal room on a 12-hour dark cycle at a room temperature of 27°C and with free access to food and water for 4 days [14]. The animals were fed with standard rat pellets and filtered water.

2.3. Acute toxicity investigation of *Costus afer* and snail slime extract

0.5 g of the crude methanol extract from *Costus afer* leaves and snail slime were evaluated for their toxicity in albino mice. The test was carried out in two phases. In the phase I of the study, nine albino mice were randomized into three groups of three mice for both *Costus afer* and Snail slime extract. They were given 10 mg/kg, 100 mg/kg and 1000 mg/kg body weight dose respectively of the *Costus afer* extract, and Snail Slime, administered intraperitoneally (i.p.). The albino mice were observed for changes in physical appearance, gross behavioral change and death in the first 4 hours and subsequently daily for 21 days [9].

In view of the result obtained from phase 1 treatment, phase II treatment was carried out using another fresh set of three albino mice randomized into three groups of one mice each and given 1600 mg/kg, 2900 mg/kg and 5000 mg/kg body weight of the extract dose to determine acute toxicity if there was no death.

2.4. Preparation and sequential extraction of the bioactive component of *Costus afer* leaf extract

The plant leaves were washed, air dried and pulverized to enhance the penetration of the extracting solvents into the plant cells so as to facilitate the release of the active ingredients or principles using Corona hand grinder. It was first defatted with Petroleum ether so that the presence of oil in the plant leaf will not affect the animal when the extract is administered to the animal. The finely ground and air dried *Costus afer* leaves (200 g) was sequentially extracted with solvents of increasing polarity (petroleum ether, acetone, methanol and water). The water extract was prepared in the same way as the methanol and acetone extracts. The residue was removed by filtration, while the filtrate was concentrated (distilled, evaporated and vacuum dried) under reduced pressure by a rotary evaporator at 40°C and the aqueous extract was distilled off at 100°C.

2.5. Extraction of snail slime from giant African land snail

The method used by [1], [2] was employed for the preparation and extraction of snail slime from the giant African Land Snail. The precipitates were freeze dried at (-4°C) to obtain greyish–brown flakes of the snail slime extract, which was then pulverized into fine powder, bottled and stored in a desiccator for further studies.

2.6. Qualitative phytochemical screening of extracts

Phytochemical analysis of freshly prepared *Costus afer* methanol leaf extracts were performed to evaluate the detection of various constituents using procedures described by [6]. The methanol leaf extract of *Costus afer* was subjected to tests like alkaloid, flavonoids, saponins, phenols, tannins, phlobatanins and cardenolides for the identification of its various active constituents by standard methods.

3. Results and discussion.

The percentage of the extraction yield for the plant using different solvents like Petroleum ether, methanol, acetone, and water was determined as: 0.85%, 6.27 %, 1.75 % and 2.06 % respectively. The acute and sub-acute toxicity profile of *Costus afer* and the Snail slime in a normal Swiss Albino Mice was established to be non- toxic at 5000 mg/kg body weight of the Mice using Lorke's LD₅₀



method.

From an aspect of physicochemical analysis of the snail slime there was *indication* that a high quantity of protein was present in the snail slime as compared to its carbohydrate and fat content [3]. Investigation of the solubility profile indicates that the snail slime was partially soluble in distilled water at ordinary room temperature but moderately soluble at its boiling point. The snail slime was not soluble in n-hexane, petroleum ether, methanol acetone, ethanol, aqueous ammonia, dilute and concentrated (HCl, H₂SO₄, and NaOH at room temperature. There was a noticeable slight difference in its solubility enhancing effect at temperature of 33°C and 45°C. The toxicology of the mice was assessed according to Lorke's method [11].

Acute toxicity study of *Costus afer* methanol leaf extract and Snail Slime on mice showed that no mice died within 24 hours after intraperitoneal (i.p) administration with the plant extract. Also the LD₅₀ at 5000 mg/kg body weight approves the plant extract and the slime to be safe on the account of the method of [4] and [11]. Both at the lower (10 mg/kg b.w) and highest dose (5000 mg/kg b.w) no significant change was observed in the body weight and the behavioral parameters used to evaluate the toxicity for example, hair, eyes, mucous membrane, salivation, sleep, coma, tremor, diarrhea, morbidity and mortality [9].

4. Conclusions

The result obtained shows that the Costus afer methanol leaf extract and Snail slime are non-toxic in sub-acute and acute dose of 5000 mg/kg. Generally, the solubility status of snail slime in most liquids as well as both acidic and alkaline medium shows insoluble and slightly soluble; this may go a long way to prove snail slime as a carrier of chemical and biological materials for use as nanoparticles in medical and pharmaceutical industry.

Acknowledgements

The authors are very thankful to Technicians of the Science Laboratory Technology of Federal

Polytechnic Bali for their technical assistance during this investigation. Also we acknowledge Mr. Agu Magnus who assisted in the collection of the plant from Ohia Umuewi in Njaba L.G.A., Imo State.

References

- [1] Adikwu M. V. (2005). Evaluation of snail mucin motifs as rectal absorption enhancer for insulin in non-diabetic rat models. *Biol, Pharm Bull.*2005; 28 (9): 1801-1804.
- [2] Adikwu, M. U. and Ikejiuba C. C. (2005). Some physiological and wound healing properties of Snail mucin. *Boll. Chim. Farm.*144:1-8.
- [3] Adikwu, M. U. and Nnamani P. O. (2005). Some physiological and toxicological properties of Snail mucin. *Bio research* 5:1-6.
- [4] Agu, M.O., Barminas J.T., Ukwubile C.A., Hotton J.A (2015). Acute toxicity investigation of methanol leaf extract of *Costus afer* and Snail slime extract on Swiss Albino Mice. *American Journal of Chemistry and Application.*vol. 2, No.6, pp141-147.
- [5] Anaga, A. O, Njoku C. J. Ekejiuba E. S. Esiaka M. N. Asuzu I. U. (2004). Investigation of the methanolic leaf extract of *Costus afer* Ker for Pharmacological activities in vitro and in vivo. *Phytomedicine* (2-3), 242-248.
- [6] Anyasor, G.N, Ogunwenmo K. O, Oyelana O. D, and Akpotenure B.G, (2010). Phytochemical constituents and antioxidant activities of aqueous and methanol stem extract of *Costus afer* – Ker Gawl. (Costaceae), *African Journal of Biotechnology*, Vol. 96 No.31 pp 4880–4884.
- [7] Bukil, H. M. (1985). The useful plants of West Tropical Africa. Vol. 1 Royal botanic gardens.
- [8] Fox R. S. & Ruppert E. E, and Bacnes R. D. (2004). *Invertebrate Zoology: a functional evolutionary approach.* Belmont, CA: Thomas–Brooks Cole.
- [9] Guinnin F.D. Felix, Jean Robert Klotoe, Jean-Marc Ategbro (2017). Acute Toxicity Evaluation of Ethanolic Extract of *Aristolochia albidula* Duch. Leaveson Wistar Rats Liver and Kidney Functions. *Int. J. Pharm. Pharm Sci*, Vol. 9, Issue 7, 35-40
- [10] Iwu M. M. (1983). Traditional Igbo Medicine Institutes of African Studies, University of Nigeria, Nsukka, pp: 122–144.
- [11] Lorke D. (1983). A new approach to a practical acute toxicity testing. *Arch. Toxicol.* 53, 275–283.
- [12] Nyananyo, B. C. (2006). Plants from the Niger Delta. *International Journal of Pure and Applied Science* 3(4),21–25pp.
- [13] Solawoye, M. O, and Oyesika O. O. (2008). *Textbook of medicinal plant from Nigeria.* University of Lagos press, Nigeria, pp: 628.
- [14] Ukpabi, C. F. Agbafor K. N. Ndukwe O. K., Agwu, Nwachukwu S. N. (2012). Phytochemical composition of *Costus afer* extract its alleviation of carbon tetrachloride induced hepatic oxidative stress and toxicity. *Int. J. of Modern Botany.* 2(5): 120-126.

**ABSTRACT CCT:- 011**

Akas Patrick*, Adenekan Olapeju, Amiolemen Sunday, Ogidan John, Omoyajowo Koleayo

National Centre for Technology Management, South West Office, Victoria Island Lagos

Email: akas.patrick@yahoo.com**EFFECTS OF THE PRESENCE OF OIL WELL IN SOUTH- EAST NIGERIA ON QUALITY OF CASSAVA (*Manihot esculenta Crantz*): A CASE STUDY OF ANAMBRA WEST LOCAL GOVERNMENT AREA****1. Introduction**

Oil spill is the release of a liquid petroleum hydrocarbon into the environment, especially marine areas due to human activity, and it is a form of pollution (Etkin, 2000). In Nigeria, 50% of oil spills is due to corrosion, 28% to sabotage and 21% to oil production operations (Nwilo, 2005). 1% of oil spills is due to engineering drills, inability to effectively control oil wells, failure of machines, and inadequate care in loading and unloading oil vessels (Nwilo, 2005). Most of the oil pipes and tanks in the country are very old and lack regular inspection and maintenance.

Thousands of barrels of oil have poured into the environment through some of the corroded pipes and tanks. The oil industry located within oil communities has contributed immensely to the growth and development of the country, but unsustainable oil exploration activities has rendered areas such as Niger Delta region in Nigeria, one of the five most severely petroleum damaged ecosystems in the world. (Inya, 2012). There is no doubt that the Nigerian oil industry has impacted on the country in a variety of ways at the same time. However, on the negative side, petroleum exploration and production also have adverse effects on farming, as that is the traditional means of livelihood of the oil producing communities (Ezekwesili, 2010).

There is need to make significant progress in tackling the problem of oil spillage on cassava production and also harness more information on the effect of oil spillage on the crop production. Furthermore, the result from the spillage on the cassava planted by farmers may lead to fatalities, job losses among the farmers. Oil spillage will damage soil nutrient, subsequently damaging the agricultural produce. The exploration of oil within the location will have a degree of contamination or may have an impact on the food product thereby making it unfit for human consumption.

Cassava is third largest source of food carbohydrates in the tropics, after rice and maize. Cassava is a major staple food in the developing world, providing a basic diet for over half a billion people (FAO, 2007). In terms of agriculture, Cassava has played and

still continues to play a remarkable role in the agricultural development in Nigeria. It has been transformed from minor crop and recently into a cash crop (Ahmadu, 2012). It is one of the dominant carbohydrate rich staple crops grown in most countries in continental Africa (John, 2006), especially in Nigeria (Nzekwe, 2006). Though Nigeria is the highest producer of cassava in the world, she is also the world largest consumer, leaving nearly nothing for export. More than 80 % of Nigeria's populace consume cassava (Babawale, 2001).

2. Methodology

The objective of this study is to examine the effects of the presence of oil well on Cassava. 5 Cassava samples were collected at different locations near the oil well. The samples were analyzed for heavy metals using an atomic absorption spectrophotometer to determine metal ions such as Copper, Lead, and Cobalt, Chromium, Cadmium, Zinc, and Nickel in cassava. Proximate analysis was conducted for the cassava samples to determine the nutritional value, such as crude protein, carbohydrate content, ash, crude fibre, crude fat, moisture content and mineral composition such as potassium, magnesium, calcium and sodium, zinc and copper.

3. Results and discussions

The study shows that the heavy metal in cassava samples were as follows iron (158.5mg/kg WHO 50mg/kg), manganese (7.0mg/kg, WHO 2mg/kg), chromium (6.1 mg/kg, WHO 0.05mg/kg), cobalt (2.5 mg/kg, WHO 0.1 mg/kg) and lead (1.8 mg/kg WHO 0.3mg/kg). The concentrations of these heavy metals in the sample were observed to be higher than the WHO allowable levels in food. However, the concentrations of copper (13.8 mg/kg, WHO, 73.30 mg/kg), Nickel (3.2 mg/kg, WHO, 67.9mg/kg), cadmium (0.2mg/kg WHO, 0.2mg/kg), falls within allowable levels. The effect of high concentration of these heavy metals in samples indicated that high concentrations of iron in food can causes cause joint pain, liver diseases, heart failure and in men, inability to get or maintain an erection. High concentration of chromium in food sample can cause Lung



cancer, kidney diseases (WHO 2004). Excess cobalt in food can cause damage to the kidney, liver, pancreas and heart (Edward 2013).

Excess manganese can lead to neurological effect like Parkinson disease, respiratory diseases and reproductive effect such as decrease fertility.

Lead concentration is high, which can easily cross the placenta and damage the fetal brain and may also cause development of autoimmunity, in which a person's immune system attacks its own cells leading to diseases such as rheumatoid arthritis, diseases of kidney, nervous system and circulatory system. (Casarett and Doull, 1996) The proximate analysis revealed high level of carbohydrate (71.38%), crude protein (9.10%), and crude fibre (5.20%), with low crude fat (1.56%) Ash content (4.01%). The ash values of cassava analyzed are high, suggestive of high metal content. The result obtained from all the cassava samples analyzed clearly revealed high concentration of iron, manganese; chromium, cobalt, and lead are not within allowable limit. The results obtained from this study posit that the concentration of copper, nickel and cadmium are within the allowable limit. However, the consumption of this food crop over a long time could result to the bioaccumulation of these heavy metals in the living tissues of man and animals. This may indicate a future adverse effect on humans and animals.

The presence of high concentration of some of these heavy metals in cassava poses a serious threat to human blood system and may be carcinogenic and neurologically dangerous. This study recommends that adequate supply of portable water to the community for domestic use and irrigation should be made adequate, thus farming activities should be carried out in areas ($r > 19.4\text{km}$) far away from

the oil well (Geological survey, 2016).

References

1. Ahmadu, J.A (2012). Effect of Oil spillage on cassava production in Nigeria Delta region of Nigeria. Department of Agricultural Economics Extension services, Faculty of Agriculture University of Benin, Benin City, Nigeria.
2. Babawale, O.O (2001). Comparative study of manual and improved processing equipment for Cassava. Processing of the 35th Annual conference of the Agricultural Society of Nigeria held at Abeokuta, Ogun State. September, 16-20.
3. Casatte, C. and Doull, D. (1996). Heavy metal and Health World Resource Institute. Washington
4. Edward, J. (2013) Toxic metals: the health dangers of cobalt in food Samples-Global healing. Centre publishing January 15, 2013.
5. Etkin, S. A. (2000). Financial costs of oil spill worldwide. Oil spill intelligence Report, cutter. Information corps, Arlington Massachusetts USA. Pp 346.
6. Ezekwesili, C.N (2005). In-Situ burning of oil Spills. Journal of Research of the National Institute of Standards and Technology. Vol. 2, 246 -265.
7. Food and Agriculture Organisation (2007). National Nutrient Database for Standard Reference.
8. John, U. (2006). Growth and yield cassava as influence by fertilizer types in the coastal plain soil in Uyo Southern. Nigeria journal of Sustainable Tropical Agricultural Research 18: 99-102.
9. Inya, A.E (2012). The Nigeria State, Oil Exploration and Community interest, issues and perspective. University of Port Harcourt, Nigeria
10. Nwilo, P.C. and Badejo, T. O. (2005). Oil spill problems and Management in the Niger Delta. International oil spill Conference, Miami, Florida USA.
11. Nzekwe, L.S. (2006). Technology adoption of improved practice by cassava farmers in. Agricultural development programme (ADP) zone of Ogun State proceeding of the 35th Annual conference of the agricultural society of Nigeria University of Agricultural Abeokuta Nigeria, pp 331.
12. World Health Organisation, (2004). Sulphate in drinking back ground document for development for WHO guideline for drinking water quality, pp1-16



ABSTRACT CCT-: 015

Abubakar U. A.^{1*}, U. A. Birnin-Yauri², C. Muhammad², and A. A. Muhammad³

1. Department of Chemistry, Gombe State University, Gombe-Nigeria.
2. Department of Pure and Applied Chemistry, Usmanu Danfodiyo University, Sokoto.
3. Department of Pharmacology and Toxicology, Usmanu Danfodiyo University, Sokoto.

Email: aausmaseen@gmail.com

SYNTHESIS, CHARACTERIZATION AND ANTIBACTERIAL ACTIVITY OF SOME MIXED DRUG METAL (II) COMPLEXES OF SULFAMETHOXAZOLE AND AMPICILLIN TRIHYDRATE

ABSTRACT: The emergence of new infectious diseases, the resurgence of several infections that appeared to have been controlled and the increase in bacterial resistance have created the necessity for studies directed towards the development of new antimicrobials. Mixed drug metal (II) complexes of Co, Ni and Cu with Sulfamethoxazole (SMX) and ampicillin trihydrate (AMP) as ligands were synthesized and characterized by standard procedures i.e. (elemental chemical analysis C.H.N.S, FTIR, Molar conductivity, melting point and decomposition temperature and solubility test). On the basis of these studies, a six coordinated octahedral geometry for all these complexes has been proposed. The standard drugs and its mixed complexes were also tested for their antibacterial activity using agar diffusion method against *Salmonella typhi* (gram negative bacteria) and *Staphylococcus aureus* (gram positive bacteria). The results of the zones of inhibition showed that the complexes of Co, Ni and Cu at 20 µg/disc has antibacterial activity on *Staphylococcus aureus* (24.3, 22.3 and 24.0 mm) and *S. typhi* (15.3, 14.0 and 9.7 mm) respectively.

Keywords: synthesis, sulfamethoxazole, ampicillin trihydrate, *Salmonella typhi*, *Staphylococcus aureus*.

1. Introduction

Metals have an esteemed place in medicinal chemistry. First row transition metals represent the d-block elements which lie between group IIA and IIIA of the periodic table. Their d-shells are in process of filling. This property of transition metals resulted in the foundation of coordination complexes. Metal complex or coordination compound is a structure consisting of a central metal atom, bonded to a surrounding array of molecules or anions (ligands) (Rafique *et al.*, 2010). Transition metal complexes are cationic, neutral or anionic species in which a transition metal is coordinated by ligands (Cox, 2005). Mixed ligand complexes with metal ion bound to two different and biochemically important ligands have aroused interest as model for metallo-enzymes.

The physiologically interesting mixed ligand complexes of transition metals with amino acids play an important role in biological systems and have been a subject of great interest for researchers (Shivankar *et al.*, 2003). Metals not only provide templates for synthesis, but they also introduce functionalities that enhance drug delivery vectors (Obaleye *et al.*, 2012). Many organic drugs require interaction with metals for activity. They interact with metals at their target site or during their metabolism or disturb the balance of metal ion uptake and distribution in cell and tissue.

The unique properties of metal complexes tend to offer advantages in the discovery and development of new drugs (Obaleye *et al.*, 2012). Here in this paper we are describing synthesis and characterization of cobalt (II), nickel (II) and copper (II) complexes, sulfamethoxazole [4-amino-N-(5-methyl-3-isoxazolyl) benzenesulfonamide], and ampicillin trihydrate.

2. Materials and methods

2.1. Reagents and instruments

All chemicals and solvents used were of analytical grade. Pure sample of Sulfamethoxazole, molecular formula C₁₀H₁₁N₃O₃S and molecular weight 253.28, was obtained from Bristol Scientific Company, Lagos Ampicillin trihydrate from Central Drug House, New Delhi. Metal salts CoCl₂.6H₂O, NiCl₂.6H₂O and CuCl₂. 2H₂O were of Merck chemicals. Analytical Reagent grade hydrated metal chlorides from Bristol Scientific Chemicals were used for the preparation of the complexes. Elemental analysis (C, H, N and S) were carried out using micro analytical technique on CHNSO Elemental analyzer at Universiti Teknologi Petronas (UTP) Malaysia. The Infrared spectra of ligand and metal complexes were recorded on KBr pellets in the range 4000-450 cm⁻¹ on Perkin Elmer FTIR spectrophotometer. Melting points were recorded using melting point apparatus.

2.2 Synthesis

To a hot ethanolic solution (20 cm³) containing 2.0 mmole (0.506 g) of sulfamethoxazole, ethanolic solution (20 cm³) containing 2.0 mmole, (0.806 g) of ampicillin trihydrate were added to ethanol solution (20 cm³) 2.0mmole of a metal chloride (hydrate) under constant stirring. The pH of the reaction mixture was adjusted to 7.5–8.5 by adding 10 % alcoholic ammonia solution and refluxed for about 3 h. The precipitated solid metal complex was filtered off under hot conditions and washed with hot ethanol, petroleum ether (40–60 °C) and dried over anhydrous CaCl₂ in a vacuum desiccator (Munde *et al* 2010).



2.3 Antibacterial activities

The antibacterial activity of the ligand and metal complexes were tested *in vitro* against Bacteria: *Staphylococcus aureus* and *Salmonella typhi* by the paper disc plate method. The compounds were tested at the concentration 0.50 and 1.0 mg mL⁻¹ in DMSO and compared with known antibiotics *viz.* ciprofloxacin.

3. Results and discussion

The physical characteristics and molar conductance data of the ligands and its metal complexes are given in Table 1. The analytical data of the complexes revealed 1:1 mole ratio (metal:ligand) and corresponds well with the general formula [ML] (M =Co (II), Ni (II), Cu (II)). The magnetic susceptibilities of the Cu (II) and Ni (II) complexes at room temperature were found to be consistent with square-planar geometry and that of the Co (II) complex with

high-spin octahedral structures having two water molecules coordinated to the metal ion. The presence of two coordinated water molecules was confirmed by TG/DT analysis. The metal chelate solutions in DMSO showed low conductance, supporting then non-electrolyte nature of the complexes.

3.1 IR spectra

FTIR spectral data of the complexes and standard drugs in Table 3.2 showed the most important absorption bands. The presence of strong absorption bands at 3507 cm⁻¹ in the spectrum of ampicillin trihydrate was attributed to $\nu(\text{O-H})$ vibration frequencies (Waziri *et al.*, 2014). This absorption band shifted to 3477 cm⁻¹, 3460 cm⁻¹ and 3445 cm⁻¹ in cobalt (II), nickel (II) and copper (II) complexes respectively indicating the formation of coordination bond between the central metal atom and (O-H) of the ampicillin trihydrate.

Table 1. Analytical Data of the Complexes and Ligands

Complexes	Yield (%)	Colour	M.P. (°C)	Λ S cm ² mol ⁻¹	Molar conductance
[Co(SMX)(AMP)]	59.50	Pink	245 (D)	18.20	6.08
[Ni(SMX)(AMP)]	61.90	Yellow	238 (D)	28.71	6.72
[Cu(SMX)(AMP)]	58.33	Green	234 (D)	20.13	7.12
(AMP)	ND	White	198-199	-	4.10
(SMX)	ND	White	169-171	-	4.19

Key: SMX = Sulfamethoxazole, AMP = Ampicillin trihydrate, ND: Not determined, D = decomposed

From Table 1, the percentage yield of the [Co(SMX)(AMP)], [Ni(SMX)(AMP)] and [Cu(SMX)(AMP)] are 59.50, 61.90 and 58.33 and all the complexes decomposed at a temperature range of 234°C to 24°C

Table 2. Infrared Spectral Data of the Complexes and the Ligands (cm⁻¹).

Complexes(cm ⁻¹)	$\nu(\text{O-H})$	$\nu(\text{N-H})$	$\nu(\text{C=O})$	$\nu(\text{S=O})$	$\nu(\text{M-N})$	$\nu(\text{M-O})$
[Co(SMX)(AMP)]	3477	3386	1639	1134	588	476
[Ni(SMX)(AMP)]	3460	3173	1620	1125	576	428
[Cu(SMX)(AMP)]	3445	3339	1657	1128	578	420
AMP	3507	3445	1773	-	-	-
SMX	3470	3015	1633	1337	-	-

Table 3. Antibacterial Activities of the complexes and the ligands against *S. aureus* and *S. typhi*

Complexes/Ligands	zone of inhibition (<i>S. aureus</i>)		<i>S typhi</i>	
	10 $\mu\text{g}/\text{cm}^3$	20 $\mu\text{g}/\text{cm}^3$	10 $\mu\text{g}/\text{cm}^3$	20 $\mu\text{g}/\text{cm}^3$
[Co(SMX)(AMP)]	19.7 ± 0.58	24.3±0.58	11.6 ± 0.58	15.3±1.15
[Ni(SMX)(AMP)]	18.0 ± 0.00	21.3±1.15	13.7± 0.58	14.0±0.00
[Cu(SMX)(AMP)]	20.7 ± 0.58	24.0±0.00	8.7 ± 1.15	9.7±0.58
[(SMX)(AMP)]	15.2 ± 0.60	20.0±0.00	8.2 ± 0.58	8.6±0.58
(SMX)	12.7 ± 1.15	16.3±0.58	6.3 ± 0.58	7.6±0.58
(AMP)	14.0 ± 0.00	17.7±0.58	8.0±0.00	9.3± 1.15

The appearances of such spectral bands suggest the coordination to the respective metals as reported by (Ahmed *et al.*, 2011) in which the band at 1633 cm⁻¹ was assign to $\nu(\text{C=O})$ in free sulfamethoxazole. This band is observable in the spectra of three complexes at 1639 cm⁻¹, 1620 cm⁻¹ and 1657 cm⁻¹ confirming the coordination of

sulfamethoxazole to the respective metals. The strong absorption in the range of 550-595 cm⁻¹ and 420-500 cm⁻¹ of the metal complexes have been assigned to $\nu(\text{M-N})$ and $\nu(\text{M-O})$ stretching frequencies respectively, supporting the coordination of the ligands to respective metal ions through Nitrogen and oxygen atoms respectively (Osowole *et al.*, 2015). It was



therefore suggested, based on the chelate theory (Chang *et al.*, 2010), that increasing the number of chelate rings may improve the antimicrobial activities of the complexes. The strong absorption bands at 3445 cm⁻¹ and 3015 cm⁻¹ in AMP and SMX were assigned as $\nu(\text{N-H})$ band (Khan and Asnani, 2011; Gulcan *et al.*, 2012). On coordination, these bands shifted to 3386 cm⁻¹, 3173 cm⁻¹ and 3339 cm⁻¹ in the spectra of Co (II), Ni (II) and Cu (II) complexes respectively indicating the coordination of the amino group's nitrogen to the metal (II) ions without deprotonation (Beyrambadi *et al.*, 2011). This is in closed agreements with the bands obtained by (Osowole *et al.*, 2015).

3.1 Antibacterial activity

The measured zone of inhibition of the complexes as well as the ligands against *Staphylococcus aureus* and *Salmonella typhi* were presented in Table 3. The comparison of the biological activity of the *Salmonella typhi* (gram negative) bacteria and *Staphylococcus aureus* (gram positive) the biological activities of the metal complexes are higher than the free ligands towards the gram positive and gram negative bacteria, in addition, the antibacterial activity of the complexes follow the order [Co(SMX)(AMP)] > [Cu(SMX)(AMP)] > [Ni(SMX)(AMP)] > (SMX)(AMP) > (SMX) > (AMP) against *Staphylococcus aureus*. But with *Salmonella typhi*, the antibacterial activities of the complexes reduced in the following order (AMP) < (SMX) < (SMX)(AMP) < [Cu(SMX)(AMP)] < [Ni(SMX)(AMP)] < [Co(SMX)(AMP)]. It is evident from the above data that the antibacterial activity significantly increased on coordination.

It was suggested that suggested that the ligands with nitrogen and oxygen donor systems inhibit enzyme activity (Fayad *et al.*, 2012) Coordination reduces the polarity of the metal ion mainly because of the partial sharing of its positive charge with donor groups within the chelate ring system (Raja *et al.*, 2011). The increase in the antibacterial activities of the complexes as compared to the free ligands may be due to to the electropositive nature of metals, ultimately enhancing their antibacterial (Nazir *et al.*, 2013).

Reference

1. Ahmed, E. M., Marzouk, N. A., Hessein, S. A. and Ali, A. M. (2011). Synthesis, Reactions and Antimicrobial activity of some new thienopyridine and thienopyrimidine derivatives. *World Journal of Chemistry*, 6:25-31.
2. Beyrambadi, S. A., Hoseini, H. E., Housaindokht, M. R. and Morsali, A. (2011). Synthesis,

- experimental and theoretical characterization of Cu (II) complex of @- chloropyrimidine. *Science Research Essentials*, 6(20): 4341-4346.
3. Chang, E., Simmers, C. and Knight, A., (2010). Cobalt complexes as antiviral and antibacterial agents. *Pharmaceuticals*, 3, 1711-1728
4. Cox, P. A. (2005). Instant Notes Inorganic Chemistry. 2nd ed. New York: BIOS Scientific Publishers, 237:1001-2299.
5. Fayad, N. K., Taghreed, H. A. and Ghanim, F. H. (2012). Synthesis, Characterization and Antibacterial Activities of Mixed Ligand Complexes of some Metals with 1-nitroso-2-naphthol and L-phenylalanine, *Chemistry and Materials Research*, 2(5): 18-29.
6. Gulcan, M., Sonmmez, M. and Berber, I. (2012). Synthesis, Characterization and antimicrobial of a new pyrimidine Schiff base and its Cu(II), Ni(II), Co(II), Pt (II) and Pd (II) complexes. *Turkey Journal of Chemistry*, 36:189.
7. Khan, F. R. and Asnani, A. J. (2011). Synthesis, anti-ulcer and anti-secretory activity of some new substituted 2 (pyrimidylsulfanyl) Benzamidazoles Derivatives. *International Journal of Research in Pharmaceutical and Biomedical Sciences*, 2(2):695-700.
8. Munde, A. S., Jagdale, A. N., Jadhav, S. M. and Trimbak, K. C. (2010). Synthesis, characterization and thermal studies of some transition metal complexed of asymmetric tetradentate Schiff base ligand. *Journal of the Serbian of Chemical Society*, 75(3):349-359.
9. Nazir, F., Bukhari, I. H., Arif, M., Riaz, M., Raza, S. A. Bokari T. H., and Jamal, M. A. (2013). Antibacterial Studies and Schiff bases metal complexes with some novel antibiotics. *International Journal of Current Pharmaceutical Research*, 5(3):40-46.
10. Obaleye, J. A., Tella, A. C. and Bamigboye, M. O. (2012). Metal complexes as prospective antibacterial agents in: B. Valprasad ed. 2012. A Search for Antibacterial Agent. Rijeka: InTech. Rijeka, Croatia, 197-219.
11. Osowole, A. A., Sherifah, M. W. and Alaoluwa, K. A. (2015). Synthesis, characterization and antimicrobial activity of some mixed trimethoprim Sulfamethoxazole Metal Drug Complexes. *World Applied Sciences Journal*, 33(2):336-342.
12. Rafique, S., Idrees, M., Nasim, A., Akbar, H. and Athar, A. (2010). Transition metal complexes potential therapeutic agents. *Biotechnology and Molecular Biology Reviews*, 5(2):38-45.
13. Raja, S. R., Jisha, J. and Mary, N. L. (2011). Antibacterial Studies of Schiff Base Complexes and Polymer supported Schiff Base Complexes. *International Journal of Institute Pharmaceutical Life Sciences*, 1(2):49-56.
14. Shivankar, V.S., Vaidya, R.B., Dharwadkar, S.R., and Thakkar, N.V., (2003). Synthesis, Characterization, and Biological Activity of Mixed Ligand Co (II) Complexes of 8- Hydroxyquinoline and some Amino Acids synth. *React. Inorg.Met-Org and NanoMet.Chem.* 33:1597- 1622.
15. Waziri, I., Ndahi, N. P., Mala, G. A. and Fugu, M. B. (2014). Synthesis, Spectroscopic and Biological Studies of Cobalt (II), Nickel (II) and Iron (III) mixed antibiotic metal complexes. *Scholars Research Library*, 6(5):118-122.

**ABSTRACT CCT-: 024**

Lubabatu Muazu Jodi¹, Lawal Gusau Hassan¹, Lawal Muhammad Abubakar² Abdullahi Muhammad Sokoto¹, Muibat A. Obianke¹ and Aminu Bayawa Muhammad^{1*}

1. Department of Pure and Applied Chemistry, Usmanu Danfodiyo University, Sokoto.

2. Department of Crop Science, Usmanu Danfodiyo University, Sokoto.

Email: ambayawa@yahoo.com

EMPIRICAL OPTIMIZATION OF ULTRASOUND-ASSISTED ALKALINE CATALYSED TRANSESTERIFICATION OF *Lannea acida* SEED OIL TO BIODIESEL

ABSTRACT: Biodiesel is produced from wide range of feedstock although, for both economics and food security reasons, there is more emphasis on non-edible oils, such as seed oils of *L. siceraria*, *H. brasiliensis* among others. *Lannea acida* is one of those plants with seeds having significant oil content (42.79%). In this work Box-Behnken response surface methodology design was used to investigate and optimise the transesterification of *L. acida* oil into biodiesel with the help of ultrasound following initial acid-catalysed esterification of the oil due to its high free fatty acid content. Effect of four factors, catalyst concentrations methanol/oil ratio temperature and time, was investigated. And physicochemical properties of the biodiesel were determined according to standard procedures. The results of regression analysis revealed that two linear terms (Methanol/oil ratio and catalyst concentration), and three quadratic terms (respective squares of methanol/oil ratio, catalyst concentration and reaction temperature) significantly influenced the biodiesel yield. The model obtained, with coefficient of determination (R^2) of 91% (R^2 -adj = 90.53%; R^2 -pred = 89.06%) was found to adequately account for the experimental data. Results of validation experiments, with biodiesel yield of 99.05±0.22 %, was in agreement with the model predictions. Analysis of the biodiesels by GC/MS, shows that the biodiesel to contain mainly methyl esters of octadecadienoic acid (19.44%), octadecanoic acid (19.32%), hexadecanoic acid (14.93%) and octadecanoic acid (11.49%). The produced biodiesel has specific gravity (0.89), kinematic viscosity (6.62 Cst), aniline point (45°C), flash point (90°C), pour point (-5°C), cloud point (16.33°C), and sulphur content (0.03%) which are within the ASTM D6751 and EN 41214 standards, implying its suitability for use as fuel in diesel engines.

Keywords: *Lannea acida*, Box-Behnken design, optimization, biodiesel, alkaline catalysis, transesterification.

1. Introduction

The increasing decline in fossil fuel reserves coupled with their negative environmental impact are increasingly motivating search for alternative renewable fuels [1,2]. Biodiesel is one of such promising fuels suitable for use in diesel engine [2,3]. It is renewable and produces much fewer harmful emissions than conventional petrodiesel [4,5]. Thus significant utilization of biodiesel has been projected to significantly help in decreasing carbon dioxide, sulphur dioxide, unburned hydrocarbon, and particulate matter emissions from automobiles [6].

Biodiesel is produced from wide range of feedstock [7-9] although, for both economics and food security reasons, there is more emphasis on non-edible oils [8,10], such as seed oils of *L. siceraria* [11], *H. brasiliensis* [12] among others [3]. *Lannea acida* is one of those plants with seeds having significant oil content (42.79%). It is a deciduous shrub or tree (1.5 to 10 m tall and bole of 50 - 70 cm in girth) is widely distributed throughout West Africa and particularly in the northern part of Nigeria. It has red to purple-black clusters of fruits with oil-rich kernels [13].

In this work we report our investigation on optimisation of alkaline catalysed transesterification of seed oil of *Lannea acida*. Box-Behnken response surface experimental design was used to investigate and optimise the transesterification with the help of ultrasound following initial acid-catalysed esterification of the oil due to its high free fatty acid content. Effect of four factors, catalyst concentrations methanol/oil ratio temperature and time, was investigated. GC/MS (Agilent 7890A GC coupled to 5973 MSD) was used to determine the molecular composition of the biodiesel produced at the optimal process condition. And physicochemical properties of the biodiesel were determined according to standard procedures [12]. The results of regression analysis revealed that two linear terms (Methanol/oil ratio and catalyst concentration), and three quadratic terms (respective squares of methanol/oil ratio, catalyst concentration and reaction temperature) significantly influenced the biodiesel yield. The model obtained, with coefficient of determination (R^2) of 91% (R^2 -adj = 90.53%; R^2 -pred = 89.06%) was found to adequately account for the experimental data.

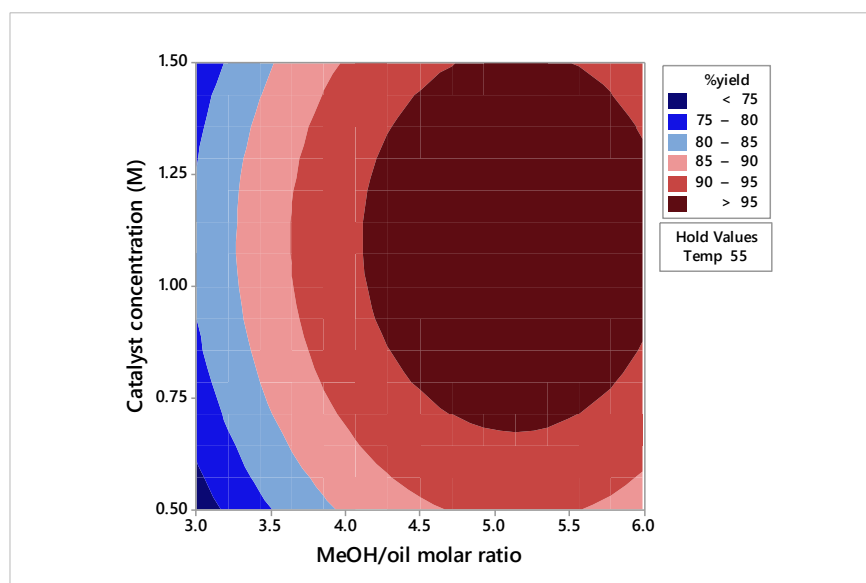


Fig. 1. Contour plot showing effect of catalyst concentration and methanol/oil molar ratio on biodiesel yield in transesterification of *L. acida* seed oil.

Fig. 1 shows that the biodiesel yield increases with an increase in catalyst concentration and methanol/oil molar ratio. Highest biodiesel yields greater than 95 % are obtained at catalyst concentrations of 0.65 to 1.50 M when the MeOH/oil ratio of 4.30 to 6.0. Optimisation results show that maximum biodiesel yield of 98.0 % can be obtained at catalyst concentration of 1.0 %, temperature of 55°C, methanol/oil ratio of 4.5. Results of validation experiments, with biodiesel yield of 99.05 ± 0.22 %, was in agreement with the model predictions. Analysis of the biodiesels by GC/MS, shows that the biodiesel to contain mainly methyl esters of octadecadienoic acid (19.44%), octadecanoic acid (19.32%), hexadecanoic acid (14.93%) and octadecanoic acid (11.49%).

The produced biodiesel has specific gravity (0.89), kinematic viscosity (6.62 Cst), aniline point (45°C), flash point (90°C), pour point (-5°C), cloud point (16.33°C), and sulphur content (0.03%) which are within the ASTM D6751 and EN 41214 standards, implying its suitability for use as fuel in diesel engines.

References

- [1] Agarwal AK, Gupta T, Shukla PC, Dhar A. Particulate emissions from biodiesel fuelled ci engines. *Energy Conversion and Management*. 2015; 94: 311-330.
- [2] Atabani AE, Silitonga AS, Badruddin IA, Mahlia TMI, Masjuki HH, Mekhilef S. A comprehensive review on biodiesel as an alternative energy resource and its characteristics. *Renewable and Sustainable Energy Reviews*. 2012; 16: 2070-2093.

- [3] Hoekman SK, Broch A, Robbins C, Cenicerros E, Natarajan M. Review of biodiesel composition, properties, and specifications. *Renewable and Sustainable Energy Reviews*. 2012; 16: 143-169.
- [4] Issariyakul T, Kulkarni MG, Meher LC, A.K. D, N.N. B. Heterogeneous catalysts for biodiesel production. *Chem. Engineering J*. 2008; 140: 77-85.
- [5] Dwivedi G, Jain S, Sharma MP. Impact analysis of biodiesel on engine performance—a review. *Renewable and Sustainable Energy Reviews*. 2011; 15: 4633-4641.
- [6] Antolin G, Tinaut FV, Briceno Y, Castano V, Pirez C, Ramirez AI. Calcium oxide as a solid base catalyst for transesterification of soybean oil. *Bioresour. Technol*. 2002; 83: 111 - 114.
- [7] Fan X, Wang X, Cheng F. Two novel approaches used to produce biofuel from low-cost feedstock. *The Open Fuels and Energy Science Journal*. 2010; 3: 23 - 27.
- [8] Gui MM, Lee KT, Bhatia S. Feasibility of edible oil vs. Non-edible oil vs. Waste edible oil as biodiesel feedstock. *Energy*. 2008; 33: 1646-1653.
- [9] Karmakar A, Karmakar S, Mukherjee S. Properties of various plants and animals feedstocks for biodiesel production. *Bioresource Technology*. 2010; 101: 7201-7210.
- [10] Haas MJ. Improving the economics of biodiesel production through the use of low value lipids as feedstocks: Vegetable oil soapstock. *Fuel Process Technol*. 2005; 86: 1087-1096.
- [11] Muhammad AB, Bello K, Tambuwal AD, Aliero AA. Assessment and optimization of conversion of *Siceraria* seed oil into biodiesel using cao on kaolin as heterogeneous catalyst. *International Journal of Chemical Technology*. 2015; 7: 1 - 11.
- [12] Muhammad AB, Obianke M, Gusau LH, Aliero AA. Optimization of process variables in acid catalysed in situ transesterification of hevea brasiliensis (rubber tree) seed oil into biodiesel. *Biofuels*. 2016: 1-10.
- [13] Maydell H-JV (1990) *Trees and shrubs of the sahel: Their characteristics and uses*; Verlag Josef Margraf: Zusammenarbeit.

**ABSTRACT CCT-: 037**

Ibrahim Abubakar Abubakar*, Abdulfatai Jimoh, Muibat Diekola Yahya, Manase Auta

Department of Chemical Engineering, School of Engineering and Engineering Technology, Federal University of Technology Minna, PMB 65, Minna, Niger State Nigeria

Email: abubakar6989@gmail.com**OPTIMIZING DEPROTEINIZATION OF CHITIN USING RESPONSE SURFACE METHODOLOGY**

ABSTRACT: The physicochemical parameter which influences the application of chitin in various fields is strongly linked to the source and the conditions of the chitin production. The condition of chitin production can be controlled by manipulating solution conditions (temperature, concentration, reaction time) and optimization of deproteinization processes. The *Callinectes pallidus* wastewas pre-treated, bleached, decolourized and demineralised which significantly affect chitin quality and yield. The design of experiments (DOE) via central composite design (CCD) of response surface methodology (RSM) was used to optimize the process parameters of deproteinization. The experimental results indicate that the crab shells waste (CSW)/chitin had 5.24/4 % moisture, 59.31/0.7% ash, 6.75/0.95 % lipid, 15.75/2.05 % crude protein and mineral 44.17/8.98 g/Kg respectively. The predicted values of the response were further validated and results suggested that the optimal condition for chitin synthesis in deproteinization; treatment temperature 70 oC, reaction time of 4 h, and concentration of NaOH 4.47 % with percentage deproteinization of 92.97 % and 91.08 % for actual and predicted respectively.

Keywords: chitin synthesis, deproteinization, crab shell waste, response surface methodology.

1. Introduction

Wastes generated from the production and processing of aquatic resources are enormous which constituting source of land and water pollutions. In view of the fact that, most of the aquatic waste easily deteriorate and littered on river banks thereby restricting tourist activities (Jang *et al.*, 2004; Mejia-Saules *et al.*, 2006; Adebayo-Tayo *et al.*, 2012). The conversion of these wastes into useful chemical materials such as chitin for industrial application is one of the major objectives of this research (Jang *et al.*, 2004; Gerente *et al.*, 2007; Sivakami *et al.*, 2013; Maram *et al.*, 2013; Mohammed *et al.*, 2014).

Chitin is a unique functional material for versatile applications with high commercial interest due to its percentage nitrogen contents compared to artificially replaced cellulose (Kumar, 2000; Yadav *et al.*, 2004; Zaku *et al.*, 2011). It can be found in an array of species in both the animal and plant kingdoms. The tradition source of chitin is the seafood waste, mostly the fish scale, crabs, prawn, lobster and shrimp shells. Chitin is the second most abundant biopolymer in nature after cellulose. It is estimated that its annual synthesis reaches 100 billion tons (Rinaudo, 2006).

Many techniques have been planned and used over the years to produce pure chitin; nevertheless, no standard technique has been adopted (Rødde *et al.*, 2007). The usual processes of chitin synthesis consist of the use of strong acids and bases under high temperatures, may cause pollution and significantly lower quality and yield of chitin (No *et al.*, 2002; Rødde *et al.*, 2007). An alternative way to solve these problems is to use organic acid during demineralization, due to corrosiveness of inorganic acids and

furthermore, improved deproteinization treatment via optimization of process parameters (Shirai *et al.*, 2001; Cira *et al.*, 2002). However, Response surface methodology (RSM) is useful statistical techniques of Design-Expert (Software 7) that can reduce the number of experimental trials, determine the significant reaction factors, and can be employed to optimize the treatment conditions (Younes *et al.*, 2012). Hence, the aim of this work was to search for modified ways of getting high quality chitin from the crab shell (*Callinectes pallidus*) via Optimizing deproteinization of chitin using response surface methodology for industrial used.

2. Material and methods

2.1 Material and chemical/reagents

The fresh samples of Gladiator Swim crab shells, *Callinectes pallidus* were obtained from Oyingbo, Lagos, Nigeria. For all experiments, reactions were carried out in Erlenmeyer flask (250 ml capacity). The major chemicals and reagents used are include lactic acid ($\text{CH}_3\text{CH}(\text{OH})\text{CO}_2\text{H}$), sodium hydroxide (NaOH), Sodium hypochloride (NaOCl) and Acetone($\text{CH}_3)_2\text{CO}$ all these chemical and reagents are analytically graded and were obtained from Sigma Aldrich and Analar BDH.

2.2 Methods

The wet crab shell waste (CSW) was thoroughly washed and oven dried at 60 °C for 10 hr, then milled and sieved through 300 μm BS sieve. 10 g of the prepared CSW were decolorized with acetone in the ratio 1:1 weight of solid to solvent (W/V) for 10 min and dried for 1 hr at ambient temperature. The



sample was bleached with 0.35 % NaOCl solution for 10 min at ambient temperature. Samples were washed with distilled water and oven dried for about 4 h at 60 °C, and milled (Nessa *et al.*, 2010; Abdulwadud *et al.*, 2013). The surface area, proximate and thermal gravimetric analyses of CSW and chitin were carried out in order to determine its quality and yield.

2.3 Demineralization of crab shell waste (CSW)

$$D_m = \frac{(A_0O - A_rR) * 100}{A_0} \quad (1)$$

Where:

D_m = Percentage demineralization (%); A_0 = Ash content before demineralization (%)

A_r = Ash content after demineralization (%); O = Weight of Sample before demineralization (g); R = Weight of Sample after demineralization (g).

2.4 Deproteinization of demineralized crab shell waste (CSW)

Three parameters which were expected to have an effects on deproteinization of demineralized CSW were identified; concentration of NaOH solution (A , %, w/v), reaction time (B , h) and treatment temperature (C , °C). The treatments were carried out with aid of central composite design (CCD) of RSM. The CCD matrix

Demineralization was carried out using modified procedures reported by Hossain and Iqbal (2014) and Divya *et al.* (2014). The CSW samples mixed with 10 % concentration of lactic acid (v/v), 2 hr reaction time and treatment temperature of 45 °C. The demineralized CSW were washed to neutrality with deionised water, oven dried at 60 °C for 4 hr, milled and labelled for further analysis (Jimohet *et al.*, 2013). The percentage demineralization was evaluated by Equation 1.0 (Ghorbel-Bellaaj *et al.*, 2011; Khorramiet *et al.*, 2012).

consisting 20 runs with three input variables were considered at low (-1), medium (0) and high (+1) level with axial point (α) added at a distance of 1.68 (Myers *et al.*, 2009; Melvin *et al.*, 2011). The percentage deproteinization was evaluated by Equation 2.0 (Ghorbel-Bellaaj *et al.*, 2011; Khorrami *et al.*, 2012). The data obtained were subjected to the Analysis of Variance (ANOVA) and optimization. The results of CCD were used to derive second order polynomial model (Equation 3).

$$D_p = \frac{(P_0O - P_rR) * 100}{P_0} \quad (2)$$

Where

D_p = Percentage deproteinization (%); P_0 = Protein content before deproteinization (%)

P_r = Protein content after deproteinization (%); O = Weight of Sample before deproteinization (g)

R = Weight of Sample after deproteinization (g).

$$Y = \beta_0 + \beta_a A + \beta_b B + \beta_c C + \beta_{ab} AB + \beta_{ac} AC + \beta_{bc} BC + \beta_{aa} A^2 + \beta_{bb} B^2 + \beta_{cc} C^2 + \dots \quad (3)$$

Where Y is the predicted response (% deproteinization); β_0 is the intercept (regression coefficient); β_a , β_b and β_c are the linear coefficient; β_{aa} , β_{bb} and β_{cc} are the quadratic coefficient; β_{ab} , β_{ac} and β_{bc} are the interaction coefficient. A , B and C are the independent variables (Manase *et al.*, 2012; Richa *et al.*, 2014).

3. Results and discussion

3.1 Characterization CSW and chitin

The result of the surface chemistry, proximate and mineral composition of Crab shell waste (CSW) and chitin were presented in Table 1. The Analysis showed that the CSW had 6.95 % moisture, 59.31 % ash, 6.75 % lipid, 15.75 % crude protein and mineral 44.17g/Kg. While chitin proximate and mineral composition were 4 %, 0.7 %, 0.95 %, 2.05 %, 8.98 g/Kg, 374 m²/g and 0.25 cm³/g for moisture, ash, lipid, crude protein, mineral, specific surface area and specific pore volume respectively. This is in agreement with the findings reported

by Fawole, *et al.*, 2007 and Adejonwo, 2010. From the results given in Table 1, it can be realized that the values of surface area analysis, proximate and mineral composition of crab shells are essential in estimating the quality of the raw material utilization for different technological processes as established in the literature (Abdul and Sarojanlini, 2012).

3.2 Thermogravimetric Analysis (TGA)

Thermogravimetric analysis (TGA) is a thermal analysis in which changes in physical and chemical properties of materials were measured as a function of increasing temperature as in Fig. 1.



Table 1: Result of proximate, mineral and surface chemistry analysis of CSW and Chitin

Sample	Moisture (%)	Ash (%)	Lipid (%)	Crude Protein (%)	CaCO ₃ (g/Kg)	Surface Area (m ² /g)	Pore Volume (cm ³ /g)
CSW	5.24	59.31	6.75	15.75	44.17	229.60	0.15
Chitin	4.00	0.70	0.95	2.05	8.98	374.00	0.25

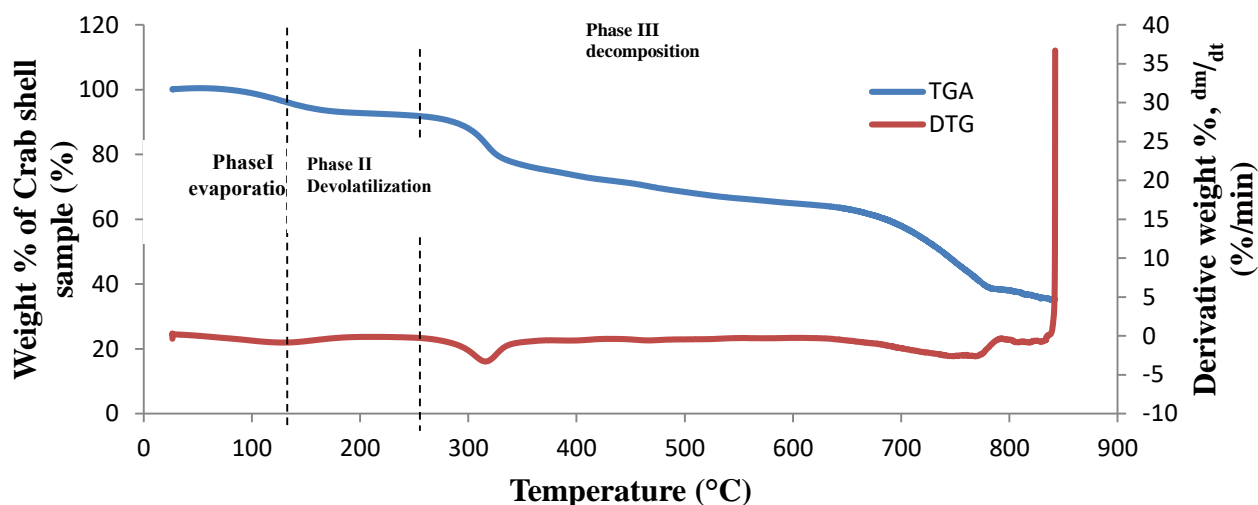


Fig. 1. Thermogravimetric Analysis (TGA) and Derivative Thermogravimetric (DTG)

The TGA details of crab shell in Fig. 1 shows mainly two major weight losses at 190 °C and the second before 310 °C respectively. The first one is due to the elimination of water molecules with respective moisture content of 5.24 % and the second one is due to the depolymerisation and decomposition of volatile products (Vijayalakshmi *et al.*, 2016).

3.2 Synthesis of chitin from crab shell waste (CSW)

The percentage demineralization of CSW was 96.41 % obtained from 10 % concentration of lactic acid (v/v), 2 hr reaction time and treatment temperature of 45°C. The value of percentage demineralization reported in this work is higher than value reported by Neith *et al.*, 2011, which may be due to differences in the approach used.

Table 2. Actual-Predicted Values and Residual for Y (Chitin)

Factors				Responses		
Run	A-Conc. of NaOH (%)	B-Time (h)	C-Temp. (°C)	Actual Value	Predicted Value	Residual
1	0	0	0	68.03	61.56	6.47
2	0	-1.68	0	71.11	70.81	0.30
3	1	1	1	91.40	91.86	-0.46
4	0	0	1.68	90.67	96.64	-5.97
5	1	-1	1	78.83	71.26	7.57
6	0	0	0	72.43	70.37	2.05
7	0	0	0	75.50	74.20	1.30
8	1	-1	-1	87.97	88.84	-0.87
9	0	0	0	75.50	74.20	1.30
10	0	0	0	75.50	74.20	1.30
11	1	1	-1	62.94	61.92	1.02
12	0	0	0	87.83	86.11	1.72
13	1.68	0	0	79.53	78.96	0.56
14	1	1	1	76.16	78.98	-2.82
15	1	-1	-1	73.82	70.60	3.22
16	0	1.68	0	80.56	80.60	-0.05
17	0	0	-1.68	79.31	80.60	-1.30
18	1	-1	1	74.53	73.60	0.93
19	1	1	-1	76.31	80.60	-4.30
20	-1.68	0	0	47.60	55.68	-8.08



In Table 2 the demineralized CSW was followed by optimization of deproteinization parameters (Concentration of NaOH, reaction time and treatment temperature). From the response surface methodology showed that the optimum conditions, deproteinization of 92.97 % at treatment temperature 70 °C, concentration of NaOH 4.47 % (v/v) and reaction time 4hr was achieved. The high values of percentage deproteinization may be due to interaction of the process parameters (temperature, time and concentration of base) lead to high quality of chitin yield (Nidheesh *et al.*, 2014). From the statistical analysis, F-value of 6.34 implies the model is significant, base Central composite design (CCD) of RSM was applied for deproteinization parameters toward achieving quality chitin. From the results given in Table 2, the predicted values of the responses for % deproteinization (Y) were calculated using Equation 3 based on the respective coefficients variables has significant effect on the quality and yield of chitin during deproteinization

Equation in Terms of Coded Factors:

$$Y = +80.60 + 8.47*A + 7.19*B + 2.98*C + 6.38*A*B - 2.54*A*C + 0.66*B*C - 3.77*A^2 - 2.33*B^2 + 1.19*C^2 \quad (4)$$

Equation in Terms of Actual Factors:

$$Y = +50.84402 + 9.81415*A + 4.42602*B - 0.82343*C + 3.19132*AB - 0.12677*A*C + 0.066042*B*C - 0.94317*A^2 - 2.32706*B^2 + 0.011918*C^2 \quad (5)$$

4. Conclusion

High quality chitin from crab shell wastes by organic acid demineralization and optimization of deproteinization process parameters. The effect of process variables on the chitin preparation and optimization of deproteinization parameters via Central composite design (CCD) of response surface methodology (RSM) improved the quality and yield of chitin. These findings suggest that the predicted values of the response were further validated and results suggested that the optimal conditions for deproteinization of chitin were 70 °C, 4 hr, and 4.47 % of NaOH with percentage deproteinization of 92.97 % and 91.08 % for actual and predicted value respectively. This technique makes it attractive for the high quality chitin and avoiding the toxicity of chemical during treatment. This research work successfully synthesized.

References

1. Adebayo-Tayo, B. C., Odu, N. N., Okonko, I. O. (2012). Microbiological and physiochemical changes and its correlation with quality indices of tilapia fish (*Oreochromis niloticus*) sold in Itu and Uyo markets in Akwa Ibom State, Nigeria. *New York Science Journal*;5(4):38-45.
2. Adejonwo, O. A., Kolade, O. Y. Ibrahim, A. O. and Oramadike, C. E. (2010). Proximate and anatomical

treatments provided in Equation 4–5. The predicted values of Y were further validated and results suggested that the optimal condition for chitin synthesis in deproteinization; treatment temperature 70 °C, reaction time of 4 h, and concentration of NaOH 4.47 % with percentage deproteinization of 92.97 % and 91.08 % for actual and predicted respectivel (Richa *et al.*, 2014). on p-value of 0.0040. The models were valid from the Standard Deviation of 6.61, Root Squared of 85 %, Mean 77.25, Adjusted R-Squared 72 %, Correlation of Variance 8.56 % , Predictected R-Squared -0.0510 and Adeq Precision 9.231.

3.3 Regression model

The quadratic regression models (Equations 4 – 5) were obtained for predicting the optimal points of chitin synthesis. The model shows that the input

- weight composition of wild brackish *Tilapia guineensis* and *Tilapia melanotheron*, *World Rural Observations* 2(3), 34–37.
3. Abdul H. and Sarojanlini, C. H. (2012). Proximate composition, Macro & Micro elements of some smoke-dried hill stream fishes from Manipur, India. *Nature & Science*.10 (1).
 4. Abdulwadud A., Muhammed, T. I., Surajudeen, A., Abubakar, J. M. and Alewo, O. A. (2013). Extraction and Characterisation of Chitin and Chitosan from Mussel Shell. *Civil and Environmental Research* 3 (2).
 5. Cira L.A., Huerta S., Guerrero I., Rosas R., Shirai K. (2000). Scaling up of lactic acid fermentation of prawn wastes in packed-bed column reactor for chitin recovery. In: Peter M.G., Domard A., Muzzarelli R.A.A., editors. *Advances in Chitin Science*. Volume IV. Potsdam University; Postdam, Germany: 2–27.
 6. Choorit, W., Patthanamane, W. and Manurakchinakorn S. (2008). Use of response surface method for the determination of demineralization efficiency in fermented shrimp shells. *Bioresour. Technol.*;99, 6168–6173. doi: 10.1016/j.biortech.
 7. Divya K., Sharrel R. and Jisha M S. (2014). A Simple and Effective Method for Extraction of High Purity Chitosan from Shrimp Shell Waste. Proc. of the Intl. Conf. on Advances in Applied Science and Environmental Engineering.
 8. Fawole, O. O., Ogundiran, M. A., Ayandiran, T. A., and Olagunju, O. F. (2007). Proximate and Mineral Composition in Some Selected Fresh Water Fishes in Nigeri. *Internet Journal of Food Safety*, Vol.9, 52-55.



ABSTRACT CCT-: 025

Muhammad A.U.¹, ¹C. Muhammad, ¹B.U. Bagudo, ¹M. Mukhtar, ²M. Musa and ³Y. Alhassan

¹Department of Pure and Applied Chemistry,

²Department of Physics, Usmanu Danfodiyo University, Sokoto.

³National Research Institute for Chemical Technology, Zaria.

Email: amumar898@gmail.com

ASSESSMENT AND OPTIMIZATION OF BIODIESEL PRODUCTION FROM NEEM SEED OIL USING SULFATED ZIRCONIA CATALYST

ABSTRACT: Response surface based on Box-Behnken design was used to investigate and optimize the reaction conditions for conversion of neem seed oil in to biodiesel with sulfated zirconia catalyst. The oil was extracted from the seed using n-hexane. Then the oil was transesterified using methanol and sulfated zirconia catalyst to biodiesel. The oil extracted and biodiesel produced were analyzed for physicochemical and fuel properties using ASTM methods. The fatty acid methyl ester was estimated using Gas Chromatography- Mass Spectrophotometry (GC-MS). The results obtained showed percentage oil yields of 40.64 ± 1.01 %. The optimum yield of 89% was obtained at the reaction temperature, reaction time, molar oil to methanol ratio and catalyst concentration, 600C, 1:12, 90 minutes and 1% wt. respectively. The model obtained has good predictive power; Methanol to oil molar ratio and reaction time followed by temperature were the major parameters that determine the response output (biodiesel yield). 11-octadecanoate methyl ester was dominant ester with 36.21% followed by methyl hexadecanoate 15.11%, methyl octadecanoate 11.42 % and methyl eicosanoate 0.82%. Some critical fuel parameters like iodine value, cetane number, kinematic viscosity, specific gravity and others determined are in conformity with ASTM D6751 requirement.

Keywords: Biodiesel, cetane number, Box-behnken design, transesterification.

1. Introduction

Energy is an essential driving factor to socioeconomic development in our present society. Its impact touches all aspect of human endeavours [1]. Petroleum based fuels are the major fuel sources used in transportation sector in most of the developing nations. Its combustion generates emissions which are nuisance to environment and adversely affect human health [2]. However, these non-renewable sources will be exhausted in near future. Recent assessments of remaining petroleum reserves show the world will soon face relentless oil supply crisis [3]. Subsequently, various alternative energy sources are under intense investigation. Among these, biofuels have been identified to be sustainable alternative with promising long term positive impact on the environment [4]. Biodiesel, in particular is recognized to be greener as well as alternative to fossil diesel due to its properties such as higher cetane number, lower smoke and particulates, and lower carbon dioxide and hydrocarbon emissions than fossil diesel. In addition, it is biodegradable and nontoxic [5, 6]

Heterogeneous solid acid catalyst has been used as an alternative to basic and enzyme catalysts since they can be used in both transesterification and esterification reaction [7]. Sulfated zirconia showed high activity and selectivity for esterification of fatty acids with alcohols [8]. Neem seeds are oil rich and have been shown to be viable source of oil for biodiesel production [9,] Thus, the aim of this study is to use response surface methodology base on Box-Behnken statistical design to study and optimize the process variable in biodiesel production using Sulfated zirconia catalyst.

2. Materials and methods

2.1. Chemical reagents

All the chemicals and reagents are analytical grade and used as procured without further purification.

2.2 Sample preparation and oil extraction

The neem seeds were obtained from Bodinga Local Government area of Sokoto state. The seeds were sorted out, dehulled, ground into powder and the oil was extracted using soxhlet extraction method n-hexane solvent.

2.3 Catalyst preparation

The solvent – free method of sulfated zirconia designated as S-ZrO₂ was prepared by Sun – et al. [10] ZrOCl₂. 8H₂O and (NH₄)₂SO₄ in a molar ratio of 1:6 were ground in an agate mortar for 20 min at room temperature, let the mixture for 18 h in open air, then the sample was calcined at 600°C for 5h.

2.4 Experimental design

Four independent variables namely reaction time, temperature, methanol to oil ratio and catalyst were selected. The experiment was designed (Response surface based on Box-Behnken) using MINITAB 17 statistical software and data was analyzed at 95 % confidence level.

2.5 Description of experimental runs

10 g of neem oil, methanol and catalyst were added as specified in the design matrix. The mixture was then refluxed at appropriate temperature (60, 62.5 or 65°C) for the specified period (60, 90, or 120 minutes). At the end, test



tube was allowed to cool and the mixture was centrifuge to remove the catalyst. The mixture was transferred in to separating funnel to separate under gravity overnight. The separated upper layer was placed into an evaporating dish and heated in water bath at 90 °C for 30 minutes, then neutralized with dilute phosphoric acid (pH 4.0). The methyl esters were then washed with hot distilled water (1:5 v/v) until the washed water had a pH of 7.0. The residual water was removed by drying the methyl esters over heated (100 °C) anhydrous sodium sulphate [23]. The percentage yield was calculated using equation 1.

$$\text{Yield (\%)} = \frac{\text{Weight of Biodiesel}}{\text{Weight of sample}} \times 100 \quad (1)$$

3. Results and discussion

Table 1. Fuel properties

Parameter	Unit	Biodiesel ASTM D6751	Values
Acid value	mgKOH/g	0.5 max	0.04 ± 0.33
Iodine value	gI ₂ /100g	130 max	36.54 ± 0.10
Kinematic viscosity	Cst	1.9 – 6.0	4.4 ± 0.00
High heating value	MJ/kg	-	48.12 ± 1.2
Flash point	°C	93 min	105

Kinematic viscosities of the produced biodiesel are within ASTM specification. Cetane number is fuel quality parameter that is related to the ignition delay time and combustion quality of a fuel, it measures the readiness of a diesel fuel to auto ignite when injected into the diesel engine [11]. Flash point is the lowest temperature at which a combustible mixture will be formed above the liquid fuel. However, higher than 55 °C reported for bottle gourd [12]. The profile of fatty acids methyl esters in neem biodiesel indicates methyl-11- octadecadienoate

3.1. Effect of process on the mean biodiesel yield

Figure 1 gives a summary of the biodiesel yield obtained for different levels of the four process variables investigated. The biodiesel yield varied from minimum of 59.54 % to maximum of 89 %. There is predominant increase in yield with increase in methanol to oil ratio. Notably, the yield increased with increase in reaction time from 60 min to 90 min, but then decreased when the reaction time was raised to 120 min. The biodiesel yield increases with increase in methanol to oil ratio and decreases with increase in temperature beyond the boiling point of methanol. Interestingly, the biodiesel yield increased with increase in both catalyst concentration and temperature when time and methanol to oil ratio are held constant at 90 minute and 9:1 respectively.

(linoleic acid ester) as the dominant ester. However, the presence of methyl hexadecanoate and methyl octadecanoate the second and third most abundant methyl esters in the produced biodiesel will enhance the stability of the diesel been them saturated compounds and less susceptible to peroxidation. Interestingly, the biodiesel produced may have higher stability due to absence of polyunsaturated esters with double and triple bonds that causes blockage in engine injection system [13].

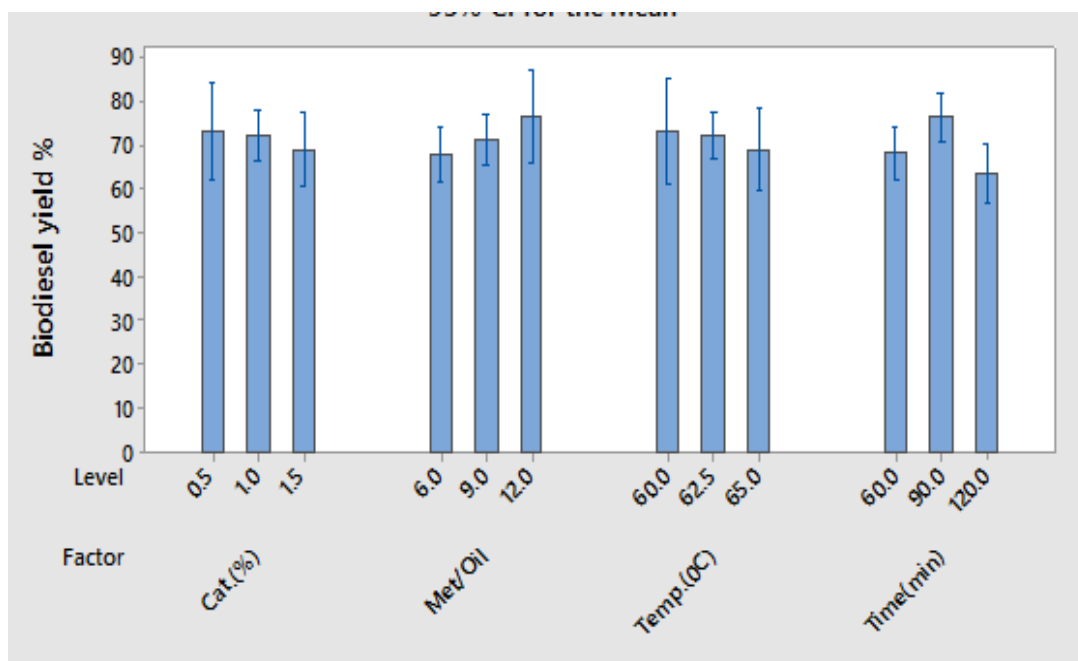


Fig. 1. Summary of the effect of the process variables on the biodiesel yield from neem seed oil.



4. Conclusion

Heterogeneous acid catalyst sulfated zirconia was successful in converting neem seed oil into biodiesel. The biodiesel yield decreases with increase in reaction temperature beyond the boiling point of the alcohol (methanol). The optimization of process variables shows that yield in excess of 85% can be obtained at 60 °C, 12:1, 0.5% and 90 minutes reaction temperature, methanol / oil ratio, catalyst concentration and reaction time respectively. The fuel parameters determined are in conformity with ASTM D6751 standard. However, evaluation of engine performance of the fuel is hereby recommended.

Reference

1. Sokoto A.M, Hassan, L. G. Salleh, M.A. Dangoggo, S.M. and Ahmad, H.G. (2013). Quality Assessment and Optimization of Biodiesel from *Lagenaria Vulgaris* Seeds Oil. *International Journal of Pure and Applied Science Technology*. **15**:55 – 65.
2. Mussatto S. I. (2016). A Closer Look at the Developments and Impact of Biofuels in Transport and Environment; What are the Next Steps? *Biofuel Research Journal*. **9**: 31-36.
3. Ogunsiyi H.O (2012). Acid and Base Catalyzed Transesterification of Mango (*Mangifera indica*) Seed Oil to Biodiesel. *IOSR Journal of Applied Chemistry*. **2**(2):18-22.
4. Muhammad A.B., Muyibat O., Hassan L.G., and Aliero, A.A (2016). Optimization of Process Variables In Acid Catalyzed In Situ Transesterification Of Hevea Bransillensis (Rubber Tree) Seed Oil Into Biodiesel. *Biofuels*. Available Online at <http://dx.doi.org/10.1080/17597269.2016.1242689>
5. Al-Zuhair S (2007). Production of biodiesel: properties and challenges. *Biofuels*. **1**:5-66.
6. Encinar J.M., Gonzalez, J.F., Rodriguez, R.A (2007). Ethanolysis of used frying oil: Biodiesel preparation and characterization. *Fuel process technology*. **88**:513-522.
7. Muhammad C., Alhassan, Y., Yargamiji, Bello, Z., and Ifeyinwa, A.I (2011). Composition and Characterization of Crude Glycerol from Biodiesel Production Using Neem Seed Oil. *Journal of Basic Applied Chemistry*, **1** (9):80-84
8. Diedhiou Djibril, Diatta, M.L., Faye, M., Vilarem, G, Sock, O., and Rigal, L. (2015). Biodiesel production from neem seeds (*Azadirachta indica* A. Juss) oil by its base-catalyzed Transesterification and its Blending with Diesel. *Research Journal of Chemical Sciences*, **5** (10): 13-19.
9. Muthu H., Sathyaselvabala, V., Varathachary, T., Kirupha Selvaraj, D., Nandagopal, J., and Subramanian, S. (2010). Synthesis of Biodiesel from Neem Oil by Two-Step Tranesterification. *Brazilian Journal of Chemical Engineering*. **27**(4), 601- 608.
10. Sun Y., Ma, S., Du, Y., Yang, J. (2005). Solvent – free preparation of nanosized sulfated zirconia with bronsted acidic sites from simple calcinations. *Journal of physical Chemistry*. **109**:2567-2572.
11. Muhammad A. B., Kabiru, B., Tambuwal, A.D nad Aliero A. A. (2015) Assessment And Optimization Of Conversion Of L. Siceraria Seed Oil Into Biodiesel Using Cao On Kaolin As Heterogeneous Catalyst. *International Journal of Chemical Technology* **7** (1): 1-11.
12. Hassan L.G., and Sani, N.A. (2010). Preliminary Studies on Biofuel Properties of Bottle Gourd (*Lagenaria Siceraria*) Seeds Oil. *Nigerian Journal of Renewable Energy*. **11**(12):20-25.
13. Sokoto A.M., Hassan, L.G., and Dangoggo, S.M (2011) Influence of Fatty Acid Methyl Ester on Fuel Properties of Biodiesel Produce from *Curcubita Popo*. *Nigerian Journal Basic and Applied Science*. **19**:81-86.

ABSTRACT CCT-: 028

Ajunwa I. *, C.O. Folayan, G.Y. Pam, A.A. Ibrahim

Department of Mechanical Engineering, Ahmadu Bello University, Zaria, Kaduna State, Nigeria

Email: unclezick@yahoo.com

INFLUENCE OF INCREASING SKIRT HEIGHT ON QUANTITY OF WOOD AND TIME CONSUMED FOR COOKING ON A WOOD STOVE

ABSTRACT: Since many globally depend on wood for their heating needs, the need of finding better ways of burning wood cannot be overemphasized. In this work a wood stove was tested without a skirt and with three different detachable skirts of varying heights to ascertain the influence of the skirts on the stove in terms of quantity of wood and time consumed for cooking. It was found that the stove tested without a skirt consumed the highest average quantity of wood and time. The wood and the time used for the water boiling test (WBT) kept reducing until the least quantity of wood and time was used when the tallest skirt, having same height as that of the pot used for the experiment. Invariably, stoves having skirts as tall as the tallest pot to be used on them have the best advantages of saving wood and time for cooking.

Keywords: detachable skirts, quantity of wood, water boiling test, wood stove.

1. Introduction

In the last few decades, the world at large and most especially the developing countries have experienced a total dependence on forest wood, which has caused hardship for especially women and children who have to move long distances in search of this wood. It was reported that more than three billion people globally depend on solid fuels including biomass fuels like wood, dung, agricultural residues and coal for their energy needs (WHO, 2005). Authors like Tietema (1991) and FAO (1997) have also asserted that there was no feasible alternative to wood as an energy source in some of the underdeveloped and developing countries in Africa and Asia.

When wood is harvested indiscriminately, there is need to develop means of burning this wood economically and efficiently. Baldwin (1987) reported that when cooking is carried out in the traditional open-fire, only 8% of the heat energy is absorbed by the water or food, 10% is lost by evaporation from the pot and 82% is lost to the surrounding. The improved cookstoves (ICSs) with skirts which avails the easiest and fastest response to this menace aim at increasing fuel combustion and heat transfer efficiencies thereby reducing the amount of wood and time used for cooking. Dale (2005) for instance determined the effect of skirt by using two pots. One skirted and the other unskirted. With the pot skirt present, he discovered that the heat transfer was 1465 W and without the skirt just about 1107 W of heat was transferred. Alex and Sadip (2009) conducted experiments both with and without the pot skirt. They reported an optimum increase in the thermal efficiency from 20.7% to 28.7% when the skirt was used.

This paper reports the influence of skirt height variations on wood stove in terms of quantity of wood and time consumed in cooking.

2. Materials and methods

2.1. Materials

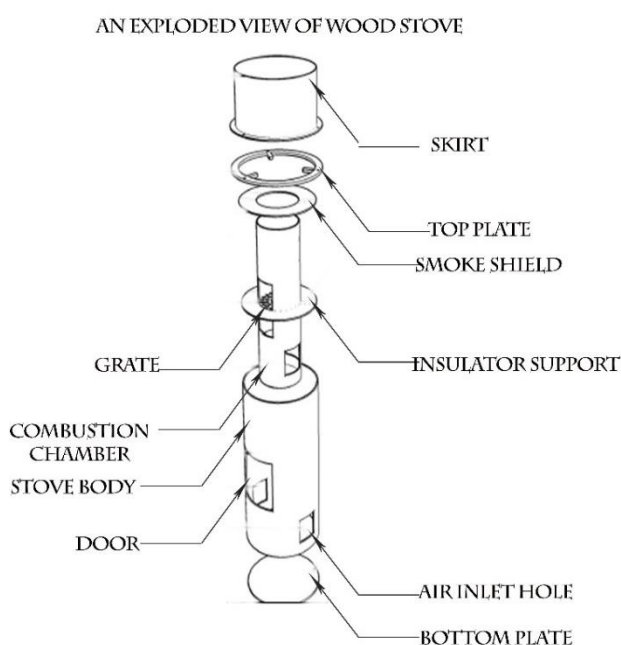


Fig. 1. An exploded diagram of the wood stove

2.2 Methods

2.2.1 Experimental Procedure

The Water boiling test (WBT) was employed in evaluating the performance of the stove. It consists of three phases: a high power (cold start) phase, a high power (hot start) phase, and a low power (simmer) phase. These three were carried out and their averages taken. High power (cold start) test: for this test, the stove was lit while cold, a pre-weighed bundle of wood was used to bring a measured amount of fresh pot of cold water to a pre-determined local boiling temperature.

High power (hot start) test: for this test, while the stove was still hot; again, a pre-weighed bundle of wood was used to bring a measured amount of fresh pot of cold water to boiling. Low power (simmering) test: this third phase followed immediately after the second phase. A weighed bundle of wood required to keep the measured amount of water that remained from the second phase of the test simmering



maintained at the boiling point for 45 minutes was recorded. In each case of the experiment, the mass (kg) of fuel before and after the experiment for each test, initial and final temperature (°C) of water, time (min) in starting and ending the experiment were noted and recorded.

3. Results and discussion

3.1. Results

The bar chart representations for the WBT for quantity of wood consumed.

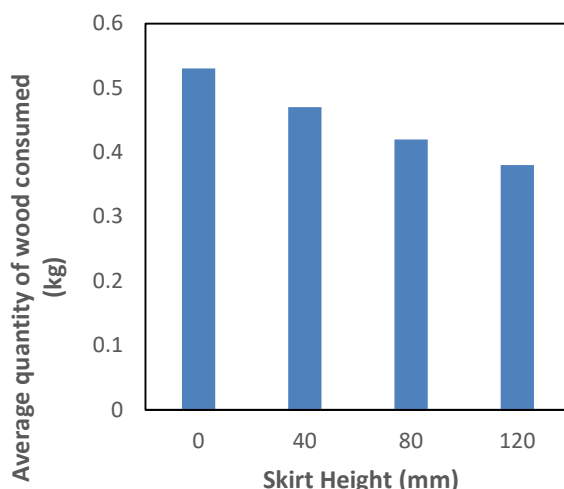


Fig. 2. Bar chart of average quantity of wood consumed (kg) for the WBT for the stove and skirts with increasing heights (mm)

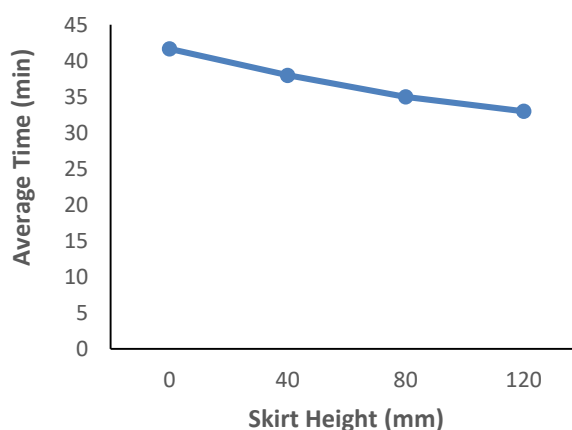


Fig. 3. Graph of the average time (min) taken for the WBT with increasing skirt height (mm)

1.2 Discussions

Fig. 2 shows the values (bars) of the quantity of wood consumed for the WBT, it can be seen that lesser quantity of wood was used for boiling the water as skirts were used on the stove. It also shows that as skirt heights were increased from 40 mm to 120 mm, there was a continuous decrease in the average quantity of wood used to boil the water.

Without skirts, an average quantity of 0.53 kg wood was consumed by the stove for the WBT. As the 40 mm skirt height was tested, 0.47 kg quantity of wood was used up on the average. The average quantity of wood used for the WBT kept reducing as the skirt heights were increased, and just an average of 0.38 kg was consumed when the tallest skirt of height 120 mm was tested.

These values gave a trend of bars (fig. 2) decreasing from top left to bottom right –

signifying that lesser quantity of woods were used up for the WBT as skirts were used on the stove and their heights increased subsequently. It can be seen from fig.3 that, it took the longest average time (41.67 mins) for the stove (without skirt) to complete the WBT than when skirts were used on it. When the skirt 40 mm height was used on the stove, the average time for the WBT reduced to 38.00 mins, a percentage decrease of about 8.807%. This time kept decreasing as skirts with height 80 mm and 120 mm were used on the stove with skirt 120 mm height having the least average boiling time (33 mins).

The graph for this trend of average boiling time in relation to skirt height slants downwards from the top left to the downright showing an inverse relationship between average boiling time and increasing skirt height as shown in fig.3, signifying that as skirt height increased, there was a decrease in time taken to boil the



water.

Generally, there was a reduction in quantity of wood and time used in boiling the water when skirts were used because the heat from the flue gases that are normally expelled to the surrounding when skirts are not used are now availed an avenue to continuously rob on the sides of the pot for a longer time when skirts were used. As the skirts get taller, it signifies that more of this avenue is made available for the flue gases and the sides of the pot for a continuous interaction for a longer time – hence more heat transferred to the pot. With more heat transferred to the pot, boiling will be achieved in a shorter time and hence lesser wood will be burnt.

2. Conclusions

At the end of this work, it was found that there was a general decrease in the quantity of wood and time

used for cooking as skirts were tested on the stove – these advantages were both maximized with the tallest skirt which had the same height as that of the pot used for the experiment.

References

1. WHO (2005), *Indoor air pollution and health: World Health Organization (WHO), Geneva.*
2. Tietema T., Dithlodo M. and Tibone C (1991). Characteristics of eight firewood species of Botswana. *Biomass and Bioenergy 1*, 1991, 41-46.
3. FAO (1997). *Forest Products Outlook: United Nations Food and Agricultural Organization (FAO).*
4. Baldwin S.F. (1987). *Biomass stoves: Engineering design, development, and dissemination* (VITA 1600 Wilson Boulevard, Suite 500 Arlington, Virginia 22209 USA).
5. Dale A. (2005). Report on some heat transfer experiments: presented at the 2005 *ETHOS Conference*, Seattle, Washington.
6. Alex W. and M. Sandip M. (2009). Computational heat transfer analysis of the effect of skirts on the performance of third-world cookstoves.



ABSTRACT CCT-: 029

Suleiman Iguda Ladan

Department of Basic and Applied Sciences, College of Science and Technology
Hassan Usman Katsina Polytechnic, Katsina.

Email: suleimaniguda@yahoo.com

THE CHALLENGES AND PROSPECTS OF USING BIOMASS ENERGY IN NIGERIA

Biomass energy is the first ever energy used by mankind and is also the fuel which is the main stay of the global economy till the middle of the 18th Century when fossil fuel took over. Fossil fuel took over as they are not only denser in their energy content but also generated less pollution when burnt in comparison to biomass (Abbasi and Abbasi, 2010). Recently there is an increased interest in biomass energy as it is perceived as carbon neutral source of energy unlike net carbon-emitting fossil fuels of which copious use has led to global warming and ocean acidification (Abbasi and Abbasi, 2010).

Biomass is organic matter that can be burnt or decomposed to be used as source of energy. In a way biomass energy can be considered a form of solar energy since it receives its original energy from the sun through the process of photosynthesis. This solar energy is stored in plants and is available for conversion into usable forms for human use. These include burning wood, collecting methane from biogas and using energy crops for bio fuels (Newcomb, 2011).

According to Sambo (2009), biomass refers to energy sources from plant origin such as trees, grasses, agricultural crops and their derivatives as well as animal wastes. As energy form biomass may be used as solid fuel or converted via a variety of technologies to liquid or gaseous forms for the generation of electric power, heat or fuel for motive power. Biomass resources are considered renewable as they are naturally occurring and when properly managed may be harvested without significant depletion (Sambo, 2009). Since biomass is

renewable energy source its importance will increase as international energy policies and strategies focuses more heavily on renewable resources and conservation. Biomass is considered the renewable energy source with the highest potential to contribute to energy needs of modern society for both the industrialized and developing countries worldwide (Demirbas *et al*,2009). Biomass is the most important source of energy in many developing countries, most notably in sub-Saharan Africa. Although the bulk of biomass consumption is traditional burning of firewood for electricity, heating and other forms of energy, there is growing discussion of the potential to build up modern biomass energy industries in developing countries, for example, bio fuel and biogas industries (GES, 2017).

In recent years there is a resurgence of interest in the use of biomass energy due to its advantages over fossil fuels and as such its use is being utilized in the country. The aim of the paper is to examine the challenges and prospects of using of biomass energy with a view to promote its sustainable utilization. Both the traditional use of biomass and use of biomass as modern source of fuel are considered in the paper. In Nigeria, the biomass resources available include Fuelwood, agricultural wastes and crop residues, saw dust and wood shavings, animal dung/poultry droppings and municipal solid wastes. The estimated biomass energy resource potential of Nigeria can be seen on the table 1 below.

Table 1. Biomass Energy Resource Potentials of Nigeria

S/N	Biomass Resource	Quantities (million tonnes)	Energy value ('000MJ)	Resource potentials
1.	Fuel wood	39.1	531.0	43.4 million tones/year fuel wood consumption
2.	Agricultural residues	11.244	14.77	91.4 million tones/year produced
3.	Saw dust	1.8	31.433	5.2 million tones/year produced
4.	Municipal solid waste	4.075	-	30 million tones/year from 18.5 tonnes in 2015

Source: Sambo (2009), 2012) and Oluoti *et al* (2014).

From table 1 it could be seen that Nigeria has large potentials of biomass energy resources in terms of quantity and energy value. Also from the table 1, it could be observed that the energy value for municipal solid waste is not given from the source of the table which is Sambo

(2009). However, there are studies on electricity generation potential of municipal solid wastes in selected cities such as that of Daura (2016), which have shown that large amount of electricity can be generated by incineration. This clearly indicated that there is



large energy value that can be generated from the other urban centres within the country. There are several ways of utilizing biomass energy in Nigeria. Fuel-wood constitute the major source of cooking fuel in both rural and urban centres. Municipal solid waste is utilized as source of energy in form of fuels, mostly in

Lagos State. Bio-fuel production facilities are found in Ekiti, Kwara, Osun, Oyo, Kogi, Kano, Kaduna and Zamfara States. There are also sugar cane based bio-fuel plants in Adamawa State. ENPOST farm bio-gas plant is found in Ilesa, Osun State (Nwofe, 2014).

Table 2. Biomass Energy Projects in Nigeria

S/N	Biomass Resource	Location of energy project	Energy project
1	Municipal solid waste	Epe, Lagos state	Epe integrated solid waste management project.
2	Municipal solid waste	Olushasun, Lagos, Lagos State	Landfall site gas to energy project.
3	Energy crops	Ilemeso, EKiti State	Bio-fuel production complex by Global Fuels Limited
4	Energy crops (sugar cane)	Girei and Demsa local government area Adamawa State	Sugarcane based bio-fuel plants by renewable energy plant office, Adamawa State
5.	Municipal solid waste	Ikorodu, Lagos, Lagos State	Compost plant for treatment of market waste
6.	Municipal solid waste	Ikosi market, Lagos, Lagos State	Waste-to-energy plant at Ikosi market.
7.	Municipal solid waste	Ilesa town, Osun state	ENPOST biogas plant at ENPOST farm

Source: Nwofe, (2014)

In the attempt to use biomass energy in Nigeria, there are challenges that have to be considered which include:

- The rapidly growing population in the country creates increasing demand for firewood and charcoal from a diminishing supply that results to the degradation of hectares of forests and other forms of vegetation (Ladan and Mashi, 2012).
- The smoke that is generated from the burning of wood fires is a major source of air quality degradation and health risks. Many women who use firewood as fuel for cooking are exposed to smoke which poses health risk that can lead to respiratory illnesses. (Cunningham and Cunningham, 2004).
- The crops that are used as energy crops which are sugar cane and maize are predominantly food crops. Therefore, using them for energy production leads to competition with food production especially at a time now that there is the need to grow more food to feed the population and bring down rising food prices.
- There is lack of equipment and infrastructure for storing of biogas for cooking purposes and its conversion to electricity for the use of the populace particularly in rural areas where there is the need for a source of energy for cooking to reduce the use of fuel wood (Nwofe, 2014).
- Reforestation projects, agro-forestry, community woodlots and inexpensive, efficient locally produced cook stoves could help alleviate the expected shortages of fuel wood shortages that could be experienced due to promoting the use of biomass energy.
- The use of biogas as an alternative source of energy is gaining importance as it is renewable, free from carbon dioxide (CO₂) emission and is abundantly available in form of agricultural residues, cattle dung and municipal solid wastes. This is important as many Nigerians face daily struggle to find enough fuel to cook their food.
- Biomass resources, giving the right conditions can easily regenerate and will provide the needed crops for energy production without negatively impacting food resources. This is so because with careful planning a delicate balance can be reached through careful analysis before any major biomass energy operation is initiated (Newcomb, 2011).
- There are various Biomass energy researches that are ongoing in different parts of the country particularly as it relates to biogas and bio-fuels. For example, Biogas research activities are ongoing at Renewable Energy Research Centres at Sokoto and Nsukka and also in many tertiary institutions in the country. There are also some private companies such as Global Fuels Limited that engage in bio-

Despite these challenges, there are prospects for the use of biomass energy in Nigeria which include:



fuel production in several States across the federation.

There are several research and development activities that are carried out by these research centers, tertiary institutions and private

companies that will lead to the development and also promote the use of biomass energy in Nigeria in future. These Biomass energy production targets and timelines can be seen on the table 3 below.

Table 3. Biomass Energy Production Targets and Timelines in Nigeria

S/No	Type of Biomass Energy	Timeline/Quantity		
		Short (2015)	Medium (2020)	Long (2030)
1	Biomass Electricity (MW)	5	30	100
2	Improved Cook stove (No.)	300,000	500,000	1,000,000
3	Biogas Digesters (No.)	500	6,000	8,000
4	Biomass Briquetting Machine (No)	30	50	80
5	Bio-fuel (ML/day) * Bio ethane (B10)	1951	3559	8837
-	Biodiesel (B20)	730	1254	4270

Based on 13% GDP Growth rate supply projections of PMS and AGO. Source: Energy Commission of Nigeria (2012).

The utilisation of biomass energy is a viable option to the energy challenges of most developing countries with large amount of natural resources like Nigeria (Nwofe,2017). In attempting to promote the use of biomass energy there are certain challenges that should be overcome as there are bright prospects for the use of biomass energy in Nigeria.

References

- Abbasi, T. and Abbasi, S. A. (2010)-Biomass Energy and The Environmental Impacts Associated with its Utilization *Renewable and Sustainable Energy Reviews* 14 (3) DOI:<http://doi.org/10.1016/j.rser.2009.11.006>.
- Cunningham, W. P. and Cunningham, M. A. (2004)-*Principles of Environmental Science: Inquiry and Applications* McGraw Hill Higher Education Boston USA P.291
- Daura, L. A. (2016)-Electricity Development Potential of Municipal Solid Wastes in Kano Metropolis. *Journal of Scientific and Engineering Research* 3 (4):157-161.
- Demirbas, M. F., Balat, M. And Balat, H. (2009) - Potential Contribution of Biomass to the Sustainable Energy Development *Energy Conservation and Management* 50 (7):1746-1760 DOI:<https://doi.org/10.1016/i.enconman.200.03.013>.
- Global Energy Symposium (GES) (2017)-Bio-energy and Land Use in Developing Countries: The Challenge. Available at <http://www.global-economic-symposium.org/knowledgebase/the-global-environment/bioenergy>.
- Ladan, S. I. and Mashi, B. H. (2012)-Towards Effective Utilization of Renewable Energy Sources for Sustainable Development in Nigeria. A Paper presented at an International Conference on Renewable Energy organized by PTDF and UMY University Katsina.
- Newcomb, P. (2011)-What is Biomass Energy and How Does it Work? <https://www.poweredbymothernature.com/what-is-biomass-energy/>
- Nwofe, P .A. (2014)-Utilization of Solar and Biomass Energy-A Panacea To Energy Sustainability in a Developing Economy. *International Journal of Energy and Environmental Research* 2 (3) :10-19
- Sambo, A. S. (2009)-Strategic Development in Renewable Energy in Nigeria. International Association for Energy Economics. www.researchgate.net/publication/237284856-strategic
- Sambo, A. S. (2012). Policy and Plans on Renewable Energy in Nigeria. Keynote presentation, Proceedings of PTDF-UMYU International Conference on Renewable Energy, Katsina.
- Oluoti, K., Petterson, A. And Richards, T. (2014)-Nigerian Wood Waste: A Dependable and Renewable Fuel Option for Power Production. *World Journal of Engineering and Technology*.2, 234-248.



ABSTRACT CCT-: 038

Yusuf O. Usman^{1*}, K. I. Omoniyi², Olanipekun O. Idowu¹, Gero Mohammed¹, Peculiar Okoro¹

¹Basic Research Department, National Research Institute for Chemical Technology, Zaria.

²Department of Chemistry, Ahmadu Bello University Zaria, Kaduna State

Email: yusufusman1250@yahoo.com

AN ASSESSMENT OF THE POTASH BIOCATALYST POTENTIAL OF PLANTAIN PEEL RESIDUES FOR REDUCING SUGAR PRODUCTION FROM PHOENIX DACTYLIFERA SEED PIT

ABSTRACT: Chemical pretreatment of lignocellulosic biomass has been extensively investigated for sugar generation and subsequent fuel production. Alkaline pretreatment has emerged as one of the popular chemical pretreatment methods, but most attempts thus far have utilized inorganic KOH for the pretreatment process. This study aimed at investigating the potential of Bioalkali extracted from plantain peel ash as a viable alternative alkaline reagent for lignocellulosic pretreatment of *Phoenix dactylifera* compared to synthetic KOH. The combusted plantain peel ash was characterized using x-ray fluorescence spectroscopy with K₂O as the dominant oxide (54.2 wt %), the concentrations of the potash alkali (KOH) extracted were quantified titrimetrically using HCL. *Phoenix dactylifera* seed pit was pretreated using Taguchi orthogonal array to design the experiment of chemical hydrolysis. The factors of KOH/bioalkali (BioKOH) concentrations (0.022–1.950 %), Solid to liquid ratio (1:30–1:90 w/v) for varying treatment times (15–60 min) at 121 °C affecting reducing sugar production were optimized for the hydrolysis. The pretreatment condition of 0.157 % Bioalkali (BioKOH), 30 min, 1:30 w/v was determined to be the most effective as it utilized the least amount of Bioalkali (BioKOH) while generating 21.95 mg sugar/g substrate, at the same pretreatment condition, 29.35mg sugar/g was generated using inorganic KOH.

Keywords: *Phoenix dactylifera* (Date palm seed pit), Lignocelluloses, KOH, Bioalkali (BioKOH), Plantain peel, Reducing sugars

1. Introduction

Lignocellulosic biomass is a complex substrate that typically contains 50–80 % [dry basis (db)] carbohydrates that are polymers of 5C and 6C sugar units. The two polysaccharides in lignocelluloses, cellulose (~45 % db) and hemicellulose (~25 % db), are bound together by lignin (~25 % db), which is a complex three-dimensional polyaromatic matrix. Lignin is partly covalently associated with hemicellulose, thus preventing hydrolytic enzymes and acids from accessing some regions of the holocellulose to release the sugar units (Hamelinck et al., 2005).

Date pits have a hard seed coat that makes the seed components difficult to digest. It is necessary to process the seeds before feeding them to livestock. Alkali treatments increase the digestibility of fibrous materials. Application of a 9.6% NaOH solution to ground date pits decreased neutral detergent fibre (NDF) content and increased in vitro digestion rates. This treatment was more effective on finely ground date pits (4 mm vs. 8 mm) (Al-Yousef et al., 1986). (Briones et al., 2012) reported that the lignocellulosic components of date palm seed pit are: cellulose 20%, hemicellulose 55%, lignin 23% and ash 1.1%.

Partial degradation of cellulose and hemicellulose is possible during alkali pretreatment. A large number of reactions may take place at elevated temperature in the alkali conditions. The most important reactions are (Fengel et al., 1984; Pérez et al., 2010): dissolution of non-degraded polysaccharides; formation of alkali-stable end-groups referred to as peeling reactions of end groups (peeling-off); hydrolysis of glycosidic bonds and acetyl groups; decomposition of dissolved

polysaccharides.

Bio-alkali is the alkali derived from the ashes of burnt biomaterials. Agricultural materials contain a good percentage of mineral salts. When these materials are burnt in air, carbohydrates, fats, proteins and vitamins will all burn away. The resulting ashes contain oxides of these minerals. Some of these are basic oxides of potassium and sodium, which when dissolved in water yield their corresponding hydroxides (alkali). Research has shown that plantain peel ash has been used to produce soap (Yahaya et al., 2012), and lubricating grease of good quality. Hence, it is believed that alkali produced from the ash can equally be a good solvent for hydrolysis of biomass.

The aim of this work was to determine the optimum conditions for reducing sugar production from date palm seed pit (DPSP) by synthetic KOH compared with Bioalkali (BioKOH) hydrolysis. In this experiment, three factors were optimized namely KOH/BioKOH concentration, solid to liquid ratio and reaction time. Response Surface Methodology (RSM) using Taguchi L9 orthogonal array Design was applied for optimizing these independent variables.

2. Materials and methods

Extraction of BioKOH: Exactly 5 kg of plantain peels were collected from eateries in Kaduna, washed and dried by placing them in an oven at 60° C until dry enough to break with the hand. The dried peels were burnt inside the combustion pan with industrial gas burner and ash of 0.47 kg was obtained, sieved through 0.8mm sieve and then assayed using XRF, AAS/flame photometer. Exactly 0.06kg of the ashes was boiled in 1 dm³ of deionised



water for one hour at 100°C using a hot plate. The ashes were allowed to cool down, packed into a 2- liter beaker. The slurry was kept for 12 hours before draining of extract. After draining, the first extract was kept in a separate sealed container and equal volume of cold deionised water was poured into the slurry for further extraction. This was repeated the third time, and extracts kept in different glass containers. The specific gravity, pH and conductivity of the alkali was measured (Onyegbado et al., 2002; Onyekwere, 1996). The filtrate/extract which contains hydroxide of the mineral elements were then quantified titrimetrically using HCl (Uyigue et al., 2013).

Experimental design. RSM was used to find the optimum conditions for pretreatment of date palm seed pit. Taguchi L9 design with three independent variables: (a) reaction time; (b) solid to liquid ratio and (c) concentration of KOH/BioKOH was applied to maximize reducing sugar yield from lignocellulose of date palm seed pit. The experimental design created by Minitab 16 software resulted in nine experimental trials.

Mechanical treatment of date palm seed pit. Air-dried date palm seed pit was washed air dried and milled using Christy and Morris Laboratory mill, Chelmsford England, sieved through a diameter sieve of 0.8 mm, and was stored in sealed plastic bottle at room temperature. Alkali/BioAlkali pretreatment of date palm seed pit (DPSP).

One gram of milled DPSP was soaked with 30, 60 and 90 grams of 0.022, 0.157 and 1.950% (w/w) bio-alkali/KOH solution in the 250 ml Erlenmeyer flask and then autoclaved at 121°C for 15,30 and 60 minutes. After hydrolysis, the suspended material was separated using filter paper (Sharma et al., 2013; Sukri et al., 2014; Thanapimmetha et al., 2011). The total reducing sugars in the filtrate were determined by the 3,5-dinitrosalicylic acid (DNS) method described by Miller in 1959 (Miller, 1959).

3. Results and discussion

The actual concentration of the potash (i.e. KOH) in the plantain peel ash extract were measured using the titration method, wherein 0.1 M HCl was titrated against a diluted solution of potash alkali. The endpoint volumes of HCl in the titrations were 87.07,

7.03 and 0.97 cm³ for the first, second and third extract respectively given rise to potash-alkali concentrations as 19.5 g/dm³, 1.57g/dm³ and 0.22 g/dm³ respectively (Table 2). For low potash-alkali concentrations of these values, high yield of reducing sugar is possible as corroborated by the work of (Sharma et al., 2013).

This is more evident in table 1 showing XRF results of the various oxides contained in plantain peel ash. Amongst other impurities, the oxide of potassium has the highest percentage of 54 wt% hence a viable source of potash biocatalyst for DPSP hydrolysis.

Table 1. X-ray Fluorescence spectroscopy Analysis of burnt Plantain Peel Ash

Element	Concentration
Na ₂ O	0.0000 Wt %
MgO	4.8035 Wt %
Al ₂ O ₃	2.7684 Wt %
SiO ₂	11.5773Wt %
P ₂ O ₅	10.4901Wt %
SO ₃	3.2959 Wt %
Cl	5.0814 Wt %
K ₂ O	54.1881Wt %
CaO	6.9613 Wt %
TiO ₂	0.0726 Wt %
Cr ₂ O ₃	0.0000 Wt %
Mn ₂ O ₃	0.1689 Wt %
Fe ₂ O ₃	0.4582 Wt %
ZnO	0.0874 Wt %
SrO	0.0468 Wt %

Table 3. Infrared spectra analysis of DPSP Hydrolysate.

Sample	C-O	CH ₃ C-H	C=O	O-H
	m-s	M	m-s	s-broad
DPSP	1080.17	1388.79	1643.41	3387.11

M- medium, S - strong,

IR Spectra: As shown in table 3, It is evident from the spectra of DPSP hydrolysate that reducing sugar was synthesized with bands at 3387, 1643, 1388 and 1080 cm⁻¹ which indicates the presence of OH stretching vibration in OH functional groups, C=O stretching was also pronounced which serves as reducing sugar active site, CH₂ bending vibration in alkanes, C-O stretching representing pyranose ring skeletal vibration in ethers,



Table 2: Physicochemical parameters of bioalkali and inorganic alkali.

Parameters	Bioalkali			synthetic alkali		
	1 st Extract	2 nd Extract	3 rd Extract	1.950%	0.157%	0.022%
pH	12.0	11.2	10.2	13.0	12.2	11.3
Specific gravity	1.050	1.010	0.900	1.02	1.000	0.900
Cond. (mS/cm)	11.13	7.65	1.13	11.17	5.67	0.93
KOH (g/L)	19.50	1.57	0.216			
KOH(%)	1.950	0.157	0.022	1.950	0.157	0.022

Optimisation of reducing sugar production by alkali and bioalkali hydrolysis: In the present study, Taguchi L9 orthogonal array design was used to investigate the optimal conditions of the reducing sugar production from pretreated DPSP. There were three factors namely concentration of KOH/BioKOH, solid to liquid ratio and reaction time and three levels of each parameter were varied as shown in Table 4. The nine experiments were designed as shown in Table 4 and the maximum reducing sugar is 21.95 and 29.35 mg sugar/g substrate using Bioalkali (BioKOH) and synthetic KOH

respectively as observed at the experimental run number 4. The probability value (p-value) is a tool for evaluating the significance and contribution of each parameter to the production of sugar. For a one tail t-test, ($p = 0.05$). Since experimental value (0.16684763) is larger than the p value, it shows that there is no significant difference between Bio-KOH and KOH Hydrolysis of Date Palm Seed Pit (DPSP). The statistical software MINITAB release 16 was used to design the experiments and to investigate the effects of the assigned parameters on the reducing sugar production.

Table 4. Design of Experiment for Date Palm Seed Pit Using Bio alkali and KOH Hydrolysis

Run Number	Factor settings			Red. Sugar Yield (mg/g)	
	Concentration (%)	Solid : Liquid Ratio (w/w)	Reaction Time (min)	Bio KOH	KOH
1	1.950	30	15	11.25	11.68
2	1.950	60	30	9.28	8.83
3	1.950	90	60	12.36	12.90
4	0.157	30	30	21.95	29.35
5	0.157	60	60	11.95	21.09
6	0.157	90	15	10.59	14.46
7	0.022	30	60	22.56	25.41
8	0.022	60	15	16.34	17.02
9	0.022	90	30	16.09	16.36

4. Conclusions

The optimal conditions obtained through a statistical Taguchi L9 Design are successfully determined to maximize the reducing sugar production from synthetic KOH and BioKOH hydrolysis. The result indicated that the optimal conditions for reducing sugar production from pretreated date palm seed pit by synthetic KOH and BioKOH hydrolysis are 0.157 % (v/v) of KOH and BioKOH, solid to liquid ratio of 1:30 and reaction time of 30 minutes which give the maximum reducing sugar of 21.95 and 29.33 mg sugar/g substrate for BioKOH and synthetic KOH respectively. A one tailed t-test analysis at $p=0.05$ shows that there is no significant difference in the optimized hydrolysis of DPSP using BioKOH and synthetic KOH hence the overall benefit of this study is that the knowledge gap of appropriate stoichiometry for pretreatment of DPSP from alkali synthesized from ashes of plantain peel prior to release of sugar has been provided, and dumping of plantain peels in heaps in farms which is

considered adverse to soil fertility will stop.

Reference

1. Al-Yousef, Y., Belyea, R., & Vandepopuliere, J. (1986). Sodium hydroxide treatment of date pits. Paper presented at the Proceedings of the Second Symposium on the Date Palm in Saudi Arabia.
2. Briones, R., Serrano, L., & Labidi, J. (2012). Valorization of some lignocellulosic agro-industrial residues to obtain biopolyols. *Journal of chemical Technology and Biotechnology*, 87(2), 244-249.
3. Fengel, D., & Wegener, G. (1984). Wood: chemistry, ultrastructure, reactions. *Walter de Gruyter*, 613, 1960-1982.
4. Hamelinck, C. N., Van Hooijdonk, G., & Faaij, A. P. (2005). Ethanol from lignocellulosic biomass: techno-economic performance in short-, middle-and long-term. *biomass and bioenergy*, 28(4), 384-410.



5. Miller, G. L. (1959). Use of dinitrosalicylic acid reagent for determination of reducing sugar. *Analytical chemistry*, 31(3), 426-428.
6. Onyegbado, C., Iyagba, E., & Offor, O. (2002). Solid soap production using plantain peel ash as source of alkali. *Journal of Applied Sciences and Environmental Management*, 6(1), 73-77.
7. Onyekwere, C. (1996). *Cassava peels ash: An alternative source of alkali in soap production*. B. Eng. Thesis Department of Chemical Engineering, University of Port Harcourt.
8. Pérez, S., & Samain, D. (2010). Structure and engineering of celluloses. *Advances in carbohydrate chemistry and biochemistry*, 64, 25-116.
9. Sharma, R., Palled, V., Sharma-Shivappa, R. R., & Osborne, J. (2013). Potential of potassium hydroxide pretreatment of switchgrass for fermentable sugar production. *Applied Biochemistry and Biotechnology*, 169(3), 761-772.
10. Sukri, S. S. M., Rahman, R. A., Illias, R. M., & Yaakob, H. (2014). Optimization of alkaline pretreatment conditions of oil palm fronds in improving the lignocelluloses contents for reducing sugar production. *Rom Biotechnol Lett*, 19, 9006-9018.
11. Thanapimmetha, A., Vuttibunchon, K., Saisriyoot, M., & Srinophakun, P. (2011). *Chemical and microbial hydrolysis of sweet sorghum bagasse for ethanol production*. Paper presented at the World Renewable Energy Congress - Sweden; 8-13 May; 2011; Linköping; Sweden.
12. Uyigüe, L., Viele, E., & Chukwuma, F. (2013). A Preliminary Assessment of the Potash Biocatalyst Potential of Empty-Oil-Palm-Bunch (EOPB) Residues for Biodiesel Production. *Journal of Emerging Trends in Engineering and Applied Sciences (JETEAS)*, 4(3), 446-450.
13. Yahaya, L., Hamzat, R., Aroyeun, S., & Odufuwa, M. (2012). Production of Liquid detergent from the pods of Kola (*Cola nitida*). *Moor Journal of Agricultural Research*.

**ABSTRACT CCT-: 044**

Musa S. H.^{1*}, E. A. Adegbe¹, U. M. Shittu¹, A. Y. Atta¹, S. Usman¹, A. H. Idowu¹, A. Ade-Ajayi¹ and Y. Z. Safiya²

¹National Research Institute for Chemical Technology, P. M. B. 1052 Basawa – Zaria.

²Nuhu Bamalli Polytechnic, Zaria Kaduna State, Nigeria

Email: shmy2k4@gmail.com

EXTRACTION AND SOME CHARACTERISTICS OF TAMARIND SEED STARCH AS A BIOPOLYMER

ABSTRACT: In the recent years, starch have raised great interest since sustainable development policies tend to expand with the decreasing reserve of fossil fuel and the growing concern for the environment. Starch made from tamarind seeds is considered to be the cheapest non-edible starch with many industrial applications. Tamarind fruits are used for edible purposes and seeds are wasted. Characterization of this starch such as the proximate analysis results in substantial value addition for its biodegradability and many industrial applications. Some examples have been presented to elucidate that tamarind seed starch are promising materials for various applications and their development is a good solution for reducing the consumption of petroleum resources based materials and environmental problem.

Keywords: tamarind seeds, starch, biodegradability, proximate.

1. Introduction

The tamarind tree (*Tamarindus indica* L.) belonging to family Caesalpiniaceae is found in both tropical and subtropical regions of the world [Shlini Purushothaman, Siddalinga Murthy K R, 2011]. Tamarind fruits are used for edible purposes and seeds are generally thrown away. These seeds could be used for producing starch which is used for sizing in textile industry and as a general adhesive material. Starch is the most abundant carbohydrate reserve in plants and is found in leaves, flowers, fruits, seeds, different types of stems and roots. Starch is used by plants as source of carbon and energy [Smith, 2001]. Among the natural polymers, starch is of interest. It is regenerated from carbon dioxide and water by photosynthesis in plants [Ephraim Nuwamanya *et al.*, 2010]. Owing to its complete biodegradability, low cost and renewability, starch is considered as a promising candidate for developing sustainable materials. In view of this, starch has been receiving growing attention since 1970s [Isabelle Vroman and Lan Tighzert, 2009].

Many efforts have been exerted to develop starch-based polymers for conserving the petrochemical resources, reducing environmental impact and searching more applications [P. A. Pawar *et al.*, 2008]. Starch is considered a promising candidate for developing sustainable materials. In view of this, starch has been receiving growing attention since the 1970s.

Many efforts have been exerted to develop starch-based polymers for conserving the petrochemical resources and reducing environmental impacts.

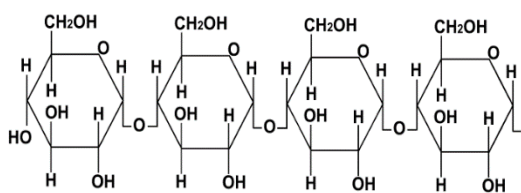
Starch is an important naturally occurring polymer of glucose, with diverse applications in food and polymer science, found in roots, rhizomes, seeds, stems, tubers and corms of plants, as microscopic granules having characteristic shapes and sizes [Kaur *et al.*, 2006]. Each starch typically contains several million amylopectin molecules accompanied by a much larger number of smaller amylose molecules. Starch made from tamarind seeds is non-edible. These seeds are generally thrown away and hence their use results in substantial value-addition. This is one of the cheapest available non-edible starch [Phani Kumar G.K, Gangarao battu, Kotha N.S. Lova Raju.]. A crude extract of tamarind seed is rich in polysaccharides ranges from 60 – 80%

which contains glucose, xylose and galactose [Kumar *et al.*, 2008].

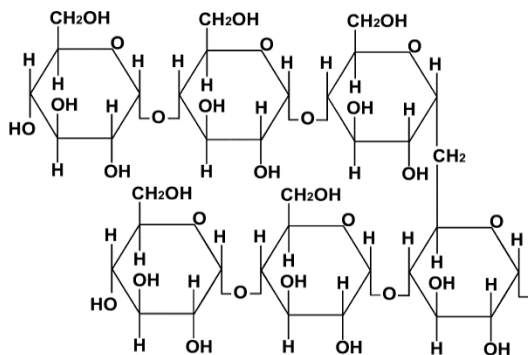
Starch structure

Starch is mainly composed of α -D-glucopyranose polymers bound by α – 1, 4 and α 1, 6 – glycoside links. These links are formed between the first carbon (C₁) of one molecule and fourth (C₄) or the sixth (C₆) of the second one [Cameron *et al.*, 2007]. As the aldehyde group on one end of a starch polymer is always free, these starch polymers always possess at least one reducing tip. The other end of the polymer is an irreducing tips. Depending on the degree of polymer branching occurring in a starch molecule, there may be great number of irreducing tips. The formation of α – links in a starch molecule enable some parts of starch polymers to generate helix structures; this is determined by the orientation of hydroxyl (-OH) groups on the first carbon atom (C₁) and the pyranose ring. Studies on the starch's chemical properties and structure have established that it is composed of two components, both also polysaccharides: amylose (20 – 30%) and amylopectin. The ratio of these compounds varies subject to the source or origin. [Marcin *et al.*, 2009]. Amylose is a linear portion of starch it is a polymer of glucopyranosyl monomers linked to each other by α (1 – 4) linkages. Amylopectin has some backbone as amylose, but it is a branched polymer of α (1 – 6) monomer linkages [Cura *et. al.*, 1990]. The molecular weights of amylose and amylopectin have been estimated to be about 10⁵ and 10⁸ Da respectively. [Mahsa *et al.*, 2002]. Both amylose and amylopectin consist of glucopyranose molecules, yet the structural differences between these two polymers determine their different properties [Marcin *et al.*, 2009].

Depending on the botanical origin of the plant, starch granules can have different shapes (sphere, platelet, polygon...) and size (from 0.5 to 175 μ m). These granules are composed of two α -D-glucopyranose homopolymers, the amylose and the amylopectin. Their proportions in the granules depend directly on the botanical source. In addition, starch also contains, in much smaller proportions, other compounds such as proteins, lipids and minerals.



Amylose



Amylopectin

2. Methodology

The seeds of *Tamarindus indica* were washed thoroughly with water to remove the adhering materials. Then, the reddish testa of the seeds was removed by heating seeds in sand in the ratio of 1:4 (Seed: Sand). The testa was removed. The seeds were crushed lightly. The crushed seeds of *Tamarindus indica* were soaked in water separately for 24 h and then boiled for 1 h and kept aside for 2 h for the release of mucilage into water. The soaked seeds were taken and squeezed in a muslin bag to remove marc from the filtrate. Then, equal quantity of acetone was added to precipitate the mucilage. The mucilage was separated. The separated mucilage was dried at temperature 50°C, powdered and passed through sieve number 80. The dried mucilage was powdered and stored in airtight container at room temperature [Phani Kumar G.K *et al.*, 2011].

2.2 Proximate analysis

The proximate analyses were carried out using AOAC 1984 methods and are shown in Table 1.

Table 1. Proximate analyses of Tamarind Seed Starch

Proximate composition	Percentage composition (%)
Moisture content	10.800
Ash content	0.080
Lipid	0.241
Protein content	14.310
Fibre content	1.800
Carbohydrate content	81.769
Viscosity	498.0 @ 60rpm

3. RESULTS AND DISCUSSIONS

From the above proximate analysis results, it shows that tamarind seed starch was found to be high in carbohydrate contents of 81.769%, protein 14.310%, moisture content of 10.8%, ash content of 0.080%, fibre content of 1.800% and viscosity of 498.0 at 60rpm. The spectra obtained were analysed for presence/absence of key functional groups by comparison with a standard FTIR correlation table. Scanning electron microscopy

was used to evaluate the smoothness, roughness and compatibility of the starch through morphological analysis.

The high carbohydrate contents, qualifies the starch as promising raw material for conventional biopolymers.

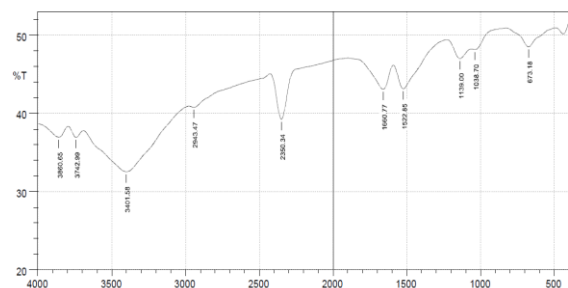


Fig. 1. FTIR spectra of the tamarind starch

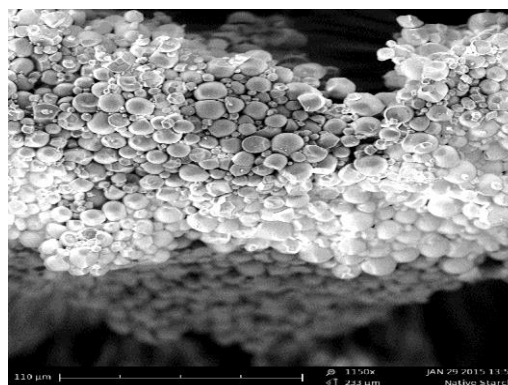


Plate 1. SEM for tamarind starch

4. Conclusion

This work has shown that it is possible to extract starch from seeds of tamarind for biodegradable polymer synthesis. The starch produced can be harnessed for industrial and domestic for future applications.

References

- Shlini Purushothaman*, Siddalinga Murthy K R, 2011, Extraction of β -galactosidase and β -glucosidase from the seeds of *Tamarindus indica*. *International Journal of Biomolecules and Biomedicine (IJBB)* ISSN: 2221-1063 (Print) 2222-503X (Online) Vol. 1, No.3, p. 8-17.
- Smith, A. M. (2001). The biosynthesis of starch granules. *Biomacromolecules*, 2(2), 335-341. <http://dx.doi.org/10.1021/bm000133c>. PMID:11749190.
- Isabelle Vroman * and Lan Tighzert, 2009 Biodegradable polymers; *Materials* 2009, 2, 307-344; doi:10.3390/ma2020307 ISSN 1996-1944 www.mdpi.com/journal/materials
- Ephraim Nuwamanya, Yona Baguma, Naushad Emambux, John Taylor anRubaihayo Patrick, 2010. Physicochemical and functional Characteristics of Cassava Starch in Ugandan varieties and their progenies. *Journal of Plant Breeding and Crop Science* Vol. 2(1), pp 001 – 011.
- Phani Kumar G.K *, Gangarao battu, Kotha N.S. Lova Raju 2011, Isolation and Evaluation of Tamarind Seed Polysaccharide being used as a Polymer in Pharmaceutical Dosage Forms. *RJPBCS* Vol. 2 Issue 2 Page 274 – 290
- Kaur, L., Singh, J., & Singh, N. (2006). Effect of cross-linking on some properties of potato (*Solanum tuberosum* L.) starches. *Journal of*
- Cura J.A, and Krisma C.R., (1990), cereal grains: A study of their alpha - 1, 4 - alpha 1,6



- glucopyosaccharide composition. *Starch/starke* 42 (2), pp 171 – 175.
8. Mahsa M., Arthor J., Rome, Martin C. Sandra E., Hill, Stephen E. and Harding (2003). Partial fraction of wheat starch amylose and amylopectin using xonal ultracentrifugation. *Carbohydrate Polymers* (52) pp 269 – 274.
 9. Cameron K, Wang y, Moldenhauer A 2007. Comparison of Starch Physicochemical Properties from medium Grain Rice Cultivars Grown in California and Arkansas *Starch/Stärke* 59: 600 – 608.



ABSTRACT CCT-: 045

Abdullahi I. Danfillo*¹, Zaharaddeen Sani Gano², Abdulazeez Yusuf Atta², Atinuke E. Akintunde³

1. Department of Chemical Engineering, Ahmadu Bello University, Zaria, Kaduna State, Nigeria
2. Petrochemicals & Allied Department, National Research Institute for Chemical Technology, Zaria-Nigeria
3. Otto-von-Guericke University, Universitätsplatz 2, 39106, Magdeburg, Germany

Email: aidanfillo68@gmail.com

A BENCH SCALE LABORATORY PRODUCTION OF BROWN SUGAR FROM SUGARCANE

ABSTRACT: In this work, a bench scale production of brown sugar was carried out from sugarcane using the open pan technology. The work was carried out to generate laboratory data for use in design, modelling and simulation of sugar processing plant using the open pan technology. The sugarcane sample was first subjected to proximate analysis for characterization purposes and subsequently used in the production of the brown sugar. The results of proximate analyses showed that the cane sugar has 63.9% water content, 23.84% fibre content, and 12.26% sugar content. However, a sugar recovery of 9.3% was achieved in the production processes.

1. Introduction

Sugars are a major form of carbohydrate and are commonly found in all green plants. They occur in significant amounts in most fruits and vegetables. Sugar is used as sweetening agent, in the food industries, in pharmaceutical industries and as preservatives; therefore, the need for sugar in our day to day activities is of paramount importance.

The Nigerian sugar market has an estimated potential of 1.7 million tons, according to the United States Development of Agriculture (USDA). Data obtained from the National Sugar Development Council (NSDC) reveals that the country's sugar consumption in 2012 was 1,108,980 tons even as domestic production was 10,843 tons. Hence within the period under review, 1,098,137 tons were imported into Nigeria, costing the country a total of \$517,222,527 (USDA, 2013). Nigeria has a land potential of over 500,000 hectares of suitable cane fields capable of producing over 5 million metric tons of sugarcane. When processed efficiently, these can yield about 3 million metric tons of sugar, according to (NSDC, 2002).

Generally, Sugar is produced using two technologies, thus the Open Pan System (OPS) and the Vacuum Pan System (VPS) technologies. The major difference between the OPS and VPS technology is the method of evaporating or boiling the juice. While evaporation is carried out under atmospheric pressure in the OPS, it is carried out under suitable vacuum in the VPS. The OPS system is usually adopted by the local producers, producing sugar in a small quantity while the VPS system is capital intensive and therefore mostly carried out at industrial capacities. Moreover, the VPS is more energy efficient than the OPS and because of the presence of vacuum, the extracted cane juice boils at a lower temperature thus reducing the effect of inversion.

The Nigerian sugar industry remains underdeveloped and the Government of Nigeria through the National Sugar

Development Council (NSDC) intends to foster sugar production. Since domestic demand is by far higher than domestic supply, the commodity is largely imported. Raw sugar was the 2nd agricultural import in Nigeria in terms of quantity (after wheat) and the 3rd in terms of value (after wheat and palm oil) for the period 2005-2010 (NSDA, 1996).

Therefore, the work was carried out on a bench scale laboratory experiment to optimized the production of brown sugar on a particular variety of sugarcane, M-21 Variety of sugarcane.

2. Materials and methods

Brown sugar is a sucrose sugar product with a distinctive brown color due to the presence of molasses. Raw sugar cane was basically characterized by quantifying its moisture, fibre and sugar content using proximate analysis.

2.1 Moisture content analysis

Moisture Content (or water Content) is the amount of water evaporated from the sugarcane upon drying to a constant weight. The conventional way is to report moisture content on a wet (or total weight) basis.

2.2 Fibre content analysis

Fibre content analysis is the total weight of fibre after digesting and drying of the sugarcane to a constant weight.

2.3 Equipment material and reagent used

The equipment material and reagent used are: knives, juice extractor, suitable beakers of different sizes, vacuum oven, weighing balance, pH meter, refractor(brix) meter, crystallization pan, thermometer, filtration funnel, filter paper, hot plate, water bath, CaOH as the reagent, and sugarcane as the material used.



2.4 Open pan system (OPS)

Procedure for the production of brown sugar M-21 sugarcane samples were first washed to make them free of impurities. The washed samples were cut into small pieces and their juice was extracted using a bench top juice extractor. The extracted juice was then clarified using slaked lime prepared in the required Ph. The clarified juice was then purified and concentrated via evaporation. Brown sugar crystals were finally obtained via crystallization of the concentrated juice. The crystals were further separated from the molasses via a centrifuge machine. For improved sugar recovery, sugarcane samples were subjected to multiple juice extractions commonly 3 to 4 times for each samples.

3.0 Results and discussions

3.1 Moisture Content

Table 1. Initial Weight of samples and dishes.

Samples	Weight of Dishes (g)	Weight of Samples (g)	Weight of Dishes + Samples (g)
A	66.28	10.13	76.41
B	66.21	10.03	76.24
C	66.99	10.12	77.11

Table 2. Weight of Samples Taken After 1hr Intervals.

Interval (H)	A (G)	B (G)	C (G)
1	71.6	71.7	71.9
2	70.0	70.1	70.8
3	69.9	69.8	70.8
4	69.9	69.8	70.7
5	69.9	69.8	70.7

Weight of Dried Samples	Weight of Samples + Dishes (G)	Weight of Samples (G)
A	69.9	3.62
B	69.8	3.59
C	70.7	3.71

Percentage moisture content of samples

$$\%MC_i = \frac{(\text{initial weight of sample})_i - (\text{final dry weight of sample})_i}{(\text{Initial weight of sample})_i} \times 100$$

$$\%MCA = \frac{(10.13 - 3.62)}{10.13} \times 100 = 64.26\%$$

$$\%MCB = \frac{(10.03 - 3.59)}{10.03} \times 100 = 64.21\%$$

$$\%MCC = \frac{(10.12 - 3.71)}{10.12} \times 100 = 63.34\%$$

Percentage Fibre Content

$$\%Fbi = \frac{\text{final weight of dried sample}_i \times 100}{\text{Initial weight of fresh sample}_i}$$

Initial weight of fresh sample_i

Final Weight of Dried Samples after Digestion

Percentage Fibre Content

$$\%Fbi = \frac{\text{final weight of dried sample}_i \times 100}{\text{Initial weight of fresh sample}_i}$$

Initial weight of fresh sample_i

Final weight of dried Samples after digestion

	Samples+ Dishes (G)	Samples (G)
A	68.7	2.42
B	68.6	2.39
C	69.4	2.41

	Samples + Dishes (G)	Samples (G)
A	69.9	3.62
B	69.8	3.59
C	70.7	3.71

$$\%FbA = \frac{2.42}{10.13} \times 100 = 23.89\%$$

$$\%FbB = \frac{2.39}{10.03} \times 100 = 23.83\%$$

$$\%FbC = \frac{2.41}{10.12} \times 100 = 23.81\%$$

$$\%FbB = \frac{2.39}{10.03} \times 100 = 23.83\%$$

$$\%FbC = \frac{2.41}{10.12} \times 100 = 23.81\%$$

Weight of Sugar Content

Sugar content_i = (weight of dry sample before digestion) _i - (weight of dry samples after digestion) _i

$$SCA = 3.62 - 2.42 = 1.2g$$

$$SCB = 3.59 - 2.39 = 1.2g$$

$$SCC = 3.71 - 2.41 = 1.3g$$

Percentage Sugar Content

$$\%S G_i = \frac{(\text{weight of sugar})_i}{(\text{initial weight})_i} \times 100$$

$$\%S CA = \frac{1.2}{10.13} \times 100 = 11.85\%$$

$$\%SCB = \frac{1.2}{10.03} \times 100 = 11.96\%$$

$$\%SCC = \frac{1.3}{10.12} \times 100 = 12.85\%$$

Total Weight of Sugarcane Crushed = 800g.

Therefore,

$$\text{Percentage recovery} = \frac{(\text{total weight of sugar} / \text{total weight of sugarcane}) \times 100}{= (74.2/800) \times 100}$$

$$= 9.3\%$$

$$= 9.3\%$$

Table 1 shows the initial weight of the dishes and the three sugar cane samples (A, B and C). Table 2 shows the different samples of sugarcane heated in an oven at an interval of one hour, taking note of the change in weight until the sample attend constant weight. The samples finally attained a constant weight after four hours, thereby calculating the moisture content to be 63.9%.

The fibre content was also determined after digesting the sugarcane sample in five successive portions of boiling water for 10 minutes each, allowing to drain after each digestion. After the last digestion, the samples were dried at the temperature of boiling water, cool and weigh quickly to determine the fibre content to be 23.9%.



The total amount of sugarcane crushed was 800g. Open pan system was used in the

production of the sugar and the yield obtained was 9.4%.

Table 3.

S/N	Volume	Weight	Brix	Baume	pH	gH ₂ O/gCaO
1	258	282.6	30.4	16.9	5.34	5.78
2	178	182.3	19.4	10.8	5.46	9.78
3	295	298	13.4	9.4	5.60	16.22
4	487	378.52	11.4	6.3	5.72	18.69
5	431	435	7.36	4.1	5.82	28.98

Table 4. Percentage Recovery Evaluation of Sugar from 800g of Sugarcane

Extract No.	1					
Crystallization Step	1	2	3	4	5	Total
	8.51	6.98	5.8	4.5	2.1	27.89
Extract No.	2					
Crystallization Step	1	2	3	4	5	Total
	7.9	6.2	5.0	4.1	2.0	25.2
Extract No.	3					
Crystallization Step	1	2	3	4	5	Total
	4.5	4.0	2.0	1.9	1.0	13.4
Extract No.	4					
Crystallization Step	1	2	3	4	5	Total
	2.0	2.2	1.51	1.0	0.0	6.71
Extract No.	5					
Crystallization Step	1	2	3	4	5	Total
	1.0	0.0	0.0	0.0	0.0	1.0
Total Weight of Sugar	74.2					

4. Conclusion

The entire work showed the result of the production of brown sugar from M-21 variety of sugarcane in a laboratory bench scale. The water (moisture) content in this variety of sugarcane was 63.4, the fibre content 23.9 and the sucrose yield was 9.4 which is a very good yield compared to the literature that says "Sugar recovery from existing OP plants range from 6-7% (Chungu, Kimambo, & Bali, 2001).

Acknowledgements

The authors' wishes to appreciate the support of National Research institute for Chemical Technology, Zaria towards the success of this work.

References

- (2012). Retrieved from World Sugar Research Organisation: <http://www.wsro.org/AboutSugar/FactsaboutSugar.aspx>
- Chungu, A., Kimambo, C., & Bali, T. (2001). Assessment of Village Level Sugar Processing Technology in Tanzania. Dar Es Salaam: Mkuki Na Nyota.
- National Sugar Development Council. (2002). NSDC. Nigeria: NSDC.
- USDA. (2013). New York: United State Department of Agriculture. National Sugar Development Council (NSDC, 2002). Nationwide survey on industrial and domestic consumption of sugar in Nigeria.
- National Sugar Development Council (NSDC, 1996): Annual Report for the year ended. NSDC Publication.



ABSTRACT CCT-: 048

Ibrahim A.A., M. Dauda, G.Y. Pam and M.B. Abdullahi

Department of Mechanical Engineering, Ahmadu Bello University, Zaria, Kaduna State, Nigeria

Email: ahamadii80s@gmail.com

DESIGN, CONSTRUCTION AND TESTING OF SOLAR STILL HAVING SUBMERGED FLAT ABSORBER PLATE

ABSTRACT: A solar still with a submergible flat absorber plate was designed and constructed. The submergible flat absorber plate was introduced to increase absorption of solar radiation and to improve on the heat transfer rate of the absorber. The still was tested for three days, with 10 litres of raw water in the first day, then 20 and 30 litres on the second and third day of the experiment respectively. Distillates of 753 ml/day, 826 ml/day and 744 ml/day respectively were obtained in the first, second and third day of the experiment. The efficiencies obtained for the first, second and third day of the experiment were 82.35%, 82.99% and 83.82% respectively. The pH value of the distilled water was 7.7, which is within acceptable range (World Health Organisation (WHO), 2007). The cost of the solar still as of 2014 was N7, 600.00.

1. Introduction

Water is one of the most vital ingredients for the sustenance of all living things. Portable water can be defined as water fit for human consumption. Water is used for agriculture, irrigation and domestic purposes. Over two-thirds of the earth's surface is covered with water of which around 97 % is salty, 2.6% is present as icebergs and only less than 1% of water is within human reach (Kumar, 2015). Distillation is a good method of obtaining portable water. However, the conventional distillation processes such as thin film distillation, multi – effect fresh evaporation, reverse osmosis and electrodialysis are techniques that require a lot of energy and are not feasible for large fresh water demands. Therefore, solar distillation is a promising method and an alternative way for providing small communities in remote areas and islands with portable water. In fact, it has been reported that for such places, solar distillation could be the most favorable means of portable water supply (Medugu and Ndatuwong, 2009). Indeed, several solar still designs have been developed. One of the current objectives among researchers is the improvement of the overall efficiency of the system (Iloje, 1998). As such, research is still on going on the improvement of solar stills. The objective of this research was to design and construct a solar still having submerged flat absorber plate and to determine its performance. The submerged flat absorber plate was incorporated so as to improve the heat transfer to the un-distilled water.

2. Materials and methods

2.1. Design of solar distillation plant

2.1.1 Design Considerations

The most important factor in solar powered systems is the Heat transfer rate from the absorber to the load. The major consideration is to minimize heat lost and maximise absorption of solar radiation. Other

considerations were:

- The design of the still was based on the month of lowest insolation which is August here in Zaria Kaduna state, Nigeria.
- The still was designed for one litre of distilled water per day.
- Latitude of Zaria was used as angle of inclination of the collector.

2.2 Material selection

2.2.1 Still Basin and Submerged Plates

The material for the basin and the submerged flat plate has to be of high absorptivity or less reflectivity and transmissivity (Ibrahim *et al.*, 2015). A black painted aluminium sheet (205W/m²°C) was used.

2.2.2 Side walls

The material for the wall which serves as external casing and support to the top cover should be rigid and be of low thermal conductivity to prevent heat losses. For better efficiency, wood (0.147W/m²°C) was used at the outer part, while sawdust (0.08W/m²°C) was used at the inner part in between the basin and the wood.

2.2.3 Top Cover

The top cover as can be seen in, has to be transparent to allow solar radiation to get to the absorber therefore, glass of area 0.36m² was used based on the design calculation.

2.2.4 Channel

Aluminium sheet was used to develop the distilled water channel for distillate collection at the outlet.

2.4. Testing of the solar still

The solar still was tested to determine its productivity, efficiency and capacity.



Plate 1. Showing submerged flat plate
 Plate 2. Showing the solar still

3. Results and discussion

3.1 Results

The temperature difference between water and the glass. Temperature difference between water and the glass can be seen in figure 2.

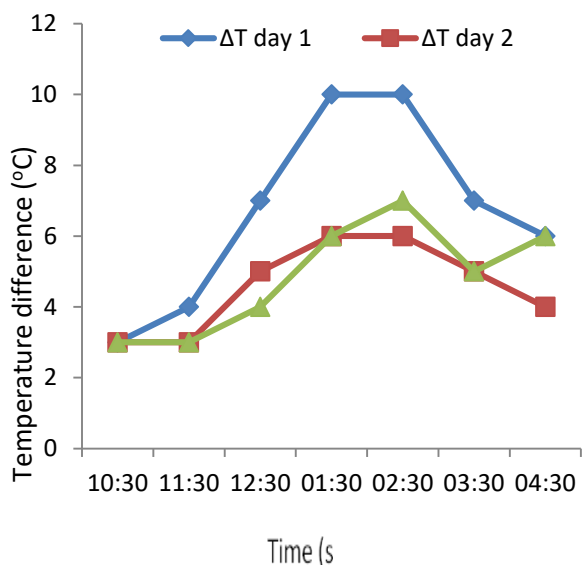


Fig. 1. Temperature difference between water and glass for day 1, 2 and 3.

3.1.2 Distillate yield

Fig. 2 shows the yield obtain on each day of the experiment.

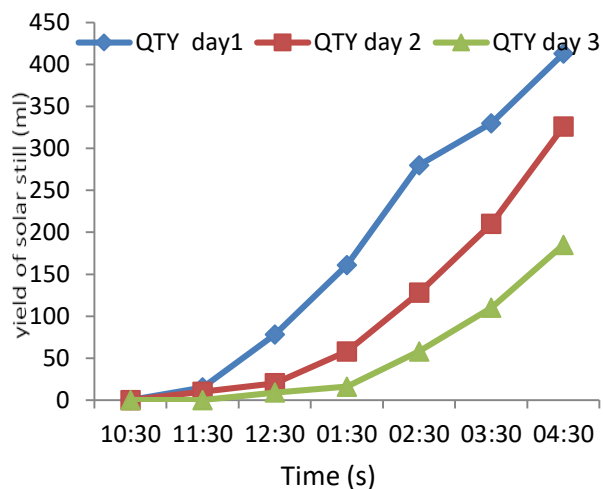


Fig. 2. Commulative distillate at hour interval between 10:30 am to 4:30 pm for day 1, 2, and 3 respectively.

3.1.3 Daily distillate

Figure 3 shows the yield obtain from the still for the three days of experiment.

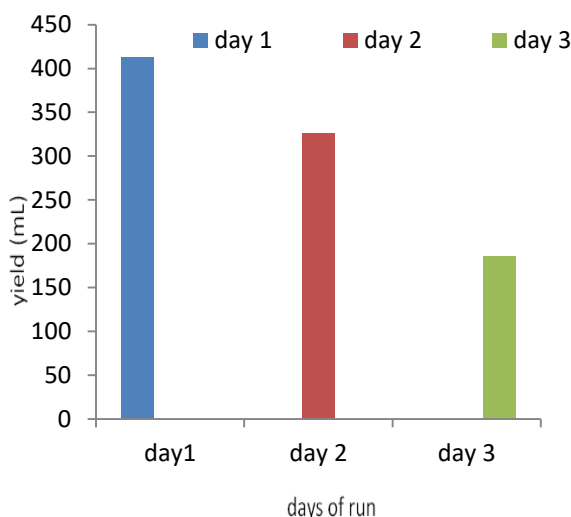


Fig. 3. Total yield for day 1, 2 and 3 of solar still running between 10:30 am to 4:30 pm

3.2 Efficiency and capacity of the still

Table 3.1 show the efficiency (η) and capacity (mL/day) of the solar still with submerged flat absorber on the first, second and third day of the experiments.

The pH value of the distilled water was measured to be 7.7. The solar still is affordable with a total cost of N7, 600.00.

3.3. Discussion

From the result of temperature difference between water and glass as shown in figure 2, it can be seen that on the first day of the experiment with the solar still containing 10 litres of inlet un distilled water, the temperature difference was higher than that of the second and third day of the experiments where the still contained 20 and 30 litres of inlet water respectively. The high temperature difference on the first day was due to low quantity of inlet water to absorb the heat being released by the absorber. It is the temperature difference that



brought about vaporisation, though when the difference was much convective heat loss increased.

Figure 2 and 3 shows that the productivity of the still reduces with increase in inlet water. Highest productivity was obtained on the first day of experiment with solar still containing 10 litres of un distilled water during the sunshine hours of experiment. But the still with 20 liters of water yielded the highest daily distillate

because it utilizes the stored heat in the water at night for vaporization, while on the third day with solar still having 30 litres of un distilled water gave the least productivity.

The daily efficiencies and capacities of the solar still in the three days of test did not go in correlation with the result of figure 1 and 2 because of variation in whether condition at night.

Table 3.1. Showing the efficiency and capacity of the still.

Still Type	Day 1		DAY 2		Day 3	
	η %	(mL/day)	η %	(mL/day)	η %	(mL/day)
Submerged Flat Absorber	82.26	753	84.43	826	82.86	753

Efficiency (η) = $\frac{Q_e}{H_s}$ Solar still capacity (m_c) = $\frac{Q_e}{L}$ Q_e - heat energy used H_s - Incoming solar energy, L- Latent heat of vaporisation

There was a reasonably high solar still efficiency of above 80% in all the days of experiment as can be seen in table 3.1, which shows that the solar still had a high performance. The pH value of the distilled water was within the accepted range (6.5 -8.5) (WHO, 2007).

4. Conclusion

A small size solar still having submerged flat absorber plate was designed and constructed for experimental purpose. The solar still was found to have performed better with an inlet of 10 litres of un distilled water. The solar still efficiency and capacity at 10 litres of inlet un

distilled water is 82.26% and 753 mL/day.

References

1. Ibrahim A.A., Dauda M., Pam G.Y. and Obada D.O. (2015) Design, Construction and Performance Comparison of Two Solar Stills Having Different Absorber Design. NIJOTECH Vol. 34 No. 4, pp 761-767.
2. Kumar P.V., Kumar A. Prakash O. And Kaviti A.K. (2015) Solar stills system design: A review Renewable and Sustainable Energy Reviews 51:153–181
3. Medugu D.W. and Ndatuwong L.G. (2009) Theoretical analysis of water distillation using solar still. International journal of Physical Sciences Vol. 4 (11), pp. 705-712. ISSN 1992-1950.
4. World Health Organisation (2007) Revised background document for development of WHO Guidelines for Drinking-water Quality WHO/SDE/WSH/07.01/1



ABSTRACT CCT-: 049

Ibrahim A.A., M. Dauda, G.Y. Pam and I. Ajunwa

Department of Mechanical Engineering, Ahmadu Bello University, Zaria, Kaduna State, Nigeria

Email: ahamadii80s@gmail.com

PERFORMANCE COMPARISON OF A SUBMERGED V-PATTERN ABSORBER STILL AND THE CONVENTIONAL BASIN STILL

ABSTRACT: Solar still having a submerged V-pattern absorber and the other having its basin as the absorber were both successfully designed and constructed. Both stills were tested under the same conditions from 10:30 am to 4:30 pm. 10 litres of inlet raw water was poured into each stills. The distillates obtained from the still with the submerged V-pattern absorber and the conventional basin still were 710 mL/day and 843mL/day respectively. While their efficiencies were 81.77% and 83.30% respectively. The experiment showed that the conventional basin still had better performance in all the days of experiments. The total cost of producing the submerged absorber solar still is N8,030.00 while that of the conventional solar still was N7,070.00.

1. Introduction

Large quantities of fresh water are required in many parts of the world for agricultural, industrial and domestic uses. Lack of fresh water is a prime factor inhibiting regional economic development. The oceans constitute an inexhaustible source of water but are unfit for human consumption due to their salt content, in the range of 3 % to 5 %. Seawater and sometimes brackish water desalination constitutes an important option for satisfying current and future demands for fresh water in arid regions. Solar distillation is now being successfully practiced in numerous countries in the Middle East, North Africa, Southern and Western United State, and Southern Europe to meet industrial and domestic water requirements (Pinar, 2003).

Several works have been done on solar stills; Alpesh et al. (2011), devised a model which will convert dirty/saline water into pure/portable water using a renewable source of energy (i.e. solar energy). His design model produces 1.5 litres of pure water from 14 litres of dirty water during six hours. The efficiency of the plant was 64.37%. Muafag S.K. (2007) worked on the Effect of Water Depth on the Performance Evaluation of Solar Still. In his work, different depths of brackish water (0.5cm, 2cm, 3cm, and 4cm) with TDS of 5000ppm were tested under the same climatic conditions in Mutah University. A six-month study showed that the still productivity is strongly dependent on the climate, design and operational conditions.

This work intends to compare the performance of a developed submerged v-pattern absorber still and the conventional basin still.

2. Materials and methods

2.1 Design of solar distillation plants

2.1.1 Design Considerations.

Heat transfer rate from the absorber to the load (un distilled water) is of utmost importance in any solar powered system. The major consideration is to minimize heat losses and

maximise absorption of solar radiation. Other considerations were:

- i. The design of the stills was based on the month of lowest insolation which is August here in Zaria Kaduna state, Nigeria.
- ii. The stills were designed for one litre of distilled water per day.
- iii. Latitude of Zaria was used as the angle of inclination of the collector.

2.2 Material selection

2.2.1 Still basin and submerged plates

The material for the basin and the submerged V-pattern plate which serves as the absorbing bodies for the incoming solar radiation has to be of high absorptivity or less reflectivity and transmissivity (Ibrahim et al., 2015). A black painted aluminium sheet (205 W/moC) was used.

2.2.2 Side Walls

The material used to build the walls, which serves as external casing and support to the top cover should be rigid and be of low thermal conductivity to prevent heat losses. For better efficiency, wood (0.147 W/moC) was used at the outer part, while saw dust (0.08 W/moC) was used at the inner part in between the basin and the wood.

2.2.3 Top Cover

The top cover has to be transparent to allow solar radiation to get to the absorber. Therefore, glass was used of area 0.36m² based on the design calculation and thickness of 4 mm.

2.3.4 Channel

Aluminium sheet was use to develop the distilled water channel for distillate collection at the outlet.

2.4. Testing of the Solar Stills

The solar stills were tested to determine their distillate productivity, efficiency and capacity.



Plate 1. Development of v-pattern absorber

3. Results and discussion

Temperature readings of the inner glass and the water were taken and recorded at hourly intervals. Fig. 3 shows a plot of the temperature difference between water and glass for the two stills. Figure 4 is a graph of the cumulative distillates obtained at hourly intervals for the two stills.



Plate 2. The two solar stills

It can be seen from fig. 3 that the temperature difference of the submerged v-pattern solar still was higher than that of the conventional basin still which means more heat will be lost in the submerged v-pattern solar still because of the high temperature difference. The more the heat loss the lesser the energy available for water vaporisation. This is the reason while the conventional basin solar still produced more distillate than the submerged v-pattern absorber solar still as it can be seen in fig. 4 below.

Other possible reasons why the submerged v-pattern absorber solar still had lower distillate were that some surfaces of the absorber do cast shadow on other surfaces thereby preventing solar insolation from reaching those surfaces especially when the sun is not at the meridian.

3.1 Plots Showing Readings Taken from Stills

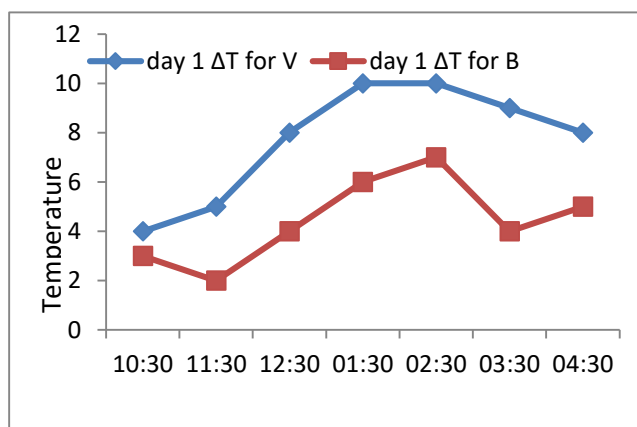


Fig. 3. Temperature difference between water and glass against time.

Where ΔT for V: temperature difference between water and glass for submerged v-pattern still.

ΔT for B: temperature difference between water and glass for the conventional still.

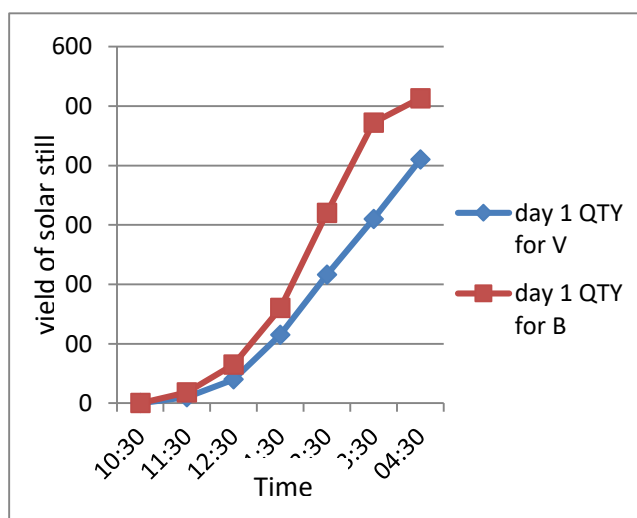


Fig. 4. A plot of cumulative distillate against time

Where QTY for V: distillate from submerged v-pattern still

QTY for B: distillate from conventional basin still.

3.2 Efficiency and capacity of the stills

As shown in table 3.1, the efficiency (η) and capacity (mL/day) of the still without submerged absorber (conventional basin still) is higher than that of the still with submerged v-pattern absorber.

3.3 Cost

The total cost of production of the submerged v-pattern solar still was eight thousand and thirty naira only (N8, 030. 00) while that of the conventional solar still is seven thousand seventy naira only (N7, 070.00).



Table 1. Showing the efficiency and capacity of the still.

Still Type	Day 1	
	η %	(mL/day)
V- pattern absorber	81.65	750
Without Submerged Absorber	83.30	843

Efficiency (η) = Q_e/H_s ; Solar still capacity (me) = Q_e/L Q_e - heat energy used; H_s - Incoming solar energy; L- Latent heat of vaporisation

4. Conclusion

The productivity, efficiency and capacity of a developed submerged V-pattern absorber solar still and the conventional still were both determined and compared. From the result of the comparison, it can be concluded that adding submerged v-pattern absorber plate to solar still does not improve on the distillate yield or on the efficiency of the solar still.

References

- Pinar I. A. (2003). “Theoretical and Experimental Investigations on Solar Distillation of IyteGulbahceCompus Area Seawater”, Izmir Institute of Technology, Turkey.
- Alpesh M., Arjun V., Nitin B., & Dharmesh L. (2011) LDesign of Solar Distillation system, International Journal of Advance Science and Technology, Vol 29 pg 67-74.
- Muafag S., Tarawneh K. (2007). “Effect of Water Depth on the Performance Evaluation of Solar Still” Mechanical Engineering Department, Faculty of Engineering, Mutah University, P. O. Box 7, Karak 61710, Jordan.



ABSTRACT CCT-: 057

Ahmed Rufai Dahiru^{1,3,*}, Jani Kangas¹, Juha Tanskanen¹ Ulla Lassi²

1. Chemical Process Engineering Research Unit, Faculty of Technology, P.O. Box 4300, University of Oulu, Finland
2. University of Oulu, Research Unit of Sustainable Chemistry, P.O. Box 3000, FI-90014 Oulu, Finland
3. Department of Planning Research & Statistics, Ministry of Environment, Sokoto State, Nigeria

Email: elrufai10@yahoo.co.uk

MFI-TYPE ZEOLITE MEMBRANES FOR THE SEPARATION OF CO₂/N₂ MIXTURES

ABSTRACT: Two MFI-type zeolite membranes were tested in the separation of CO₂/N₂ mixtures. Parameters such as separation factor (α), gas permeability (\dot{P}) and CO₂ permeate flux (J) were used to determine the membrane performance. The separation between CO₂ and N₂ take place due to preferential adsorption of CO₂ that hinders the N₂ permeation unto the membrane pore network. The highest membrane performances of the feed gas compositions were achieved with low CO₂ gas composition, and at low temperature separation experiments. Under these conditions, the obtained α , \dot{P} and J were 2.9, $5.3 \times 10^{-7} \text{ mol s}^{-1} \text{ m}^{-2} \text{ Pa}^{-1}$ and $20.9 \text{ kg m}^{-2} \text{ h}^{-1}$ respectively.

1. Introduction

One of the greatest challenges in the 21st century has been how to correlate the ever increasing population growth, emission reduction and energy-demand. This is clearly visible to the several projections reported to that effect. According to the projection reported by Intergovernmental Panel on Climate Change, unless current trends in energy production and use have been revisited, the increased concentration of greenhouse gases in the atmosphere could ultimately disrupt the societal, economic development and environmental consequences of both the present and future generations (IPCC 2000). In principal terms, the major challenge is concentrate and purification of CO₂ in the exist stream.

CO₂ an important greenhouse gas, does not have any useful heating value in the downstream processes. Recent advances in the capture of carbon dioxide envisaged in the utilization of the captured carbon dioxide for further uses, such as in other chemical syntheses, or enrichment in greenhouses for plant growth. Therefore, this study focuses on the recovery of carbon dioxide from gas mixtures, as part of the HighBio2 project in which the University of Oulu is a partner.

2. Materials and methods

Carbon dioxide (999.99%) and nitrogen (99.99%) were purchased from AGA. The separation of CO₂/N₂ mixture was done using two supported hydrophobic high silica MFI type zeolite membranes (ZSM5-I and ZSM5-II). The experiments were carried out by sealing the membrane with O-rings and then placed in a stainless steel module surrounding by heating mantle. The flows of pure gas component were controlled by mass flow controller. The flows of each of the pure gas components were set at 2 l/min and monitored in the automatic monitoring system in the Labview. The laboratory equipment is originally from Xytel Europe B.V., but has undergone a multitude of changes during the

experimental work. The tests for the selected gas compositions were done at low (300K), and high (373K, 473K) temperatures. For the high temperature separation experiments, the membrane cell was also heated with the electric furnace. However, in the low temperature separation experiments, the membrane cell was heated only using the heating mantle.

In all the separation experiments, the feed and permeate pressures were kept constant at 6 bar and 1 bar respectively. After the pressures had stabilized, and the desired temperature was attained, the permeate flow rates were measured from the installed flow meter in the system. The temperature and pressure relative to the atmospheric pressure readings were also taken from the installed thermometer and monometer respectively. The feed, permeate and retentate samples were taken using the gas tight syringe at their respective outlets and injected into column of gas chromatography-equipped with thermal conductivity detector (GC-TCD). The average of the feed, permeate and retentate from the GC analysis of each of the samples were taken and converted to normal temperature and pressure (NTP) conditions through the usage the ideal gas equation. The separation factors of the samples were calculated from Eq. (1).

$$\alpha = \frac{y_{CO_2}/y_{N_2}}{x_{CO_2}/x_{N_2}}, \quad (1)$$

where α is the separation factor, y and x are the average molar fractions at the exit of the permeate, and the retentate respectively.

Furthermore, the membrane permeability of each of the samples were calculated from Eq. (2).

$$\dot{P} = \frac{F_x}{A \cdot \Delta p}, \quad (2)$$

where \dot{P} is the Permeance of gas x [$\text{mol s}^{-1} \text{ m}^{-2} \text{ Pa}^{-1}$], F_x is the flow rates of gas x [mol s^{-1}], A is the unit area of membrane [m^2], and Δp is the partial pressure difference between the feed and the permeate [Pa].



Additionally, the CO₂ permeation fluxes of the samples were calculated from Eq. (3).

$$J = \frac{\mathcal{F}}{A}, \quad (3)$$

where J is the CO₂ permeation flux [kg m⁻² h⁻¹], and \mathcal{F} is the permeate flow rate [kg h⁻¹].

3. Results and discussions

Table 1 presents the comparison of results obtained from this study and those reported in the literature. Figure 1-4 depicts the separation factors, gas permeances and CO₂ permeation flux obtained from this study.

Table 1. Comparison of the results in this study and the literature results reported on CO₂/N₂ separation using zeolites membranes.

Zeolite Membrane	Temp (K)	Feed (CO ₂ :N ₂)	$\alpha_{\text{CO}_2/\text{N}_2}$	CO ₂ Permeance (mol s ⁻¹ m ⁻² Pa ⁻¹)	CO ₂ PF (kg m ⁻² h ⁻¹)	Ref.
ZSM-5	300	1:1	2.9	5.3 x 10 ⁻⁷	20.9	This work
SAPO-34	300	1:1	16	9.8 x 10 ⁻⁷	0.7	Poshusta <i>et al.</i> (2000)
K-Y	313	1:1	30.3	1.8 x 10 ⁻⁶	14.3	Kusakabe <i>et al.</i> (1999)
K-ZSM-5	323	1:1	2	4.5 x 10 ⁻⁸	0.4	Masuda <i>et al.</i> (1998)
B-ZSM-5	300	6:1	12.6	2.6 x 10 ⁻⁷	5.1	Bernal <i>et al.</i> (2004)

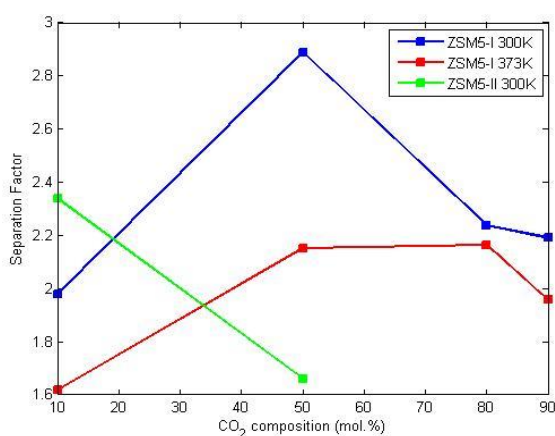


Fig. 1: Separation factors as function of CO₂:N₂ feed ratio at 300K and 373K under constant feed pressure of 6 bar and permeate pressure of 1 bar.

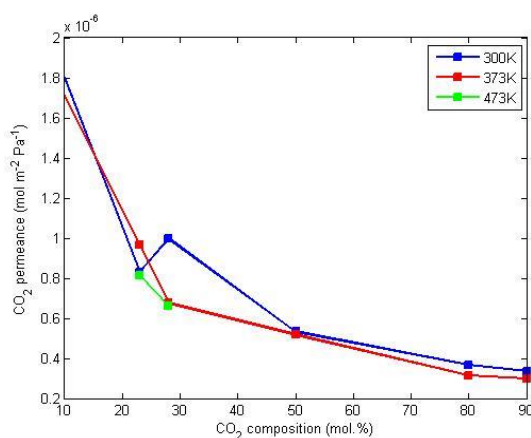


Fig. 2: CO₂ permeances as function of CO₂ feed compositions at 300K, 373K and 473K and constant feed and permeate pressures of 6 bar and 1 bar respectively.

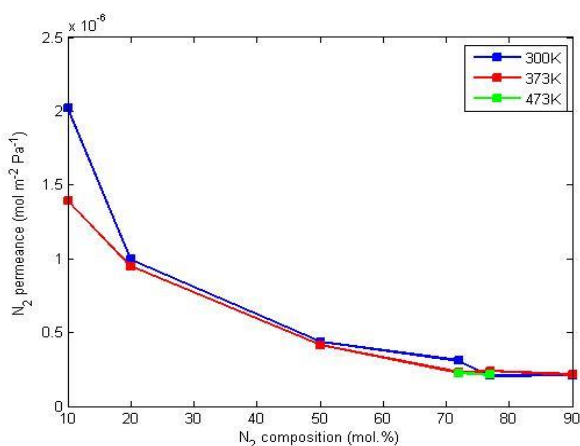


Fig. 3. N₂ permeances as function of N₂ feed compositions at 300K, 373K and 473K and constant feed and permeate pressures of 6 bar and 1 bar respectively.

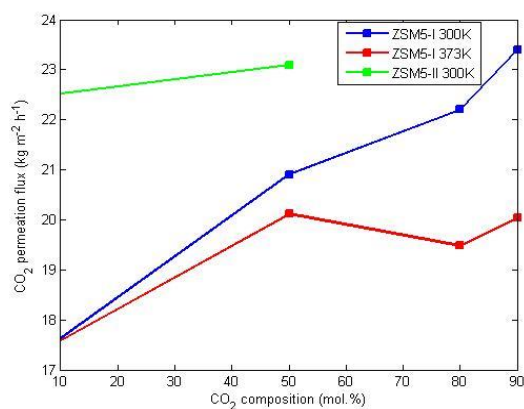


Fig. 4. CO₂ permeation fluxes as function of CO₂ feed composition of the ZSM5-I at 300K, 373K and ZSM5-II at 300K under constant feed pressure of 6 bar and permeate pressure of 1 bar.



4. Conclusion

Two MFI-types zeolite membranes (ZSM5-I and ZSM5-II) were tested in the separation of CO₂ from CO₂/N₂ mixtures in a laboratory scale experiments. Separation factor, gas permeability and CO₂ permeate flux were the parameters used to determine the membrane performance. The highest membrane performances of the feed gas compositions were achieved with low CO₂ gas composition, and at the low temperature separation experiments.

Acknowledgement

The authors are grateful to the financial support by EU/ Interreg Nord program within the research project of “HighBio2 – Biomass to Energy and Chemicals”. The first author acknowledges the Sokoto State Government

Higher Scheme Programme.

References

1. Bernal, M. P., Coronas, J., Menéndez, M. and Santamari, J. (2004). Separation of CO₂/N₂ Mixtures Using MFI-Type Zeolite Membranes. *AIChE J.* 50 (1), 127–135.
2. IPCC. (2000). IPCC special report: Emission Scenarios. Available: <http://www.ipcc.ch/pdf/special-reports/spm/sres-en.pdf>.
3. Kusakabe, K., Kuroda, T., Uchino, K., Hasegawa, Y. and Morooka, S. (1999). Gas Permeation Properties of Ion-Exchanged Faujasite-Type Zeolite Membranes. *AIChE J.* 45 (6), 1220–1226.
4. Masuda, T., K. Hashimoto, F. Kapteijn, and J. A. Moulijn, J. A. (1998). Selective Permeation of CO₂ from Mixture Gas of CO₂ and N₂ through ZSM-5 Zeolite Membrane. *Proc. ICIM'98*, Nagoya, Japan.
5. Poshusta, J. C., Tuan, V. A., Pape, E. A., Noble, R. D. and Falconer, J. L. (2000). Separation of light gas mixtures Using SAPO-34 Membranes. *AIChE J.* 46 (4), 779–789.



ABSTRACT CCT-: 008

Liman M. G.¹ and D. Umar²

1. Department of Pure and Applied Chemistry, Faculty of Science, Usmanu Danfodiyo, Sokoto. Nigeria
2. National Research Institute for Chemical Technology (NARICT), Zaria

Email: gidado.liman@udusok.edu.ng

DETERMINATION OF HEAVY METALS IN LOCALLY PROCESSED MEAT SOLD IN SOKOTO METROPOLIS, SOKOTO STATE

ABSTRACT: This study reports the concentration of heavy metals (Fe, Zn, Cu and Pb) using Atomic Absorption Spectroscopy (AAS) in four samples of dry meat: (kilishi, balangu, danbun-nama and tsire), which are widely consumed in Sokoto Metropolis, Sokoto State, Northern Nigeria. The results of iron (Fe) for kilishi, balangu, danbun-nama and tsire were (0.0986, 0.0795, 0.127 and 0.1075) mg/g respectively. The concentration of zinc (Zn) for kilishi, balangu, danbun-nama and tsire were (0.0401, 0.0397, 0.0236 and 0.0459) mg/g respectively. Similarly, the concentration of copper (Cu) in the same samples were (0.00276, 0.00312, 0.000488 and 0.00276) mg/g and also, the concentration of lead (Pb) for kilishi, balangu, danbun-nama and tsire were (0.0468, 0.0123, 0.0132 and 0.0308) mg/g respectively. The results showed that the concentrations of Fe, Zn, Cu and Pb in the samples of the dry meat are lesser than the permissible limits set by WHO and therefore indicates that the metals are within tolerance limits and may be safe for consumption, although there may be danger of bioaccumulation.

1. Introduction

With increasing industrialization, more and more metals are entering into the environment. These metals stay permanently because they cannot be degraded in the environment. They enter into the food material and from there they ultimately make their passage into the tissue (Baykov *et al.*, 1996). Lead, cadmium, mercury and arsenic are among the main toxic metals which accumulate in food chains and have a cumulative effect (Cunningham and Saigo, 1997). Heavy metals often have direct physiologically toxic effects and are stored or incorporated in living tissues (Baykov *et al.*, 1996). A study carried out by John and Jeanne (1994) showed that levels of arsenic, cadmium, mercury and lead were detected in several tissues of goats; the results showed that the levels of the above metals were found to be very high and generally above the permissible level. Similarly, the distribution and localization of some heavy metals in the tissues of some calf organs were detected, the most affected organs, which showed higher levels of trace metals, were livers, kidneys and small intestines (Horky *et al.*, 1998). Lead is a metabolic poison and a neurotoxin that binds to essential enzymes and several other cellular components and inactivates them (Cunningham and Saigo, 1997). Toxic effects of lead are seen on haemopoietic, nervous, gastrointestinal and renal systems (Baykov *et al.*, 1996). Food is one of the principle environmental sources of cadmium (Baykov *et al.*, 1996). As cadmium moves through the food chain it becomes more and more concentrated as it reaches the carnivores where it increases in concentration by a factor of approximately, 50 to 60 times (Daniel and Edward, 1995). Toxic effects of cadmium are kidney dysfunction, hypertension, hepatic injury and lung damage (John and Jeanne, 1994). Cadmium chloride at teratogenic dose induced significant alterations in the detoxification enzymes in the liver and kidney

(Reddy and Yellamma, 1996). Animals vary in their arsenic accumulation depending upon the type of food they consume (John and Jeanne, 1994). Acute arsenic exposure can give symptoms with rapid onset of headache, nausea and severe gastrointestinal irritation (Allan *et al.*, 1995). Similarly, increase in levels of copper causes liver and brain damage, which may follow haemolytic crisis (Judith, 1994). Zinc concentrations were found to be highest in meat, liver, fish and eggs (Janet and Carl, 1994).

2. Material and methods

All reagents used were of analytical grades throughout the experiment. All glass wares used were properly washed with detergents, soaked in 6M HCl overnight and rinsed several time with distilled water. All samples (fresh and roasted meats) were from two (2) different species of animal i.e cow and ram. From each of the species, fresh and roasted meats of (balangu, kilishi, tsire and dambun-nama) were collected from different suya spots at different locations in Sokoto metropolis of Sokoto state, Nigeria and a total of twenty (20) samples were collected. Ten (10) samples from cow (balangu, kilishi, tsire, dambun-nama and fresh of each individual roasted meat) and another ten (10) samples from ram (i.e. balangu, kilishi, tsire, danbun-nama and fresh of each individual roasted meat). Three replicate samples for Balangu, Kilishi and Tsire were collected, while one sample of Dambun Nama was collected because one spot was available at the study area. The samples were put in a fresh polyethene bag each and labeled, and were taken immediately to laboratory for treatment.

2.1. methods

The samples were individually washed with distilled water in the laboratory in order to remove any contaminant apart from the target metals. The samples were cut into pieces each



at a time using a clean knife. The samples were dried in an oven at 80 °C overnight. The samples were grinded into fine powder after drying using a ceramic mortar and pestle. Accurately 2.0g of each of the powdered samples were weighed in a porcelain crucible. The fine powdered samples in the crucibles were ignited in a muffle furnace at 600°C for three (3) hours.

The samples were then removed from the furnace and allowed to cool in a desiccator and a perfect grayish ash was obtained. Five (5) cm³ of 6M HCl was added to the crucible to dissolve the ash. Further, the crucibles containing acid solution were kept on a hot plate and digested to obtain a clean solution. The final residue was dissolved in 0.1M Nitric acid (HNO₃) solution and made up to 25 cm³ in sample bottles. All the treated samples were taken to science central laboratory, UDUS for AAS analysis (Stewart et al., 1974).

3. Results and discussion

The following tables contain the result of the analyzed samples in different concentrations.

The results obtained from the Atomic Absorption Spectroscopy (AAS) analysis have shown that these heavy metals Zn, Fe, Cu and Pb were all present in all the samples of the dry meat (kilishi, balangu, danbun-nama and tsire) analyzed as shown in Tables 3.1 and 3.2 respectively. The concentration of Fe in all the samples of the dry meats analyzed falls below the Recommended Dietary Allowances (RDAs) given by the Food and Nutrition Board (FNB) which is between 11 mg – 15 mg. The concentration of Zn in all the analyzed samples of dry meat falls below the RDAs given by Food and Nutrition Board which is between 2 mg - 13 mg. Zinc is an essential element in human diet. Too little Zn can cause problems; however, too much Zn is harmful to human health (ATSDR, 2004). The concentration of Cu in all the analyzed samples of dry meat falls below the RDAs given by Food and Nutrition Board which is between 0.2 mg – 1.3 mg. The concentration of Pb in all the analyzed samples of dry meat falls below the RDAs given by Food and Nutrition Board which is between 0.1 to 0.5 mg.

Table 1: Concentration of heavy metals in locally processed cow meat

S/No	Sample name	Fe (mg/g)	Zn (mg/g)	Cu (mg/g)	Pb (mg/g)
1	Balangu P	0.0795	0.0397	0.00312	0.0123
2	Meat F	0.0691	0.0390	0.003	0.0122
3	Dambun-nama P	0.127	0.0236	0.000488	0.0132
4	Meat F	0.124	0.0221	0.000411	0.0130
5	Kilishi P	0.0986	0.0401	0.00197	0.0468
6	Meat F	0.0916	0.0411	0.00192	0.0462
7	Tsire P	0.1075	0.0459	0.00276	0.0308
8	Meat F	0.1071	0.0451	0.00273	0.0311

Key: P = Processed meat, F = Fresh meat.

Table 2. Concentration of heavy metals in locally processed ram meat

S/No	Sample name	Fe (mg/g)	Zn (mg/g)	Cu (mg/g)	Pb (mg/g)
1	Balangu P	0.185	0.148	0.1860	0.063
2	Meat F	0.129	0.289	0.110	0.004
3	Dambun-nama P	0.989	0.411	0.143	0.089
4	Meat F	0.239	0.510	0.121	0.070
5	Kilishi P	0.388	0.612	0.133	0.028
6	Meat F	0.138	0.104	0.1290	0.0312
7	Tsire P	0.433	0.663	0.288	0.0308
8	Meat F	0.321	0.214	0.184	0.0422

Key: P = Processed meat, F = Fresh meat

4. Conclusion

From the result obtained, the concentrations of these heavy metals (Zn, Fe, Cu and Pb) in the samples of locally processed meat (balangu, kilishi, danbun– nama and tsire) analyzed falls below the Recommended Dietary Allowances set by the Food and Nutrition Board (FNB).

The samples of the locally processed meat suggest that they are free from these heavy metals poisoning. However, it should be noted that, bioaccumulation effect may manifest later in life due to prolonged usage.



References

1. Agency for Toxic Substances and Disease Registry (ATSDR), (2005). Toxicological Profile for Zinc, U. S Department of Health and Human Services, Public Health.
2. Allan G. O., Robert A. C., O'Reilly D. S. J., Stewart M. J., and James S., (1995). Clinical biochemistry. 2nd Edn, Harcourt Brace and Company Ltd., pp: 114 – 115.
3. Baykov B. D., Stoyanov M. P., and Gugova M. L., (1996). Cadmium and lead bioaccumulation in male chickens for high food concentrations. Toxicology environmental chemistry. 54: 155 – 159.
4. Cunningham W. P., and Saigo B. W., (1997). Environmental science a global concern. 4th Edition, WMC Brown publisher, New York, pp: 389.
5. Daniel B., and Edward A. k., (1995). Environmental science, earth as a living planet. John Willey and Sons, Inc. New York, pp: 278-279.
6. FNB, (2011). Food and Nutrition Board, at the Institute of Medicine.
7. Horky D., Illek J., and Pechova A., (1998). Distribution of heavy metals in calf organs. Vet. Med., 43: 331 – 342.
8. Janet C. K., and Carl L. K., (1994). Modern nutrition in health and disease. 8th Edn, part I, pp: 227 – 228.
9. John H. H., and Jeanne I. R., (1994). Food additives, contaminants and natural toxins, modern nutrition in health and disease. 8th Edn, part II, pp: 1597 – 1598.
10. Judith R. T., (1994). Modern nutrition in health and disease. 8th Edn, part I., pp: 237- 240.
11. Reddy A. T. V., and Yellamma K., (1996). Cadmium chloride induced alteration in the detoxification enzymes of rat liver and kidney. Pollution. Res., 15: 371 – 373.
12. Stewert, E.A Max, H.G John, A Parkinson and Christopher Q (1974), Chemical Analysis of Ecological Materials, Blackwell scientific publishers London, p13-243

**ABSTRACT CCT-: 062**Opeoluwa O. Fasanya¹, Rbed Isa¹, Sharafadeen Gbadamasi¹, Abdulazeez Y. Atta¹, Baba Y. Jibril²

1. Petrochemicals & Allied department, National Research Institute for Chemical Technology, Zaria

2. Department of Chemical Engineering, Ahmadu Bello University, Zaria, Kaduna State, Nigeria

Email: Unclezick@yahoo.com**KEY COMPONENTS OF CATALYSTS FOR METHANOL STEAM REFORMING: A SHORT REVIEW****1. Introduction**

There are concerns with regards to high levels environmental pollution rising from the use of fossil fuels. This and the reduction in fossil fuel levels are some of the factors attracting interest in renewable energy research. A variety of energy solutions have been identified; one of which is the use of hydrogen. More than 50 million tons of hydrogen is generated each year from fossil fuels by industry for these purposes (1). About half of the hydrogen produced world over is via methane steam reforming or natural gas reforming (2). This is an energy intensive process requiring temperatures as high as 700°C and results in high CO₂ emissions. The production of hydrogen from alcohols is an attractive route that has gained acceptance due to low energy requirements and a cleaner carbon footprint. Hydrogen driven PEMFC function with virtually no harmful emissions. Gaseous hydrogen has an energy density of 120 MJ/kg which is approximately three times that of gasoline. Transportation, handling, delivery and its low volume energy density (13kJ [dm]⁻³) of hydrogen (3) are however major challenges. In situ reforming of alcohols and hydrocarbons has been identified as means of tackling this problem (4).

Methanol has been considered as an excellent source of hydrogen. Properties such as low conversion temperatures (200-300°C), high hydrogen to carbon ratio (4:1) and the absence of C – C bond reducing soot formation have resulted in many researchers suggesting methanol as a viable alternative for commercial hydrogen generation (5, 6). Storage of methanol when compared to methane which is presently a primary source of hydrogen via methane steam reforming is also easier to handle as present liquid fuel dispensing technologies can be used (7). An added advantage is the relatively lower operating temperatures of methanol steam reforming (MSR) when compared to methane steam reforming which occurs at temperatures between 750-1000°C and pressures between 30-40 bar (7). The problem however associated with steam reforming of methanol are the products which accompany the formation of hydrogen which include carbon dioxide (CO₂), carbon monoxide (CO) and methane (CH₄). CO is detrimental to Proton exchange

membrane fuel cell (PEMFC), as poisoning of electrodes occur with CO concentrations as low as 10ppm (8).

Despite being the focus of research for the past the decades, work in this area is not losing steam. Typically copper-based catalysts specifically Cu-ZnO systems have been widely employed as commercial catalysts for methanol steam reforming, the CuZnOAl₂O₃ formulation in particular. These catalysts are well tuned towards the methanol steam reforming (MSR) process and are also used for methanol synthesis and the water gas shift reactions (9). Copper-based catalysts generally favor H₂ production with a high selectivity towards CO₂ (10) and a relatively high amount of CO selectivity especially for PEMFC use. But Inherent weaknesses such as sintering at high temperatures and low thermal stability are still a major concern. New ideas in the areas of catalyst composition, morphology and also reaction conditions are continuously being tested. The use of promoters, varying methods of synthesis and composition are factors which have significant effects on catalyst stability. Advances in surface sciences and nanotechnology to also alter the morphology are being explored in other to develop new catalysts and optimize existing catalysts. This review seeks to look at research work carried out over the last decade in catalyst composition applied in methanol steam reforming and highlight the more recent attempts at developing catalysts with low CO selectivity and high H₂ yield.

1.2 Catalyst Composition

MSR catalysts can be divided into two groups based on composition. Copper-based catalysts and group VIII-X based catalysts. The copper catalysts are generally characterized by high activity and selectivity while the second group have higher stability. Copper-based catalysts have been widely used for generating hydrogen from methanol (11). Though the CuZnO pairing is also used for methanol synthesis, water gas shift reaction and hydrogenation of CO_x (12).

The drawbacks of copper-based catalysts include pyrophoricity and deactivation at moderately high temperatures (11, 13), poor thermal stability at temperatures above 270°C is often experienced. Kawamura et al based on



their findings concluded that the dispersion of copper on zinc oxide improved catalytic activity for methanol conversion and reduced carbon monoxide selectivity compared with that of traditional catalysts (14). Zinc increases Cu dispersion resulting in increased activity of the metal catalyst (15). Increased dispersion is often tied to improved reducibility of CuO (16) which is responsible for increased catalytic activity of CuO/ZnO.

1.2.1 Zinc Oxide (ZnO)

Initially, ZnO was thought to just provide a means of increasing catalyst activity by providing increased Cu dispersion, it has now been shown to play a much larger role in the catalytic process. ZnO characteristically cracks methanol molecules and has been commonly utilized as a promoter and/or support for MSR (17). This Cu-ZnO pairing has been widely investigated due to high activity in methanol reforming. It has been suggested that a synergistic effect arises from the contact of ZnO with Cu as the binary catalyst is much more active than each component on its own (10). Tests have shown that reforming can take place on bare ZnO though with low selectivity towards hydrogen at temperatures between 180°C and 300°C (18). High temperature reforming (temperatures above 380°C) was carried out on ZnO-Al₂O₃ by the Yang group (19). Methanol conversion of almost 100% was gotten at 420°C with CO selectivities below generally 10%. Related work though revealed that MSR on ZnO has CO₂ selectivity as high as 99% depending on reaction conditions (20). Further buttressing this point is the high selectivity of CO₂ seen on ZnPd/ZnO particles. Heggen et al., (21) were able to show using aberration-corrected electron microscopy, electron energy loss spectroscopy and in situ heating experiments, that ZnO patches formed on the surface of ZnPd/ZnO catalysts. The ZnO patches rapidly increased selectivity towards CO₂ as the MSR reaction progressed.

The formation of a Cu-Zn alloy is thought to positively influence the reforming process evidenced by the work of Sanches et al., (22). They showed that a correlation between an increase in the Cu lattice constant and methanol conversion led to higher activity. The formation of the Cu-Zn alloy can be favoured by carrying out reduction with a gas possessing a high reduction potential such as H₂/CO mixture.

Various morphologies of ZnO have yielded varying levels of catalyst activity. Karim et al., (23) showed that more faceted ZnO brought about better catalyst activity. They compared ZnO of different morphologies with the same amount of palladium on each catalyst.

Cu, Pd and Au were deposited on ZnO nanorods grown by Danwittayakul and Dutta (18, 24) with H₂ selectivity of 25% being reported at 350°C. Low selectivity reported is probably due to the ZnO to cordierite ratio on which the ZnO rods were grown on. The duo further impregnated Cu on ZnO microballs (25) which resulted in an increased H₂ selectivity of 43%. The improved activity seems to be not only as a result of more copper being available for the reforming process but also the larger surface area of ZnO. Nakajima et al., (26) though silent on the H₂ selectivity demonstrated the process using ZnO nanowires, having CO selectivity of 5.7%.

The final nature of the ZnO; i.e surface area, morphology and polarity ratio strongly depends on the synthesis conditions (27).

1.2.2 Alumina

Addition of promoters to the traditional CuZnO matrix have yielded promising results in reduction of CO selectivity. Widely investigated promoters include CeO₂, Al₂O₃ and ZrO₂. The use of Al₂O₃ has yielded higher Cu dispersion but reduced catalytic activity once 10wt% is exceeded. The reduced activity has been attributed to high level of interaction between CuO and Al₂O₃ which not only leads to an increase in reduction temperature but also a reduction in copper surface area (16, 28). This translates to less methanol being adsorbed on the Cu surface. Higher levels of Al₂O₃ might result in more formation of methyl formate and formaldehyde as seen in reforming experiments carried out on Al₂O₃ (28, 29). Interestingly though, the work of Jones et al., (28); revealed that in using Al₂O₃ nanoparticles as support, lower CO selectivities were observed at higher temperatures. Postulating that the use of nanoparticles results in a more active copper surface being made available.

In summary, the addition of Al₂O₃ has been found to improve surface area, mechanical strength and prevent sintering (30).

1.2.3 Zirconium

Attention however has gravitated towards the use of zirconium as a promoter and more recently as a primary support (31, 32). CO selectivity with ZrO₂ is usually very insignificant (22). Catalyst reducibility and thermal stability are greatly increased by ZrO₂ addition. Playing a role similar to ZnO, ZrO₂ is able to also improve Cu dispersion often evidenced by diminishing peaks in XRD of ZrO₂ containing powders (33). This property is attributed to the amorphous phase of ZrO₂ in the catalyst (16). When compared with ZnO, highly dispersed ZrO₂ possesses a large



number of surface hydroxyl groups which aid in stabilizing Cu⁺ and promoting activity (33). In methanol synthesis, ZrO₂ serves as an adsorption site for CO₂ hydrogenation. In MSR however it is able to adsorb methanol and improve the mobility of lattice oxygen (33). ZrO₂ is able to lower the Al and weaken the interaction between CuO and Al₂O₃ to avoid CuAl₂O₄ spinel formation which retards MSR. Stability of ZrO₂ promoted Cu/ZnO/Al₂O₃ catalysts is dependent on striking a balance between Al₂O₃ and ZrO₂. Also, Cu-Zn alloy formation improved in the presence of ZrO₂ (22).

Utilizing zirconia and dysprosium (Dy), Silva et al., (9) synthesized a novel CuZrDyAl catalyst which had better selectivity and activity than commercial CuZnOAl₂O₃ catalyst at 180°C. They attributed their success to being able to achieve increased Cu reducibility brought on by the high level of Cu dispersion and the enhanced Cu interaction with the Zr matrix.

Cerium

Reports indicate that the use of 10wt% CeO₂ as a promoter increases catalyst life time, increases methanol conversion and H₂ selectivity for a CuZnOAl₂O₃ catalyst (34). In contrast, Huang et al reported that even though CeO₂ did improve Cu dispersion and mechanical properties of the catalyst, it did however weaken the MSR reaction (16).

Other metals

Promotion of MSR reactions using precious metals is also receiving attention. Gallium promoted CuZnO tests carried out by Toyir et al resulted in a double yield of H₂ when compared with the non-promoted catalyst. Their tests on the Ga impregnated catalysts also solely pure H₂ and CO₂ product was attainable at 320°C (35). These results were rather impressive considering that CO selectivity usually increases with increase in temperature.

2. Conclusion

Increased H₂ selectivity and reduced CO selectivity are the key factors which affect the choice of catalyst used for MSR. Various configurations are still being explored but the Cu/ZnO/Al₂O₃ catalyst still remains the commercial catalyst of choice even with the drawbacks associated with it. It is believed that the perfect support will allow for increased dispersion of copper on its surface and thereby result in increased activity. Research in this area continues and new configurations are constantly being investigated.

References

1. Trincado M, Banerjee D, Grutzmacher H. Molecular Catalysts for hydrogen production from alcohols. *Energy Environ Sci.* 2014;7:2464-503.

2. Sharma S, Ghoshal SK. Hydrogen the future transportation fuel: From production to applications. *Renewable and Sustainable Energy Reviews.* 2015;43:1151-8.

3. Ribeirinha P, Boaventura M, Lopes JCB, Sousa JM, Mendes A. Study of different designs of methanol steam reformers: Experiment and modeling. *International Journal of Hydrogen Energy.* 2014;39:19970-81.

4. Sa S, Silva H, Brandao L, Sousa JM, Mendes A. Catalysts for methanol steam reforming - A review. *Applied Catalysis B: Environmental* 2010;99:43-57.

5. Huang T-J, Chen H-M. Hydrogen Production via steam reforming of methanol over Cu/(Ce,Gd)O₂-X catalysts. *International Journal of Hydrogen Energy.* 2010(35):6218-26.

6. Kim T, Jo S, Song Y-H, Lee DH. Synergetic mechanism of methanol-steam reforming reaction in a catalytic reactor with electric discharges. *Applied Energy.* 2014(113):1692-9.

7. Chen W-H, Cheng T-C, Hung C-I. Modelling and simulation of microwave double absorption on methanol steam reforming for hydrogen production. *International Journal of Hydrogen Energy.* 2011(36):333-44.

8. Qi Z, He C, Kaufman A. Effect of CO in the anode fuel on the performance of PEM fuel cell cathode. *Journal of Power Sources.* 2002;111(2):239-47.

9. Silva H, Mateos-Pedrero C, Ribeirinha P, Boaventura M, Mendes A. Low-temperature methanol steam reforming kinetics over a novel CuZrDyAl catalyst. *Reaction Kinetics, Mechanisms and Catalysis.* 2015;115(1):321-39.

10. Yong ST, Ooi CW, Chai SP, Wu XS. Review of methanol reforming Cu-based catalysts, surface reaction mechanisms, and reaction schemes. *International Journal of Hydrogen Energy.* 2013;38:9541-52.

11. Mrad M, Hammoud D, Gennequin C, Aboukais A, Abi-Aad E. A comparative study on the effect of Zn addition to Cu/Ce and Cu/Ce-Al catalysts in the steam reforming of methanol. *Applied Catalysis A: General.* 2014(471):84-90.

12. Muhamad EN, Irmawati R, Taufiq-Yap YH, Abdullah AH, Kniep BL, Grgsdies F, et al. Comparative study of Cu/ZnO catalysts derived from different precursors as a function of aging. *Catalysis Today.* 2008;131:118-24.

13. Wang C, Boucher M, Yang M, Saltsburg H, Flytzani-Stephanopoulos M. ZnO-modified zirconia as gold catalyst support for the low-temperature methanol steam reforming reaction. *Applied Catalysis B: Environmental.* 2014(154-155):142-52.

14. Kawamura Y, Yamamoto K, Ogura N, Katsumata T, Igarashi A. Preparation of Cu/ZnO/Al₂O₃ catalyst for micro methanol reformer. *Journal of Power Sources.* 2005(150):20-6.

15. Ma Y, Guan G, Shi C, Zhu A, Hao X, Wang Z, et al. Low-temperature steam reforming of methanol to produce hydrogen over various metal-doped molybdenum carbide catalysts. *International Journal of Hydrogen Energy.* 2014;39:258-66.

16. Huang G, Liaw B-J, Jhang C-J, Chen Y-Z. Steam reforming of methanol over CuO/ZnO/CeO₂/ZrO₂/Al₂O₃ catalysts. *Applied Catalysis A: General.* 2009;358(1):7-12.

17. Danwittayakul S, Lakshman K, Al-Harhi S, Dutta J. Enhanced hydrogen selectivity via photo-engineered surface defects for methanol steam reformation using zinc oxide-copper nanocomposite catalysts. *Applied Catalysis A: General.* 2014;471:63-9.

18. Danwittayakul S, Dutta J. Zinc Oxide nanorods based catalysts for hydrogen production by steam reforming of methanol. *International Journal of Hydrogen Energy.* 2012;37:5518-26.

19. Yang M, Li S, Chen G. High-temperature steam reforming of methanol over ZnO-Al₂O₃ catalysts.



- Applied Catalysis B: Environmental. 2011;101(3):409-16.
20. Halevi B, Lin S, Roy A, Zhang H, Jeroro E, Vohs J, et al. High CO₂ Selectivity of ZnO Powder Catalysts for Methanol Steam Reforming. *The Journal of Physical Chemistry C*. 2013;117:6493-503.
21. Heggen M, Penner S, Friedrich M, Dunin-Borkowski RE, Armbrüster M. Formation of ZnO Patches on ZnPd/ZnO During Methanol Steam Reforming – A Strong-Metal-Support-Interaction Effect? *The Journal of Physical Chemistry C*. 2016;120(19):10460-5.
22. Sanches SG, Flores JH, Avillez RRD, Silva MIPd. Influence of preparation methods and Zr and Y promoters on Cu/ZnO catalysts used for methanol steam reforming. *International Journal of Hydrogen Energy*. 2012;37:6572-9.
23. Karim AM, Conant T, Datye AK. Controlling ZnO morphology for improved methanol steam reforming reactivity. *Physical Chemistry Chemical Physics*. 2008;10:5584-90.
24. Danwittayakul S, Dutta J. Controlled growth of zinc oxide microrods by hydrothermal process on porous ceramic supports for catalytic application. *Journal of Alloys and Compounds*. 2014;586:169-75.
25. Danwittayakul S, Dutta J. Two step copper impregnated zinc oxide microball synthesis for the reduction of activation energy of methanol steam reformation. *Chemical Engineering Journal*. 2013(223):204-308.
26. Nakajima H, Lee D, Lee M-T, Grigoropoulos CP. Hydrogen production with CuO/ZnO nanowire catalyst for a nanocatalytic solar thermal steam-reformer. *International Journal of Hydrogen Energy*. 2016(41):16927-31.
27. Mateos-Pedrero C, Silva H, Pacheco Tanaka DA, Liguori S, Iulianelli A, Basile A, et al. CuO/ZnO catalysts for methanol steam reforming: The role of the support polarity ratio and surface area. *Applied Catalysis B: Environmental*. 2015;174:67-76.
28. Jones SD, Neal LM, Hagelin-Weaver HE. Steam reforming of methanol using Cu-ZnO catalysts supported on nanoparticle alumina. *Applied Catalysis B: Environmental*. 2008;84(3):631-42.
29. Mrad M, Gennequin C, Aboukaïs A, Abi-Aad E. Cu/Zn-based catalysts for H₂ production via steam reforming of methanol. *Catalysis Today*. 2011;176(1):88-92.
30. Perez-Hernandez R, Mendoza-Anaya D, Martinez AG, Gomez-Cortes A. Catalytic steam reforming of methanol to produce hydrogen on supported metal catalysts. *Hydrogen Energy - Challenges and Perspectives: Intech*; 2012. p. 147-74.
31. Lopez P, Mondragon-Galicia G, Espinosa-Pesueira ME, Mendoza-Anaya D, Fernandez ME, Gomez-Cortes A, et al. Hydrogen production from oxidative steam reforming of methanol: Effect of the Cu and Ni impregnation on ZrO₂ and their molecular simulation studies. *International Journal of Hydrogen Energy*. 2012;37:9018-27.
32. Pérez-Hernández R, Gutiérrez-Martínez A, Espinosa-Pesqueira ME, Estanislao ML, Palacios J. Effect of the bimetallic Ni/Cu loading on the ZrO₂ support for H₂ production in the autothermal steam reforming of methanol. *Catalysis Today*. 2015;250:166-72.
33. Park JE, Yim S-D, Kim CS, Park ED. Steam reforming of methanol over Cu/ZnO/ZrO₂/Al₂O₃ catalyst. *International Journal of Hydrogen Energy*. 2014;39:11517-27.
34. Minaei S, Haghghi M, Jodeiri N, Ajamein H, Abdollahifar M. Urea-nitrates combustion preparation of CeO₂-promoted CuO/ZnO/Al₂O₃ nanocatalyst for fuel cell grade hydrogen production via methanol steam reforming. *Advanced Powder Technology*. 2017;28(3):842-53.
35. Toyir J, Ramírez de la Piscina P, Homs N. Ga-promoted copper-based catalysts highly selective for methanol steam reforming to hydrogen; relation with the hydrogenation of CO₂ to methanol. *International Journal of Hydrogen Energy*. 2015;40(34):11261-6.

**ABSTRACT CCT-: 040**

Anyim P. B.^{1*}, Okibe F. G.², Gadimoh S.¹, Salisu Z.M.¹, Daniel D.¹, Chibuzo-Anakor N.C.¹, Oddy-Obi I. C.¹, Suleiman M. A.¹, Lawal O.M.¹ and Ukpong M.K.¹.

1. Department of Textile Technology, National Research Institute for Chemical Technology, Zaria, Nigeria
2. Department of Chemistry, Ahmadu Bello University, Zaria, Nigeria

Email: ginikaanyim@gmail.com

ASSESSMENT OF HEAVY METALS CONTAMINATION OF BRASSICA OLERACEA L. CULTIVATED ON FARMLANDS ALONG HUNKUYI-ZARIA ROAD, NIGERIA

ABSTRACT: The aim of the present work was to determine possible heavy metal contamination of *Brassica oleracea* L cultivated along Hunkuyi-Zaria road. Standard procedure for the analysis of metals by Atomic Adsorption Spectrometry (AAS) was used to determine the concentration of the heavy metals in the samples. Results showed that Cu content of edible tissues of the vegetable ranged from 0.9 to 1.6 mg/kg; Pb 9.1 to 99.5 mg/kg; Cd 0.4 to 1.2 mg/kg; Zn 48.7 to 61.8 mg/kg and Cr 1.0 - 17.8 mg/kg during dry season. The results obtained for heavy metals levels in wet season were, Cu 1.1 to 22.4 mg/kg; Pb 59.7 to 336.6 mg/kg; Cd 0.4 to 1.1 mg/kg; Zn 68.8 to 95.6 mg/kg and Cr 6.6 to 28.5 mg/kg. The average values for lead, cadmium, zinc, copper and chromium were, 33.690, 0.360, 19.930, 0.580 and 5.180 mg/kg respectively. These average values were higher than WHO permissible limits of 0.900, 0.000, 0.000, 8.000, and 0.003 mg/kg for copper, lead, cadmium, zinc and chromium in vegetables respectively. Target Hazard Quotient (THQ) for lead across the three sampling stations was above 1.000 for both seasons with the highest value recorded at farm three of the wet season. THQ-based risk assessment in this study thus indicates that, the consumption of cabbage from the study area poses serious toxicological risk with respect to lead in all the seasons.

1. Introduction

Uptake of heavy metals by plants and subsequent accumulation along the food chain is a potential threat to animal and human health (Sprynskyy et al., 2007). The absorption of heavy metals by plants is one of the main routes of entrance into the food chain (Jorda, 2006).

Vegetables are common diet consumed by most human populations due to their rich vitamins, fibres and anti-oxidant content (Mohammed and Khamis, 2012). However, vegetables cultivated on contaminated soils take up heavy metals in quantities large enough to cause health problems to their consumers. This study was aimed at assessing some heavy metals contamination of *Brassica oleracea* L. cultivated on farmlands along Hunkuyi-Zaria road, Nigeria.

2. Materials and methods**2.1 Collection, preservation and preparation of sample**

The research was conducted on the irrigated *Brassica oleracea* L obtained from farms along Hunkuyi-Zaria road. The study area is located in Kudan Local Government Area of Kaduna State. Samples were collected twice in the year 2012 from three different farms: 1, 2 and 3. The first round of sampling was carried out in March towards the end of the dry season while the second round was in September at the peak of the rainy season. Fresh matured edible cabbage was randomly handpicked from farms: 1, 2 and 3 each during dry and wet seasons. All the samples were washed and dried in an oven at 80°C (Larry and Morgan, 1986).

Each sample was grounded into a fine powder, sieved and finally stored in a 250cm³ screw capped plastic bottle appropriately labeled. Exactly 2g of each of the cooled grounded

sample was weighed out into a Kjaedahl flask mixed with 20cm³ of concentrated perchloric acid and concentrated nitric acid in the ratio 1: 4 by volume respectively and left to stand overnight. Thereafter, the flask was heated at 70°C for about 40 min; the temperature was increased to 120°C for about 20 min. The mixture turned black after a while (Erwin and Ivo, 1992). The digestion was completed when the solution became clear and the appearance of white fumes. The digest was allowed to cool, and then filtered into 100 cm³ volumetric flasks and diluted to the mark with distilled water after washing the residue with distilled water. The filtrate was transferred into a screw capped bottle for analysis.

2.2. Sample analysis

Metal concentration in the digests was determined by Atomic Absorption Spectrophotometry, using Shimadzu Atomic Absorption Spectrophotometer (model AA-6800, Japan) equipped with Zeeman background correction and graphite furnace at National Research Institute for Chemical Technology (NARICT), Zaria-Nigeria. The calibration curve was prepared by running different concentrations of standard solutions. The instrument was set to zero by running the respective reagent blanks. Average values of three replicates were taken for each determination and were subjected to statistical analysis.

2.3 Statistical analysis

Data collected were subjected to statistical test of significance using the Analysis of Variance (ANOVA), Independent t-test, Pearson product moment correlation coefficient. The estimated daily metals intake from cabbage in this study was determined according to Addo et al., (2012) following equation (1).

Target Hazard Quotient (THQ) was computed using equation (2).

$$EDI = C_{\text{metal}} \times DAC \times C_{\text{factor}} / (BW) \dots \dots \dots (1)$$

Where C_{metal} (mg/kg) is the concentration of heavy metals in contaminated vegetable; DAC (kg/day) represents the daily average consumption of cabbage; C factor is the conversion factor = 0.085. BW is the body weight.

$$THQ = [W_{\text{plant}}] \times [M_{\text{plant}}] / RfD \times Bo \dots \dots \dots (2)$$

Where $[W_{\text{plant}}]$ is the daily intake of vegetables (kg per day of fresh weight), $[M_{\text{plant}}]$ is the concentration of metal in the vegetable (mg/kg). RfD is the oral reference dose for the metal (mg/kg) body weight per day), and Bo is the human body mass (kg).

3. Results

3.1 Concentration of metals in the edible cabbage (*Brassica oleracea*) tissues. The Mean concentration of Copper, lead, Cadmium Zinc and chromium, in samples of edible cabbage (*Brassica oleracea*) tissues from the three established sampling stations for the two seasons are presented Figures 3.1 and 3.2. The mean concentration of Cu in cabbage during dry season ranged from 0.9 mg/kg (farm 3) to 1.6 mg/kg (farm2); Pb in cabbage ranged from 9.1 mg/kg (farm 1) to 99.5 mg/kg (farms 2 and 3); Cd concentration in cabbage ranged from

0.4 mg/kg (farm 3) to 1.2 mg/kg (farm1); Zn ranged from 48.7 mg/kg (farm 2) to 61.8 mg/kg (farm 1) while Cr ranged from 1.0 mg/kg (farm 1) to 17.8 mg/kg (farm 2). The metal levels in wet season ranged as follows- the mean concentration of Cu in cabbage ranged from 1.1 mg/kg (farm1) to 22.4 mg/kg (farm 3); Pb ranged from 59.7 mg/kg (farm1) to 336.6 mg/kg (farm3); Cd ranged from 0.4 mg/kg (farm 3) 1.1 mg/kg (farm 2); Zn ranged from 68.8 mg/kg (farm 3) to 95.6 mg/kg (farm 1) while Cr ranged from 6.6 mg/kg (farm 3) to 28.5 mg/kg (farm 2).

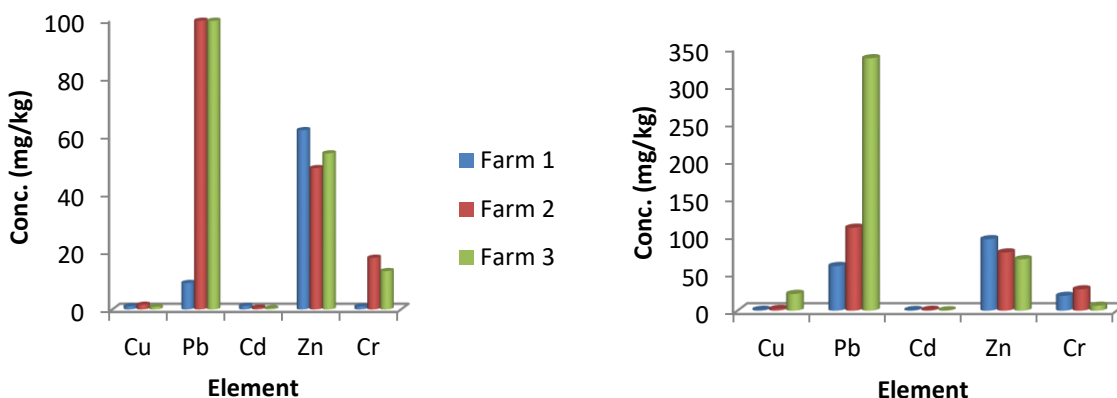


Fig. 1: Spatial distributions of metal concentration in edible tissues of *Brassica oleracea* L across sampling stations during dry season (**Fig. 2**) wet season.

3.2 Estimated daily intake

Table 1: Estimated daily metal intake (mg/kg b.w. /day) across the farms during dry season brackets indicate the RDI for females.

Element	Copper	Lead	Cadmium	Zinc	Chromium
Farm 1	0.53	4.42	0.58	30.02	0.49
Farm 2	0.78	48.33	0.29	23.65	8.65
Farm 3	0.44	48.33	0.19	26.13	6.41
Average	0.58	33.69	0.36	19.93	5.18
UL (mg/ day)	10.00	0.240	0.064	40.00	130 µg/day
RDI (mg/ day)	0.900	0.00	0.00	11(8)	0.003-1.5

**Table 2:** Estimated daily metal intake (mg/kg b.w. /day) across the farms during wet season brackets indicate the RDI for females.

Element	Copper	Lead	Cadmium	Zinc	Chromium
Farm 1	0.53	28.99	0.39	46.4	9.62
Farm 2	1.12	53.86	0.53	37.79	13.84
Farm 3	10.88	163.63	0.19	33.42	3.21
Average	4.20	65.49	0.37	39.20	8.89
UL (mg/day)	10.00	0.240	0.064	40.00	130µg/day
RDI (mg/day)	0.900	0.00	0.00	11(8)	0.003-1.5

Table 3: Target Hazard Quotient (THQ) of metals in edible Cabbage tissue during wet season.

Element	Copper	Lead	Cadmium	Zinc	Chromium
Farm 1	0.0012	7.85	0.37	0.044	0.0061
Farm 2	0.0027	14.57	0.51	0.0036	0.0087
Farm 3	0.026	44.28	0.18	0.0032	0.002
Average	0.01	22.23	0.35	0.017	0.0056

3.3 Discussion

The concentration of metals in the vegetable crop were significantly high above the value recommended by FAO/WHO (2001) except for Cu and Zn which were below the maximum recommended limit of 73.3 and 99.4 mg/kg respectively. The elevated levels of Pb far exceeded the recommended limit (of 0.3 mg/kg) in the sample especially during wet season could indicate other source such as vehicular emission than contaminants from irrigation water. Concentration of Cd of all the sample under investigation was above the maximum permissible concentration (of 0.2mg/kg) of Cd (FAO/WHO 2001).

This high level of Cd might be due to the use of cadmium-containing phosphate fertilizers. High concentration of metals observed in the vegetable crop could be as a result of high traffic density along that road. This is in agreement with the results of Abechi *et al.*, (2010). There was a generally increase in the average metal levels of samples collected during rainy season as compared to samples collected during dry season. This could be attributed to the possibility of runoffs from the surrounding land containing metal salts being washed into the farmlands (Lawal and Audu, 2011).

The difference in Cu, Pb, and Cd levels of cabbage between dry and wet season was not statistically significant ($p > 0.05$). However, the difference in Zn concentration between the two seasons was statistically significant ($p < 0.05$) with the concentration in wet season significantly higher than the dry season. This could be attributed to the dissolved salts of Zn present in the environment that get to the root of the of the crop at the on- set of the rain The difference in Cu, Pb, Cd and Cr levels of edible cabbage tissues across farms 1 and 2; 1 and 3; 2 and 3 respectively were statistically significant

(ANOVA $p < 0.05$). There was no significant difference in Zn levels across the farms (ANOVA $p > 0.05$). Significance differences observed could be due to the original soil content and anthropogenic activities such as the fertilizer applied to the farms the previous year.

Positive Correlation was observed between Cu and Pb ($r=0.941$); Cu and Zn ($r=0.037$); Cd and Zn ($r=0.313$); Cd and Cr ($r=0.115$). On the other hand, negative correlation was observed between Cu and Cd ($r=-0.453$); Cu and Cr ($r=-0.0341$); Pb and Cd ($r=-0.583$); Pb and Zn ($r=0.011$) and Pb and Cr ($r=-0.149$). Significant correlations were observed between Cu and Pb; Pb and Cd at 99% and 95% confidence levels respectively. The significant positive correlation observed between these elements indicates that increase in one elemental content of edible cabbage tissues brings about increase in the other and vice versa. It also shows that the same source is responsible for their presence at the concentrations determined. The reverse is the case in the case of negative correlation.

Estimated Daily Intake (EDI)

The estimated daily intake (EDI) of heavy metals is widely used to describe the safe levels of metallic intake through food consumed (Udiba et al, 2015). It also combines data on the levels of heavy metals in foodstuff with quantities of food consumed on the daily basis (Udiba et al., 2015). In this study the average seasonal daily copper, lead cadmium, zinc and chromium intake for people living in Zaria and its environs through the consumption of cabbage cultivated along Hunkuyi road were estimated and compared with the recommended daily intakes/or allowances (RDI) and the upper tolerable daily intakes for the metals (UL) (Tables 1 and 2). Tolerable



Daily Intake (TDI) is an estimate of the amount of elements in air, food or drinking water that can be taken in daily over a lifetime without appreciable health risk. The average values of the estimated daily intake for lead, cadmium and chromium were above the RDI and UL while copper intake was below the RDI and UL, zinc intake was above the RDI and below UL for both seasons (Table 1 and 2).

Target Hazard Quotients (THQ)

The THQ is the ratio between exposure and the reference oral dose (RfD). If the THQ is less than one, there is no obvious risk. THQ-based risk assessment method indeed provides an indication of the risk level due to exposure to pollutants (Chary et al., 2008). The average THQs for individual metals across the study area were all below 1.00 lead (Pb) being the only exception. Tables 3 and 4 show that the THQ for lead across the three farms were all above 1.00 for both seasons with the highest value recorded at farm three of the wet season. THQ-based risk assessment in this study thus indicates that, the consumption of cabbage from the study area poses serious toxicological risk with respect to lead intoxication irrespective of the season.

4. Conclusion and recommendation

The results obtained from this study have shown that there is increased danger of growing vegetable crops by Hunkuyi road Zaria. This could also be applicable to other major roads. The study showed that abundant concentration of heavy metals especially Pb, Cr and Cd could be directly related to the amount in the environment including the soil. The average values of the estimated daily intake for lead, cadmium and chromium were above the RDI and UL while copper intake was below the RDI and UL; zinc intake was above the RDI and below UL for both seasons. The average THQs for individual metals across the study area were all below 1.00 lead (Pb) being the only exception. THQ-based risk assessment in this study thus indicates that, the consumption of cabbage from the study area poses serious toxicological risk with respect to lead intoxication irrespective of the season. Therefore, a clean-up procedure should be embarked on to reduce the heavy metal concentration in the soil

either by use of bioremediation, particularly phytoremediation which involves the use of plants in the detoxification of the soil. With respect to the information obtained from this study, a research should be carried out on the source of irrigation water to actually ascertain the major source of these pollutants. Also routine and periodic assessment of metal pollution in agricultural soils in relation to vegetable production and depending on waste water irrigation in dry season is important because of the potential risk posed to animals and human through food chain.

Reference

1. Abechi, E.S., Okunola, O.J., Zubairu, S. M. J., Usman, A.A. and Akpene, E. (2010). Evaluation of heavy metals in roadside soils of major streets in Jos metropolis, Nigeria. *Journal of Environmental Studies*. 2(6): 387-389
2. Addo M. A., Darko, E.O., Gordon, C., Nyarko B. J. B. (2013), *e-Journal of Science & Technology*, 3(8), 71-83.
3. FAO/WHO, (2001). Codex Alimentarium Commission. Food additives and Contaminant. Joint FAO/WHO food Standards Program, ALINORM 01/2A, pp:1-289.
4. Erwin J.M, Ivo N. (1992). Determination of Lead in tissues: A pitfall due to wet digestion procedures in the presence of sulphuric acid. *Analyst*. 17: 23-26.
5. Jordao C.P., Nascentes C.C., Cecon P.R., Fontes R.L.F. and Pereira J.L. (2006). Heavy metal availability in soil amended with composted urban solid wastes. *Environmental Monitoring and assessment*, 112, 309–326
6. Larry R.W. and Morgan J.T. (1986). Determination of Plant Iron, Manganese and Zinc by wet digestion procedures. *J. Food Agric.*, 37: 839-844.
7. Lawal, A. O. and Audu, A. A. (2011). Analysis of heavy metals found in vegetables from some cultivated irrigated gardens in the Kano metropolis, Nigeria. *Journal of Environmental*
8. Sprynskyy M., Kosobucki P., Kowalkowski T. and Buszewsk B. (2007). Influence of clinoptilolite rock on chemical speciation of selected heavy metals in sewage sludge.
9. Udiba U. U., Bate Garba, Mahmud Abdullahi, Umar Shitu, Zakariyya Ahmad, Agboun T. D. T, Ozogu, A. N. (2015), Evaluation of the Pollution Status of River Galma Basin in the Vicinity of Dakace Industrial Layout, Zaria, Nigeria (in press)
10. Mohammed N.K and Khamis FO (2012). Assessment of heavy metal contamination in vegetables consumed in Zanzibars, *Natural Science* 4(8), 588-594. <http://dx.doi.org/10.4236/ns.2012.48078>

**ABSTRACT CCT-: 067**

Gbadamasi S.^{1*}, O. O. Fasanya¹, A. R. Isa¹, A. O. Umar¹, Z. S. Gano¹, A. Y. Atta¹, B. Y. Jibril², B. Mukhtar², B. O. Aderemi².

1. Petrochemicals & Allied Department, National Research Institute for Chemical Technology, Zaria
2. Department of Chemical Engineering, Ahmadu Bello University, Zaria, Kaduna State, Nigeria

Email: engrsharaf2009@hotmail.com

AROMATIZATION OF LIQUEFIED PETROLEUM GAS OVER ZnO/ZSM-5 CATALYSTS

ABSTRACT: Aromatization of liquefied petroleum gas (LPG) was investigated over ZnO/ZSM-5 prepared via impregnation method. Three ZnO/ZSM-5 catalysts with different ZnO loading were synthesized and the performance was investigated in a fixed-bed reactor. The synthesized catalysts were characterized using N₂-adsorption-desorption, XRD, SEM-EDX, and UV-Vis techniques. The activity results revealed that the reaction proceeds via bifunctional mechanism viz cracking, oligomerization, cyclization, and isomerization on the ZSM-5, and dehydrogenation over the ZnO. Remarkably, over 90% LPG conversion was recorded for the three catalysts and the high conversion was sustained even at 5 h of sampling. However, of the three catalysts, 2wt.% ZnO/ZSM-5 is the most selective catalyst to aromatics formation, with ~51% aromatics selectivity. The superior performance of 2 wt.% ZnO/ZSM-5 was attributed to the presence of more ZnO as compared to 0.5wt.% ZnO/ZSM-5, and presence of superior mesopore area, BET total surface area, pore volume and pore sizes than 5wt.% ZnO/ZSM-5.

1. Introduction

The commercial interest of LPG aromatization is well demonstrated with the development of several processes. The major interest of these processes is to allow the conversion of low value gaseous alkanes produced in remote fields into valuable and easier to be transported aromatics (benzene, toluene, xylene and ethylbenzene (BTX and EB)). Light aromatics are used as blending agents in the refineries to improve the octane rating of gasoline, and as major raw materials for petrochemical industries. The transformation of LPG to BTX and EB proceed over bifunctional catalysts (metallic and acidic sites) and involves series of reaction steps, viz cracking, dehydrogenation, cyclization, isomerization, oligomerization and aromatization. The series of reactions and the complexity involves makes the preparation of high performing catalysts very difficult [1, 5].

H-ZSM-5 is the most studied catalyst for this type of reaction, because of its unique structure and its ability to enhance all the reactions stages involve during the aromatization reactions. However, its ability to produce light alkanes during the protolytic cracking steps reduces its selectivity to aromatics and EB [6]. Also, high acidity from the HZMS-5 is responsible for olefins oligomerization and cyclization but it's not suitable for dehydrogenation that is key in aromatics formation [7]. To address this challenge, ZSM-5 has been doped with Ga [1, 5, 8, 9], Zn [7, 10-12], Pt [13, 14], Mo₂C [4, 15], Re [16, 17], Mo [9] with the aim of achieving better aromatics selectivity. Keen attention has been placed on Zn/HZSM-5 catalysts both from a fundamental and an applied point of view. Ai Sha *et al.* [2] studied the aromatization of n-butane over 6 wt.%ZnO/HZSM-5(26) and reported a conversion of 99.9%. Though more emphasis was on the conversion, but further analysis revealed aromatics selectivity of 29.5%

and gas selectivity of 70.5%. In another report by Baradaran *et al.* [7], they studied the aromatization of propane over ZnO/HZSM-5 using 0.5 wt.% ZnO. They reported improved aromatics selectivity and attributed the catalyst performance to the presence of ZnO and HZSM-5 crystallinity.

Though there have been significant reports in open literature on the use of ZnO/HZSM-5 as catalyst for propane and butane aromatization, but limited research has been done on its usage in LPG aromatization. Therefore, the main goal of the present study is to investigate the aromatization of LPG over ZnO/ZSM-5(50). Different ZnO/ZSM-5(50) with varying ZnO loading were synthesized and the catalytic activity investigated in fixed-bed reactor and the products analyzed using an online GC.

2. Experimental**2.1. Catalysts preparation**

The ZSM-5(50) (CBV 5524G, Zeolyst International) used as support for the catalyst synthesis was first calcined at 550 °C for 5 h to convert the ZSM-5(50) to HZSM-5(50) from its ammonium form and labelled CAT1. 0.5, 2 and 5 wt.% ZnO were subsequently impregnated into the CAT1 using the wetness impregnation method with Zn(NO₃)₂.6H₂O (≥99%, JHD Chemical) as ZnO precursor. In a typical synthesis, calculated amount of finely grinded CAT1 was dispersed in de-ionized water and a solution of Zn(NO₃)₂.6H₂O containing calculated amount of ZnO was added drop-wise. The excess water was evaporated on a hot plate under stirring conditions at ~70 °C. The obtained sample was oven dried at 80 °C for 17 h and subsequently calcined at 550 °C for 5 h. The obtained catalysts were labelled CAT2, CAT3 and CAT4 respectively.

2.2 Catalysts characterization

The N₂ sorption isotherms of the samples were measured on a V-Sorb 2800P Surface Area and Porosimetry Analyzer at 77 K. Prior to the analysis, all samples were pretreated at 250 °C for 9 h under vacuum to remove water and any dissolved gasses. The surface areas were calculated by BET method and the BJH method was applied to the adsorption branch of the isotherms to determine the pore size distribution and pore volume of the catalysts. The XRD patterns of the catalysts were recorded on a PXRD PANalytical EMPYREAN diffractometer equipped with Cu-K α ($\lambda = 1.5406 \text{ \AA}$) radiation source operating at 40 mA and 40 kV in the 2θ range of 5° to 60°. The scan step size was 0.013° s⁻¹ and the ZnO crystallite size was calculated using the Scherrer equation from the diffraction peak at d(100). The morphological features of the catalysts were taken on an ultra-high vacuum and high-resolution FEI-XL-30 scanning electron microscope. The ultraviolet-visible (UV-Vis) spectra were

obtained from Shimadzu UV – 2500PC Series spectrometer, using methanol as reference.

2.3 Catalysts activity tests

The catalysts activity was investigated for the aromatization of LPG at atmospheric pressure in a fixed-bed reactor (Finetec finereactor–4100) with a length of 55 cm and 11 mm internal diameter. For every reaction, 80 vol.% of N₂, 20 vol.% of LPG and 1.0 g of mixture of catalyst and diluent (powdered glass beads) were used. Upon attaining the reaction temperature, the system is allowed for 1 h to stabilize, after which samplings are made after every 1 h. The products were analyzed online using a gas chromatograph (BUCK Scientific, model 910) equipped with a TCD connected to both molesieve 13X and Hayescp D columns, and an FID connected to a 60 m \times 0.53 mm \times 5 μ m Restek MXT–1 capillary column.

3. Results and discussion

3.1 Catalysts characterization

Table 1: Physicochemical properties of the synthesized catalysts

Catalysts	BET (m ² /g)	Micropore area (m ² /g)	Mesopore area (m ² /g)	Average pore volume (cm ³ /g)	Average pore size ^a (Å)	ZnO crystallite Size ^c (Å)
CAT1	358.7	225.1	133.6	0.1919	34	–
CAT2	360.6	244.3	116.3	0.1750	29	460
CAT3	339.7	248.7	91.0	0.1615	29	537
CAT4	299.6	227.8	71.8	0.1429	26	403

a BJH adsorption average pore diameter. *b* BJH adsorption pore volume. *c* Calculated by using Scherrer equation based on XRD results

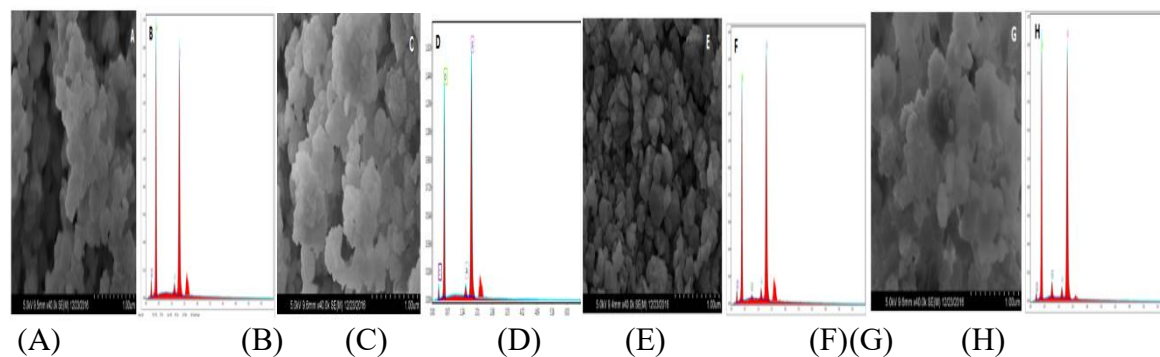


Fig. 1. SEM images of (A) CAT1, (C) CAT2, (E) CAT3, (G) CAT4 and EDX images of (B) CAT1, (D) CAT2, (F) CAT3, (H) CAT4

The textural properties of CAT1 and the corresponding catalysts were investigated using N₂ adsorption–desorption analysis and the results are summarized in Table 1. The results obtained shows that CAT1 has a BET surface area of 358.7 m²/g, an average pore volume of 0.1919 cm³/g and an average pore size of 34 Å. In addition, the microporous section contributed an area of 225.1 m²/g to the BET surface area, which is almost twice the mesopore area of 133.6 m²/g. However, there

was a noticeable decrease in the BET surface area of the catalysts as ZnO was impregnated. ZnO impregnation resulted into possible surface coverage of the mesopore section of the catalysts as evident from Table 1, and the decrease in surface area increases with increase in ZnO loading. Furthermore, there was also decrease in the average pore volume and average pore size of the catalysts upon impregnation of ZnO. Expectedly, this decrease increases with increase in the ZnO

loading and could be associated to partial pore blockage by the impregnated ZnO. Though there was a decrease in the average pore size, however, the final pore size still falls within the mesoporous region as per IUPAC classification. This is a desirable property as it would enhance diffusivity during the aromatization reaction.

Fig. 1 shows the SEM images and the corresponding EDX of the support, CAT1 and the catalysts, CAT2, CAT3 and CAT4. The images revealed highly crystalline ZSM-5(50) with hexagonal morphology. Upon impregnating ZnO, there was no observable change in the morphology of the parent ZSM-5(50), as the tetragonal is maintained. Though, the presence of ZnO could not be clearly seen from the SEM images, however, the EDX result confirm its presence. In addition, ZnO could not be detected in for CAT2, and the could be associated to the detection limit of the machine used, as CAT2 only contains 0.5 wt.% ZnO.

Fig. 2 shows the XRD patterns for the support (CAT1) and the corresponding catalysts (CAT2, CAT3 and CAT4). The results show that the crystalline nature of the ZSM-5(50) was maintained upon calcination to obtain CAT1. The patterns for CAT2, CAT3, and CAT4 showed similar diffraction peaks as the parent CAT1, except for slight increment of the peak at $2\theta = 31.1^\circ$, 34.3° , and 36° . These peaks at $2\theta = 31.1^\circ$, 34.3° , and 36° correspond to the (100), (002), and (101) hexagonal structured ZnO respectively (JCPDS 01-079-0208). The ZnO crystallite sizes of the catalysts, calculated by Scherrer equation, using the peak d(100) are presented in Table 1. The results reveal that the average crystallite size of ZnO in each catalyst is larger than the corresponding pore diameter of the support, CAT1. This observation suggests that some particles of the active component are deposited on the external surface of the CAT1 during impregnation and consequently, decrease in mesopore area.

Table 2: Composition of the used LPG

LPG Component	Composition (%)
Methane	0.08
Ethane	1.93
Propane	3.37
Butane	94.48
Pentane	0.14

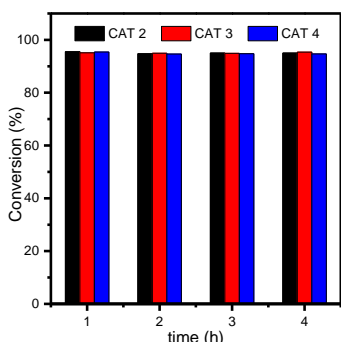


Fig. 4. LPG conversion at 520 °C and catalyst: diluent = 50%:50%

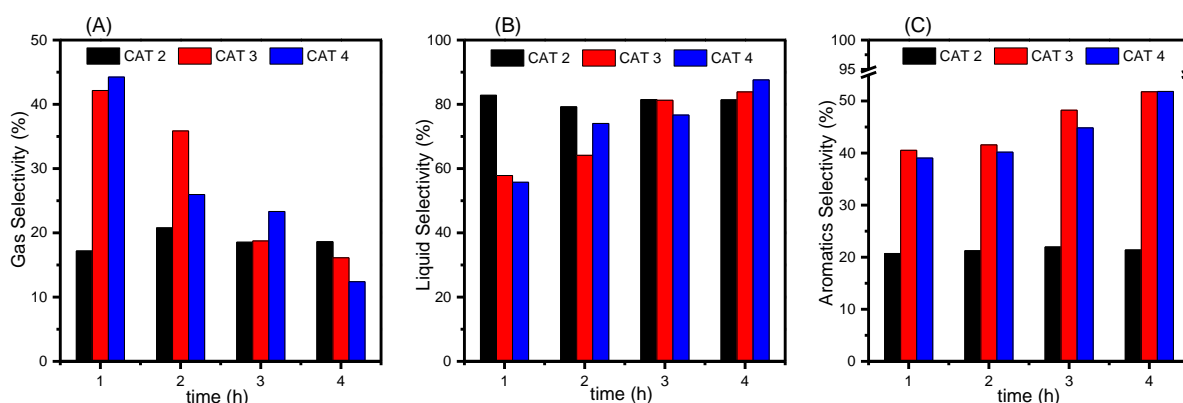


Fig. 5. (A) Gas, (B) Liquid, and (C) Aromatics Selectivity at 520 °C and catalyst: diluent = 50%:50%



The catalytic activity test was carried out in a fixed-bed reactor at 520 °C and 580 °C, at atmospheric pressure, and using liquefied petroleum gas (LPG) as the feed. As can be seen from Table 2, the used LPG is made up of butane, propane, ethane pentane, and methane, with butane being the major component. The products of the aromatization reactions are grouped into two, viz, gas component (majorly methane and ethane) and liquid component (BTX, EB and C9+). The conversions of the three synthesized catalysts at 520 °C are presented in Fig. 4. All the catalysts show high conversion of about 95%, and this was sustained even after 4 h of reaction. These high and comparable conversions could be attributed to the presence of similar catalysts structure and comparable acidity as there was no structural modification during synthesis. As reported by Ai Sha *et al.* [2], the conversion of LPG proceeds via cracking, isomerization, dehydrogenation and oligomerization reactions, and the structures of ZSM-5 and its acidity are desirable tools in achieving these goals. On the other hand, the gas, liquid and aromatics selectivity varies from one catalyst to the other (Fig. 5). For all the catalysts, the gas selectivity decreases with increase in reaction time, except for CAT 2 that shows almost same gas selectivity throughout the reaction (Fig. 5(A)). A gas selectivity, as high as ~45% and ~42.5% were obtained for CAT 4 and CAT 3 respectively at 1 h of sampling. However, at 4 h of on stream analysis, the gas selectivity for CAT 3 and CAT 4 decreased to a value below 20%, and this could be associated to the conversion of the gaseous component to the liquid component of the product.

The liquid (BTX, EB and C9+) and the aromatics (BTX and EB) selectivity for the synthesized catalysts are shown in Fig. 5 (B) and (C) respectively. As shown in Fig. 5B, the liquid selectivity for CAT 2 is greater than 80% for all the reaction time. However, when this is compared to the aromatics selectivity (Fig. 5 (C)), it is event that most of the liquid product produced by CAT 2 are C9+. On the other hand, the liquid selectivity for CAT 3 and CAT 4 increases with increasing sampling time until an impressive value of greater than 80% (Fig. 5 (B)). In addition, the aromatics selectivity for CAT 3 and CAT4 increases with an increase in sampling time. All these results indicate that the presence of ZnO in the catalysts improve its selectivity to aromatic compounds. As reported by Ivanova *et al.* [10] and Caeiro *et al.* [20], the presence of ZnO in aromatization reaction enhances the dehydrogenation and oligomerization steps and consequently improves the formation of aromatics and EB compounds. Therefore, the superior

performance of CAT 3 and CAT 4 in the present study could be easily associated with the presence of more ZnO in the CAT 3 and CAT 4. Comparing the performances of CAT 3 and CAT 4, it is evident that CAT 3 performed comparable to CAT 4 though containing less amount of ZnO than CAT 4. This observation is attributable to the superior mesopore area, BET total surface area, pore volume and pore sizes of CAT 3.

4.0 Conclusion

The present study investigated the effect of ZnO loading on ZSM-5 for the aromatization of LPG. Based on the obtained results and subsequent discussions, it is concluded that:

1. *The aromatization of LPG proceeds via a bifunctional mechanism as the reaction requires ZnO sites for dehydrogenation steps and acidic protonic sites for oligomerization and cyclization steps.*
2. *Irrespective of the amount of ZnO used, the reaction proceeds via the same reaction steps and similar product composition was obtained.*
3. *Of the three synthesized catalysts, CAT 3 (containing 2 wt.% ZnO) has the superior performance, which is attributed to the presence of more ZnO as compared to CAT 2, and presence of superior mesopore area, BET total surface area, pore volume and pore sizes than CAT 4.*

References

1. Liu, R.-l., et al., *Aromatization of propane over Ga-modified ZSM-5 catalysts.* Journal of Fuel Chemistry and Technology, 2015. **43**(8): p. 961-969.
2. Ai Sha., N.L.H., et al., *Catalytic conversion of n-butane over Au-Zn-modified nano-sized HZSM-5.* Chinese Journal of Catalysis, 2013. **34**(6): p. 1262-1266.
3. Solymosi, F. and A. Széchenyi, *Aromatization of isobutane and isobutene over Mo2C/ZSM-5 catalyst.* Applied Catalysis A: General, 2004. **278**(1): p. 111-121.
4. Song, Y., et al., *An effective method to enhance the stability on-stream of butene aromatization: Post-treatment of ZSM-5 by alkali solution of sodium hydroxide.* Applied Catalysis A: General, 2006. **302**(1): p. 69-77.
5. Ogunronbi, K.E., N. Al-Yassir, and S. Al-Khattaf, *New insights into hierarchical metal-containing zeolites; synthesis and kinetic modelling of mesoporous gallium-containing ZSM-5 for propane aromatization.* Journal of Molecular Catalysis A: Chemical, 2015. **406**: p. 1-18.
6. Lukyanov, D.B. and T. Vazhnova, *Aromatization activity of gallium containing MFI and TON zeolite catalysts in n-butane conversion: Effects of gallium and reaction conditions.* Applied Catalysis A: General, 2007. **316**(1): p. 61-67.
7. Baradaran, S., et al., *Isobutane aromatization in the presence of propane as a co-reactant over H-ZSM-5 catalysts using different crystallization times.* Journal of Industrial and Engineering Chemistry, 2015. **27**: p. 354-361.
8. Krishnamurthy, G., A. Bhan, and W.N. Delgass, *Identity and chemical function of gallium species inferred from microkinetic modeling studies of*



- propane aromatization over Ga/HZSM-5 catalysts. *Journal of Catalysis*, 2010. **271**: p. 370–385.
9. Themba, E.T. and S.S. Michael, *Aromatization of n-hexane over Ga, Mo and Znmodified H-ZSM-5 zeolite catalysts*. *Catalysis Communications*, 2015. **72**: p. 49–52.
 10. Ivanova, I.I., et al., *Surface species formed during propane aromatization over Zn/MFI catalyst as determined by in situ spectroscopic techniques*. *Journal of Molecular Catalysis A: Chemical*, 2009. **305**(1-2): p. 47-53.
 11. Oscar, A.A., A.E. Griselda, and B.P. Liliana, *Catalytic conversion of natural gas with added ethane and LPG over Zn-ZSM-11*. *Applied Catalysis A: General*, 2000. **190**: p. 169–176.
 12. Berndt, H., G. Lietz, and J. Viilter, *Zinc promoted H-ZSM-5 catalysts for conversion of propane to aromatics: II. Nature of the active sites and their activation*. *Applied Catalysis A: General*, 1996. **146**: p. 365-379.
 13. Reschetilowski, W., et al., *Influence of platinum dispersion on the ethane aromatization on Pt/H-ZSM-5 zeolites*. *Applied Catalysis*, 1991. **78**(2): p. 257-264.
 14. Takayuki, K., M. Masami, and Y. Tatsuaki, *Aromatization of butane on Pt-Ge intermetallic compounds supported on HZSM-5*. *Applied Catalysis A: General* 2000. **194–195**: p. 333–339.
 15. Solymosi, F. and A. Szechenyi, *Aromatization of isobutane and isobutene over Mo2C/ZSM-5 catalyst*. *Applied Catalysis A: General* 2004. **278**: p. 111–121.
 16. Linsheng, W., O. Ryuichiro, and I. Masaru, *Selective Dehydroaromatization of Methane toward Benzene on Re/HZSM-5 Catalysts and Effects of CO/CO2 Addition*. *Journal of Catalysis*, 2000. **190**: p. 276–283.
 17. Jianjun, G., et al., *Dehydrogenation and aromatization of propane over rhenium-modified HZSM-5 catalyst*. *Journal of Molecular Catalysis A: Chemical*, 2005. **239**: p. 222–227.
 18. Premanathan, M., et al., *Selective toxicity of ZnO nanoparticles toward Gram-positive bacteria and cancer cells by apoptosis through lipid peroxidation*. *Nanomedicine: Nanotechnology, Biology and Medicine*, 2011. **7**(2): p. 184-192.
 19. Goh, E.G., X. Xu, and P.G. McCormick, *Effect of particle size on the UV absorbance of zinc oxide nanoparticles*. *Scripta Materialia*, 2014. **78**: p. 49-52.
 20. Caeiro, G., et al., *Activation of C2–C4 alkanes over acid and bifunctional zeolite catalysts*. *Journal of Molecular Catalysis A: Chemical*, 2006. **255**(1-2): p. 131-158.
 21. Van der Mynsbrugge, J., et al., *Theoretical Analysis of the Influence of Pore Geometry on Monomolecular Cracking and Dehydrogenation of n-Butane in Brønsted Acidic Zeolites*. *ACS Catalysis*, 2017. **7**(4): p. 2685-2697.
 22. Seddon, D., *Paraffin oligomerisation to aromatics*. *Catalysis Today*, 1990. **6**(3): p. 351-372.

**ABSTRACT CCT-: 042**Alhassan Y.^{1*} and N. Kumar²

1. National Research Institute for Chemical Technology, P.M.B. 1052, Zaria, Nigeria

2. Delhi Technological University, 110042 New-Delhi, India

Email: lahassan897@yahoo.com**HYDROTHERMAL LIQUEFACTION OF *Jatropha curcas*: ENERGY EVALUATION AND RECOVERY**

ABSTRACT: Hydrothermal liquefaction (HTL) process, a super-specialty biomass conversion technique has received attention, recently. In this research, the HTL of whole *Jatropha curcas* biomass was conducted to produce bio-crude oil in a high pressure reactor at 350 °C. The products yields (bio-crude oil and residue) and degree of liquefaction are evaluated. In addition, the total energy recovery of the bio-crude oil was evaluated. The modified Van Krevelen diagram showed higher effective H/C ratio (1.3-1.8) was found, with corresponding O/C ratio (0.56-0.83). The bio-crude oil HHV obtained was 28.56 ± 0.73 (MJ/kg). It is therefore deduced that, biomass liquefaction into bio-crude oil is an efficient technique for the production of bio-crude oil with improved energy potential for transportation.

Keywords: Energy recovery, Oxygenated compounds, Bio-crude oil and Yields.

1. Introduction

Hydrothermal liquefaction [HTL], is an environmentally friendly process by which biomass including agricultural wastes is converted to obtain liquid fuel and chemicals at temperature range from 423K-623K; yielding bio-char, bio-crude or heavy oil and gaseous products. This is because; all the products (bio-char, aqueous phase, gas and bio-oil) obtained from this process are energy dense constituents. Liquid products (bio-oil and aqueous phase) formed the greater portion of the liquefaction products

Energy recovery is the central in considering the economic sustainability of biofuels. The final energy recovery of fuels determined its application as transportation fuel. This is defined as the ratio of the energy in total biomass conversion, to total energy that could be recovered from the combustion of such a fuel obtained from the biomass. Also, the heat recovery and losses are taking into consideration [1].

Carbon and hydrogen content of liquid fuels are important energy indicators, since, a complete fuel combustion is said to occur when; all carbon and hydrogen are converted into carbon dioxide and water, respectively. Principally, the evaluation of such net energy ratio requires the understanding of the mass, energy recovery and elemental balances at each step of the entire process [2]. An effective representation of such energy density is in the value of its H/C and O/C ratios; since fuels and feedstock energy content increases with decreasing O/C and increasing H/C ratio [3], [4].

Jatropha curcas has rich oil content, making it suitable for biodiesel production. According to Alhassan et al. [3], *Jatropha* de-oiled cake, formed aromatic oil via condensation and hydrolysis reactions, yield high bio-oil product. In this papers, energy evaluation of bio-crude

oil obtained from the HTL of de-oiled *Jatropha curcas* seed cake was conducted. The carbon, nitrogen and energy recoveries of the feedstock and product was evaluated.

2. Materials and method

The HTL of *Jatropha curcas* seed was conducted in reactor unit of 100 mL capacity (Fig. 1). The reactor is made-up of stainless steel container which is completely immersed into a heater, such that the maximum working temperature of 600 °C and pressure of 120 MPa are obtainable. Biomass-water slurry mixture is loaded into the reactor in the ratio (1:10), while Na₂CO₃ is used as catalyst and Nitrogen gas is purged into the reactor. Detailed procedure and feedstock characterization has already been reported in our previous works [3]. Equations (1-3) are employed to evaluate the recovery of individual elements.

3. Results and discussion

The hydrogen content in the product was found to be uniformly distributed and independent of the product yield, ranging from 4.23 wt% – 6.02 wt%. Hydrogen recovery (HR) was slightly different from the trend. However, the possible variation could be due to the production of hydrogen-rich compounds during the secondary reactions in the production process. It was presumed that, HTL proceeds via step-wise reactions including; hydrolysis, decarboxylation, rearrangements etc, which are increasing the H/C ratio. For example, decarboxylation reaction favored the production of high quality fuel due to its improvement in the H/C ratio. Fig. 2 presents the modified Van krevalen diagram of bio-crude oil. Carbon content increases with increasing product yield.

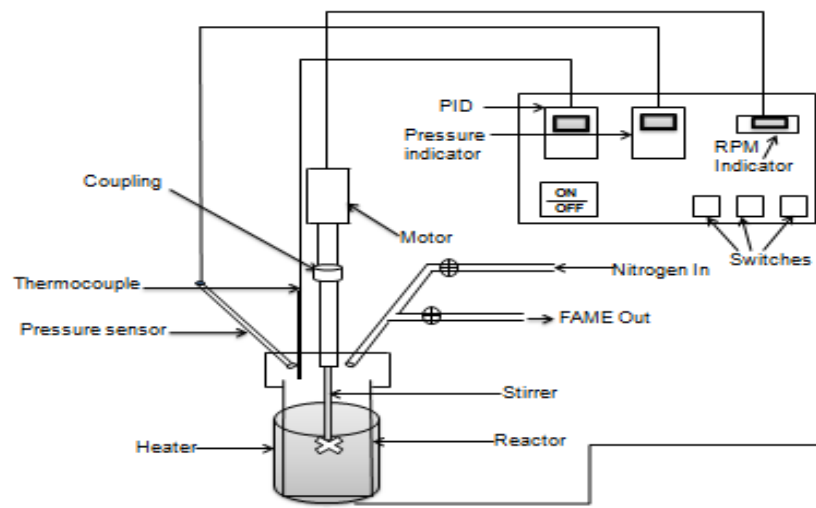


Fig. 1: Schematic diagram of the hydrothermal liquefaction reactor used

$$HR (\%) = \text{Mass}_{(\text{Product})} \times \text{Hydrogen}_{(\text{of Product})} / \text{Mass of Hydrogen}_{(\text{Feedstock})} \times 100 \text{ (Eqn.1)}$$

$$CR (\%) = \text{Mass}_{(\text{Product})} \times \text{Carbon}_{(\text{Product})} / \text{Mass of Carbon}_{(\text{Feedstock})} \times 100 \text{ (Eqn.2)}$$

$$ER (\%) = \text{HHV}_{(\text{Product})} \times \text{Mass of Product} (\%) / \text{HHV}_{(\text{Feedstock})} \times \text{Mass}_{(\text{Feedstock})} \times 100 \text{ (Eqn.3)}$$

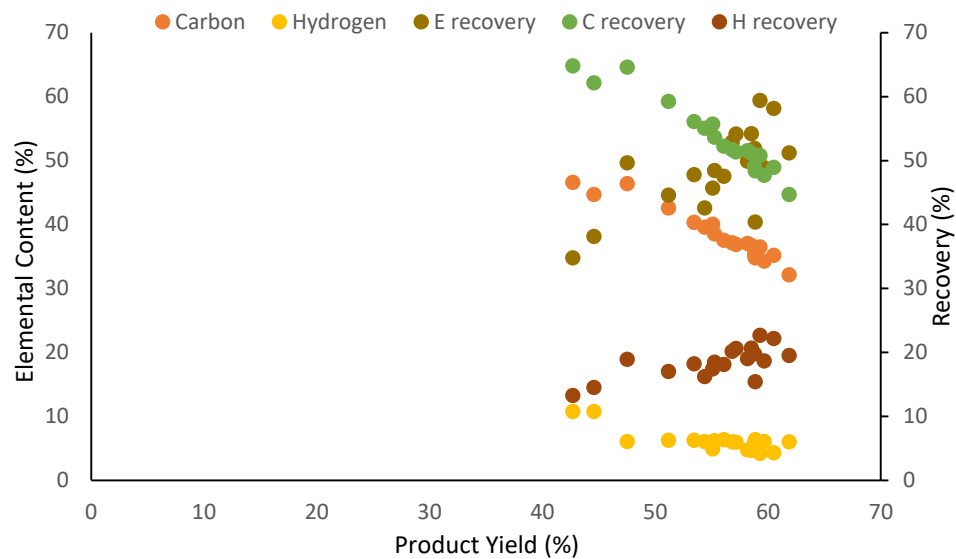


Fig. 2: Modified Van krevalen diagram of bio-crude oil

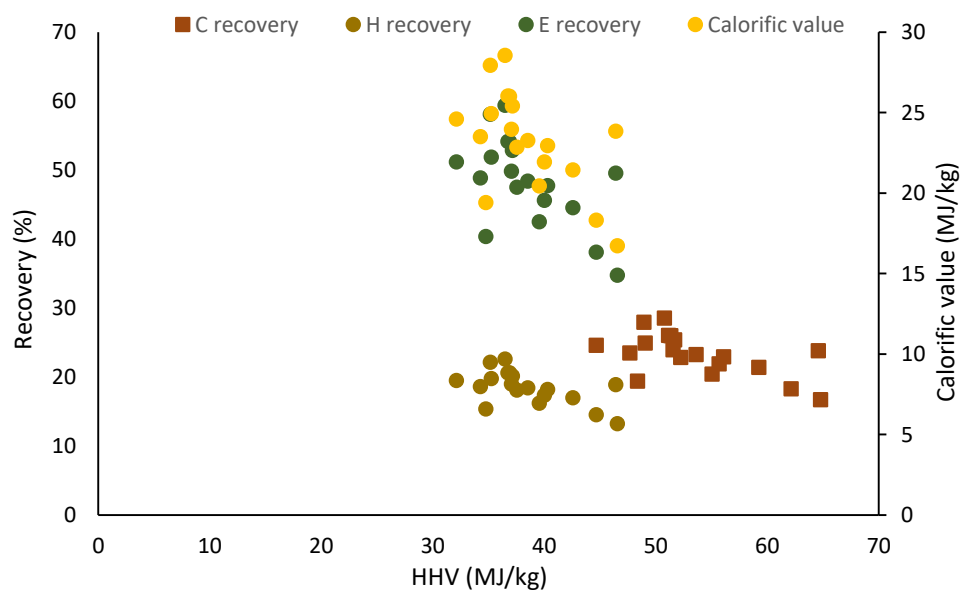


Fig. 3: Energy recovery profile of bio-crude oil



This is because, carbon bond, though stable, but has high tendency for the formation of lower molecular weight compounds. Since, multitude of reactions are taking place, at this point (β -O-4) bond of the biomass, it was proposed that at supercritical point of water, for example; less energy intense reactions are a preferentially favoured. Carbon and hydrogen are positive energy indicators in bio-crude oil, while nitrogen, sulfur and oxygen are negative energy indicators. As such the H/C ratio of bio-crude oil greater than 1.5 indicates the potential for transport application [4].

The energy recovery, is the product of the heating value and the yield of oil obtained from the HTL process. The ER ratio, on the other hand, highlights the total energy recovered from the bio-crude to the energy input of dry feedstock [5]. This parameter is largely affected the reaction conditions employed in HTL, except for the effect of catalyst. From the results, ER largely varied due to interchanging composition of the bio-crude with increasing reaction conditions. It was presumed that, at lower and less severe reaction conditions, including temperature, pressure and time, primary reactions are predominant reactions [6]. These reactions are characterized by high molecular weight products and low energy content.

As the thermal degradation of *Jatropha curcas* seed is prolonged, and reaction conditions got severer, secondary reactions, such as aromatization, decarboxylation and rearrangement reactions are favoured [7]. These are responsible for increasing lower molecular weight compounds and consequently yield increasing H/C compounds. Fig. 3 presents the energy recovery profile of *Jatropha curcas* seed bio-crude oil. As envisaged, the higher heating value (HHV), was calculated using Dulong's formula reported elsewhere [3]. The lowest ER for H was in the range of 32.42 – 46.31 (MJ/kg), while that of carbon was in the range of 44.67 – 64.78 (MJ/kg). Cumulatively, the *jatropha curcas* seed bio-crude had low calorific value

in the range of 16.73 – 28.56 (MJ/kg). This is quite low as compared to other feedstock including microalgae [1], mixed culture algae [2] reported by different authors.

4. Conclusions

The hydrothermal liquefaction of Jatropha curcas seed was conducted and the energy recovery parameters are evaluated. Energy indicators including carbon and hydrogen recoveries were evaluated. Accordingly, although Jatropha curcas seed bio-crude oil showed good energy recovery in the range of 32.42 – 46.31 (MJ/kg), such is low compared to other feedstock, specifically, microalgae. It is recommended that co-liquefaction of the seed could improve the energy recovery.

References

- [1] M. P. Caporgno, E. Clavero, C. Torras, J. Salvadó, O. Lepine, J. Pruvost, J. Legrand, J. Giralt, and C. Bengoa, "Energy and Nutrients Recovery from Lipid-Extracted Nannochloropsis via Anaerobic Digestion and Hydrothermal Liquefaction," *ACS Sustain. Chem. Eng.*, vol. 4, no. 6, pp. 3133–3139, 2016.
- [2] W. T. Chen, Y. Zhang, J. Zhang, L. Schideman, G. Yu, P. Zhang, and M. Minarick, "Co-liquefaction of swine manure and mixed-culture algal biomass from a wastewater treatment system to produce bio-crude oil," *Appl. Energy*, vol. 128, pp. 209–216, 2014.
- [3] Y. Alhassan, N. Kumar, and I. M. Bugaje, "Hydrothermal liquefaction of de-oiled *Jatropha curcas* cake using Deep Eutectic Solvents (DESs) as catalysts and co-solvents," *Bioresour. Technol.*, vol. 199, pp. 375–381, 2016.
- [4] L. Nazari, Z. Yuan, S. Souzanchi, M. B. Ray, and C. Xu, "Hydrothermal liquefaction of woody biomass in hot-compressed water: Catalyst screening and comprehensive characterization of bio-crude oils," *Fuel*, vol. 162, pp. 74–83, 2015.
- [5] J. Zhang, W. T. Chen, P. Zhang, Z. Luo, and Y. Zhang, "Hydrothermal liquefaction of *Chlorella pyrenoidosa* in sub- and supercritical ethanol with heterogeneous catalysts," *Bioresour. Technol.*, vol. 133, pp. 389–397, 2013.
- [6] D. Chiaramonti, M. Prussi, M. Buffi, A. Maria, and L. Pari, "Review and experimental study on pyrolysis and hydrothermal liquefaction of microalgae for biofuel production," *Appl. Energy*, pp. 1–10, 2016.
- [7] L. Zhang, B. Zhou, P. Duan, F. Wang, and Y. Xu, "Hydrothermal conversion of scrap tire to liquid fuel," *Chem. Eng. J.*, vol. 285, pp. 157–163, 2016.

**ABSTRACT CCT-: 032**

Audu E.A., A. A. Nuhu, M.E. Isah, A. Abubakar

Department of Basic Research, National Research Institute for Chemical Technology, PMB 1052, Zaria.

Email: ephraim.audu@yahoo.com**PHYTOCHEMICAL SCREENING AND SPECTROSCOPIC STUDY OF THE LEAVES OF ADINA MICROCEPHALA**

ABSTRACT: The study was carried out to assess the phytochemical conduct and to conduct spectroscopic evaluation of *Adina microcephala* leaves. The leaves were subjected to serial exhaustive serial soxhlet extraction using ethyl acetate as extraction solvent. The preliminary phytochemical screening of the ethyl acetate extract revealed the presence of alkaloids, glycosides, cardiac glycosides, flavonoids, saponins and tannins and triterpenoids. The Fourier transform infrared spectroscopy (FTIR) result of the ethyl acetate extracts indicated the presence of fatty acids and show major absorption bands typical of O-H, C-H, C=O and C=C stretch. C-O stretch was also observed. The gas chromatography-mass spectrometry (GC-MS) analysis result revealed mostly the presence of the following fatty acids: hexadecanoic acid, tetradecanoic acid, octadecanoic acid and octadec-9-enoic. The study provides significant information on the phytochemical composition and spectroscopic data which can be used for application in medicine and other fields.

Keywords: *Adina microcephala*, GC-MS, fatty acids, hexadecanoic acid, phytochemical.

1. Introduction

Traditional medicine has been in existence from the time immemorial as major African socio-cultural heritage (Okigbo and Mmeka, 2006). Traditional Medicine has been the focus for wider coverage of primary health care delivery in Africa and the rest of the world (Elujobaet *al.*, 2005). Research on the chemical constituent of the plants and pharmaceutical screening may lead to development of new drugs derived from plants (Olatunji and Atolanii, 2009).

A medicinal plant is a plant which one or more of its parts contains substance that can be used for therapeutic purposes or which can be used for drug synthesis. Many licensed drugs used today originated from medicinal plants used in traditional medicine (Akobi, 2004). The plant *Adina microcephala* (Delile) also known as *Breonadiamicrocephala* is from the family Rubiaceae. Common names are Adina, African teak, matumi, red wood, milamandia, mdogowe, mgwina, mugonha, mugunya and yombe (Hyde *et al.*, 2013).

Adina microcephala is a medium to large evergreen tree about 30 – 40meter in height and the trunk is 80cm in diameter, leaves in whorls of 3 to 5 near the end of the branches; lanceolate to narrowly elliptic, leathery, dark green with the mid rib yellow, raised conspicuously. It is also found in Plateau state and Zaria and some other places in Nigeria (Offiah *et al.*, 2011).

The plant has been found usefully in the treatment of ailments such as, diarrhea, ringworm, diabetes, in modulation of anxiety and depression other uses includes the treatment of cardiovascular diseases and heart failure (Offiah *et al.*, 2011)

2. Materials and methods**2.1 Preliminary analysis****2.1.1 Sample collection and identification**

The leaves of *Adina microcephala* was collected from rivers in samaru, under Sabon Gari local Government, Kaduna State. The plant was identified at the herbarium of Botany Science Department, Ahmadu Bello University, Zaria-Nigeria with voucher number 900383.

Extraction

The pulverized plant material (500g) was weighed out and packed in a thimble and placed inside a soxhlet extractor. Solvent (500ml) and anti-bumping chips were put into a 1L round bottom flask and heated on a heating mantle. The solvent in the extracted was recovered using a rotary evaporator at 40°C and the extract was exposed to the atmosphere for all the residual solvent to evaporate.

2.2 Laboratory analysis:**2.2.1 Phytochemical Screening**

The phytochemical components of the plant extracts were screened according to the methods described by Sofowora (2008).

2.2.2 FTIR

The FTIR analysis of the extracts was carried out using FTIR-8004s spectrophotometer (Shimadzu model) scanning the sample through 4000-400cm⁻¹.

2.2.3 GCMS

The GC-MS analysis was carried out in a GC-QP2010 PLUS (Shimadzu model) which was set to scan mode.



3.0 Results and discussion

Table 1: Phytochemical Analysis of Methanol and Ethyl Acetate Extracts of *Adina microcephala*

Phytochemical constituents	Ethyl acetate Extract
Saponin	-
Tannin	-
Cardiac glycosides	+
Triterpenoids	+
Alkaloids	+
Anthraquinones	-
Flavonoids	+

Key: -: not detected, +: present

Table 2: FTIR result of the ethyl acetate extract

Bands cm^{-1}	Functional group
3403.51	O-H stretch
3392.90	O-H stretch
2934.79	C-H stretch
1633.76	C-C stretch
1714	C=O stretch
1268.24	C-O stretch

3.1 Phytochemical Analysis

The present study on the ethyl acetate extract of *Adina microcephala* confirms the presence of alkaloids, cardiac glycosides, flavonoids, tannins, saponins and triterpenoids. The presence of these compound is believed to be responsible for the curative properties of the plant. Alkaloids, which are basic plants compounds containing nitrogen in their chemical structure as part of the heterocyclic ring, were found in the plant; this may be responsible for the marked physiological activities of the plant. Alkaloids have been used medically as antimicrobial, antidiarrhoeal, and antihelmintic agent. The plant extract also contains flavonoids, cardiac glycosides and triterpenoids, which have been reported to have anti-diarrheal and antimicrobial activity. The plant has also been reported to have anti-inflammatory properties which are possibly due to phytosterols (Gadre and Gabhe, 1993). The cardiac glycosides therapeutically have the ability to increase the force and power of heart-beats without increasing the amount of oxygen needed by heart muscle. They can thus increase the efficiency of the heart-beat without strain to the oxygen (Hunt *et al.*, 1980). As a result of the presence of cardiac glycosides. The use of *Adinamicrocephala* in herbal medicine for the treatment of cardiovascular problems may be sustained. Presence of flavonoids will be an evidence for the use of the plant in herbal treatment of cancer. Flavonoids are polyphenolic compounds with an anti-oxidant property (Chew *et al.*, 2009). They enhance the effect of vitamin C and also known to be biologically

active against liver toxins, tumor, viruses and other microbes, allergies and other inflammations.

3.2 Fourier Transform Infrared (ftir) Analysis

The FTIR result of the ethyl acetate extract reveals the presence of functional groups as shown in table. The functional groups present confirmed the presence of alkaloids, glycosides, cardiac glycosides, flavonoids and triterpenoids.

3.3 Gas Chromatography-Mass Spectrophotometry Analysis

GC-MS analysis of ethyl acetate extract of *Adina microcephala*, indicated the presence of pentadecanoic acid, tetradecanoic acid, hexadecanoic acid, octadecanoic acid and octadec-9-enoic acid visible in peaks 6, 8, 9, 10 and 11. The most prominent of this peaks are 9 and 11 with an area % of 30.34 and 35.29 respectively.

Palmitic or hexadecanoic acid is the most common fatty acid (saturated) found in animals, plants and microorganisms (Gunstone *et al.*, 2007). Its formula is $\text{CH}_3(\text{CH}_2)_{14}\text{CO}_2\text{H}$. It is a major component of palm trees but can also be found in meats, cheeses, butter and dairy products. Hexadecanoic acid has antimicrobial, nematicide, hemolytic 5-alpha reductase inhibitor and antioxidant activity. It has also found wide application in the production of soaps and cosmetics products.

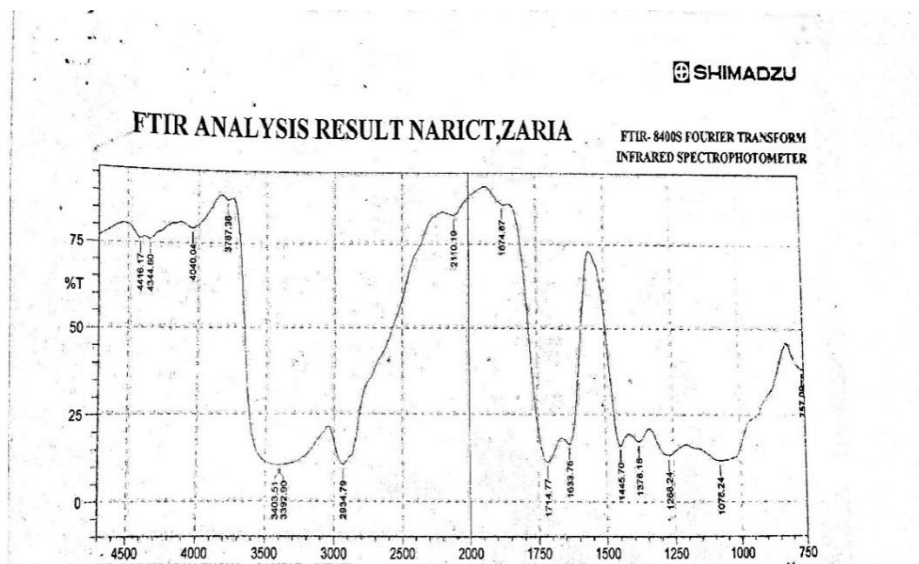


Fig. 1: FTIR spectrum of methanolic extract of *Adina microcephala*

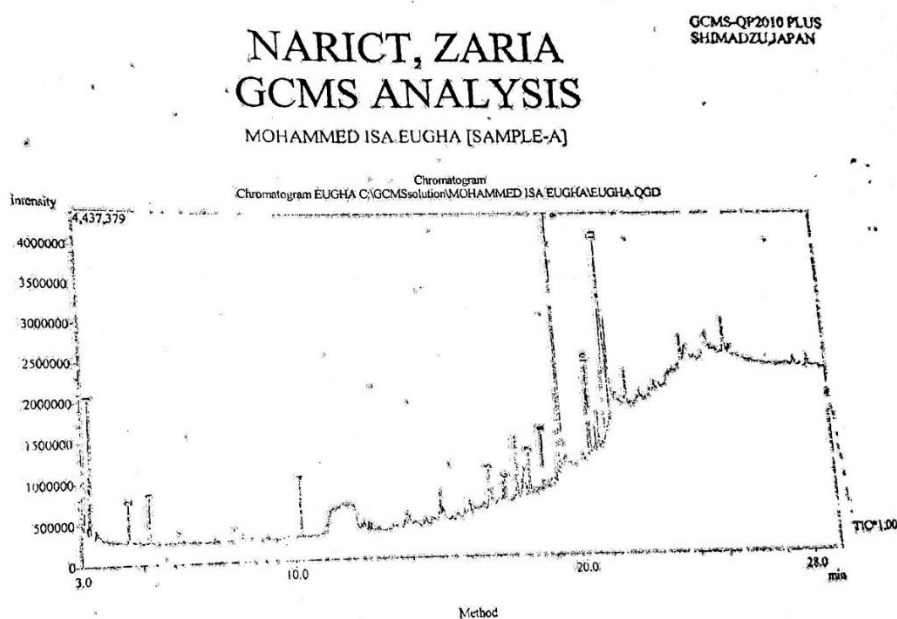


Fig. 2: GCMS spectrum of methanolic extract of *Adina microcephala*

4. Conclusion

The classes of phytochemicals have been demonstrated to have biological activity. The FTIR and GC-MS analyses showed the fatty acid profiles with hexadecanoic acid also known as palmitic acid and tetradecanoic acid or myristic acid being most prominent. They have antifungal and antibacterial properties. Therefore, it can be source of active antimicrobial agents for the development of drugs for the prevention and treatment of diseases.

Acknowledgement

The authors wish to acknowledge the management of the National Research Institute for Chemical Technology (NARICT) Zaria, for the opportunity to present this paper. Our gratitude also goes to Mallam U. S. Gallah for identifying the plant of study

References

1. Akobi, I. C. (2004). The preliminary Phamaconostic Evaluation of leaves, stems and

roots of *Waltheriaindica*, A.B.U. Zaria, Nigeria. Page 11-33

2. Chew Y. L, Goh, J. K, Lim, Y. Y (2009). Assessment of vitro Antioxidant Capacity and polyphenolic composition of medicinal herbs from Leguminosea in peninsular Malaysia. Food chem. 119:373-374
3. Elujoba, A. A., Odeleye, O. M and Ogunyemi, C. M (2005). Traditional Medical Development for medical and dental primary Healthcare Delivery System in Africa. *African Journal of Traditional, Complementary and Alternative Medicine* 2(1): 46-61
4. Gadre, A. P and Gabhe, S. Y., (1993). Identification of some sterols of *Breonadialsalicina* by GC-MS. *Indian Journal of Pharmaceutical Science*. pp 168
5. Gunstone, F. D., John L. Harwood and Albert J. Dijkstra (2007). *The lipid handbook*. 3rd ed. Boca Raton; CRC Press. ISBN 978-0849396885.
6. Hunt S., Goff, J. L and Holbrook, J (1980). *Nutrition, Principles and Chemical Practice*. John Wiley and Sons, New York, pp 49-52.
7. Hyde, M. A., Wursten, B.T. and Ballings, P (2013). *Flora of Zimbabwe: species information: Breonadialsalicina*
8. Offiah, N. V, Makama, S, Elisha, I. L, Makoshi, M. S, Gotep, J. G, Dawurung, C. J, Oladipo, O. O,



- Lohlum, A. S and Shamaki, D (2011) Ethnobotanical survey of medicinal plants used in the treatment of animal diarrhoea in Plateau State, Nigeria *BMC Veterinary Research*, 7:36
9. Okigho, R. N and Mmeka, E. C (2006). An Appraisal of Phytomedicine in Africa *KMITL Science and Technology Journal*.6 (2):83-93
 10. Olatunji, A. G and Atolani, O (2009). Comprehensive scientific demystification of *Kigelia africana*: *African Journal of Pure and Applied Chemistry* 3 (9): 158-164
 11. Sofowora (2008). Medicinal plants and traditional medicine in Africa. Third, edition John Wiley and Sons Ltd. pp 181-2004
 12. Zambia Forest Department, (1979). Timbers of Zambia, *Adina microcochala* and *Amblygonocarpus andongensis*. Zambia Forest Department, Division of Forest Products Research, Timbers of Zambia Technical Note (5) 7

**ABSTRACT CCT-: 041**Shehu U.^{1*}, M.T. Isa², B. O. Aderemi², T. K. Bello², H.I. Audu¹, U. M. Shittu¹, A.F. Ade-Ajayi¹

1. National Research Institute for Chemical Technology, P.M.B 1052 Zaria, Nigeria

2. Department of Chemical Engineering, Ahmadu Bello University, Zaria, Nigeria

Email: Unclezick@yahoo.com**PROPERTIES OF CHEMICALLY MODIFIED BAOBAB POD/SISAL FIBRE REINFORCED LOW DENSITY POLYETHYLENE HYBRID COMPOSITE**

ABSTRACT: *The present study determined the effect of sodium hydroxide (NaOH) treatment on the properties of baobab pod/sisal fibres reinforced low-density polyethylene (LDPE) hybrid composites. Used to treat the fibres, were different concentrations of NaOH 2 -10 wt% at 2 wt% interval. The hybrid composites were compounded using two roll mills machine and compressed in a mold using hydraulic press at a pressure of 10 kN and temperature of 120 °C. The fibre content of the hybrid composites was 10 wt% with baobab and sisal fibre ratio of 1:1. Tensile, impact, hardness, water absorption and morphological analysis were conducted on the produced hybrid composites. The mechanical properties of the hybrid composite increased with increase NaOH concentration up to 6 wt%, while the water absorption decreased with increase in concentration of NaOH solution. The morphology revealed that surface cracks and voids were more in hybrid composites produced with untreated and fibres treated at higher concentrations of NaOH.*

Keywords: *Mechanical Properties, Baobab, Sisal, Polyethylene, Hybrid Composite, Sodium hydroxide.*

1. Introduction

Currently, attention is shifting to natural fibres as Substitute for man-made fibres such as glass, carbon, Kevlar, because of their nonbiodegradability and lack of sustainability (Mishra et al., 2004; Jawaid et al., 2011 and Abdulkhalil et al., 2012). However, natural fibres have setbacks of being hydrophilic and of low mechanical properties. Treatment of natural fibres using different methods has been demonstrated to solve the problem associated with hydrophilic nature of the fibres (Li et al., 2007; Paul et al., 2010 and Liu et al., 2011). Treatment of fibres improves interlocking at the interface thereby providing improved adhesion with matrix (Kumar et al., 2011), and subsequently improved properties. Also, to improve on the properties of the composite, a single fibre may not be able to provide, thus combing two or more different fibres in matrix is also a way by which improved properties of natural fibre reinforced composites can be accomplished.

Combining two or more fibres in matrix or a fibre incorporated in combined matrices result to hybrid composite. Tailoring the properties of these types of composite materials, could achieve balance of properties, weight and cost savings (Saha et al., 1996).

Natural fibre reinforced hybrid composites have found use in sliding panels, bearings, bushings, because of the improved properties achieved by chemical treatment and hybridization (Singh et al., 2014).

Despite various reported works on the use of natural fibres as reinforcement in composites, the report on the use of baobab (*Adansonia digitata*) fibre or its combination with other fibres as reinforcement in composite is scanty. But, reports are available on its use in rope making, basket nets, fishing line (Sidibe et al., 2002). Investigation showed it has potential as

reinforcement when treated (Shehu, 2016). This work is thus aimed at studying the effect of alkali (NaOH) treatment on the properties of baobab pod fibre hybridized with sisal fibre in low density polyethylene composites.

2. Experimental

2.1 Materials

The baobab pod and sisal fibres were obtained from National Research Institute for Chemical Technology (NARICT), Zaria, Nigeria. The fibres, modified with sodium hydroxide (97 % purity, BDH Chemical, Poole, England) before use. The matrix was low density polyethylene obtained from Chemical store, Zaria.

2.2 Methods

2.2.1 Treatment of baobab and sisal fibres

The baobab and sisal fibres were treated with 2, 4, 6, 8 and 10 wt% of sodium hydroxide solutions respectively to remove some of the lignin, wax, pectin and other impurities. After the treatment the fibres were removed and rinsed severally with distilled water until a neutral pH was reached. Drying was done in oven at 50 °C for 20 min.

2.2.2 Hybrid composite production

The baobab pod/sisal fibres content of the hybrid composite was 10 wt% (5 wt% baobab pod fibre and 5 wt% sisal fibre). Preliminary work by Shehu, U (2016) showed that at 10 wt% loading, most of the mechanical properties were highest for baobab fibre reinforced low density polyethylene. The procedure used by Shehu, U (2016) was adopted for the production of the hybrid composites.

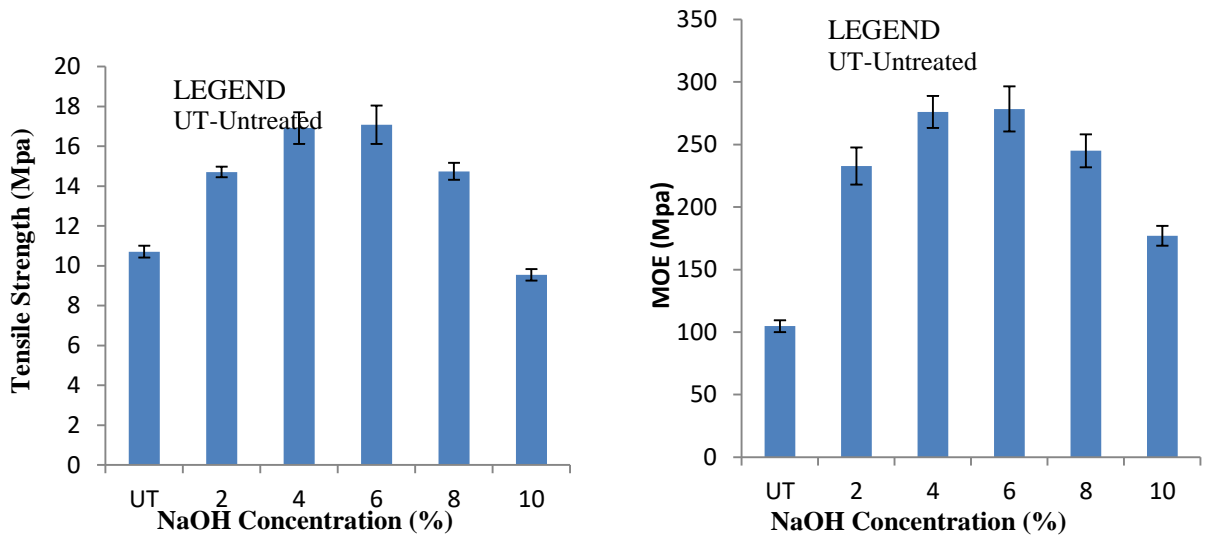


Fig. 1 and 2: Effect of Fibre Treatment on the Tensile Strength and Modulus of Elasticity of the Baobab/Sisal Hybrid Composite

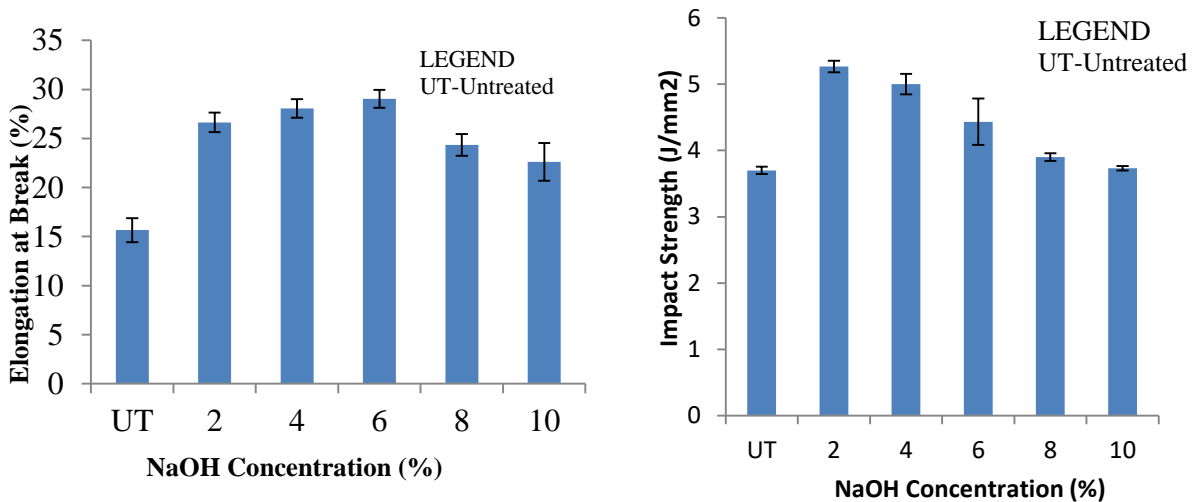


Fig. 3 and 4: Effect of Baobab/Sisal Fibre Treatment on the Elongation at Break and Impact Strength of the Hybrid Composite

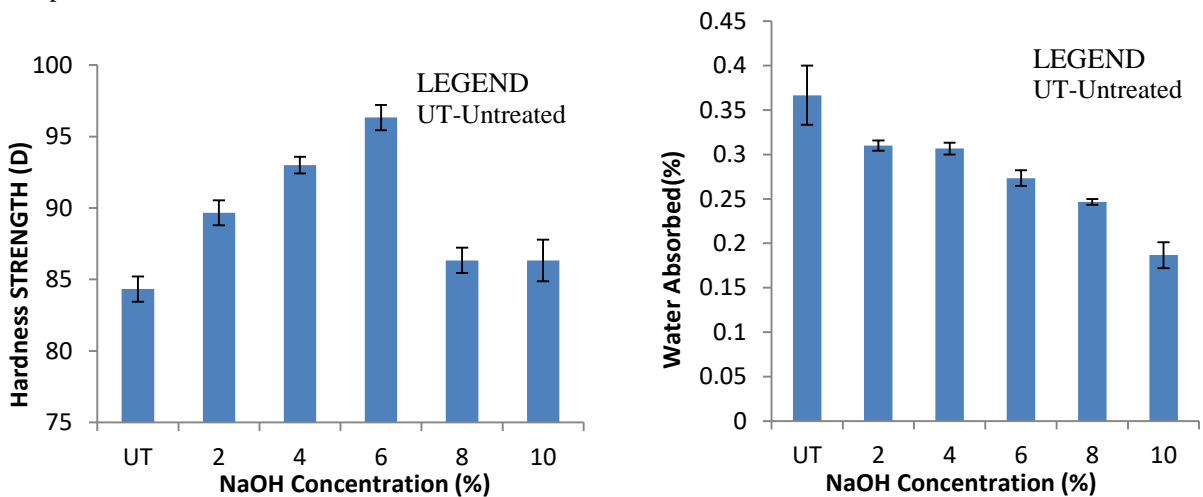


Fig. 5 and 6: Effect of Baobab/Sisal Fibres Treatment on the Hardness Strength and Water Absorption of the Hybrid Composite

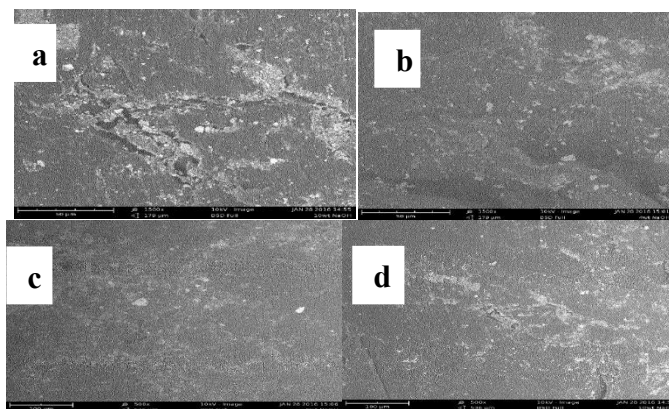


Plate 1: SEM Micrograph of (a) 50:50 untreated, (b) 4 wt% NaOH, (c) 6 wt% NaOH and (d) 10 wt% NaOH treated hybrid sisal: baobab fibre hybrid composite.



2.3 Characterization of Samples

2.3.1 Mechanical test: tensile strength, impact test and hardness test

ASTM D638 (1987) was adopted for the tensile test using an Instron Machine Model 3369, System Number 3369K1781. From the tensile test, tensile strength, modulus of elasticity and percentage elongation at break were obtained. The impact test was conducted according to ASTM D256 (1987) using the Charpy impact testing machine, Capacity 15 J and 25 J serial number 412-07-15269C.

The hardness test was performed according to ASTM D2240 using Shore Duro-meter test.

2.3.2 Water absorption test

Water absorption test was conducted using ASTM D570-98 (2005). Using Equation 1 the percent water absorbed was calculated. Where W_i is initial weight of dry sample and W_f is final weight of wet sample.

$$\% \text{water absorbed} = \frac{W_f - W_i}{W_i} \times 100$$

Three test samples were used in each of the tests and the average taken.

2.3.3 Morphological analysis using scanning electron microscope (SEM)

The morphological analysis of the samples was conducted using Phenom tm Prox scanning electron microscope. The samples size was 2 mm x 2 mm thinly coated with gold, transferred to the SEM machine where they were observed and images captured.

3. Results and discussion

3.1 Effect of Treatment on Tensile Strength and Modulus of Elasticity (MOE)

Figure 1 and 2 presents the effect of varying NaOH treatment concentration on the tensile strength and modulus of elasticity of baobab/ sisal fibre reinforced low density polyethylene hybrid composite.

A positive treatment effect was observed with fibres treated with 2 wt%, 4 wt%, 6 wt% and 8 wt% NaOH solution respectively. They showed 36 %, 45 %, 55 % and 34 % increase respectively in their tensile strength values over the untreated hybrid composite. While the highest modulus of elasticity occurs at 6 wt% NaOH treatment. The positive treatment effect noted, occurred because of the alkali treatment resulting to in an improvement in the interfacial bonding. This was so because of increase in extra sites for mechanical

interlocking, therefore promoting more resin-fibre interpenetration at the interface (Bledzki et al., 1999 and Kabir et al., 2012). Increasing the concentration of NaOH solution to 8 wt% and 10 wt% resulted to lower modulus of elasticity and tensile strength than the untreated hybrid composite. This decrease in the modulus and tensile strength might be because of excess delignification of the fibres, which results in weakening or damaging of the fibres (Bledzki et al., 1999).

3.2 Effect of NaOH Treatment on Elongation at Break

Figure 3 and 4 presents the effect of varying NaOH treatment concentration on the percentage elongation at break and impact strength of baobab/ sisal fibres reinforced low density polyethylene hybrid composite.

The modification of fibre with 2 wt%, 4 wt% and 6 wt% NaOH solutions lead to 6 %, 10.7 % and 14.7 % increase in hardness value of the composite compared with the untreated fibre composite. The noted increase in hardness value could results from strong interface, closed packing arrangement in the composite and increase in stiffness and the dispersing of the fibres properly into the matrix because of the treatment (Kumar et al., 2011; Wang et al., 2007; Modibbo et al., 2009; John et al., 2013 and Kaymakci et al., 2013).

3.4 Effect of Treatment of Surface Morphology

Plate 1 a-d show the surface morphology of the untreated and 4 wt%, 6 wt% and 10 wt% treated hybrid composite.

Conclusions

In conclusion treated Baobab pod/Sisal fibre were used to reinforce low density polyethylene successfully and the mechanical, physical and morphological analysis were conducted.

References

1. Abdulkhalil, H. P. S., Bhat, I. U. H., Jawaid, M., Zaidon, A., Hermawan, D., Hadi, Y. S., Bamboo fibre reinforced biocomposites: A review, *Materials and Design*, 42 (2012) 353- 368.
2. Araga, R. A. L., Hassan, A., Yahya, R., Thermal and tensile properties of treated and untreated red balau (*Shorea Dipterocarpaceae*) filled LDPE composites, *Journal of Science and Technology*, 3 (2) (2011) 7-27.
3. Abdulkhalil, H. P. S., Bhat, I. U. H., Jawaid, M., Zaidon, A., Hermawan, D., Hadi, Y. S., Bamboo fibre reinforced biocomposites: A review, *Materials and Design*, 42 (2012) 353- 368.
4. Li, X., Tabil, L.G., Panigrahi, S., Chemical treatment of natural fibre for use in natural fibre-reinforced.

**ABSTRACT CCT:- 063**

Suleiman M.A., M.K. Yakubu, S. Gadimoh, Z.M. Salisu, P.S. Ukanah, A. N. Ozogu, B. Anyim, O.M. Lawal, D. Daniel and I.C. Oddy-Obi

Department of Textile Technology, National Research Institute for Chemical Technology, Zaria-Nigeria.

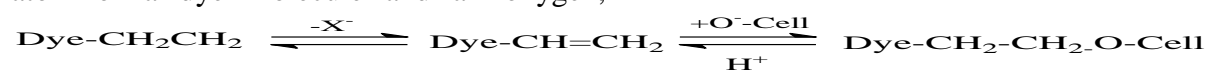
Email: mohammed_suleiman89@yahoo.com**THE STUDY OF THE RHEOLOGY AND PROPERTIES OF CORN STARCH DYED WITH REACTIVE DYE**

ABSTRACT:- The study of the rheology of corn starch dyed with reactive dye was carried out. The dyeing was carried out with different concentration of dye solution giving rise to difference in the depth of shade obtained. The amount of dye fixed on the starch were also determined indicating that the higher the concentration of the dye solution used the higher the amount of dye retained until saturation point was reached. The physical properties of the dyed and undyed starch which include viscosity, refractive index, gelation temperature were determined and compared. Intrinsic viscosity values obtained for the dyed starch are 0.21 and 0.075, gelation temperatures are 65 and 62, the refractive indices obtained are 33.6 and 34.0 respectively.

1. Introduction

Starch is an abundant bio-based polymer which attracts great attention since the 1970's (Lu et al., 2009). It has an estimated world production to the tune of about 66 million tons from year 2008 (Sugih, 2008). Starch has a general formula of $(C_6H_{12}O_5)_n$ and mostly found in plants. The main sources of starch are corn, with other sources such as potatoes, tapioca, rice etc. Starch generally contains 25 to 30% amylose and 75 to 80% amylopectins with varying shapes such as sphere and platelets, with sizes mostly between ranges of 0.5-1.75 μ (Luc, 1992)

Starch has enormous uses which cut across several strata of lives such as food and beverage industries, agriculture, construction, Textile and allied industries in production of colour and dyes. Reactive dye as defined by Rys and Zollinger (2003) is a coloured compound which has a suitable groups capable of forming a covalent bond between a carbon atom of a dye molecule and an oxygen,



(Nkenoye, 2008)

2. Experimental section**2.1 Materials**

Sodium hydroxide (NaOH) (Sigma Aldrich), Sodium Carbonate (Na_2CO_3) (Sigma Aldrich), conc. Sulphuric acid (H_2SO_4) (Sigma Aldrich), Remazol Red dye, Distilled water H_2O , Corn (Samaru Zaria).

2.2 Maize starch extraction

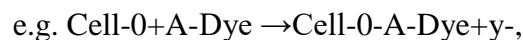
1 kg of maize was soaked in 5 Liters of water

2.3 Dyeing of starch

20 g of corn starch was weighed, 4 mls of 1% solution of remazol red dye was added to form

nitrogen, and sulphur atom of a hydroxyl, an amide group respectively of the substrate. Reactive dyes can be classified into two: Nucleophilic substitution and Nucleophilic addition.

In the nucleophilic substitution types reactive dyes, the dyes react with the cellulose by a Nucleophilic substitution mechanism, whereby a leaving group in the dye structure is displaced as a result of an attack by the cellulosate anions (Cell-0).



In the Nucleophilic addition type reactive dyes, the dyes are characterized by the fact that the dye-fibre reaction (or attachment) is that of addition, whereby a positively polarized unsaturated carbon-carbon double bond in the dye reactive group is attached by a Nucleophilic group present in the fibre (cellulosate anion).

for about 24 hrs, after which it was grinded into a slurry. The slurry was filtered using a nylon cloth and the filtrate was allowed to settle for about 12 hrs. The corn particle been denser than water tend to settle at the bottom of the container. The water was decanted out leaving the corn starch residue, which was dried in a tray under the sun for 3 days (Adamu et al, 2013). The dried starch was grinded into fine particles and finally weighed.

Percentage of starch recovered was calculated as follows

$$\text{Starch recovered (\%)} = \frac{\text{weight of starch(g)}}{\text{weight of sample(g)}} \times 100$$

a paste of corn starch. The paste was then topped with 16 mls of water to obtain 20 ml solution. The solution was heated at 40 °C in a thermostart for an hour followed by the



addition of a mixture of 5 mls of 1% solution of a mixture of NaOH + Na₂CO₃. The solution was left for about 1 hour. The solution was filtered using a filter paper. The residue was rinsed with water and dried in a vacuum oven and finally grinded to moderate fineness.

The procedure was repeated for the 10 samples of 5 g of corn starch but in each case varying the volume of the dye solution from 1-10 mls respectively and topping the mixture with the required volume of water to obtain 20 mls of the solution and adding 5 mls of a mixture of NaOH + Na₂CO₃ (Adamu *et al*, 2013).

2.4 Determination of the amount of dye retained by corn starch

2 g of each of the 10 dyed starch samples was weighed on a microbalance and each sample was transferred into 10 different flat bottom flask labelled from 1 to 10 respectively. 5 mls of conc. H₂SO₄ was added to each sample in the flat bottom flask and stirred vigorously. 100 mls of distilled water was also added to each of the 10 samples which was also stirred and left over night. The solution was filtered using a filter paper, the filtrate of each sample was run in a UV-Visible spectrophotometer and finally the results was recorded.

2.5 Determination of gelation temperature of corn starch

g of undyed corn starch was weighed and dispersed in a 100 mls of water in a 500 mls beaker. The mixture was heated gently in a water bath while stirring constantly using a stirrer. The commencement of gelatinization was noted which is indicated by the presence of little bead-like lump of geletinized starch to appear and the temperature at which this occur is the gelatinization temperature. The procedure was repeated for the dyed corn starch.

2.6 Determination of Refractive index

The refractive index of both samples were determined with Abbe refractometer (Bellingham and Stanley, Tunbridge well kent, UK). Three readings were taken for each sample and the average value reported according to ASTM D1209 (Test Method for Refractive Index).

2.7 Determination of the viscosity of corn starch

6 g of the dyed corn starch was dispersed with 300 mls of distilled water. The mixture was heated using a hot plate while stirring was maintained until paste occurred to give a 2% concentration of starch paste. The starch was allowed to cool at room temperature. The

viscosity of the starch paste was measured using brookfield viscometer. The absolute viscosity readings were obtained in mPas and the shear stress was also noted. The starch paste was diluted with water using the formulae

$$C_1 V_1 = C_2 V_2$$

Water was added to obtain concentration of 1.8, 1.6, 1.4, 1.2, 1.0, 0.8, respectively. The same procedure was carried out but in this case using the dyed corn starch, the viscosity measurement and shear stress were obtained. The relative viscosity (η_{rel}), specific viscosity (η_{sp}) for both starches were calculated.

3. Results and discussion

3.2 Description of starch powder

From Plates 1, the colour of the starch to a large extent depends on the source of extraction. The colour of corn starch is yellowish white. Furthermore, the colour of the dyed starch as depicted from plate 2 is pink due to the effect of the remazol red dye presence in the starch. The pink coloured starch improve the aesthetic property of the starch. This dyed starch has found uses as starch-reactive dye pigment in emulsion paint formulation inconcordance with the work of Adamu *et al* (2013).

The odour of both starches are relatively odourless. The presence of odour indicate the presence of microbial activities on the starch, which will futher degrade the starch since starch is biodegradable. The texture of both starches are very fine when grounded into powder. This enhance dispersability of the starch in water.

3.3 Description of the depth of shade of dyed starch

The variation of the depth of the shade of the dyed starch due to the difference in the volume of the dye solution used in the dyeing of the starch. These gives varying colour ranges.

3.4 Gelatinization temperature

The gelation temperature of the undyed starch paste is lower than the dyed paste. This is due to the swelling power of the dyed starch paste being higher than the undyed, also the effect of the reactive dye on the starch molecule thus forming covalent bonds between the reactive dye molecules and the starch molecule which tend to increase the gelation temperature of the dyed starch paste.



3.5 Viscosity of paste

From Table 2, it is evident that the viscosity of the undyed starch is higher than that of the dyed starch. This could be attributed to the presence of the dyed molecules in the dyed starch, thus forming covalent bond linkages between the dyed molecules and the starch molecules of the starch.

Thus from the graph of η_{sp}/C against C where C is the concentration. The curve of the undyed starch paste is positive and extrapolating the curve gives the intrinsic viscosity value of the undyed starch paste of 0.75, since the intrinsic viscosity is independent of concentration of the starch solution used. The curve of the dyed

starch is negative and thus extrapolating the curve gave intrinsic viscosity of 0.21. This is due to the formation of covalent bonds between the dye molecules and the starch molecules in the paste.

3.6 Amount of Dye retained in the Starch

From the fig 2. The value of the constant obtained is 0.9968 thus multiplying this value by the absorbance gives the actual amount of dye retained by the starch in grams, thus converting the value obtained to Kg showed that the amount of dye retained is directly proportional to the concentration in g/L until saturation is reached.

Table 1: Physical properties of starch and paste

	Undyed corn starch	Dyed corn starch
Colour of powder	Yellowish white	Pink
Colour of paste	Milky	Pink
Odour	Odourless	Odourless
Appearance of powder	Fine	Fine
Viscosity of paste	High	Medium
Gelatinization Temperature(°C)	62	65
Refractive index	33.6	34.0
Percentage recovery (%)	61	61

Table 2: Viscosity of dyed and undyed corn starch paste

Conc (%)	Abs visc of dyed starch	Abs visc of undyed starch	Relative visc of dyed	Relative visc of undyed	Specific visc	Specific visc of undyed	η_{spd}/C	η_{spu}/C
2.0	11.7	14.0	1.0500	1.2480	0.0500	0.2480	0.0250	0.1240
1.8	12.1	13.6	1.0796	1.2138	0.0796	0.2138	0.0442	0.1188
1.6	12.3	13.2	1.1014	1.1818	0.1014	0.1818	0.0634	0.1136
1.4	12.4	12.9	1.1071	1.1518	0.1071	0.1518	0.0765	0.1084
1.2	12.5	12.6	1.1221	1.1238	0.1221	0.1238	0.1018	0.1032
1.0	12.5	12.4	1.1210	1.1071	0.1210	0.1071	0.1210	0.1071
0.8	12.4	12.0	1.1121	1.0714	0.1121	0.0714	0.1402	0.0893

Table 3: Absorbency of dyed starch dissolved in H₂SO₄

sn	Abs	Amount of dye retained(g)	Amount of dye retained (kg)	Concentration (g/L)	Volume (mls)
1	0.161	0.1600	32.00	0.5	1
2	0.183	0.1824	36.48	1.0	2
3	0.188	0.1873	37.48	1.5	3
4	0.204	0.2033	40.66	2.0	4
5	0.213	0.2130	42.46	2.5	5
6	0.301	0.3000	60.00	3.0	6
7	0.292	0.2910	58.20	3.5	7
8	0.268	0.2671	53.42	4.0	8

Table 4: Calibration table

sn	Abs	Amount of dye retained(g)
1	0.0000	0.00
2	0.0513	0.01
3	0.1006	0.02
4	0.1526	0.03
5	0.1989	0.04
6	0.2473	0.05
7	0.3017	0.06



Plate 1: Sample of dyed starch



Plate 2: Sample of undyed starch

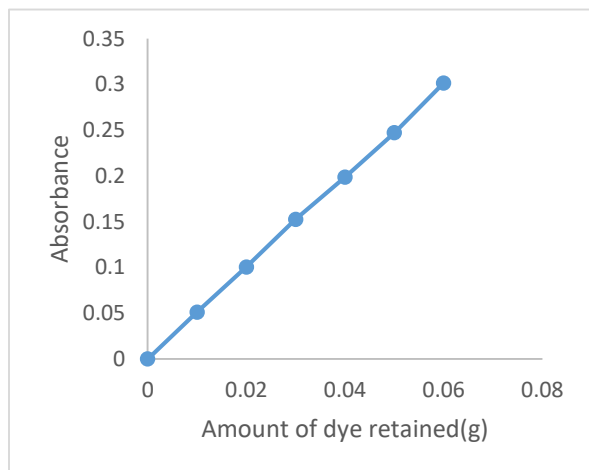


Fig 1: Calibration Curve

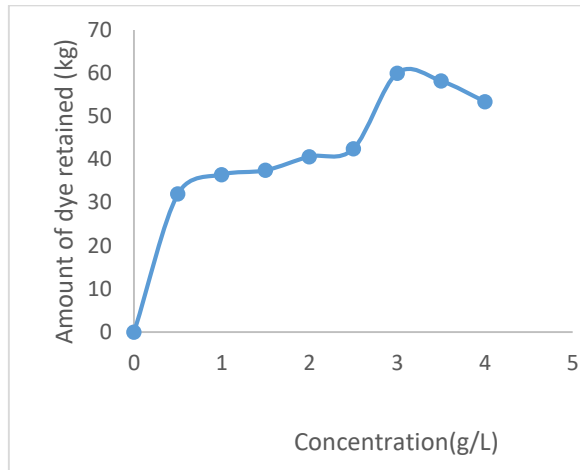


Fig 2: Amount of dye retained in the starch

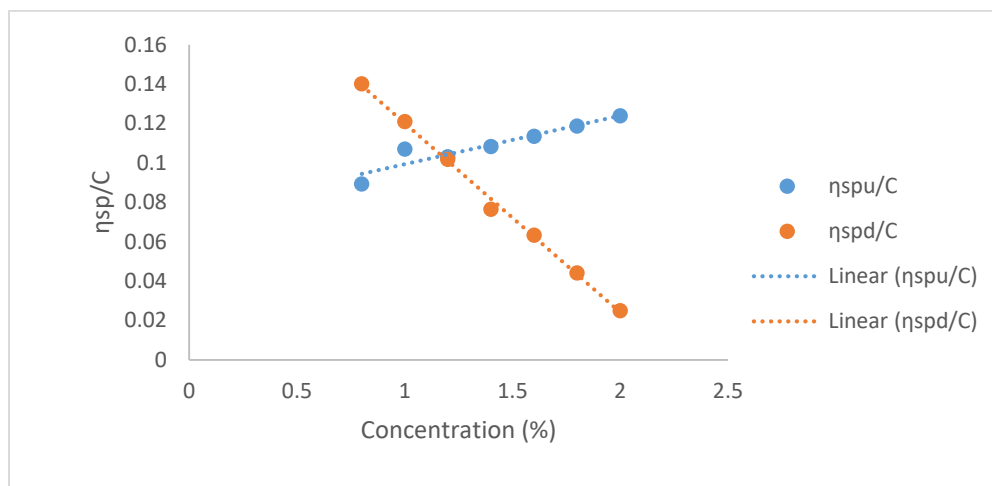


Fig 3: Viscosity of dyed and undyed starch paste.

Furthermore, from the graph it is seen that the dye molecules react with a particular group in the starch chain thus forming covalent bond, when this site are all exhausted it starts to react with other groups leading to a sharp rise in curve before it starts descending

4. Conclusion

The starch produced in this work is relatively of high quality with properties meeting the requirement for most commercial uses. The rheological properties obtained of the starch paste reveals that the viscosity of the undyed starch paste is higher than that of the dyed starch paste. The dyeing of starch with reactive dye varies with the concentration of the dye solution used given rise to different shade and

absorbance of the dyed starch is varies with concentration of the dye solution used.

References

1. Lu D.R, Xiao C.M, and Xu S.J. (2009) Starch-based completely bio degradable polymer materials, Express Polymer Letter, 3(6),366-375
2. Luc A. (1994), Agro Polymer and Starch Based Materials, www.biodeg.net/biomaterial.html.
3. Nkeonye P.O (2009) Chemistry and Application of pigments, Unpublished MSc Lecture Notes, Ahamdu Bello University Zaria, Nigeria.
4. Sugih A.K (2008) Synthesis and Properties of Starch based Materials, University of Groningen.
5. Zollinger H. (2003) Colour Chemistry 'Synthesis, properties and application of organic dye and pigment' 3rd edition. ISBN-10:3706390233
6. Adamu A.K, Yakubu M. K. and Summonu O.K (2013) Preparation of Starch-Reactive Dyed pigment to be used in Emulsion Paint Formulation. IJCEBS,1(1). ISSN 2320-4087

**ABSTRACT CCT-: 003**

Isa H. Katsayal*, U. A., Agunu, A. A. Nuhu, and Z. Abdulhamid

Department of Pharmacognosy and Drug Development, Faculty of Pharmaceutical Sciences, Ahmadu Bello University, Zaria- Nigeria

Email: hassanatuisa@gmail.com**ANTIMICROBIAL PROPERTIES OF NAUCLEA DIDERRICHII (RUBIACEAE) LEAF EXTRACTS**

ABSTRACT: This work explored the antimicrobial potential of *Nauclea diderrichii* (Rubiaceae) formerly known as *Sarcocephalus diderrichii*, a plant that is highly valued in ethno medicine for the treatment of various infectious diseases by traditional medical healers. The pulverized leaf of *N. diderrichii* was extracted successively using cold maceration method with hexane, ethyl acetate and methanol. The extracts were qualitatively screened for the presence of secondary metabolite, and then tested in vitro for activity against six clinical isolates. Preliminary phytochemical screening of the extracts revealed the presence of carbohydrates, saponins, tannins, alkaloids, cardiac glycoside, phenolic compounds, phytosterols, triterpens and flavonoid. All the bacterial strains were sensitive to the extracts with different zones of inhibition ranging from 10 mm – 20 mm whereas the two fungal strains were resistant to all the extracts. The minimum inhibitory concentration (MIC) ranges between 7.5 mg/ml – 240 mg/ml for all the bacterial strains whereas the minimum bactericidal concentration (MBC) result ranges from 15 mg/ml – 60 mg/ml for all the bacterial strains.

1. Introduction

Medicinal substances from plants have being in used throughout the world for human health care from time immemorial. This is especially in Africa where underdevelopment and poverty have made a large percentage of the people to rely almost entirely on traditional medical practices and folkloric use of plants (Egharevbu *et al.*, 2010). More so, with the WHO Alma-Ata declaration of 1978 encouraging developing and poor countries to incorporate traditional medicines of proven efficacy into the orthodox practice in order to bridge the widening gap in accessing primary healthcare by the citizen since more than 70% of the population in these countries already patronize traditional medicine (WHO, 1978; African Health Monitor Report, 2003). The efficacy of some of these traditional herbal remedies has been proven by various researchers.

Infectious diseases are major causes of morbidity and mortality in the developing world and accounts for about 50% of all deaths (El- Mahmood, 2009). Most of the current antimicrobials have considerable limitations in terms of their spectrum, side effects and their widespread overuse has led to increasing clinical resistance of previously sensitive microorganisms and to the occurrence of uncommon infections. Plants used for traditional medicines contain a wide range of substances that can be used to treat chronic as well as acute infectious diseases and have therefore become sources of important drugs. Antimicrobial properties of medicinal plants are being increasingly reported from different parts of the world. One such plant renowned for its wide use in African folklore is *Nauclea diderrichii*. The plant is native to some African countries including Nigeria. The vernacular names are Brimstone tree; African peach (English) and Tuwon biri; Goron biri (Hausa).

The leaf of *N. diderrichii* is used locally in different forms for the treatment of skin diseases, measles, fever, stomach problem, gonorrhoea, menstrual problem, tumours and diarrhea (Addo-Danso *et al.*, 2012; Alqasim *et al.*, 2013). Despite these potentials, there is no known scientific evidence to validate these claims, therefore the present study aimed at evaluating the antimicrobial properties of the leaf to provide bases for its utilization as such and to link scientific facts with some of its traditional uses with the hope of attracting more research attention to the plant for development of new drugs.

2. Materials and method

Sample plant of the leaf was authenticated as *Nauclea diderrichii* by a staff in the Herbarium Unit of the Department of Biological Sciences, Ahmadu Bello University, Zaria and assigned Herbarium specimen number 16677. Sufficient quantity of leaf was obtained in the month of October, 2015, dried under the shade for ten days and comminuted to powdered form using pestle and mortar, stored in a sterile airtight container before use.

Extraction of the powdered leaf was done using the method described by (Kokate, *et al.*, 2003). Figure 1 showed the extraction procedure for twelve days. The filtrates were evaporated to dryness, on a water bath at 55 °C after which the solidify extracts were stored in desiccator for subsequent use.

2.1 Preliminary Phytochemical Screening

The leaf extracts (hexane, ethyl acetate and methanol) were subjected to phytochemical screening in order to identify the phytochemical constituents using the method described by (Sofowora, 2000).

2.2 Clinical Isolates and Culture Media Used

Microbial strains consist of four bacterial strains, two each for gram positive and negative respectively and two fungal strains were used following the method of Nayan and Shukla, (2011).

The microbial strains were obtained from the Department of Microbiology, Ahmadu Bello University, Zaria. The culture media used are Mueller Hinton agar (MHA), Mueller Hinton broth (MHB), Potato Dextrose agar and Nutrient agar (NA). These media were used for sensitivity tests, determination of minimum inhibitory concentration (MIC) and Minimum Bactericidal Concentration (MBC).

2.3 Preparation of stock solution

The extracts, about 2.4 gram each of hexane, ethyl acetate and methanol extracts of the leaf of *N. diderrichii* were weighed and dissolved in 10 ml of Dimethyl Sulphur Oxide to obtain a concentration of 240 mg/ ml as an initial concentration of the extracts used for the antimicrobial screening. From the stock solution, two-fold serial dilutions were made to obtain 120, 60 and 30 mg/ ml concentrations of each of the extracts. Standard antibiotics Ciprofloxacin (Maxi care Nigeria Co.) and Fluconazole (Layofil Chem. Italy) were used as the positive control drugs for both antibacterial and antifungal screening respectively.

2.4 Determination of Antimicrobial Activity

To determine the antimicrobial effect of the extracts of *N. diderrichii* leaf, agar well diffusion method was employed. The standardized inocula of both the bacterial and fungal isolates were streaked on sterilized Mueller Hinton and potato dextrose agar plates.

The wells were properly labeled according to different concentrations of the extracts. Each well was filled with approximately 0.2 ml of the extracts. The plates were allowed to stay on the bench for about an hour to enable the extracts to diffuse into the agar. The plates were then incubated at 37 °C for 24 hours (plates of Mueller Hinton agar) while the plates of potato dextrose agar (for fungal growth) were incubated at room temperature for about 4 days. A clear zone that were completely devoid of growth around the wells were measured and recorded. Minimum inhibitory concentration was determined to know the lowest concentration in the series without visible sign of growth and minimum bactericidal concentration was also determined to know whether the antimicrobial effect of the extracts was bacteriostatic or bactericidal.

Generated data were statistically analyzed and expressed as mean ± standard error of mean (SEM) for all values.

3. Results and discussion

A zone of observable inhibition of growth of each organism served as a criterion for declaring an extract sensitive and was indicated by a clear zone around the well. Methanol extract gave the highest zone of inhibition followed by n- hexane while ethyl acetate gave the least zone of inhibition ranging between 10- 20mm compared to the positive control. However, all the three extracts exhibited no effects on the two fungal strains (table 1). From table 2, the MIC exhibited by the organisms range between 7.5 - 240 mg/ ml of the extracts. The gram positive microbes showed MIC range of 7.5 - 30 mg/ ml while gram negative showed MIC of 240 mg/ ml. MBC depicted by the test organisms range between 15 - 60 mg/ ml, this was only observed in gram positive bacterial and could not be determined in gram negative bacteria.

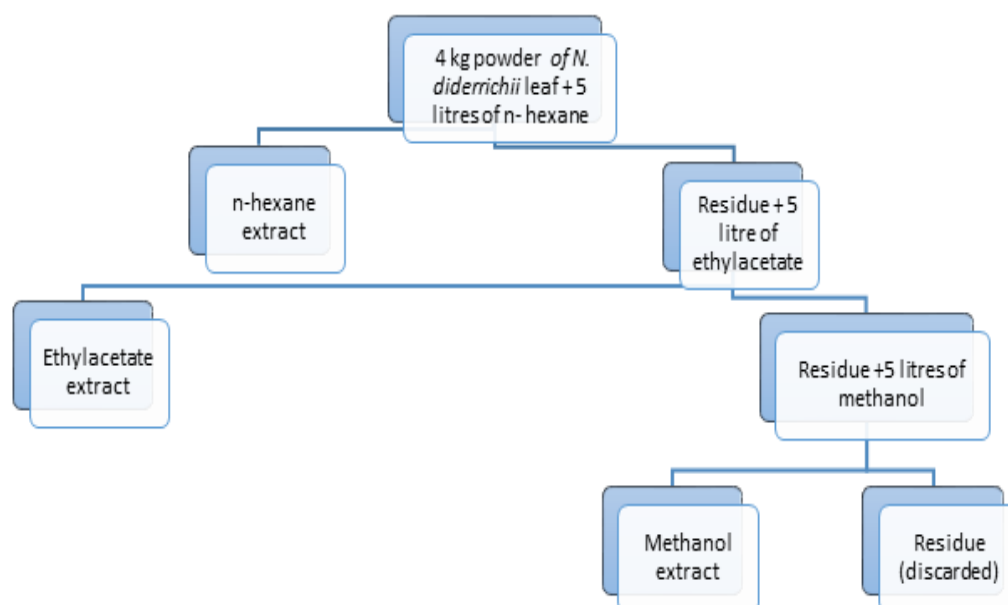


Fig. 1: Flow chart for the extraction of *Nauclea diderrichii* leaf



Table 1: Determination of Zones of inhibition of extracts in the presence of positive controls (mm) ± SEM

Test organism	Conc mg/ml	Methanol extract	Ethyl acetate extract	n-hexane extract	Ciprofloxacin and Fluconazole (10 µg/ml)
Zones of Inhibition (mm)					
<i>Bacillus subtilis</i>	240	20.33 ± 0.33	15.67 ± 0.33	16.33 ± 0.88	35.00 ± 0.00
	120	18.33 ± 0.33	13.67 ± 0.33	13.33 ± 0.88	
	60	17.33 ± 0.33	12.00 ± 0.00	11.33 ± 0.67	
	30	15.67 ± 0.67	10.33 ± 0.33	3.33 ± 3.33	
<i>Staphylococcus aureus</i>	240	18.00 ± 0.58	13.00 ± 0.00	17.33 ± 0.33	37.00 ± 0.00
	120	15.67 ± 0.33	11.00 ± 0.00	15.33 ± 0.33	
	60	15.00 ± 0.00	3.67 ± 0.67	12.67 ± 0.67	
	30	13.33 ± 0.67	3.33 ± 3.33	10.67 ± 0.67	
<i>Escherichia coli</i>	240	15.67 ± 0.33	0.00 ± 0.00	16.00 ± 1.16	40.00 ± 0.00
	120	-	-	-	
	60	-	-	-	
	30	-	-	-	
<i>Pseudomonas aeruginosa</i>	240	16.33 ± 0.88	0.00 ± 0.00	15.33 ± 0.67	37.00 ± 0.00
	120	-	-	-	
	60	-	-	-	
	30	-	-	-	
<i>Candida albicans</i>		-	-	-	31
<i>Aspergillus niger</i>		-	-	-	35

Note: Three Determinations were made in each case and the Average Taken, - = No Activity

Table 2: Minimum Inhibitory Concentrations and Minimum Bactericidal Concentrations of *Nauclea diderrichii* Leaf Extracts

Test Organisms	MIC (mg/ ml)			MBC (mg/ ml)		
	methanol	Ethyl acetate	n-hexane	Methanol	Ethyl acetate	n-hexane
<i>Staphylococcus aureus</i>	7.5	30	15	15	60	30
<i>Bacillus subtilis</i>	7.5	15	30	15	30	60
<i>Escherichia coli</i>	240	ND	240	ND	ND	ND
<i>Pseudomonas aeruginosa</i>	240	ND	240	ND	ND	ND
<i>Candida albicans</i>	ND	ND	ND	ND	ND	ND
<i>Apergillus niger</i>	ND	ND	ND	ND	ND	ND

Note: ND = not determined

4. Conclusion

The study revealed that the leaf of *N. diderrichii* contain secondary metabolites that are responsible for its antimicrobial activity, thus support the use of this plant by traditional medical practitioners in treatment for different kind of ailments, especially skin infections.

Acknowledgement

The authors are grateful to the management of the Department Pharmacognosy and Drug Development for their supports, and to Mal. Sani a traditional herbal practitioner of Layin Zomo, Zaria for the collection of the plant.

References

- Addo-Danso, S. D., Bosu, P. P., Nkrumah, E. E. Pelz, D. R. Coke, S. A. and Adu-Bredu, S. (2012). Survival and Growth of *Nauclea diderrichii* and

- Pericopsis elata in Monoculture and Mixed-Species Plots in Ghana. *Journal of Tropical Forest Science* 24(1): 37-45.
- African Health Monitor report (2003). Traditional medicine our culture, our future. Vol. 4: 1.
- Alqasim, A. M., Gabriel, O. and Uthman, I. I. (2013). Plant Remedies Practiced by Keffi People in the Management of Dermatoses. *Journal of Medicinal Plants Studies* 1(5): 112-118.
- Egharevba, H. O., Abdullahi, M. S., Okwute, S. K. and Okogun, J. I. (2010). Phytochemical Analysis and Broad Spectrum Antimicrobial Activity of *Laggera pterodonta* (DC.) Sch. Bip. (Aerial Part). *Researcher*. 2(10):35-40.
- El-Mahmood, M. A. (2009). Antibacterial activity of crude extracts of *Euphorbia hirta* against some bacteria associated with enteric infections. *Journal of Medicinal Plants Research*. 3(7):498-505.
- Kokate, C. K., Kumar S. and Kumar V. (2003). *Practical Pharmacognosy*. Vallabh Prakashan, New Delhi, India. 4:107-111.
- Nayan, R. B. and Shukla, V. J. (2011). Antibacterial and antifungal activities from leaf extracts of *Cassia*



- fistula. *Journal of Advance Pharmaceutical Technology Research*. 2(2): 104–109.
8. Sofowora, A. (2008). *Medicinal Plants and Traditional Medicine in Africa*. Spectrum Books Limited, Ibadan, Nigeria. 3rd Edition. Pp. 200-202.
 9. World Health Organization Declaration of Alma-Ata (1978), International Conference on Primary Health Care, Alma-Ata, USSR, 6-12 September 1978.

**ABSTRACT CCT-: 050**Ugochi J. Okoduwa^{*,†}, Olabode H. Olabimtan^{*}, Adebola F. Ade-ajayi^{*}, Zaharaddeen S. Gano^{*}

National Research Institute for Chemical Technology, Basawa – Zaria, Nigeria

Email: judithsplendour@gmail.com**EFFECTS OF DIFFERENT DRYING METHODS ON SOME PROXIMATE PROPERTIES OF ONION POWDER: A COMPARATIVE STUDY**

ABSTRACT: Onion powders were produced using three different drying methods namely oven drying and freeze drying. The effects of these methods on the proximate properties of the onion powders were investigated and it was observed that the amount of water loss by the onion samples followed the trend: oven drying (uniform) > freeze drying > oven drying (stage wise). Furthermore, it is worthy of note that powdered onion samples obtained via the freeze drying method retain its natural characteristic odour and colour similar to that of fresh onions while those obtained via other methods had more of the other proximate properties than the freeze dried onions.

Keywords: Onion powder, freeze drying, proximate, oven drying.

1. Introduction

Onion (*Allium cepa*), a very commonly used vegetable, ranks third in the world production of major vegetables [1]. It is a strong-flavored vegetable used in a variety of ways, and its characteristic flavor, biological compounds and medical functions are mainly due to their high organo-sulphur compounds[2]. Onion is one of the most economically viable horticultural crop in Nigeria after tomatoes [3]. In the peak season production is most times in excess leading to spoilage and wastage of the onions as they cannot be preserved properly in humid conditions [4]. Hence the need to preserve the excess produced to ensure its availability as well as prolonging its shelf life.

Dehydrated onion, canned onion and onion pickle are better ways of preserving onions for exportation. Free water is extracted from the vegetables during the drying process so that microorganisms do not survive and reproduce [1]. Drying process involves the application of heat to vaporize water and removal of moist air from the dryer. Large quantities of onions are dehydrated, but substantial quantities are imported. To retain quality, it is important to dry the onions down to not more than 5%, preferably 4% or less.

Health conditions such as scurvy, dropsy, catarrh, chronic bronchitis can be treated with onions. They also serve as domestic remedy for colic and scurvy when mixed with common salt. For clearer vision it is applied to the eyes and locally to allay irritation of insect bites and scorpion stings [5]. Among the various methods used in preserving onions, dehydration (drying) is considered most effective particularly in terms of product quality. Several methods have been adapted for the preservation of onions one of which is dehydration.

The aim of dehydrating onion into powder is to produce a concentrated product which when properly packaged has a long shelf life, after which it can simply be reconstituted without substantial loss of flavour, colour and aroma [1].

Methods such as freeze drying, convective stage wise drying, solar drying, fluidized bed drying, vacuum drying, osmotic dehydration have been employed in the processing of onions [1].

Freeze drying- technically known as lyophilization, or cryodesiccation is a dehydration process typically used to preserve a perishable material or make the material more convenient for transport. Freeze drying produces the highest quality food product compared to other methods of drying as it has the advantage of little loss of flavour or aroma [6].

Convective Stage wise drying – this is a method of drying the onions at different temperatures and time intervals and their respective weight taken.

In this work, powdered onion was produced on lab scale and some of its proximate parameters analyzed.

2. Materials and methods

2.1 Sample collection

Some purple species of onions were sourced from a local market around Basawa, Zaria and stored at room temperature prior to use for this work.

2.2 Sample preparation

The outer layer of the onions was peeled off and washed to remove adhering soil and dirt. They were then left in a sieve to drain excess water. The onions were cut into thin rings and placed in evaporating dishes.

2.3 Drying methods

Three drying methods were considered with their respective temperature, timing and sampling conditions. The samples were dried using a hot air drying oven (by Genlab) and a freeze dryer (LGJ-12 by Beiging Songyuanhaxing technologies)

2.3.1 Straight drying

60g of the sliced onion was weighed into a clean pre weighed evaporating dish and then



placed in a hot air drying oven at 95°C. The sample and dish was intermittently weighed until constant mass. This was tagged sample A.

2.3.2 Stage-wise drying.

2.3.2.1 Stage-wise drying with sliced sample

60g of the sliced onion sample was weighed into a clean pre-weighed evaporating dish and then placed in a hot air oven at 95°C for 30mins after which the temperature was varied to 70°C for 45mins, then to 55°C for 60mins, and finally to 45°C for 45mins. The dish was weighed at every interval until constant mass was achieved.

2.3.2.2 Stage-wise drying with blended sample

60g of the sliced onion sample was weighed into a clean pre-weighed evaporating dish and then placed in a hot air oven at 95°C for 30mins after which the temperature was varied to 100°C for 30mins, then to 70°C for 45mins, then to 55°C for 60mins and finally to 45°C for 45mins. The dish was weighed at every interval until constant mass was achieved. This was tagged sample C.

2.3.3 Freeze drying.

50g of blended onions was placed into the drying pan in the freeze drier at the temperature of -56°C under vacuum of 100pa for 7hrs this was tagged sample D. All analyses were done in triplicate.

2.4 Proximate analysis

The following physicochemical parameters of the dried onions were studied:

- Ash content (Expulsion of volatile organic matters).
- Moisture Content.
- Lipid (Fat and oil content)
- pH
- Colour
- Odour.

These parameters were determined according to the method approved by the association of official analytical chemist [7].

3. Results and discussions

Figure 1 depicts the rate of moisture loss in the sliced onions at 95°C. The mass decreased with time and became constant at 210mins where the moisture loss was 86%. At this time, it was

observed that the physical properties of the dried onions like the colour and odour were significantly affected to the extent of partial denaturing. To minimise denaturing, the stage wise drying was employed and results are as shown in Figure 2 which shows low moisture removal of 40% compared to that obtained in Fig. 1. One of the possible ways of improving the moisture removal is by producing slurry of the onion via blending. Figure 3 shows the results of the stage wise drying with the blended onion. Moisture removal of 50% was achieved under the considered drying time, thus making it a little bit above the one obtained with the sliced samples but lower than the one obtained at 95°C. The results therefore suggest that in order to achieve drier onions that are not denatured, longer time is needed using the stage wise drying approach. The freeze drying method was further employed on the onion samples and the results showed that a moisture loss of 82% was achieved under 420mins. Although this method takes longer drying time and moisture loss a little below that obtained at 95°C, the physical properties of the samples particularly the odour remained like that of fresh onions.

Fig. 4 shows the results of proximate analysis carried out on the dried onion samples. From the figure, Sample C was found to be more acidic than Samples A, B and D. These results showed that onions are acidic in nature. Allen *et. al.*[8] reported that onions with lower acid content are more favourable for human consumption as compared to those with higher acid content. The Ash content was found high with Sample C and lowest with Samples B and D. Lipid content was found highest with Sample C and lowest with Sample B. Sample C (stage wise drying of blended onions) was found to have the highest ash content thus suggesting that it has less volatile compounds. Moreover, it has more fats and oils from the high lipid content present.

The odour of sample D was found to be more like the raw onions, while the sample A, B, and C had burnt smell. It was observed that the colour of the samples became lighter with decrease in temperature. The freeze dried samples were lighter brown in colour compared to the heated samples that were dark brown. Freeman *et al.*[9], found that freeze-dried onion retained more of the characteristic flavor components of fresh onion, as judged by sensory tests, than hot air drying methods for onion.

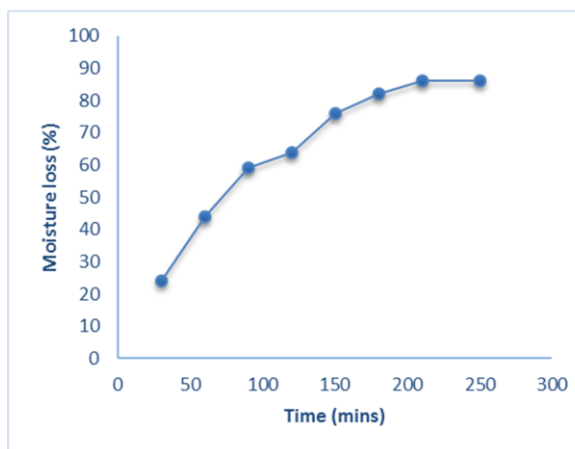


Fig. 1: Moisture loss for straight drying of sliced onions at (95°C)

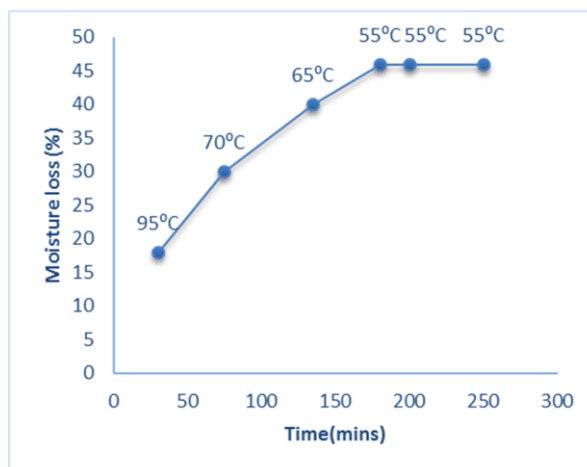


Fig. 2: Moisture loss for stage wise drying of sliced onions

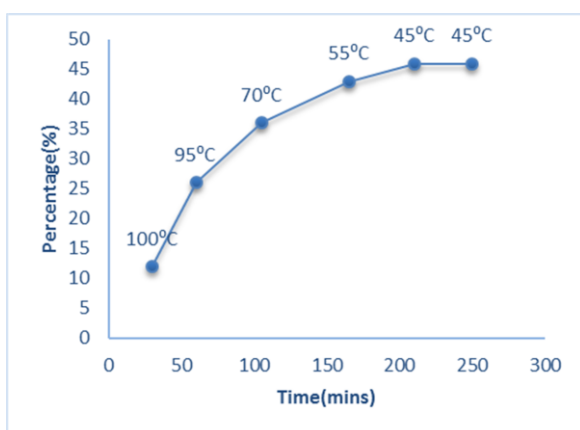


Fig. 3: Moisture loss for stage wise drying of blended onions

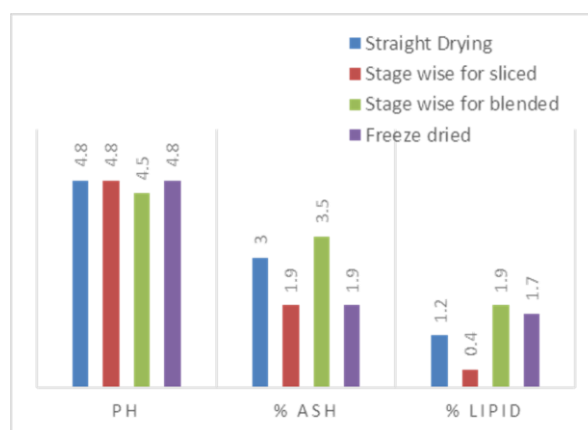


Fig. 4: pH, ash and lipid contents of hot air, stage wise and freeze dried samples

4. Conclusion

The oven dried (uniform) onion had the highest moisture removal of 86% while the oven dried (stage wise) onions had the lowest moisture removal of less than 50%. However, the blended part took shorter time to dry compared to the sliced part. The freeze dried onions had a good moisture loss of 82% with minimal denaturing and almost fresh aroma but takes longer time to dry and it is very expensive to achieve. For further studies, the vitamins, elemental composition and protein content of the freeze dried onion should be determined and compared with the hot air dried onion.

References

- Mitra, J., S. Shrivastava, and P. Rao, Onion dehydration: a review. *Journal of food science and technology*, 2012. 49(3): p. 267-277.
- Mota, C., et al., Convective drying of onion: Kinetics and nutritional evaluation. *Food and Bioproducts Processing*, 2010. 88(2): p. 115-123.

- Igbadun, H.E., A. Ramalan, and E. Oiganji, Effects of regulated deficit irrigation and mulch on yield, water use and crop water productivity of onion in Samaru, Nigeria. *Agricultural water management*, 2012. 109: p. 162-169.
- Sangwan, A., A. Kawatra, and S. Sehgal, Nutritional evaluation of onion powder dried using different drying methods. *Journal of Dairying, Foods and Home Sciences*, 2010. 29(2): p. 151-153.
- Augusti, T.K., Therapeutic and medicinal values of onions and garlic. *Onions and allied crops*, 1990. 3: p. 93-108.
- Liapis, A.I. and R. Bruttini, 11 *Freeze Drying. Handbook of industrial drying*, 2014: p. 259.
- Kelrich, K., ur. (1990) *Official methods of analysis*. Arlington, VA: Association of Official Analytical Chemists/AOAC.
- Allen, M.L., et al., The effect of raw onions on acid reflux and reflux symptoms. *American Journal of Gastroenterology*, 1990. 85(4).
- Freeman, G.G. and R.J. Whenham, Changes in onion (*Allium cepa* L.) flavour components resulting from some post-harvest processes. *Journal of the Science of Food and Agriculture*, 1974. 25(5): p. 499-515.

**ABSTRACT CCT-: 010**

Feka D.P., Gwani H., Kutman N.A., Elemike C.

Nigerian Institute of Leather and Science Technology, Samaru-Zaria, Nigeria

Email: fekapaschal@yahoo.com**EFFECT OF SOAKING AND FERMENTATION ON THE PROXIMATE COMPOSITION AND ANTI-NUTRITIONAL PROPERTIES OF SEEDS OF *Senna occidentalis*****1. Introduction**

This study evaluates the effect of two methods of pre-treatment (soaking and fermentation) on the proximate and anti-nutritional composition of underutilized seeds of *Senna occidentalis*. Crude fibre value was higher with fermentation (14.84%) and lower with soaking (4.93%), crude protein was also higher with fermentation (17.28%), soaking yielded a higher carbohydrate content (55.44%), while fermentation yielded the least (42.55%), the highest crude lipid was obtained from the untreated *Senna* seeds (3.85%) and the lowest from the soaked seeds (1.87%), total ash percentage ranged from 2.71% to 4.88%, percentage reduction in phytate, saponin, alkaloids, hydrogen cyanide was higher with fermentation (46.88%, 75.51%, 3.67%, 36.92% respectively), while reduction in tannins and oxalate was higher with soaking (20.81% and 69.5%). This work revealed that the protein and crude fibre composition of fermented seeds was improved by the fermentation process, ash content was least for fermented seed. Fermentation better reduced the anti-nutritional content of the seeds. Fermented seeds of *Senna occidentalis* have the potential to partially replace soybean as an alternative protein and fibre source in animal feed formulation upon improvement of the fermentation process.

2. Materials and Methods**2.1 Plant collection**

The pods of *Senna occidentalis* were collected from Jamaá village, Zangon-Shanu, Zaria and identified in the biological Science herbarium of the Department of Plant Science, Ahmadu Bello University Zaria, Kaduna State, Nigeria.

2.2 Preparation of sample

Matured dried pods of *Senna occidentalis* were dehulled, grounded to release the seed from coat. The grounded seeds (300g) were divided into three parts; a part (100g) was grounded into fine powder. Another part (100g) was soaked for five hours and drained using cheese cloth, dried indoors for 5 days then ground. The last part (100g) was soaked with warm

water covered, fermented for 3 days (induced with yeast), drained of the water and dried indoors for 5 days. Samples were stored in well labeled sample bottles.

2.3 Proximate analysis

Moisture content, ash content, lipid content, crude fibre, crude protein of the samples was determined by the methods described by A.O.A.C 1980. Carbohydrate was determined by difference (Muller and Tobin, 1980).

Quantitative determination of anti-nutrients Phytate was determined as described by Reddy et al (1982); Tannins was determined as described by Pearson (1976); Oxalate was determined as described by Oke (1969); Alkaloid was determined by the gravimetric methods of Harbone (1984); Saponin was determined as described by (Obadoni and Ochuko, 2001) and Hydrogen cyanide was determined by the method described by A.O.A.C (1980).

3. Results and discussion

Result shows the seed to be a good source of protein, crude fibre, crude lipid and carbohydrate. A significant increase of about 32.29% and 33.89% between the moisture content of the untreated, soaked, and fermented was recorded. Adamu et al. (2013) recorded an increase in the moisture content from 11.5% to 27% for raw and fermented seeds of *Cassia tora*. The moisture content was seen to increase in fermented and soaked seeds, probably due to the fermentation and soaking period respectively (Igbabul, et al 2014). Untreated seed is an excellent source of fibre; the soaked sample showed a decrease of 52.78% of the crude fibre obtained in the untreated seed, while the fermented seed showed a significant increase of about 42.15% obtained in the untreated seeds. The crude fibre of the seeds ranged from 4.93% to 10.44% to 14.84% for the soaked, untreated and fermented seeds respectively. This is higher than the range of 3.81%, to 3.83% to 3.86% obtained for soaked, boiled and raw seeds of a wild legume, *Mucuna pruriens* (Nwaoguikpe et al. 2011), but comparable to the crude fibre content of seeds of *Senna obtusifolia* (10.18%) carried out by Ingweye et al. (2010).

Table 1: Proximate composition of untreated and pretreated seeds of *Senna occidentalis*.

constituent	Untreated	Soaked	Fermented
Moisture content	14.40%	19.05%	19.28%
Ash	4.88%	3.18%	2.71%
Crude protein	17.06%	15.53%	17.28%
Crude lipids	3.85%	1.87%	3.34%
Crude fibre	10.44%	4.93%	14.84%
carbohydrate	49.38%	55.44%	42.55%

Table 2: Qualitative test for some anti-nutrients

Anti-nutrient	Untreated	Soaked	fermented
Saponins	++	+	+
Tannins	+++	++	++
Alkaloids	+++	+++	++

Table 3: Percentage increase/decrease in anti-nutritional properties of untreated and pretreated seeds of *Senna occidentalis*.

Anti-nutrient	Untreated	Soaked	Fermented
Phytate	0.6436%	0.5680%	0.3383%
Tannins	10.8063%	8.5626%	9.7702%
Oxalate	0.8195%	0.2530%	0.4950%
Saponins	4.9000%	2.1000%	1.2000%
Alkaloids	19.6360%	19.0400%	18.9180%
Hydrogen cyanide	0.0065%	0.0043%	0.0041%

% Increase= increase/original number x 100; % Decrease=decrease/original number x 100

The ash content for the untreated seeds was 4.88%, this is higher than that of *Seena obtusifolia* (3.70%) and seed of *Cassia tora* (4.69%), however, the ash content for the fermented *Senna occidentalis* is lower (2.71%) than the fermented seed of *Cassia tora* (7.99%), indicating a less mineral composition in the former, the ash content of the soaked *Senna occidentalis* seeds showed a decrease of about 34.84% from the untreated seeds, the loss in ash content may be due to leaching of soluble mineral into the processing water during soaking and fermentation respectively (Igbabul, et al 2014).

Crude protein content was found to compare with that of some wild legumes (*Tamarindus indica* 14% and *Atylosia scarbaeoides* 17.3%), Arinathan et al. (2003). Protein content is higher than that of the raw seeds of *Cassia tora* (13.9%), but lower than that of *Senna obtusifolia* (29.54%) and of soya bean (38%) as recorded by Augustine and Klein (1989). The seeds were generally found to be low in crude lipids, this, however is higher than the lipid content of *Mucuna pruriens* (2.69%, 2.51% and 2.51% respectively for the raw, boiled, soaked and boiled seeds) and *Senna obtusifolia* (2.31%), but much lower than the raw (16.01%) and fermented (18.36%) seeds of *Cassia tora*. A significant increase was observed for total carbohydrate with the soaked seeds, while a significant decrease was observed for the fermented seeds. A reduction in carbohydrate content has been reported in fermented seeds of *Cassia tora* (from 58.33% to 35.25%) also

an increase of 14.16% have been reported for the soaked and boiled seeds of *Mucuna pruriens*.

Soaking reduced the protein content, fermentation increased the protein content, as was reported in locust bean (*Parkia bighbosa*) fermentation (Ibrahim and Antai, 1986). The decrease in carbohydrate in the fermented sample could be attributed to the conversion of oligosaccharides to simple sugars or the utilization of the carbohydrate nutrient as source of energy by the fermenting micro-organism for growth and metabolism, the increase in carbohydrate in soaked sample could be explained in terms of the significant reduction in protein concentration. The reduction in crude fibre may be as a result of solubilization during soaking. Ibrahim and Antai (1986) reported an increase of liquid content during fermentation of Africa locust beans.

Anti-nutritional factors studied are presented in table 4. Result showed Alkaloids with highest percentage composition, a 20.81% decrease in the tannin content of the soaked sample was recorded. The saponin content of the soaked sample decreased by about 57.14%, the fermented seeds showed a less significant decrease (about 75.51%), while about 9.62% was recorded for the tannin content, a significant decrease in the phytate content (about 46.88%) was also recorded; reduction in phytate content for fermented seed agrees with result reported by Ijarotimi and Aroge, 2005. Oxalate content of the fermented seed decreased by about 40.24%, significant



decrease (about 69.5%) was observed for the oxalate content of the soaked sample. the alkaloid content of the fermented sample reduced (by 3.67%) than that of the soaked sample (2.85%). The reduction in tannin, phytate and saponin are consistent with results obtained by Adamu et al (2003), Tamburawa (2010), Balogun (2013) and Audu et al, (20013), than the reduction obtained in this research (3.67%).

Various studies have reported considerable reduction in anti-nutritional factors in traditional legumes by fermentation involving lactic acid bacteria (Barber and Achinewhu, 1992). Among the two methods the tannin content was best reduced by soaking method (although not sufficiently reduced). Result of this research shows that fermentation is more effective for reducing phytate, saponins, alkaloids and hydrogen cyanide while soaking is more effective for reducing tannins and oxalate.

Reference

- Adamu, H.M. Ushie, O. A & Elisha, B. (2013). Chemical and Nutrient Analysis of Raw and Fermented Seeds of Cassia tora. *Journal of Physical Sciences and Innovation*.5 (1):125-136.
- Arinathan, V. Muhan, V. R & Debritte, A.J. (2003). Chemical Composition of Certain Tribal pulses in South India. *International Journal of Food Science Nutrition*.54:209-217.
- Audu, S. Aremu, S.M & Lajide, L.O. (2013). Effects of Processing on Physiochemical and Anti-Nutritional Properties of Black Turtle Bean (*Phaseolus vulgaris*) Seed Flour. *Orient Journal Chem*. 29(3).
- Balogun, B.I. (2013). Effects of Processing Methods on Anti-nutrient levels of *Bauhinia monandra kurz* seeds. *PAT* 9(2):88-101.
- Barber, L. I & Achinewhu, S. C. (1992). Microbiology of Ogiri Production from Melon Seeds (*Citrullus vulgaris*). *Nigerian Food Journal* 10:129-135.
- Harbone, J.B. (1984). *Phytochemical Method*, Chapman and Hall, Ltd., London (2nd Ed) PP.12-56.
- Ibrahim, M.H & Antai, S.P. (1986). Chemical Changes during the Fermentation of African Locust Bean (*Parkiafilicoidea welw*) Seeds for production of Daddawa'. *Plant Foods Human Nutrition*.36:179-184.
- Igbabul, B. Hiikya, O & Amove, J. (2014). Effect of Fermentation on the Proximate Composition and Functional Properties of Mahogany Bean (*Afzeila Africana*) flour. *Current Research in Nutrition and Food Science*.2(1).
- Ijarotimi, S. O & Aroge, F. (2005). Evaluation of the Nutritional Composition, Sensory and Physical Properties of a Potential Weaning Food from locally Available Food Materials-Bread Fruit (*A. atilis*) and Soybean. *Journal of Food Nutrition Science*.4:411-412.
- Ingweye, J.N. Kalio, G.A. Ubua, J.A & Umoran, E.P. (2010). Nutritional Evaluation of Wild Sickle Pod (*Senna obtusifolia*) Seeds from obanliku, South-Eastern Nigeria. *American Journal of Food Technology*. 5:1-12.
- Muller, H. G. & Tobin, G. (1980). *Nutrition and food processing*. Croomhelm, London.
- Nwaoguikpe, R.N. Braide, W. & Ujowundu, C.O. (2011). The Effect of Processing on the Proximate and Phytochemical compositions of *Mucuna pruriens* seeds (velvet beans). *Pakistan Journal of Nutrition*.10(10).947-951.
- Obadoni, B.O & Ochuko, P.O (2001), Phytochemical studies and comparative efficacy of the crude extract of some homeostatic plants in Edo and Delta State Nigeria. *Global J. Pure Applied science*, 8: 203-208.
- Oke, O.L. (1969). Oxalic acid in Plants and in Nutrition. *World Review of Nutrition and Dietetics*. S. Karger Basel(Ed) P.262.
- Pearson, D.A. (1976). *Chemical Analysis of Foods*, 7th Ed, Churchill Livingstone, Edinburgh.
- Reddy, N.R. Sathe, S.K. & Sakunle, D.K. (1982). Phytates in Legumes and Cereals. *Advances in Food Research*.28:1-92.
- AOAC (1980). *Official Methods of Analysis*, (13th Ed). Association of Official Analytical Chemist, Washington DC. USA.

ABSTRACT CCT-: 030

Ozogu A. N*, Gadimoh S., Salisu Z., Suleiman M. A., Ukanah P. S., Anyim P. B., Lawal O. M., David S. D., Oddy-Obi I. C., Ukpong M. K., and Chubuzo-Ankor N. C.

Textile Technology Department, National Research Institute for Chemical Technology, Zaria-Nigeria.

Email: donagbe@yahoo.com

LOW COST BIODEGRADABLE ADSORBENT MATERIAL FOR THE REMOVAL OF METHYLENE BLUE FROM AQUEOUS SOLUTIONS: A REVIEW

ABSTRACT: This review discusses the methods for the removal of dyes from the wastewater effluents. Wastewater effluents contain synthetic dyes which cause a potential hazard to the environment; hence these dyes need to be removed from the water bodies. Adsorption process has been found to be one of the best treatment methods for Methylene blue (MB) removals. Adsorption is found to be very effective and cheap method among the all available dye removal methods. From literatures, promising economic adsorbents from different biosorbents for the removal of MB from wastewater has being compiled for year 2012, and 2013. The control of water pollution is increasingly important in recent years, the use of physical/chemical treatments such as membrane filtration, reverse osmosis, coagulation/flocculation and fenton reagents are expensive. The use of different biosorbent as an alternative low cost adsorbent in the removal of methylene blue has been extensively studied and compiled, together with their adsorption capacities and experimental conditions such as adsorbent dose, pH of the solution, temperature and equilibrium time. However, it is evident from the results of experiments in the literatures surveyed that various low-cost adsorbents have shown good potential for MB. Therefore, studies related to searching for efficient and low cost adsorbents derived from existing resources are gaining importance for the removal of dyes.

Keywords: Methylene blue, Adsorption, Low-cost adsorbent, Waste water.

1. INTRODUCTION:

Dyes are coloured compounds which are widely used in textiles, printing, rubber, cosmetics, plastics, leather industries to colour their products, results in generating a large amount of coloured wastewater. Dyes are mainly classified into anionic, cationic, and non-ionic dyes (Ravi *et al.*, 2016). Textile industries are placed in the first position in using dyes for coloration of fiber (Reisch *et al.*, 1996, Rahman *et al.*, 2010). Dyes are chemical compounds which attach themselves to fabrics or surface shells to impart colour. The results of waste water from textile and manufacturing industries is a major challenge for environmental managers (Ho *et al.*, 2001), as dyes are water soluble and produce very bright

colours in water with acidic properties. It has been projected that textile and manufacturing industries are using more than 10,000 commercially available (worldwide) dyes and the consumption of dyes in textile industry is more than 1000 tones/year and about 10-15% of these dyes are discharged into waste streams as effluents during the dyeing processes (Reisch *et al.*, 1996). Methylene blue is a common dye mostly used by industries involves in textile, paper, rubber, plastics, leather, cosmetics, pharmaceutical and food industries, which has a chemical formula $C_{16}H_{18}ClN_3S \cdot 2H_2O$, with molecular weight 319, and its chemical structure is shown in Figure 1.

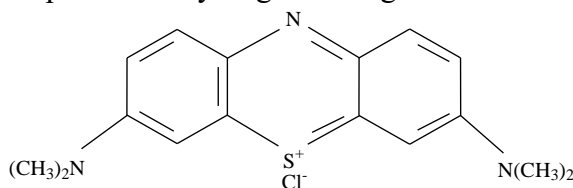


Figure 1: Chemical structure of Methylene Blue (MB) dye

The aim of this review is to provide a summary of recent information concerning the use of low-cost materials as sorbents. For this, an extensive list of sorbent literature on methylene blue has been compiled.

2. TREATMENT METHODS FOR COLOR REMOVAL:

Methods of dye wastewater treatment have been reviewed recently (Young *et al.*, 1997, and Lian *et al.*, 2009,). There are several reported treatment methods for the removal of dyes from effluents, and these technologies can be divided into three categories: chemical method, physical method, and biological method, (Young *et al.*, 1997). However, all these methods have advantages and drawbacks, because of the high cost and disposal problems. The main components of dye molecules are the chromophores, which are responsible for producing the colour, and the auxochromes, which can not only supplement the

chromophore but also render the molecule soluble in water and give enhanced affinity (to attach) toward the fibers (Gupta *et al.*, 2009).

2.1. Physical Methods:

Physical treatment method includes membrane filtration process, reverse osmosis, electrolysis and adsorption techniques. The major drawback in this technology, especially membrane filtration is limited to life time before membrane fouling occurs, and as such the cost of periodic replacement must thus be included in any analysis of their economic viability. Among all the physical treatments, adsorption process has been reported to be the most effective method for water decontamination (Da, *et al.*, 2001). Adsorption



is known to be a promising technique, which has great importance due to the ease of operation and comparable low cost of application in the decoloration process. For the purpose of removing unwanted hazardous compounds from contaminated water at a low cost, much attention has been focused on various naturally occurring adsorbents such as chitosan, zeolites, fly ash, coal, paper mill sludge, saw dust, and various clay minerals (Rafatullah *et al.*, 2010).

2.2. Chemical Treatment

The major agents of chemical treatment of dye wastewater are coagulants/ flocculants (Shi *et al.*, 2007). It involves the addition of substances such as calcium, aluminum, or ferric ions in to the effluent, as such flocculation is induced. Furthermore, Mishara *et al.*, 2006, and Yue *et al.*, 2008 have report the use of other agents for chemical processes

such as, ferric sulphate, and some synthetic organic polymers.

2.3. Biological Methods

Biological treatment of wastewater is an alternative and most economical method as compare to physical and chemical methods. Biodegradation methods such as adsorption by (living or dead) microbial biomass, fungal decolorization, bioremediation systems and microbial degradation are commonly used in the treatment of industrial effluents. Microorganism such as yeasts, bacteria, fungi and algae are able to accumulate and degrade different pollutants, but due to some technical constraints their applications is often restricted (Bekchanov *et al.*, 2012). Researchers have made a lot of efforts to focus on the adsorption technology for dye remediation from wastewater

Table 1: Existing and Emerging processes for dyes removal (Foo *et al.*, 2012).

Physical/chemical Methods	Method description	Advantages	Disadvantages
Fenton reagents	Oxidation reaction using mainly H ₂ O ₂ -Fe(II)	Effective decolorization of both soluble and insoluble dyes	Sludge generation
Ozonation	Oxidation reaction using ozone gas	Application in gaseous state: no alteration of volume	Short half-life (20 min)
Photochemical	Oxidation reaction using mainly H ₂ O-UV	No sludge production	Formation of by-products
Activated carbon	Dye removal by adsorption	Good removal of a wide variety of dyes	Regeneration difficulties
Membrane filtration	Physical separation	Removal of all dye types	Concentrated sludge production
Ion exchange	Ion exchange resin	Regeneration: no adsorbent loss	Not effective for all dyes

3. Agricultural Waste Materials Used as Low Cost Adsorbent

The use of biomass (dead or living), fungi, algae and other microbial cultures in the removal of methylene blue was the subject of many recent researches. Biological materials used to accumulate and concentrate dyes from aqueous solution are termed as bioadsorbents. Major disadvantage in these biomaterials is its non-selective (i.e. it cannot isolate each pollutant and get it removed independently of one another) all the target and nontarget contaminants, if present are concentrated on the surface of the adsorbent. Bioadsorption is a novel approach, and considered to be relatively superior to other techniques because of its low cost, simplicity of design high efficiency, availability and ability to separate wide

(Boukhelifi *et al.*, 2013). Recent literature on the methods of removal of dye from wastewater focuses on MB adsorption.

4. Sources of Dyes and its Classification

Dyes are mainly derived from natural sources without any chemical treatment (Kadolph *et al.*, 2008), such as plants, insects, animals and minerals. Dyes derived from plant sources are indigo and saffron, insects are cochineal beetles and lac scale insects, animal sources are derived from some species of mollusks or shellfish, and minerals are ferrous sulfate, ochre. Industries such as textile, printing, paper, carpet, plastic, and leather use dyes to provide colour to their products. These dyes are always left in industrial waste and consequently discharged into the water body.

**Table 2:** Various Researchers' observations on differences in adsorption capacity with Metal hydroxide sludge at different pH.

Researchers	Dye	Adsorption capacity	References
Gupta et al.	Rhodamine B	1.16×10^{-5} mol/g	Gupta <i>et.al.</i> ,2004
Manoj Kumar Sahu et al.	Safranin-O	89.4 mg/g	Sahu <i>et.al.</i> ,2015
Kong, Chun-yan	Lead (Pb)	38.2 mg/g	Kong <i>et.al.</i> ,2011

Conclusions

Based on the literature reviewed so far, it was found that, recently, there has been an increase in production and utilization of dyes, resulting in an increase in environmental pollution. Different techniques have been utilized for removal of toxic organic compounds from waste water such as filtration, coagulation/flocculation, ion exchange, adsorption, fenton reagent technique, and photocatalytic methods have been used. Chemical and biological methods found to be limited as they are often involving high investment and functional costs. Among all the methods available for separation of pollutants from waste waters, the adsorption shows possible method for treatment and removal of organic pollutants in waste water treatment. Adsorption follows surface phenomenon and more advantageous over the other available methods because of its low capital, operation costs and simple design. The results of the literatures above and methods employed during the researches lead to a conclusion that for removal of MB using bio-materials, a combination of different processes involving adsorption yields a rewarding result. Finally, from the available data in literatures, it suggests that MB removal can be achieved to some extent by low cost adsorbent, as some have advantages where by many of them are renewable and available natural resources which are currently under use.

References:

1. Ahmed M.N. and Ram R.N., Removal of basic dye from wastewater using silica as adsorbent, *Environ. Pollut.*, 77, 79–86, 1992.
2. Bekchanov, M., Lamers, J. P. A., Karimov, A. and Müller, M. Cotton, *Water, Salts and Soums*, 329–344, 2012.
3. Benoit Boulinguez, Pierre Le Cloirec and Dominique Wolbert, Revisiting the Determination of Langmuir Parameters Application to Tetrahydrothiophene Adsorption onto Activated Carbon, *American Chemical Society*, Volume 24 (13), 2008, pp. 6420–6424
4. Boukhlifi F., Chraïbi S. and Alami M., Evaluation of the Adsorption Kinetics and Equilibrium for the Potential Removal of Phenol Using a New Biosorbent, *J. Environ. Earth Sci.*, 3, 181–191, 2013
5. Da. A. browski. Adsorption from theory to practice, *Adv. Colloid Interface Sci.*, 2001.
6. Foo K.Y. and Hameed B.H., Dynamic adsorption behavior of methylene blue onto oil palm shell granular activated carbon prepared by microwave heating, *Chem. Eng. J.*, 203, 81–87, 2012.
7. Gupta V (2004) Removal of rhodamine B, fast green, and methylene blue from wastewater using red mud, an aluminum industry waste. *Ind Eng Chem Res* 43: 1740-1747.
8. Gupta V.K. and Suhas, Application of low-cost adsorbents for dye removal--a review, *J. Environ. Manage.*, 90, 2313–42, 2009.
9. Ho YS, Chiang CC (2001) Sorption studies of acid dye by mixed sorbents. *Adsorption* 7: 139-147.
10. Kadolph S (2008) Natural Dyes: A Traditional Craft Experiencing New Attention. *The Delta Kappa Gamma Bulletin* 75: 14.
11. Kong CY (2011) Adsorption Characteristics of Activated Red Mud for Lead Removal. *Asian Journal of Chemistry* 23: 1963.
12. Lian, L, L. Guo, C. Guo, Adsorption of Congo red from aqueous solutions onto Ca-bentonite, *J. Hazard. Mater.*, 161 (2009), pp. 126–131.
13. Mishra A. and Bajpai M., The flocculation performance of Tamarindus mucilage in relation to removal of vat and direct dyes, *Bioresour. Technol.*, 97, 1055–1059, 2006.
14. Mohammed M.A., Shitu A. and Ibrahim A., (2014). Removal of Methylene Blue Using Low Cost Adsorbent: A Review. *Research Journal of Chemical Sciences*. ISSN 2231-606X. Vol. 4(1), 91-102.
15. Rafatullah M., Sulaiman O., Hashim R. and Ahmad A., Adsorption of methylene blue on low-cost adsorbents: A review, *J. Hazard. Mater.*, 177, 70–80, 2010.
16. Rahman Muhammad Bozlor, Shinichi Shibata, CSiddiqua Farah Diba and Magali Uono; Low Cost Biodegradable Adsorbent Material for the Removal of Dissolved Dyes from Aqueous Solutions: An Economical Process: *IACSIT International Journal of Engineering and Technology*, Vol.2, No.5, October 2010 ISSN: 1793-8236.
17. Ravi Vital Kandisa, Narayana Saibaba K.V, Khasim Beebi Shaik, and R. Gopinath, (2016). Dye Removal by Adsorption: A Review. *J Bioremediat Biodegrad* 7:371. doi: 10.4172/2155-6199.1000371.
18. Reisch.M. S, (1996) Asian textile dye makers are a growing power in changing market. *Chemical & Engineering News* 74: 10-12.
19. Saha P., Das Mishra R. and Husk R., Adsorption of safranin onto chemically modified rice husk in an upward flow packed bed reactor: artificial neural network modeling, *Biotechnol. Adv.*, 44, 7579–7583, 2012.
20. Sahu MK, Patel RK (2015) Removal of Safranin-O dye from aqueous solution using modified red mud: kinetics and equilibrium studies. *RSC Advances* 5: 78491-78501.
21. Saif M., Rehman U., Kim I. and Han J., Adsorption of methylene blue dye from aqueous solution by sugar extracted spent rice biomass, *Carbohydr. Polym.* 90, 1314–1322, 2012.



22. Young. L, Y.U. Jain, Ligninase-catalyzed decolorization. *Water Res.*, 31 (1997), pp. 1187–1193.
23. Yue. Q.Y, B.Y. Gao, Y. Wang, H. Zhang, X. Sun, S. G. Wang, and R. R. Gu. Synthesis of polyamine flocculants and their potential use in treating dye wastewater, *J. Hazard. Mater. Mater*, 152, 221–227, 2008.

**ABSTRACT CCT-: 053**

Ozogu A. N., Gadimoh S., Salisu Z., Suleiman M. A., Ukanah P. S., Anyim P. B., Lawal O. M., David S. D., Oddy-Obi I. C., Ukpong M. K., and Chubuzo-Ankor N. C.

Textile Technology Department, National Research Institute for Chemical Technology, Zaria-Nigeria

Email: donagbe@yahoo.com

APPLICATION OF CRYOGENICS AS AN ENGINEERING TOOL FOR TEXTILE AND APPARELS; A REVIEW

ABSTRACT: Cryogenic treatment has been acknowledged by some researchers as means of extending tool life of many cutting tool materials, thus improving productivity significantly. Cryo-processing, a supplementary process to conventional heat treatment, involves deep freezing of materials at cryogenic temperatures to enhance the mechanical and physical properties. The execution of cryo-processing on cutting tool materials increases wear resistance, hardness, and dimensional stability and reduces tool consumption and down time for the machine tool set up, thus leading to cost reductions. This paper reviews the use of cryogenics as an engineering tool for textile and apparels. Cryogenics is the study of very low temperature (below $-150\text{ }^{\circ}\text{C}$, $-238\text{ }^{\circ}\text{F}$ or 123 K). It is not well defined at what point on the temperature scale refrigeration ends and cryogenics begins, but most scientists assume it starts at or below $-150\text{ }^{\circ}\text{C}$ or 123 K (about $-240\text{ }^{\circ}\text{F}$). The National Institute of Standards and Technology at Boulder (NISTB), Colorado has chosen to consider the field of cryogenics as that involving temperatures below $-180\text{ }^{\circ}\text{C}$ ($-292\text{ }^{\circ}\text{F}$ or 93.15 K). This is a logical dividing line, since the normal boiling points of helium, hydrogen, neon, nitrogen, oxygen, and normal air lie below $-180\text{ }^{\circ}\text{C}$, while the Freon refrigerants, hydrogen sulfide, and other common refrigerants have boiling points above $-180\text{ }^{\circ}\text{C}$.

1. Introduction

Cryogenics is the branch of physics and engineering that involve the study of very low temperature, how to produce it, and how materials behave at these temperatures. Cryogenics is important because rocket fuel (oxygen, hydrogen) must be loaded in as liquids at cryogenic temperatures. It is also used as good preservation of body tissues by cooling (Parthiban *et al.*, 2013). It is not well defined at what point on the temperature scale refrigeration ends and cryogenics begins (Bilstein *et al.*, 1996), but scientists assume a gas to be cryogenic if it can be liquefied at or below $-150\text{ }^{\circ}\text{C}$ (123.15 K ; $-238.00\text{ }^{\circ}\text{F}$).

The U.S. National Institute of Standards and Technology has chosen to consider the field of cryogenics as that involving temperature below $-180\text{ }^{\circ}\text{C}$ (93.15 K ; $-292.00\text{ }^{\circ}\text{F}$). This is a logical dividing line, since the normal boiling points helium, hydrogen, neon, nitrogen, oxygen, and normal air lie below $-180\text{ }^{\circ}\text{C}$. A person who studies elements that have been subjected to extremely cold temperatures is called a cryogenicist. The cryogenic processing on materials increases wear resistance, hardness, and dimensional stability, and reduces tool consumption and downtime for the machine tool set-up, thus leading to cost reductions (Gill *et al.*, 2010). The technique of cryogenic processing is a method that improves the physical and mechanical properties of materials such as metals, plastics and composites.

The word “cryogenic” comes from the Greek word “kryos”, which means cold, and is simply the study of materials at low temperature such as 77 K (Kalia *et al.*, 2010).

Po *et al.*, studied the effect of cryogenic treatment on the residual stresses and mechanical properties of an aerospace aluminium. In his work, the cryogenic treatment was applied to the Al alloy used for

aerospace application that had already been heat treated. It was slowly cooled without thermal shocks to approximately 89 K , held at this temperature for 24 hours and reheated slowly, it was observed that after the cryogenic treatment the residual stresses was reduced by up to 9ksi in the parent metal. Significant enhancement was observed in Stress Corrosion Cracking performance was observed, very small increase in the value of the micro hardness fatigue and tensile properties were noted after the treatment. Venkateswara *et al.*, studied on Cryogenic Toughness of Commercial Aluminum-Lithium Alloys: Role of De lamination toughening.

Based on a study of the fracture-toughness and tensile behavior of commercial aluminum-lithium alloys, 2090 and 8090 heat treated and cryogenic (77 K) temperatures, the following conclusions were drawn: All commercial alloys displayed increases in strength, uni-axial tensile-ductility, and strain-hardening rates with decrease in temperature from 298 to 77 K . The observed increase in uni-axial tensile ductility with decrease in temperature also appeared to be associated with loss of constraint from enhanced short-transverse delamination at 77 K . Eswara *et al.*, studied Mechanical behavior of aluminium–lithium alloys, Reveals significant information about the Aluminium Lithium alloys. These alloys are prime candidate materials to replace traditionally used Al alloys.

Despite their numerous property advantages, low tensile ductility and inadequate fracture toughness, especially in the through thickness directions, militate against their acceptability. Xian *et al.*, investigated the effect of mechanical properties and microstructures of 3102 Al-Alloy. In his work, the mechanical and microstructure properties of cryogenic treated Al 3102 H19, H26 or O state, were studied. The outcome of the result was that after deep cryogenic treatment, the strength of H 19 state

increased and the elongation to failure decreased but in the O state the yield strength increased but the breaking strength, elongation decreased.

2. Method of cryogenic treatment

Liquid nitrogen is generated from a nitrogen plant, and stored in storage vessels. With the help of transfer lines, it is directed to a closed vacuum evacuated chamber called cryogenic freezer through a nozzle. The supply of liquid nitrogen into the cryo-freezer is operated with the help of solenoid valves. Inside the chamber, gradual cooling occurs at a rate of 2 °C /min from the room temperature to a temperature of -196 °C. Once the sub-zero temperature is reached, specimens are transferred to the nitrogen chamber or soaking chamber where they are stored for 24 hours with continues supply of liquid nitrogen. Figure 1 illustrates the set up for cryogenic treatment (Amrita *et al.*, 2007).



Fig. 1: Set-up of cryogenic treatment in the temperature of 77 – 450 K, which consists of a well-insulated treatment chamber (right), liquid nitrogen in a Dewar vacuum flask (left), (Linde gas, sub-zero treatment of steels, technology/processes/equipment).

Cryogenic processing is capable of treating a wide variety of materials such as metals, alloys, polymers, carbides, ceramics and composites. Cryogenics is a dry process in which liquid nitrogen is converted to a gas before it enters the chamber so that it does not come into contact with the parts assuring that the dangers of cracking from too fast cooling are eliminated. The risk of thermal shock is eliminated as there is no exposure to cryogenic liquids. The whole process takes between 36 and 74 h depending on the type and weight of material under treatment. Cryogenic processing must be done correctly in order to be successful. The basic steps in a cryogenic process are as follows (Kalia *et al.*, 2010, Singh *et al.*, 2003, and Gulyaev *et al.*, 1937).

- **Ramp Down:** Cryogenics involves slow cooling of the material from room

temperature to 77 K and ramp down time is in the 4 – 10 h range.

- **Hold:** The material is soaked or held at 77 K for 20 – 30 h which depends upon the volume of the part. This is the part of the treatment in which the micro-structural changes are realized.
- **Ramp Up:** Finally, the material is brought back to room temperature. The ramp up time can be from 10 to 20 h range (Sandip *et al.*, 2012).

The ramp down time is 9 hours. A temperature of -196 °C is achieved in 9 hours. After ramping down to (-196 °C), material is soaked (hold) at this minimum temperature for 24 hours. It is again brought up to the room temperature in 9 hours known as the ramp up temperature. The total duration of the cryogenic treatment is about 42 hours. After the material is cryogenic treated, it is tempered to 150 °C. The temperature of 150 °C is achieved in 1.5 hours, kept it at this temperature for 4 hours. The material is brought back to room temperature in the next 1.5 hours. The total duration of tempering cycle is about 7 hours. Tempering is done in order to remove the stresses developed during cryogenic cooling (Rupinder *et al.*, 2010).

Principle methods of cooling

There is a variety of methods to bring parts down to the desired processing temperature. However, all methods work on the same thermodynamic principles of heat transfer. All sub-zero equipment falls into two broad categories; direct or indirect cooling.

- **Direct Cooling:** Processors can use liquid nitrogen effectively to achieve the temperatures necessary for cryo treatment and to get quick cool down rates for cold treatment. One of the most common techniques is to use a spray header system with atomizing nozzles that convert the liquid nitrogen (LIN) to very cold gas, cooling the parts as the liquid nitrogen turns into vapor and warms up. The LIN is directly converted to cold gas to cool the parts.
- **Indirect Cooling:** Mechanical freezers are an example of indirect cooling. Nitrogen and mechanical means can both be used to cool an alcohol tank where parts could be submerged for cold treatment. Carbon dioxide in the form of dry ice has also been used to attain low temperatures for cold treatment. Since the temperatures of these techniques cannot go below about -120 °C or -185 °F, they cannot be used for cryo treatment processes.

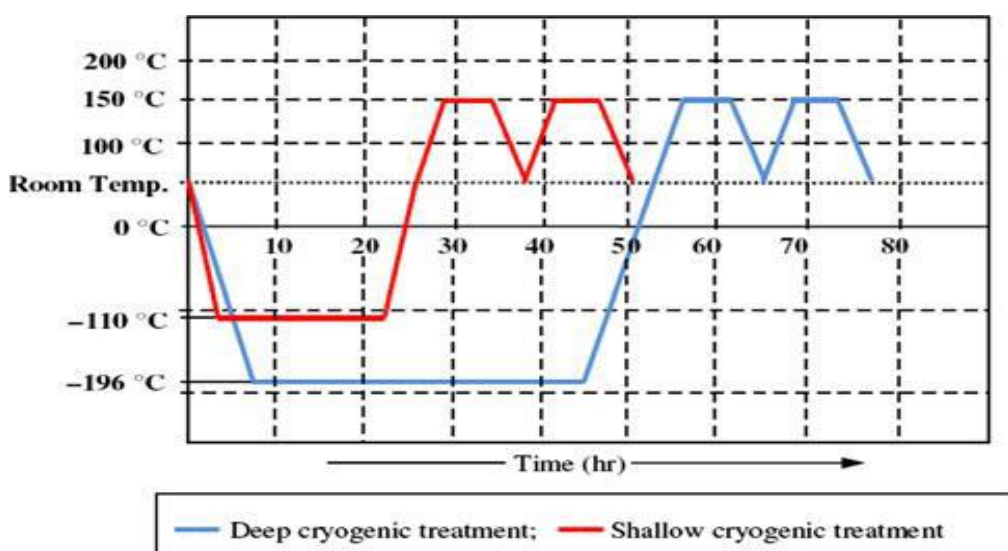


Fig. 2. Time Vs temperature for shallow cryogenic & deep cryogenic treatment (Gill *et al.*, 2011).

Types of cryogenic processes

Generally, the cryogenic treatment is classified into two types;

- **Shallow Cryogenic Treatment:** In this treatment, the material is subjected at -110 °C and held at this temperature for 18 - 25 hours and gradually brought back to the room temperature (Gill *et al.*, 2011).
- **Deep Cryogenic Treatment:** In this treatment, the material is subjected at -196 °C and held at this temperature for 24 - 72 hours and gradually brought back to the room temperature (Gill *et al.*, 2011).

Effect of cryogenic treatment

Cryogenic treatment will significantly affect the microstructure of the material. These changes in microstructure enhance the properties of the material such as hardness and wear strength of the material (Gill *et al.*, 2008).

Table 1. Cryogenic Fluids with Their Boiling Point in Kelvins.

Fluid	Boiling Point (K)
Helium-3	3.19
Helium-4	4.214
Hydrogen	20.27
Neon	27.09
Nitrogen	77.36
Air	78.8
Fluorine	85.24
Argon	87.24
Oxygen	90.18
Methane	111.7

(Cryogenic Systems by Randall Barron McGraw-Hill Book Company).

Cryogenic application in textile and apparels

a. Liquid Ammonia Mercerization

Liquid ammonia mercerizing refers to the process that truly revives the cotton through

the expression of liquid ammonia at an ultra-low temperature inside the fiber. When the fiber is treated at -33 °C liquid ammonia, the ammonia at ultra-low temperature will permeate immediately into the crystallographic structure of the fiber. Stress will be released through interior expansion, which makes the fiber cavity round and smooth, and rearranges the molecular structure, thus the crystallographic structure becomes slack and stable. This physical change makes the surface of the entire fabric smooth and bright, with solid and soft feel, so elasticity and wash-and-wear is fully achieved. (Parthiban *et al.*, 2013).

b. Cryogenic Treatment in Garment Manufacturing

Garment cutting knives and sewing needles are given cryogenic treatment, which is the process of converting the austenite state (malleable) to the martensite state (tough), such that the processed materials have increased wear, toughness, and reduced brittleness (Fu *et al.*, 2002).

c. Cry Cooling Applications in the Garment Cutting Knives

Austenite is a soft allotropic form of iron that forms at high temperature. During cooling, it gets transformed to other structures of which martensite are the desirable harder phase. But rote of cooling plays a major role in the formation of martensite. The cryogenic process can be applied on garment cutting knives and sewing needles (Satish *et al.*, 2004).

d. Cryogenic Treatment on Sewing Needles:

Sewing needles are classified by their length and thickness. The numbering system is not directly related to the length or thickness of the needles, it serves only to distinguish one needle from another. These sewing needles are cryogenically treated, and the wear resistance of garment cutting knives and sewing needles

improved (Parthiban *et al.*, 2013).



Fig. 3. Cryogenic treated garment cutting knives.



Fig. 4. Cryogenically treated sewing needles.

Conclusions

Cryogenically treated materials show a marked increase in wear resistance without any desirable change in dimensional or volumetric integrity. The material shows little or no change in yield or tensile strength. The treated material becomes less brittle, without a change in original hardness. The most significant and consistent change is the increased toughness, stability, and wear resistance. Therefore, it has less maintenance and change over, which allows for lower production cost.

REFERENCES:

1. Amrita Priyadarshini (2007), A Study Of The Effect Of Cryogenic Treatment On The Performance Of High Speed Steel Tools And Carbide Inserts. A Master's Degree Thesis.
2. Bilstein, Roger E. (1996). Stages to Saturn: A Technological History of the Apollo/Saturn Launch Vehicles (NASA SP-4206) (The NASA History Series). NASA History Office. pp. 89–91. ISBN 0-7881-8186-6.
3. Cryogenic fluids with their boiling point in kelvins (Cryogenic Systems by Randall Barron McGraw-Hill Book Company)
4. Cryogenic Systems by Randall Barron McGraw-Hill Book Company.

5. Eswara N. P., A A Gokhale and P Rama Rao, Mechanical behavior of aluminium–lithium alloys, *Sadhana* Vol. 28, Parts 1 & 2, 2003, pp. 209–246.
6. Fu S.Y., L.F. Li, Y.H. Zhang, C.J. Huang, Y.F. Xiong, (2002). Mechanical properties of SGF reinforced PA66/PP blends at RT and cryogenic temperature, proceedings of the 19th cryogenic engineering conference, France.
7. Gill S. S., Singh, H., Singh, R., Singh J., 2011, —Effect of Cryogenic Treatment on AISI M2 High Speed Steel: Metallurgical and Mechanical Characterization, *Journal of Materials Engineering and Performance*.
8. Gill SS, Singh H, Singh R, Singh J (2010) Cryoprocessing of cutting tool materials; a review. *Int J Adv Manuf Tech* 48:175–192.
9. Gill, S.S., Singh, R., Singh, H. and Singh, J., 2008, —Wear behavior of cryogenically treated tungsten carbide inserts under dry and wet turning conditions, *International Journal of Machine Tools Manuf*, 49 (3–4), P 256–260.
10. Gulyaev A (1937) Improved heat treatment of high speed steel. *Metallurgy* 12:65–70.
11. Kalia S (2010) Cryogenic processing: a study of materials at low temperatures. *J Low Temp Phys* 158:934–945.
12. Linde gas, sub-zero treatment of steels, technology/processes/equipment).
13. Parthiban M., M. R. Srikrishnan, S. Viju, (2013). Cryogenic – An Engineering Tool for Textile and Apparel. *Journal of Textile and Apparel, Technology and Management, volume 8. Issue 1*.
14. Po Chen, Tina Malone, Robert Bond, and Pablo Torres, Effect of cryogenic treatment on the residual stress and mechanical properties of an aerospace aluminium alloy, 5th Conference on Aerospace Materials, Processes, and Environmental Technology (AMPET), 2002, Von Braun Center Huntsville, Alabama.
15. Rupinder Singh, and Kamaljit Singh, 2010, —Enhancement of Tool Material Machining Characteristics with Cryogenic Treatment: A Review, Proceedings of the 2010 International Conference on Industrial Engineering and Operations Management Dhaka, Bangladesh, January 9 – 10, 2010.
16. Sandip B. Chaudhari, Sanjay P. Shekhawat, Ambepasad S. Kushwaha, (2012). Advanced Technology of Cryoprocessing for the Enhancement of Tool Material Machining Characteristics: A Review. *International Journal of Emerging Technology and Advanced Engineering*. ISSN 2250-2459, Volume 2, Issue 4.
17. Satish Kumer. S (2004). Effect of ultra-cooling on the useful life of rings & travelers, project thesis.
18. Singh PJ, Guha B, Achar DRG (2003) Fatigue life improvement of AISI 304 L cruciform welded joints by cryogenic treatments. *Eng Fail Anal* 10:1–12.
19. Venkateswara R. K. T., Weikang yu, and R.O. Ritchie, Cryogenic Toughness of Commercial Aluminum-Lithium Alloys: Role of Delamination Toughening, *Metallurgical Transactions A*, 1989, volume 20, issue 3 pp 485-497.
20. Xian quan Jiang, Ning Li, Hong He, Xiu-Jiu Zhag, Chun-chi Li, Hao Yung, Effect of mechanical properties and microstructures of 3102 Al-Alloy, *Material Science forum*, Vols 546-549, 2007, pp 845-848.

ABSTRACT CCT-: 027

Mohammed M. L.*, M. N. Almustapha, K. J. Umar, C. Muhammad, M. G. Liman and A. Uba

Department of Pure and Applied Chemistry, Usmanu Danfodiyo University, Sokoto-Nigeria.

Email: misbahubnz@gmail.com**CATALYTIC ALKENE EPOXIDATION USING CONTINUOUS FLOW REACTOR**

ABSTRACT: A polystyrene 2-(aminomethyl)pyridine supported Mo(VI) i.e., Ps.AMP.Mo complex has been successfully prepared, characterised and used as a catalyst for alkene epoxidation in a continuous reactor. The efficiency of Ps.AMP.Mo catalyst has been assessed for continuous epoxidation of 4-vinyl-1-cyclohexene with TBHP as an oxidant using a FlowSyn reactor by studying the effect of reaction temperature, feed molar ratio of alkene to TBHP and feed flow rate on the conversion of TBHP and the yield of epoxide. The catalyst was found to be active and selective for the continuous epoxidation of the substrate using TBHP as an oxidant. The continuous epoxidation in a FlowSyn reactor has shown considerable time savings, high reproducibility and selectivity along with remarkable improvements in catalyst stability compared with the reactions carried out in a batch reactor.

1. Introduction

Epoxides are used as raw materials or intermediates for the production of commercially important products for flavours, fragrances, paints and pharmaceuticals [1-2]. The production of epoxides often uses peracids including peracetic acid and m-chloroperbenzoic or chlorohydrin as oxidizing reagents in liquid phase batch reactions. However, such processes are not environmentally benign as the former produces equivalent amount of acid waste, while the latter yields chlorinated by-products and calcium chloride waste [3]. Hence, there is a strong need for cleaner catalytic epoxidation methods that employ safer oxidants and produce little waste. Soluble compounds of transition metals have been used to catalyse alkene epoxidation with good activity and increased product selectivity [4]. On the other hand, homogenous catalysed epoxidation processes are not economically viable for industrial applications due to major requirements in terms of work-up, product isolation and purification procedures.

Consequently, researchers have been focusing on developing stable heterogeneous catalysts for epoxidation by immobilisation of catalytically active metal species on organic or inorganic materials [5-7]. In this work, an efficient and selective polystyrene 2-(aminomethyl)pyridine supported molybdenum (VI) complex (Ps.AMP.Mo) has

been used as catalyst for epoxidation of 4-vinyl-1-cyclohexene using a continuous reactor. This process is atom efficient, solvent-free and uses environmentally benign tert-butyl hydroperoxide (TBHP) as an oxidant.

2. Experimental**2.1. Materials**

All chemicals used for this study were purchased from Sigma-Aldrich Co. Ltd and the purity of each chemical was verified by gas chromatography (GC). Polystyrene 2-(aminomethyl) pyridine supported molybdenum complex, i.e. Ps.AMP.Mo catalyst was successfully prepared and characterised according to the procedure reported by Mbeleck et al., 2007 [5].

2.2. Continuous alkene epoxidation in a FlowSyn reactor.

The experimental set-up of a Flowsyn continuous flow reactor is shown in Fig. 1. Samples were taken at specific time intervals and were analysed by Shimadzu GC-2014 gas chromatography. Continuous epoxidation studies were carried out following optimisation of the reaction conditions as well as extensive evaluation of the activity and reusability of the heterogeneous catalyst for alkene epoxidation in a 0.25 L jacketed stirred batch reactor.



R1 – Reagent-1 R2 – Reagent-2 S – Solvent
M – Mixing chamber CH – Column heater P1, P2 – HPLC pumps
F – Fraction collector CI – Control interface T – Temperature profile
C – Stain Steel column packed with catalyst D – Data logger

Fig. 1. Experimental set-up of a Flowsyn continuous flow reactor

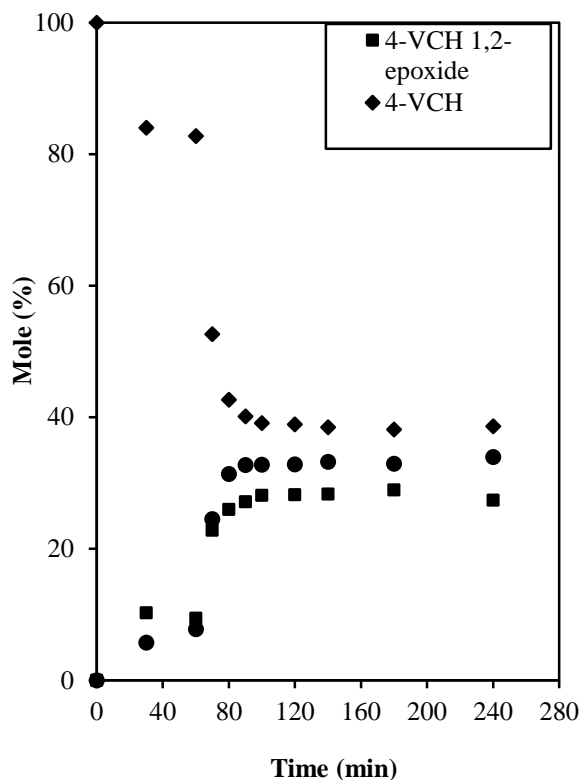


Fig. 2. Mole fractions of the various constituents in the reaction mixture for continuous epoxidation of 4-vinyl-1-cyclohexene (4-VCH) with TBHP as an oxidant

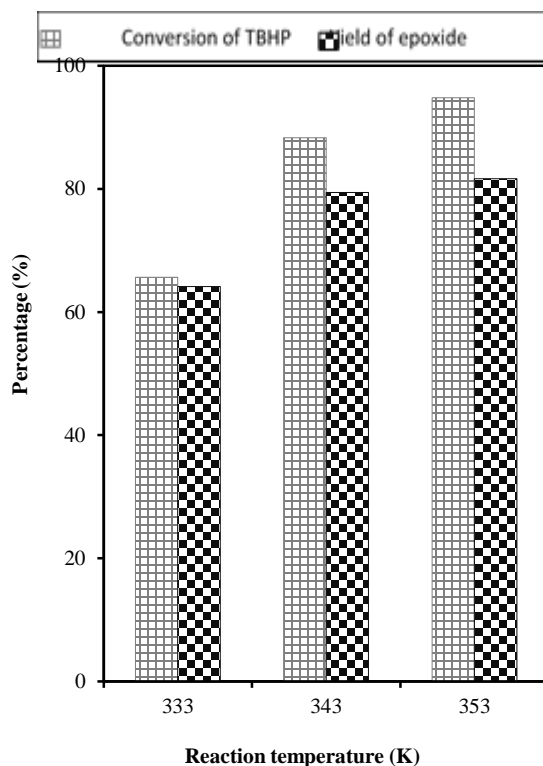


Fig. 3. Effect of reaction temperature on the conversion of TBHP and the yield of 4-VCH 1,2-epoxide at steady state for continuous epoxidation of 4-VCH with TBHP using a FlowSyn continuous flow reactor in the presence of Ps.AMP.Mo catalyst (~1.5 g) at feed flow rate: 0.1 mL/min; feed molar ratio of alkene to TBHP: 5:1.

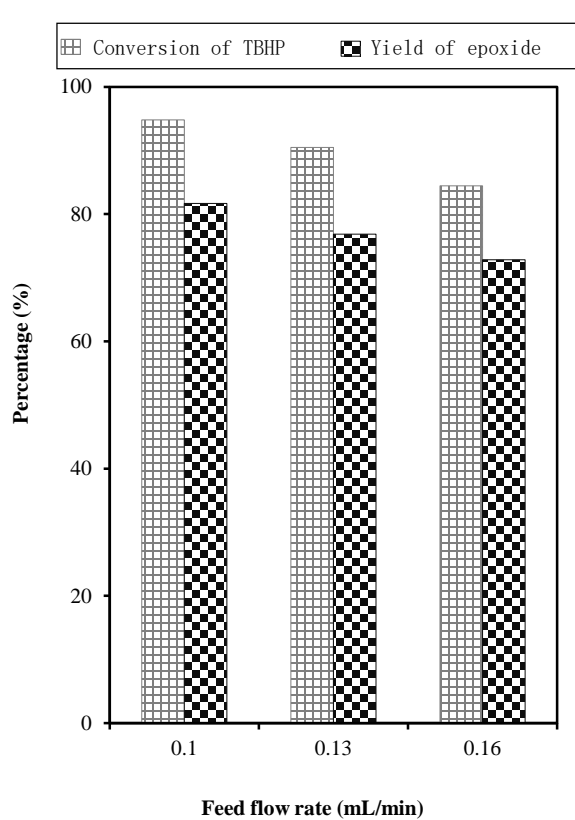


Fig. 4. Effect of feed flow rate on the conversion of TBHP and the yield of 4-VCH 1,2-epoxide at steady state for continuous epoxidation of 4-VCH with TBHP using a FlowSyn continuous flow reactor in the presence of Ps.AMP.Mo catalyst (~1.5 g) at reaction temperature: 353 K; feed molar ratio of alkene to TBHP: 5:1.

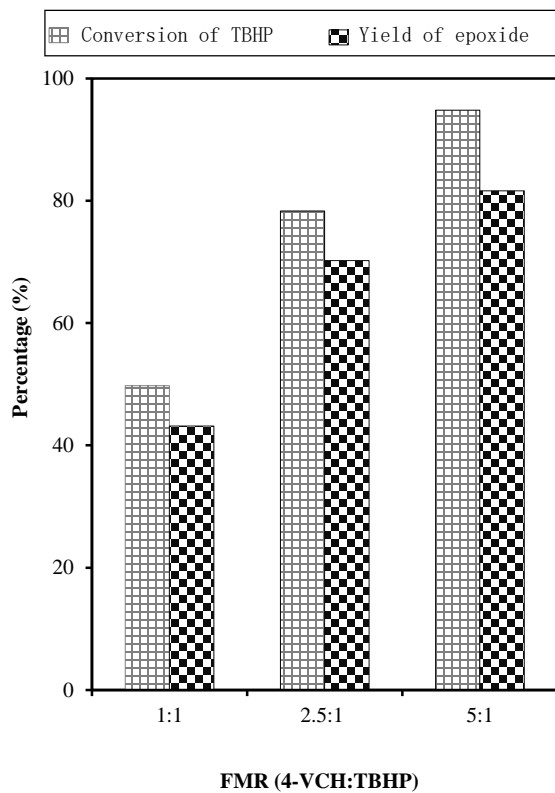


Fig. 5. Effect of feed molar ratio on the conversion of TBHP and the yield of 4-VCH 1,2-epoxide at steady state for continuous epoxidation of 4-VCH with TBHP using a FlowSyn continuous flow reactor in the presence of Ps.AMP.Mo catalyst (~1.5 g) at reaction temperature: 353 K; feed flow rate: 0.1 mL/min.



3. Results and discussion

Continuous epoxidation was carried out in a FlowSyn continuous flow reactor to study the effect of reaction temperature, feed molar ratio of alkene to TBHP and feed flow rate on the conversion of TBHP and the yield of epoxide at steady state, i.e., at 2 h. Figure 2 shows a sample plot for the steady state mole fractions of the various constituents in the reaction mixture for continuous epoxidation of 4-VCH with TBHP as an oxidant.

3.1. Effect of reaction temperature

It can be seen from Figure 3 that the conversion of TBHP and the yield of 4-VCH 1,2-epoxide at 333 K was found to be ~66% and ~64%, respectively. However, a significant increase in the conversion of TBHP (~95%) and the yield of 4-VCH 1,2-epoxide (~82%) was obtained for reaction carried out at 353 K. Hence, 353 K was selected for further optimisation studies of 4-VCH epoxidation in a FlowSyn reactor.

3.2. Effect of feed flow rate

An increase in feed residence time in the catalytic feed bed reactor by reducing the flow rate could have a positive impact on the catalytic performance in a continuous flow reaction. For instance, 4-VCH epoxidation at a feed flow rate of 0.16 mL/min gave ~84% conversion of TBHP and ~73% yield of 4-VCH 1,2-epoxide (Figure 4). However, when the residence time of the feed was increased to ~4 min by reducing the flow rate to 0.13 mL/min, the conversion of TBHP and the yield of 4-VCH 1,2-epoxide increased to ~90% and ~77%, respectively. Thus, it can be concluded that an increase in feed flow rate caused reduction in feed residence time in the reaction zone (packed column), which consequently led to decrease in both the conversion of TBHP and the yield of 4-VCH 1,2-epoxides in the continuous flow epoxidation.

3.3. Effect of feed molar ratio

Figure 5 illustrates that both TBHP conversion and the yield of epoxide increase with an increase in feed molar ratio of alkene to TBHP. The reaction carried out at a feed molar ratio of 4-VCH to TBHP of 1:1 recorded ~50% conversion of TBHP and ~43% yield of 4-VCH 1,2-epoxide. However, a significant increase in both the conversion of TBHP

(~78%) and the yield of 4-VCH 1,2-epoxide (~70%) was obtained at a feed molar ratio of 4-VCH to TBHP of 2.5:1. Therefore, it can be concluded that higher yield of 4-VCH 1,2-epoxide was obtained at 5:1 molar ratio of 4-VCH to TBHP (82%) compared to reactions conducted at 2.5:1 and 1:1 molar ratio of 4-VCH to TBHP.

4. Conclusion

Continuous alkene epoxidation using a FlowSyn reactor has enabled rapid evaluation of catalytic performance of Ps.AMP.Mo from a small quantity of reactants under different reaction conditions. The results obtained in this study show that a thorough screening of reaction parameters including reaction temperature, feed flow rate and feed molar ratio of alkene to TBHP could have a positive impact on the efficiency of a continuous flow alkene epoxidation in the presence of a heterogeneous catalyst.

Acknowledgements

The financial supports from EPSRC (grant no. EP/H027653/1) and The Royal Society Brian Mercer Feasibility award are gratefully acknowledged. One of the authors, M. L. Mohammed is thankful to London South Bank University, UK and Tertiary Education Trust Fund (TETFund), Nigeria for the PhD scholarships.

References

- (1) Siel G, Rieth R, Rowbottom KT, Epoxides, Ullmann's encyclopedia of industrial chemistry, Weinheim, Wiley-VCH, (2000).
- (2) Bauer K, Garbe D, Surburg H, Common Fragrance and Flavour Materials, 4th ed. Weinheim, Wiley-VCH, (2001).
- (3) Yudin AK, Aziridines and Epoxides in Organic Synthesis, Weinheim, Wiley-VCH, (2006).
- (4) Xia, Q.-H., Ge, H.-Q., Ye, C.-P., Liu, Z.-M., Su, K.-X., 2005. Advances in homogeneous and heterogeneous catalytic asymmetric epoxidation. Chem. Rev. 105, 1603–1662.
- (5) Mbeleck R, Mohammed ML, Ambroziak K, Sherrington DC, Saha B, Efficient epoxidation of cyclododecene and dodecene catalysed by polybenzimidazole supported Mo(VI) complex, Catal. Today, 256, 287-293, (2015).
- (6) Saha B, Ambroziak K, Sherrington DC, Mbeleck R, Liquid phase epoxidation process, US Patent 8759522 B2, (2014).
- (7) Ambroziak K, Mbeleck R, Saha B, Sherrington D, Greener and Sustainable Method for Alkene Epoxidations by Polymer-Supported Mo(VI) Catalysts, Int. J. Chem. React. Eng., 8, A125, (2010).

**ABSTRACT CCT-: 055**Bashir I.^{*1}, M. Yusuf¹, S. Gbadamasi², B. Mukhtar¹, A. Y. Atta², B. O. Aderemi¹, and B.Y. Jibril¹

1. Department of Chemical Engineering, Ahmadu Bello University, 810261 Zaria, Nigeria.
2. National Research Institute for Chemical Technology, P.M.B 1052, Zaria, Nigeria.

Email: ibrahimebd@gmail.com**PROPANE AROMATIZATION OVER HIERARCHICAL Zn/ZSM5 CATALYSTS**

ABSTRACT: Hierarchical Zn/ZSM5 catalyst with SiO₂/Al₂O₃ of 50 was synthesized via NaOH treatment of a conventional microporous ZSM5 followed by wet impregnation method of the metal precursor. Performance test was carried out in a micro fixed bed reactor and it was observed that the prepared hierarchical catalyst improved propane aromatization compared with the conventional catalyst. The hierarchical Zn/ZSM5 exhibited an external surface area S_{meso} of 137 m²g⁻¹ (about 43% of the total surface area), relatively preserved microporosity V_{micro} of 0.06 cm³/g and random intra-framework mesopores of around 5.52 nm in width, compared to S_{meso} of 151 m²g⁻¹ (about 50% of the total surface area) and V_{micro} of 0.09 cm³g⁻¹ with pore width of 4.39 nm of the conventional catalyst. XRD and FTIR results showed that the structures of the hierarchical zeolite remained relatively stable while the pyridine FTIR shows enhancement of the protonic Bronsted acidic sites. The hierarchical catalyst showed a remarkable performance with an average aromatic selectivity of 61.1% and propane conversion of 28.02% within 5 hours on stream (TOS) as compared to the conventional catalyst with 25.2% average aromatic selectivity and propane conversion of 50.1%. The hierarchical catalyst also displayed a very low C₉₊ (heavier aromatics) selectivity of 15.6% while for the microporous was 52.9% at 5 hours on stream.

Keywords: Hierarchical, Desilication, Zinc, ZSM5, Aromatization

1. Introduction

The conversion of light alkanes (C₂-C₄) into aromatic compounds mainly benzene, toluene and xylenes (BTX) is one of the major industrial processes that has attracted so much attention due to the BTX wide range of application as intermediate materials in both chemical and petrochemical industries (Tshabalala, 2009). They are used as blending mixture to enhance the octane number of gasoline. Toluene is used in the production of adhesives, benzene is extensively used in the downstream chemical processes such as production of styrene and phenol, while xylenes are essential for production of purified terephthalic acid and isophthalic acid (Akhtar *et al.*, 2012). Currently, BTX are produced from naphtha and recent research efforts are focused on developing catalyst for alternative feedstock such as light alkane aromatization.

A key research question in developing such a catalyst is the relative difference in diffusivity between light alkanes and aromatics and the effects of the difference on the BTX selectivities. However, conventional H-ZSM5 catalyst suffers quick deactivation and extreme cracking condition that leads to a large selectivity for C₁ and C₂ products. This problem was overcome by the addition of transition metals such as zinc, platinum or gallium to facilitate the dehydrogenation activity and to suppress cracking.

Despite this improvement, an important drawback of these microporous zeolites is their small pores, which is hard to be accessed by bulky reactants, this hinders diffusion because of the restricted access and slow intra-crystalline transport to and from the active sites. (Tao *et al.*, 2013).

The new mesoporous and microporous composite (hierarchical) that combine both the pore structure advantage of mesopore and the

strong acidity of zeolite, is one of the most promising materials with fast diffusive rate, and many exposed active sites (Fang *et al.*, 2010). These materials enable mass transport of larger reactants and products and allowing for reactions catalyzed by strong acidity to proceed on the mesopore surface and pore mouth and alternatively can simply serve by improving existing reactions/processes currently using zeolite catalysts (spangenberg *et al.*, 2011). Therefore, this work focuses on synthesizing hierarchical Zn/ZSM5 catalyst for light alkane aromatization.

2. Procedure

2.1 Raw materials

Commercial H-ZSM5 catalyst (Si/Al ratio 50, Zeolyst international) Sodium Hydroxide (NaOH, reagent grade, 98% anhydrous pellets), Zinc Nitrate (precursor), Nitrogen Gas (99.9% purity) Propane gas (99.9% purity).

2.2 Preparation of hierarchical H-ZSM5 catalyst (desilication using NaOH solution)

9.4 g of Parent H-ZSM5 was introduced in 300 ml of 0.3 M NaOH solution. The NaOH solution was heated at constant temperature of 65°C and the mixture was stirred for 2 hours. Then the suspension was cooled using an ice bath and later isolated by suction filtration. The residue was washed with de-ionized water until neutral pH of 7 was reached. The solid sample was then dried in an oven at 90°C for 1 hour, single ion-exchange with 0.5M NH₄Cl at 70°C for 3 hours and subsequently allowed to cool before filtration and washing. Drying was done at 95°C then calcination at 550°C for 5 hours to get the protonic Hierarchical H-ZSM5



catalyst. However, catalyst weight loss was observed which could be attributed to silica leaching during synthesis.

2.3 Zinc impregnation of the hierarchical H-ZSM5 catalysts

Zinc loading of 2 wt.% was used for the impregnation of both the hierarchical and microporous H-ZSM5. Zinc nitrate (precursor) solution was prepared by dissolving 0.608g of Zn (NO₃)₂ · 6H₂O in 100 ml of deionized water and 4.546g of the H-ZSM5 was introduced. The suspension was then stirred at 70°C and evaporated to dryness then dried in an oven at 95°C and further calcined at 550°C for 5 hours to get the modified Zn-ZSM5 Catalyst. The prepared catalysts were tested in a fixed bed micro reactor while the gas and liquid products were analyzed using a gas chromatograph (GC).

3. Results and discussion

3.1 Elemental composition

Table 1 showed that desilication or removal of framework silica atoms caused changes in the elemental composition of the parent catalyst. The SiO₂/Al₂O₃ ratio of Zn/ZSM5 decreased upon treatment with NaOH, from 47 to 26 as expected.

3.2 Structural and textural properties

3.2.1 X-ray diffraction (XRD)

From Fig. 1 decrease in intensity and crystallinity was observed for the 0.3 M-Hier-Zn/ZSM5 for all the characteristic diffraction peaks marked 'z' which could be attributed to silica leaching from the zeolite framework (desilication).

3.2.2 Fourier transform infrared measurements (FTIR)

The FTIR spectra of conventional and hierarchical 0.3 M-Hier-Zn/ZSM5 in the lattice vibration region (250-4250 cm⁻¹) are shown in Figure 2. It can be seen that the band at 450 and 550 cm⁻¹ are clearly reduced upon desilication treatment aimed at generating mesoporosity in Zn/ZSM5, which further supports the XRD data since the reduction in the aforementioned bands is an obvious reflection of crystallinity loss as well. The broadening/ decrease in intensity of the band at 1100 cm⁻¹ which is assigned to the internal (intra-tetrahedral bridged Si-OH-Al silanol) vibrations (strong bronsted acid sites) is attributed to changes in the density of strong acid sites significantly with severity in alkaline treatment (Fernandez

et al., 2010).

Also the band at 1225 cm⁻¹ signifies extra-framework aluminum species Al-(OH) or partially hydrolyzed alumina species (Lewis sites) bonded to the zeolite framework via one or two oxygen bonds. This band was observed to be decreasing with increasing alkaline treatment. These findings designated a decrease in overall or total acidity of the hierarchical samples.

3.3.3 Pyridine FTIR

The FTIR spectra of adsorbed pyridine for conventional Zn/ZSM5 and 0.3 M hierarchical Zn/ZSM5 are depicted in Figure 3. The Figure revealed the presence of Bronsted and Lewis acidic sites as observed from the appearance of IR bands near 1550 (Bronsted sites) and 1450 cm⁻¹ (Lewis sites). Upon alkaline treatment, there was a clear decrease in the intensity of 1450 cm⁻¹ band (Lewis sites) coupled with an increase in the intensity of 1550 cm⁻¹ band (protonic sites). The increase in bronsted sites could be attributed to (i) re-alumination of extra-framework alumina sites back into the zeolite framework causing a simultaneous decrease in extra framework alumina (Lewis sites) (Verboekend *et al.*, 2011) (ii) addition of H⁺ ions or protons as a result of ion-exchange could also add to the bronsted acidity. (Tshabalala, 2009).

3.3.4 N₂ sorption studies

N₂ adsorption-desorption isotherms of both microporous and mesoporous Zn/ZSM5 samples are shown in Figure 4. Whereas the textural parameters derived from the nitrogen adsorption isotherms are compiled in Table 1.1 As expected, conventional Zn/ZSM5 exhibited type I isotherm with a plateau at higher relative pressures, a typical characteristic for a microporous material. The alkaline treated samples exhibited isotherms representing both type I and IV behavior, with enhanced N₂ uptake at higher relative pressures. The increased adsorption in the relative pressure p/p₀ range >0.30 and the appearance of hysteresis loops in the desorption branch at p/p₀ ~0.40–0.50 of the treated samples indicated the development of mesopores.

3.4 Propane aromatization

The catalytic performance of conventional and hierarchical Zn/ZSM5 samples is shown in Figures 5 and 6 respectively. A gradual or steady decrease in propane conversion with time over conventional Zn/ZSM5 was observed.

Table 1: Textural properties of conventional and hierarchical Zn/ZSM5

Catalyst	Mesoporosity (%)	Si/Al ratio	S _{BET} (m ² /g)	S _{MICRO} (m ² /g)	S _{MESO} (m ² /g)	V _{TOTAL} (cm ³ /g)	V _{MICRO} (cm ³ /g)	Pore width (nm)
Zn/ZSM5	43.3	47	349	198	151	0.22	0.09	4.39
0.3M-Hier Zn/ZSM5	50.2	26	273	136	137	0.22	0.06	5.52

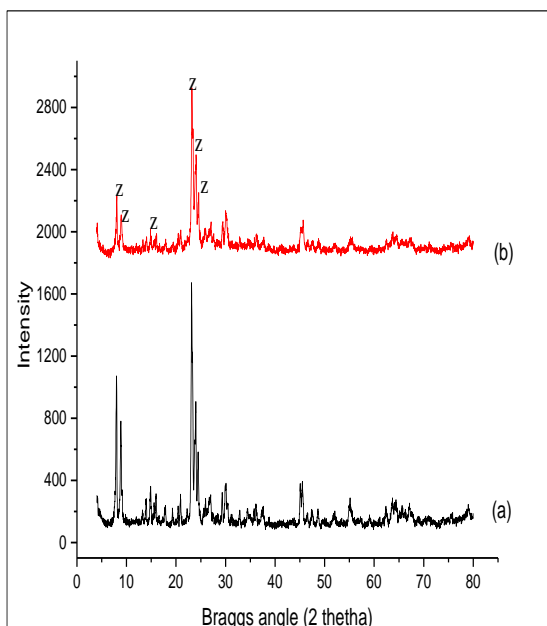


Fig. 1. XRD diffraction patterns of (a) conventional Zn/ZSM5. (b) 0.3M hierarchical Zn/ZSM5

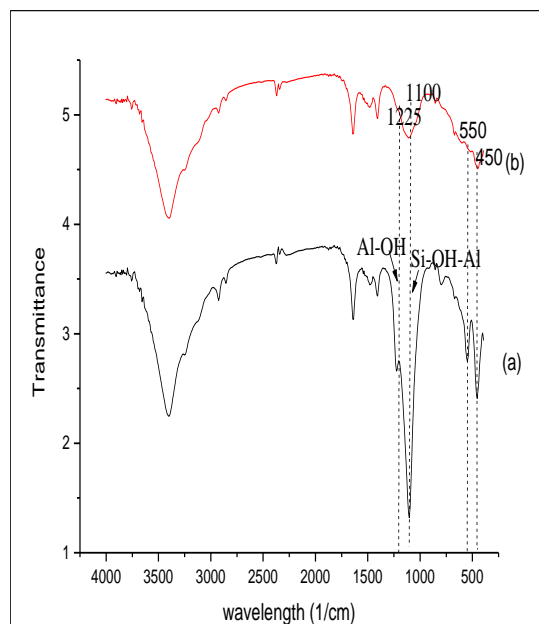


Fig. 2. FTIR patterns of (a) Conventional Zn/ZSM5 (b) 0.3M hierarchical Zn/ZSM5

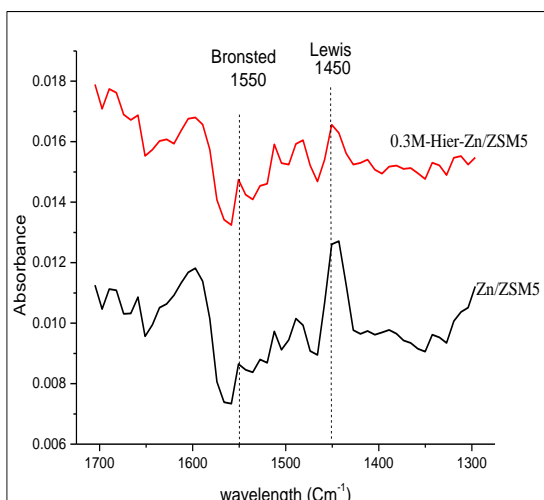


Fig. 3. Pyridine FTIR of Conventional of (a) conventional Zn/ZSM5 (b) 0.3M hierarchical Zn/ZSM5

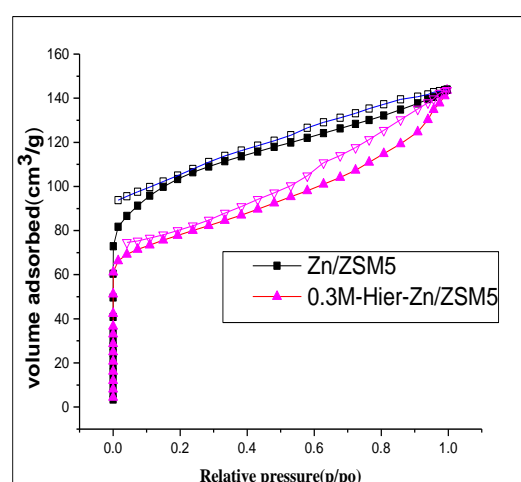


Fig. 4. Nitrogen adsorption-desorption isotherms of conventional and 0.3M-hierarchical Zn/ZSM5 samples at 77k

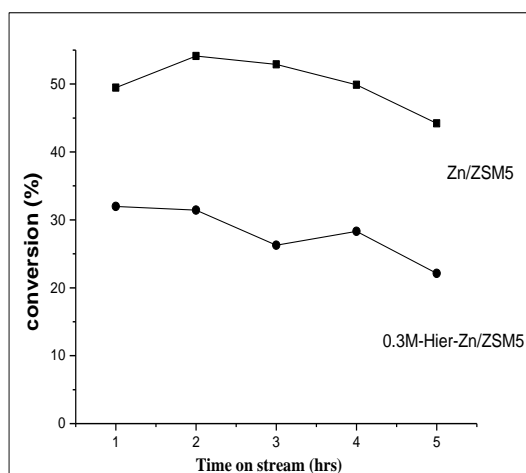


Fig. 5. Propane conversion over conventional and hierarchical Zn/ZSM5 samples

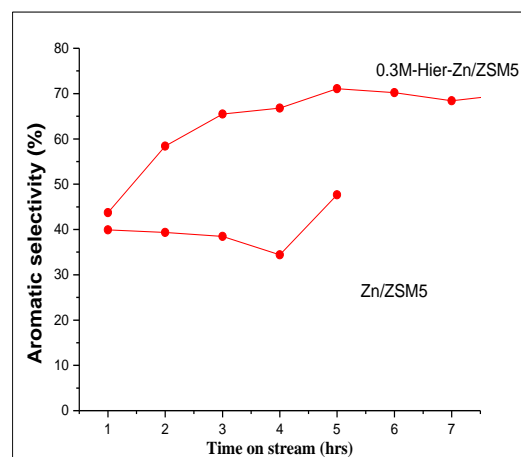


Fig. 6. Aromatic selectivity over Conventional & hierarchical Zn/ZSM5 catalysts

The maximum conversion of propane was attained at 54% and later declined to 44% as expected owing to lack of proper accessibility of the bulk molecules to acidic sites located within the zeolite cavities. While the low selectivity could be ascribed to inadequate transport of the produced desired product out of the smaller dominant microporous channels with high micropore surface area (198 m²/g) causing limitation in diffusion thereby tilting the selectivity to secondary products.

For the 0.3 M hierarchical Zn/ZSM5, a low conversion uptake was observed at 32% which consistently decreases with time to 22%. This could be attributed to loss in activity of bronsted acidic sites within the framework acquired as a result of predominant coke deposition of the catalyst causing retardation or loss in catalyst stability. Additionally, from Fig. 6, a high aromatic selectivity within the range of 58-74% was observed for the hierarchical sample which was stable within 5 hours on stream. This development could be attributed to efficient transport of the bulk reactant and desired product out of the zeolite due to bigger pore size of about 5.52 nm coupled with high micro and meso surface area of 136 and 137 m²/g that resulted to a decreased rate of deactivation caused by prevalent coke deposition.

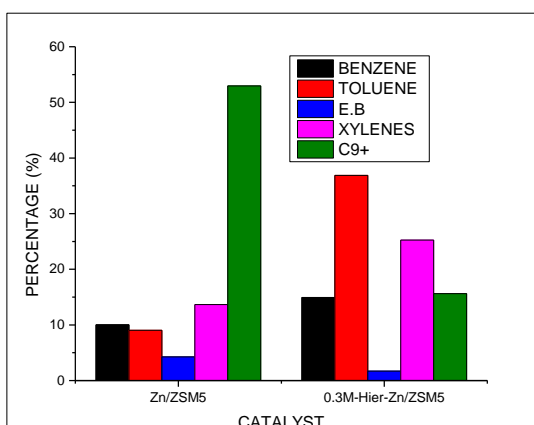


Fig. 7. Aromatic product distribution at 5 hours on stream (TOS)

Fig. 7 shows the product distribution of both catalysts. The conventional catalyst gave low aromatic selectivity of 21.5% and has high C9+ (heavier aromatics) selectivity of about 52.9%. While the hierarchical catalyst favored high toluene production and other aromatics

with least C9+ selectivity of 15.6% and aromatic selectivity of 71.1% at 5 hours on stream.

4. Conclusions

The hierarchical 0.3 M-Zn/ZSM5 catalyst was successfully synthesized and characterized using BET, XRD, XRF, FTIR and pyridine IR. The catalyst performance test was carried out at 1atm pressure, operating temperature of 540°C, propane to nitrogen ratio of 1:2 and weight hourly space velocity (WHSV) of 1200 MLg⁻¹hr⁻¹. A very high aromatic selectivity of about 71.1% and propane conversion of 22.1% was observed for the hierarchical catalyst at 5 hours on stream with a very low C9+ selectivity of 15.6% less than the conventional sample with C9+ of 52.9% selectivity. While within 5 hours on stream (TOS) an average aromatic selectivity of 61.1% was obtained while for microporous sample it was 25.2%. This shows that synthesized Hierarchical catalysts exhibited very good catalytic activity, aromatic selectivity and stability when compared with the conventional microporous catalyst.

Acknowledgements

The authors appreciate the support of the Petroleum Technology Development Fund (PTDF), Abuja, Nigeria for funding the research.

References

- Akhtar, M. N., & Ogunronbi, K. (2012). Chemical Synthesis of stable H-gallosilicic acid MFI with hierarchical pore architecture by surfactant-mediated base hydrolysis, and their application in propane aromatization. *Journal of Molecular Catalysis. A, Chemical*, 360, 1–15.
- Spangenberg, M., Taarning, E., Egeblad, K., & Hviid, C. (2011). Catalysis with hierarchical zeolites. *Catalysis Today*, 168(1), 3–16.
- Tao, H., Yang, H., Liu, X., Ren, J., Wang, Y., & Lu, G. (2013). Highly stable hierarchical ZSM-5 zeolite with intra- and inter-crystalline porous structures. *Chemical engineering journal*, 225, 686–694.
- Tshabalala, T. E. (2009). Aromatization of n -Hexane over Metal Modified H-ZSM-5 Zeolite Catalysts Synthesis, F. T., Kang, J., Cheng, K., Zhang, L., Zhang, Q., Ding, J., Wang, Y. (2011). *Zuschriften Mesoporous Zeolite-Supported Ruthenium Nanoparticles as Highly Selective Fischer – Tropsch Catalysts for the Production of C 5 – C 11*, 5, 5306–5309.
- Fernandez, C., Stan, I., Gilson, J., Thomas, K., Vicente, A., Bonilla, A., & Pórez-ramirez, J. (2010). Hierarchical ZSM-5 Zeolites in Shape-Selective Xylene Isomerization: Role of Mesoporosity and Acid Site Speciation, 6224–6233.
- D.Verbokend and Perez ramirez Article, C. (2011). *Catalysis Science & Technology*, 1(6). <https://doi.org/10.1039/c1cy00150g>.

ABSTRACT CCT-: 061Abba H.^{1*}, I.K.², Adamu, ¹A. Musa, and ³M. Iji

1. Department of Chemistry, Ahmadu Bello University, P.M.B.1045, Zaria-810006, Nigeria.
2. Nigerian Institute of Leather Science and Technology, P.M.B. 1034, Zaria, Nigeria.
3. Department of Chemistry, Abubakar Tafawa Balewa University, P.M.B. 0248, Bauchi, Nigeria

Email: habba@abu.edu.ng**EFFECT OF MOLECULAR WEIGHT AND CONCENTRATION ON PLASTICIZING EFFICIENCY OF SOME TRIMELLITATES IN POLY(VINYL CHLORIDE) (PVC)**

ABSTRACT: Sheet of pure poly(vinyl chloride) (PVC) measuring 45 x 11 x 3 mm³ was prepared to serve as control by compression moulding method. Sheets of the same dimension were also prepared by the same method after addition of 2.5, 5.0, 7.5, 10.0, 12.5, 15.0, 17.5 and 20.0 parts per hundred resin (phr) of three trimellitates [trimethyl trimellitate (TMTM), tri(isooctyl) trimellitate (TIOTM) and tri(isononyl) trimellitate (TINTM)]. Glass-transition temperature (T_g), elongation-at-break, tensile strength, leaching and migration of the control and the eight trimellitate-containing PVC sheets were determined to evaluate effects of molecular weight and concentration of the three trimellitates on their plasticizing efficiencies in the prepared PVC sheets. The experimental results showed that although both molecular weight and concentration affected plasticizing efficiency, plasticizer concentration was found to be the most important parameter. While T_g of pure PVC was 84.32oC, that of 20.0 phr TINTM-containing sample was 25.73oC, representing a decrease of 58.59oC or 69.49%. Compared to the pure PVC, the T_g of 20.0 phr TIOTM-containing sample was decreased by 37.81oC or 44.84%. The T_g of 20.0 phr TMTM-containing sample was decreased by 33.20oC or 38.19% compared to the pure PVC. Although both leaching and migration values obtained were less and followed same trend, the amount leached was relatively higher than that migrated. The plasticizing efficiencies (drastic reduction in T_g and increase in elongation-at-break, slight reduction in tensile strength and strong resistance to weight loss through leaching and migration) of the three trimellitates were found to follow the order TINTM > TIOTM >> TMTM. The trends of results were attributed to the difference in size of the three trimellitate molecules represented by their molecular weights. Being larger in size, TINTM is retained in the PVC sheets better than the relatively lower molecular weight TIOTM and TMTM as obtained from their leaching and migration values. Since the three trimellitate plasticizers work by embedding themselves between the PVC chains and spacing them apart (increasing the "free volume") and weaken the forces between the PVC molecules, thus making the PVC sheets softer and more flexible, it was not surprising that the trend in T_g reduction followed the TINTM > TIOTM >> TMTM order.

Keywords: Environment, phthalate, plasticizing efficiency, poly(vinyl chloride), trimellitate

1. Introduction

PVC is the most versatile plastic and its variety of uses comes from its ability to be formulated with different additives and with different molecular masses, giving plastics that range from rigid to pliable (Shah and Shertukde, 2003; Gill et al., 2006; Unar et al, 2010). Industrially, PVC is made from ethylene by free-radical polymerization mechanism. Unfortunately, the PVC that comes out from laboratory and industrial reactors is a hard,

rigid and brittle polymer with glass-transition temperature (T_g) of about 85oC limiting its applications where flexibility is critical (Yu et al., 2008; Rozaki et al., 2017). Consequently, plasticizers are added to PVC to reduce its T_g to even below room temperature, making it pliable and facilitate production of flexible articles such as raincoats, imitation leather, shower curtains, and disposable gloves (Rahman, 2006; Erythropel et al., 2012; Coltro et al., 2013).

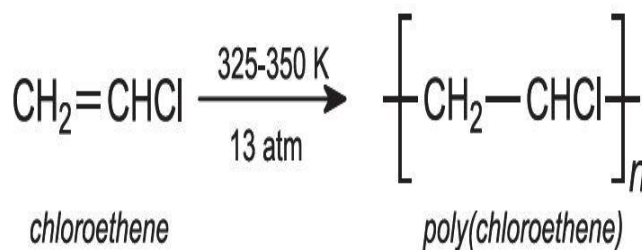


Fig. 1. Polymerization of chloroethene to PVC (Chanda and Roy, 2006)

2. Materials and methods

Sample preparation: 45 x 11 x 3 mm³ sheet of pure PVC was prepared compression moulding technique. Eight sample coupons of the same dimension were also prepared by the same procedure after addition of 2.5, 5, 7.5, 10, 12.5, 15, 17.5 and 20 phr of each of TMTM, TIOTM and TINTM.

2.2. Determination of glass-transition temperature (T_g)

T_g of the samples were determined using DSC according to the procedure of Coltro et al (2013).

2.3 Leaching and Migration tests

Procedures of Nara et al (2009) and Marcilla et al (2008) were used to test these properties of the samples.

2.4 Determination of Tensile Strength and Elongation-at-break:

These mechanical properties of the samples were determined in accordance with ASTM D-638 (Anon, 2003).

3. Results and discussion

From the experimental results displayed in Figures 1, 2 and 3, it was found that although both molecular weight and concentration affected plasticizing efficiency, plasticizer concentration was found to be the most important parameter.

3.1 Glass-Transition Temperature (T_g)

T_g or plasticizing efficiency values of the PVC sheets decreased with increase in concentration of the three trimellitates, although to slightly

different extents in the order TINTM > TIOTM >> TMTM.

3.2 Leaching and Migration

Although both leaching and migration values obtained were less and followed same trend (TMTM > TIOTM > TINTM), the amount leached was relatively higher than that migrated.

3.3 Elongation-at-break and tensile strength

While elongation-at-break of the samples increased with increase in concentration of the three trimellitates in the order TINTM > TIOTM > TMTM, tensile strength decreased in the order TMTM > TIOTM > TINTM.

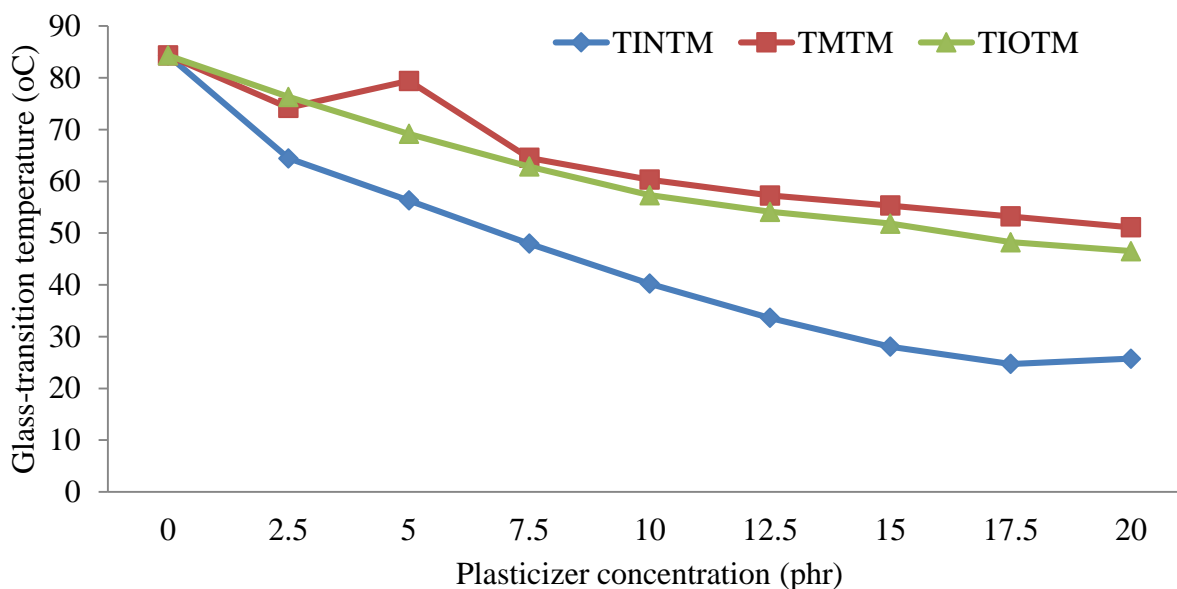


Fig. 1. Effect of concentration of TINTM, TIOTM and TMTM on the glass-transition temperature of PVC sheets.

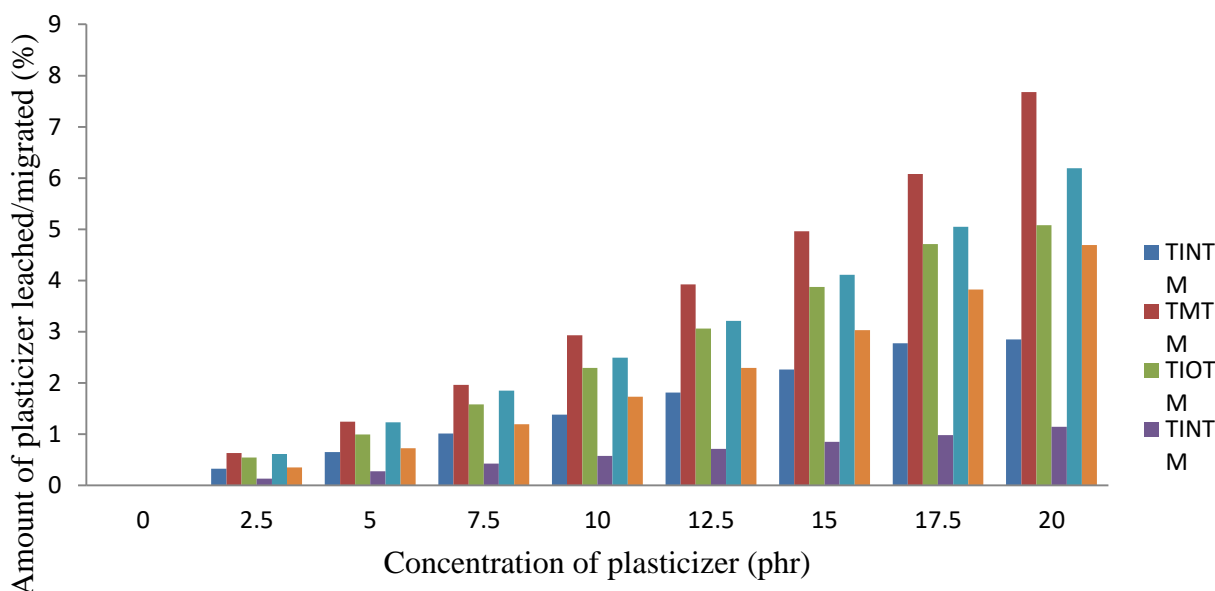


Fig. 2. Effect of concentration of TINTM, TIOTM and TMTM on their leaching and migration from the plasticized PVC sheets in 10 days.

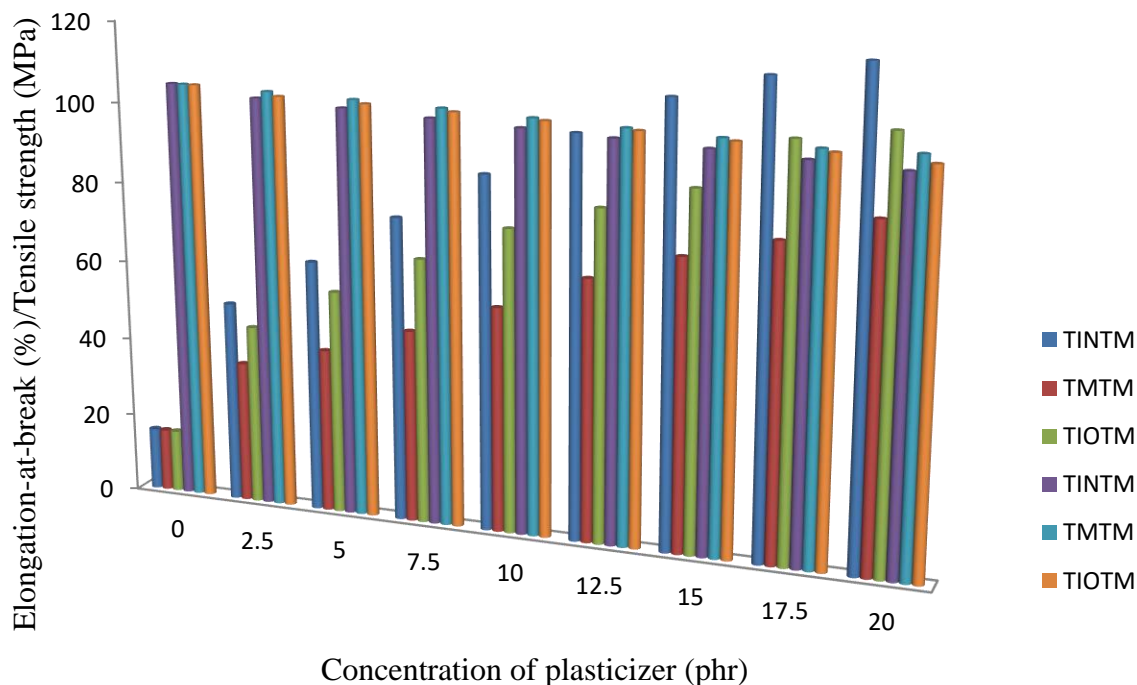


Fig. 3. Effect of concentration of TINTM, TIOTM and TMTM on elongation-at-break and tensile strength of the PVC sheets

References

Anonymous (2003). Test Method for Tensile Properties of Plastics, ASTM D-638-01. American Standards for Testing and Materials, West Conshohocken, PA. pp. 674-713

Chanda, M. and Roy, S. K. (2006). Plastics technology handbook. CRC Press, Boca Raton, pp. 1-6.

Coltro, L., Pitta, J.B. and Madaleno, E. (2013). Performance evaluation of new plasticizers for stretch PVC films. *Polymer Testing* 32 (2): 272-278.

Erythropel, H.E., Maric, M. and Cooper, D.G. (2012). "Designing green plasticizers: Influence of molecular geometry on biodegradation and plasticization properties". *Chemosphere* 86(8): 759-766.

Gill, N., Saska, M. and Negulecu, I. (2006). Evaluation of the effects of biobased plasticizers on the thermal and mechanical properties of poly(vinyl chloride). *Journal of Applied Polymer Science* 102(2): 1366-1373.

Marcilla, A., Garcia, S. and Garcia-Quesada, J.C. (2008). Migratability of PVC plasticizers. *Polymer Testing* 27(2): 221-233.

Nara, K., Nishiyama, K., Natsugari, H., Takeshita, A., and Takahashi, H. (2009). Leaching of the plasticizer acetyl tributyl citrate (ATBC) from plastic kitchen wrap.

Journal of Health Sciences 55(2): 281-288.

Rahman, M. (2006). Environmentally friendly plasticizers for poly(vinyl chloride)-Improved mechanical properties and compatibility by using branched poly(butylene adipate) as a polymeric plasticizer. *Journal of Applied Polymer Science* 100 (3): 2180-2188.

Rozaki, N.Z., Gan, SN. and Ang, D.T.-C. (2017). Environmentally friendly oil-modified polyesters as polymeric plasticizers for poly(vinyl chloride). *Journal of Polymers and Environment* 25(2): 286-295.

Shah, B. and Shertukde, V.V. (2003). Effect of plasticizers on mechanical, electrical, permanence and thermal properties of PVC. *Journal of Applied Polymer Science* 90: 3278-3284.

Unar, I.M., Soomro, S.A. and Aziz, S. (2010). Effect of Various Additives on the Physical Properties of Poly(vinyl chloride) Resin. *Pakistani Journal of Analytical and Environmental Chemistry* 11 (2): 44-50.

Yu, B.Y., Chung, J. W., and Kwak, S.-Y. (2008). Reduced migration from flexible poly(vinyl chloride) of a plasticizer containing β -cyclodextrin derivative. *Environmental Science and Technology* 42(19): 7522-7527.

**ABSTRACT CCT-: 070**Ayeni E. A.^{1*}, A. Ahmed¹, G. Ibrahim¹, V. Atinga²

1. Department of Pharmacognosy and Drug Development, Ahmadu Bello University Zaria, Nigeria
2. Department of Pharmacognosy and Drug Development, Gombe State University, Gombe Nigeria

Email: ayeniemmanuel91@yahoo.com**NUTRACEUTICAL EVALUATION OF THE AERIAL PART OF *Daucus carota* LINN.
(APIACEAE)**

ABSTRACT: The study evaluated the nutraceutical potentials of carrot (*D. carota* L.) aerial parts and suggests its pharmaceutical and nutritional utilizations. The nutritional evaluation was determined using AOAC method. The proximate analysis revealed 14.59% crude protein, lipid 10.37%, fibre 9.07%, carbohydrate 51.81%, moisture content 10.23% and the ash content was 12.99%. The mineral elements showed that the aerial parts are abundant in P (11.00), Na (5.38), Fe (3.19), K (2.25), Ca (2.02), Mn (1.15), Mg (1.02), Se (0.40), Cu (0.13), Zn (0.26), Cd (-0.02), As (0.83), Cr (0.02), Ni (0.17) and Pb (0.04). The phytochemical screening revealed the presence of steroid/triterpenes, flavonoids, alkaloids, saponins and glycosides among others which could be explored for its pharmaceutical potentials. The fixed oral doses of acute toxicity of the crude extracts were carried out on Wister Rats and no sign of toxicity and mortality was observed at 5000 mg/kg. This suggests that carrot aerial part could be potential source of vegetables supplements for mankind and also boost food security in developing countries.

Keywords: *Daucus carota*; Aerial part; Nutraceuticals; Phytochemicals; Acute toxicity

1. Introduction

Utilization of natural products especially from plants has led to drug developments, exploitation and discoveries (Cragg and Newman, 2005). Carrot (*Daucus carota* Linn), belongs to the family of Apiaceae. They are usually herbs, leaves alternate with sheathing bases. It is one of the edible root plants and it is a rich source of anthocyanins, carotenoids, β carotene, vitamins A, B and C (Bao and Chang, 1994). However, the aerial parts are usually thrown away after harvesting or after eating the edible root part and results to wastes and underutilized. The study focuses on the aerial parts nutraceutical potentials and to suggest its pharmaceutical utilization.

2. Materials and methods

2.1. Collection, Identification and Preparation of Plant Material

The aerial parts of *D. carota* were collected from the carrot sellers in Samaru market, Sabon Gari Local Government Area, Zaria, Nigeria. The Plant material was identified in the Department of Botany, ABU, Zaria and voucher specimen 12034 was obtained. The foreign materials in the plant samples were removed, air dried for 5-6 days, pulverized and stored in a polythene bag for further use.

2.2 Extraction and Phytochemical Screening of *D. carota* Aerial Part

The plant material was successively extracted by cold maceration based on solvents polarity using n-hexane, ethyl-acetate and methanol respectively. The phytochemical screening was carried out to determined secondary metabolites according to the methods described by Evans (2009).

2.3 Acute toxicity of *D. carota* Aerial Part

The acute oral dose toxicity was carried out on

apparently healthy Wister Rats of 80-120 g and the laboratory animals were sourced from the Department of Pharmacology and Therapeutics, Ahmadu Bello University, Zaria. The animals were observed for toxicity signs and mortality for 14 days as reported by OECD (2001).

2.4 Determination of Proximate and Elemental Analysis of *D. carota* Aerial Part

Acid digestion of the *D. carota* aerial part was carried out according to the standard methods of AOAC, (2005). The concentration of Fe, Mg, Zn, Cu, K and Na were determined using the flame atomic absorption spectrophotometer (AA-500-model), HACH Spectrophotometry (DR/4200) was used for phosphorus determination and Atomic Emission Spectrophotometer (A-ES- Agilent Company) were used for other elements detected. Also the proximate analyses of the *D. carota* aerial parts determined include moisture content, ash, carbohydrate, crude protein, fibre and crude lipid contents and were reported in percentage (AOAC, 2005).

2.5 Statistical Analysis

The results were analyzed and presented in tables and figures using the Statistical Package for Social Sciences (SPSS/PC; IBM Version 20.0; SPSS Inc., Chicago). The mean and standard deviation (SD) were in three replicates.

3. Results and discussion

The proximate analysis (Table 1) showed the percentage compositions of *D. carota* aerial part such as the moisture content (10.23%) which could be rich sources of water that may be utilized in the body. Also with the low percentage of moisture content the aerial part

may be stored for longer period and not susceptible to microbial attack. This is also in lined with WHO, (2007) who reported that permissible limits of moisture content must be with 12-14%. The ash content of (12.99%) dry matter obtained could be attributed to organic material and other mineral materials present in the crude drug. The percentage composition of carbohydrate (51.81%) was moderate and similar to the (55.67%) in *T. terristris* and in water spinach leaves (54.20%) (Imran *et al.*, 2007). This result is between the recommended dietary allowance of 130 g/d (FAO/WHO 2004) which shows it could be good sources of food and may contribute to daily energy requirement of a person.

The crude protein was found to be (14.59%), which was higher compared to (2.11%) in *Amaranthus viridus*, (2.90%) in *C. murale* leaves, (2.76 %) in *N. officinale*, (6.30%) in water spinach and (6.40%) in *Mormordiacae foecide* leaves (Imran *et al.*, 2007) but lower than (24.80%) in sweet potatoes leaves, (29.78 %) in *Piper guinensis*, (31.00%) (Imran *et al.*, 2007). This result conforms to the recommended dietary allowance of 13- 46 g/d for children and adults (FAO/WHO, 2004). The crude fibre (9.07%) which is similar to (7.20%) in sweet potato leaves and (13.00%) in *Tribubus terristris* leaves compared to lower percentage composition of (1.93%) in *A. viridus*, (3.82%) as reported by Akindahunsi and Salawu, (2005). This may suggest the lower deposit of lipid content in the aerial part

since lipid and fat are implicated in many human related diseases. This result is comparable to the work Idoko *et al.*, (2014); Mgbemena and Obodo (2016), who gave reports on proximate and mineral compositions of some leafy vegetables consumed in Nigeria and Feumba *et al.*, (2016) who reported nutraceutical potential of some fruits peels as sources of vegetables.

Fifteen mineral elements were detected (fig 2) which showed that *D. carota* aerial part contains macro and trace elements that function in human during muscle contraction, bone formations, growth, metabolism, osmotic balance, regulatory processes activation and other organic bimolecular activities. This result was compared with FAO/WHO (2004); Asaolu *et al.*, (2012) on required permissible limits of elements in edible plants. The presence of As, Ni, Cd, Pb and Cr is attributed to the heavy metals though they were in lower concentration which may not have effects on man when consumed as prescribed by WHO, (2007). But with the use of good agricultural practices, lower use of chemicals and fertilizer, the heavy metals could be prevented or reduced without any harmful effects when ingested over a long period of time.

The phytochemical screening (Table 2) in the n-hexane extracts and ethyl acetate revealed the absence of alkaloids, cardiac glycosides, saponins, flavonoid and anthraquinone while steroids/triterpenes was present.

Table 1. Proximate analysis of *D. carota* Aerial part

Parameters	%Moisture	%Carbohydrate	% Crude Fibre	%Crude Protein	% Crude Lipid	%Ash content
Values	10.23±0.01	51.81±0.65	9.07±0.38	14.59±1.00	10.37±0.55	12.99±0.05

Values are means ±SD (Standard deviation) of triplicate samples

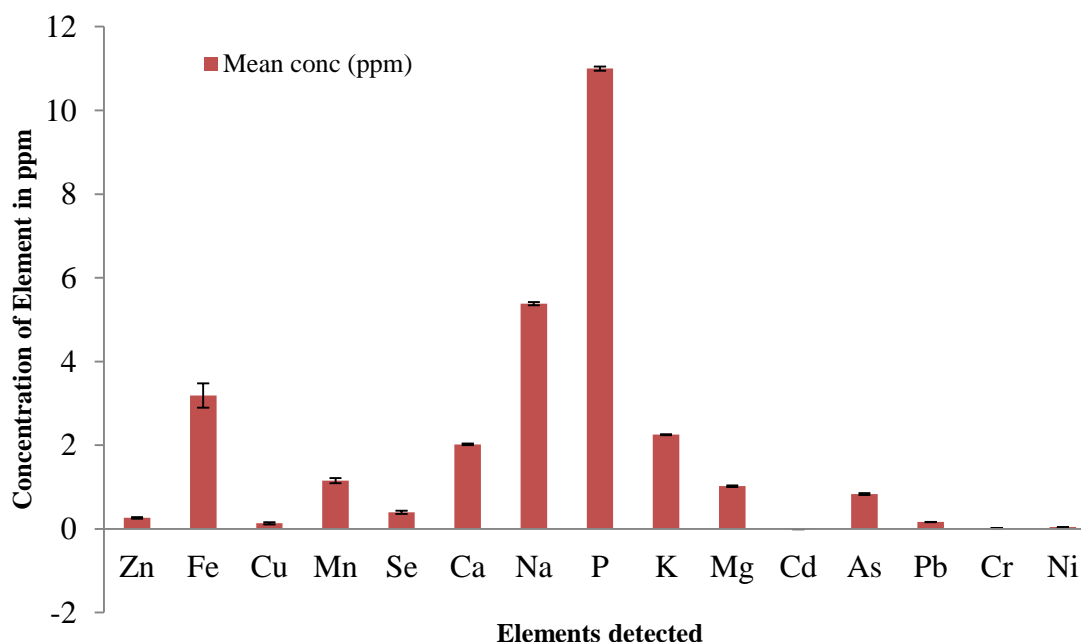


**Table 2:** Preliminary phytochemical screening of *D. carota* aerial part

Phytochemical constituents	N-hexane extracts	Ethyl-acetate extracts	Methanol extracts
Alkaloids			
Dragendorff test	-	-	+
Wagner's test	-	-	+
Mayer's test	-	-	+
Cardiac glycosides			
Keller-killani	-	-	-
Keddes test	-	-	-
Saponins			
Frothing test	-	+	+
Haemolysis test	-	+	+
Flavonoid			
Shinodas test	-	+	+
Lead acetate test	-	+	+
Anthraquinones			
Bontragers test	-	-	-
Modified bontragers test	-	-	-
Tannins			
FeCl ₃	-	+	+
Lead acetate test	-	+	+
Steroid/triterpenes			
Lieberman buchard	+	+	+
Salkowski test	+	+	+

Key: + "Present" and - "Absent"

This is attributed to the low deposit of chemical constituents in the n-hexane extracts (Evans, 2009); however, the steroids/triterpenes may be investigated for possible pharmacological activities such as antioxidant and anti-inflammatory. The ethyl acetate and methanol extracts showed the presence of saponins, flavonoids, tannins steroid/triterpenes while alkaloid is only present in methanol extracts and anthraquinone was absent in the three extracts. The presence of flavonoids and steroid/ triterpenes in the methanol and ethyl acetate extract may indicated an antioxidant activity, free radical scavenging properties, antimicrobial activity, hepatoprotective and anti-inflammatory. The presence of tannins in the ethyl acetate and methanol extracts showed that the aerial part may possess anti-nutritional factors especially when the intake is high and could also be investigated for anti-diarrhea, cardiovascular protection and anti-inflammatory properties. The acute oral toxicity of graded doses of the the n-hexane, ethyl acetate and methanol extracts were administered and no mortality or any toxic signs such as tiredness, abdominal constrict, convulsion, hyperactive, weakness, diarrhea or increased diuresis in the extracts even at a high dose of 5000 mg/kg. This could be assumed practically safe and non-toxic.

4. Conclusion

D. carota aerial parts are rich in nutrients that could be used as supplements and as vegetables for mankind which could be incorporated in daily diets and boost food security in developing countries. The extracts were considered practically safe and non-toxic at 5000 mg/kg and its further pharmaceutical utilization could be investigated.

References

- Akindahunsi, A.A. and Salawu, S.O., (2005). Phytochemical screening and nutrient-antinutrient composition of selected tropical green leafy vegetables. *African Journal of Biotechnology*. 4: 497-501.
- AOAC (2005). Official Methods of Analysis of the Association of Analytical Chemists International, 18th ed. Gathersburg, MD U.S.A. Official method.
- Asaolu, S. S., Adefemi, O. S., Oyakilome, I. G., Ajibulu, K. E. and Asaolu, M. F. (2012). Proximate and Mineral Composition of Nigerian Leafy Vegetables *J. of Food Res.*; Vol. 1, No.3; ISSN 1927-0887
- Bao. B. and Chang, K.C. (1994). Carrot juice color, carotenoids, and non-starchy polysaccharides as affected by processing conditions. *J. Food Sci.*, 59: 1155-1158.
- Cragg, G. M and Newman D. J (2005). International Collaboration in Drug Discovery and Development from Natural Sources. *Pure Appl. Chem.*, 77 (11), Pp. 1923-1942.
- Elizabeth, F. B., Obikili, E. N., Esom, A. E. and Anyanwu, G. E. (2016). Phytochemical Screening and Oral Acute Toxicity Study of Aqueous Leaf Extract of *C. giganteum* in Wistar Rats. *Journal of Phytology* 8: 22-



25

Evans, W.C. (2009). Trease and Evans Pharmacognosy. W.B. Saunder, London. 15th Edition. Pp. 140-150

FAO/WHO (2004). Vitamin and Mineral Requirements in Human Nutrition. Joint FAO/WHO Expert Consultation on Human Vitamin and Mineral Requirements (1998: Bangkok, Thailand). ISBN 92 4 154612 3 (LC/NLM Classification: QU 145)

Feumba, D. R, Ashwini Rani P. and Ragu Sai Manohar (2016): Chemical Composition of Some Selected Fruit Peels. *European Journal of Food Science and Technology* 4 (4), Pp. 12-21

Idoko, O., Emmanuel, S. A, Aguzue, O. C, Akanji, F. T, Thomas, S. A and Osuagwu, I. (2014). Phytochemical Screening, Proximate analysEs and Mineral composition of some leafy vegetables consumed in Nigeria. *Inter. J. of Adv. Chem.*, 2 (2) 175-177

Imran, M., Talpur, F.N., Jan, M. I, Khan, A. and Khan, I. (2007). Analysis of Nutritional components of some wild edible edible plants. *J. chem. Soc. Pak.* 29 (5): 500-505

Mgbemena, N. M. and Obodo, G. A. (2016). Comparative Analysis of Proximate and Mineral Composition of *Moringa oleifera* Root, Leave and Seed obtained in Okigwe Imo State, Nigeria Published with Open Access at *Journal BiNET Vol. 01, Issue 02: 57-62*

OECD (2001). Guidance Document on Acute Oral Toxicity. Environmental Health and Safety Monograph Series on Testing and Assessment No 24 (13).

WHO, (2007): Guidelines for Assessing Quality of Herbal Medicine with references to contaminations and Residues. ISBN 978 92 4 1594448 NLM Classification QU766

**ABSTRACT CCT-: 068**

B.E. Nwobi, H. A. Mohammed, V.C. Okezie, U.O. Edem, N.S. Akpan, C. Ndudi, A. Habibu, K. Muazu

National Research Institute for Chemical Technology, P.M.B 1052 Basawa Zaria

Email: Unclezick@yahoo.com**ANTIMICROBIAL INVESTIGATION OF EUCALYPTUS ESSENTIAL OIL ON SOME SELECTED BACTERIA**

ABSTRACT: *Eucalyptus* essential oil was extracted from the eucalyptus leaves and the oil was screened for antimicrobial property against six (6) bacterial isolates (*Salmonella typhi*, *Bacillus cereus*, *Staphylococcus aureus*, *Escherichia coli*, *Pseudomonas aeruginosa*, and *Bacillus subtilis*) all of which were not resistant at 100% concentration of the oil. Various zones of inhibitions (mm) were obtained with the highest found in *Bacillus subtilis* with 400mm at 100% concentration of the oil while the least zone was found in *Pseudomonas aeruginosa* with a zone of 110mm at 60% concentration of the oil. The minimum inhibitory concentration (MIC) of the oil was found highest at 50% concentration on *Staphylococcus aureus* and lowest at 30% concentration on *Bacillus cereus* and *Bacillus subtilis*. Minimum bactericidal concentration (MBC) of the oil was highest at 60% concentration on *Staphylococcus aureus* and lowest at 30% concentration on *Salmonella typhi*, *Bacillus cereus* and *Bacillus subtilis*.

Keywords: *Eucalyptus*, Essential oil, Antimicrobial, Zones of inhibition, MIC, MBC

1. Introduction

Essential oils (EOs) also called volatile or ethereal oils (Sara Burt, 2004) are aromatic oily liquids obtained from plant material (flowers, buds, seeds, leaves, twigs, bark, herbs, wood, fruits and roots). They can be obtained by expression, fermentation, effleurage or extraction but the method of steam distillation is most commonly used for commercial production of EOs (Van de Braak and Leijten, 1999). Clinical studies about the topical use of eucalyptus essential oil demonstrate that it is tolerated well both when inhaled and when applied onto the skin in topical formulations (Woolf 1999).

This study was aimed at justifying the use of eucalyptus essential oil in medicinal practices.

2. Materials and methods

2.1. Sample collection

Leaves of Eucalyptus were collected from Makarfi Forest Kaduna State and its essential oil was extracted using the steam distillation method.

2.2 Preparation of McFarland turbidity standard

The procedure for preparing McFarland turbidity standard was used in this study as described by Cheesbrough (2002).

2.3 Preparation of oil dilution (concentration)

Seven test tubes were prepared which contain one (1) ml of the Eucalyptus oil which is equivalent to 100% concentration of the oil, the second test tube had 0.8ml of the oil mixed with 0.2ml of Dimethylsulfoxide (DMSO), third test tube had 0.6ml of the oil with 0.4ml of DMSO, fourth tube had 0.4ml of the oil with 0.6ml of DMSO, 0.2ml of the oil was mixed

with 0.8ml of DMSO in the fifth test tube, this yielded a concentration of 100%, 80%, 60%, 40% and 20% respectively. Also the sixth tube had 20mg/ml of ciprofloxacin while the last test tube contains 1ml of DMSO.

2.4 Antimicrobial activity

The essential oil of eucalyptus was tested against six (6) microorganisms; *Staphylococcus aureus*, *Escherichia coli*, *Salmonella typhi*, *Shigella dysenteriae*, *Bacillus cereus*, *Bacillus subtilis* and *Pseudomonas aeruginosa* obtained from Ahmadu Bello University Teaching Hospital, Shika, Kaduna State Nigeria and preserved in McCartney bottles with slant preparations of nutrient agar.

The agar disc diffusion method was employed to determine the antimicrobial activity of the essential oils (NCCLS 1997; Khan *et al.*, 2001; Collin *et al.*, 2004).

3. Results and discussion

The difference in the susceptibility pattern of the organisms can be attributed to the various chemical compounds and functional groups found in the oil. These results are similar to those found by (Trivedi and Hotchandani, 2004; Farah *et al.*, 2001; Gamal and Sabrin, 2007; Nair *et al.*, 2008). Also, Iserin (1997), Inouye *et al.* (2001) and Cimanga *et al.* (2002) and some other researchers reported that the antimicrobial activity of an essential oil is linked to its chemical composition. The functional groups of some compounds found in most plant materials alcohol, phenols, terpenes and ketones are associated for its antimicrobial characteristics (Farah *et al.*, 2001; Alma *et al.*, 2004; Sartorelli *et al.*, 2006; Braca *et al.*, 2008; Mohammadreza, 2008; Maksimovi *et al.*, 2008).



Table 1. The mean zones of inhibition by various concentration of eucalyptus oil against selected bacteria

Organisms	Inhibition zones(mm)**						Positive control	Negative control
	100%	80%	60%	40%	20%			
<i>Salmonella typhi</i>	200	170	130	130	-		420	-
<i>Bacillus cereus</i>	250	200	190	160	120		540	-
<i>Staphylococcus aureus</i>	140	-	-	-	-		450	-
<i>Escherichia coli</i>	250	210	140	50	-		475	-
<i>Pseudomonas aeruginosa</i>	305	120	110	-	-		550	-
<i>Bacillus subtilis</i>	400	350	255	225	185		550	-

** includes diameter of disc (6mm), (-) No zone of inhibition, Positive control- ciprofloxacin
Negative control – Dimethylsulfoxide (DMSO)

Table2. Minimum Inhibitory Concentration (MIC) of Eucalyptus Oil against Selected Bacterial Isolates

Organisms	Inhibition zones(mm)**						MIC
	10%	20%	30%	40%	50%	60%	
<i>Salmonella typhi</i>	++	+	+	-	-	-	40%
<i>Bacillus cereus</i>	+	+	-	-	-	-	30%
<i>Staphylococcus aureus</i>	+++	+++	++	+	-	-	50%
<i>Escherichia coli</i>	+++	+	++	-	-	-	40%
<i>Pseudomonas aeruginosa</i>	++	+	+	-	-	-	40%
<i>Bacillus subtilis</i>	++	+	-	-	-	-	30%

(-) No turbidity; (+) low turbidity; (++) moderate turbidity; (+++) high turbidity

Table 3. Minimum Bactericidal Concentration (MBC) of Eucalyptus Oil against Selected Bacterial Isolates

Organisms	Inhibition zones(mm)**						MIC
	10%	20%	30%	40%	50%	60%	
<i>Salmonella typhi</i>	++	+	-	-	-	-	30%
<i>Bacillus cereus</i>	+	+	-	-	+	+	30%
<i>Staphylococcus aureus</i>	+++	+++	+++	++	+	-	60%
<i>Escherichia coli</i>	+++	+	+	+	-	-	50%
<i>Pseudomonas aeruginosa</i>	+++	+	+	-	-	-	40%
<i>Bacillus subtilis</i>	++	+	-	-	-	-	30%

(-) No growth; (+) low growth; (++) moderate growth; (+++) high growth

References

- Alma MH, Nitz S, Kollmannsberger H, Digrak M, Efe F T, Yilmaz N (2004). Chemical Composition and Antimicrobial Activity of the Essential Oils from the Gum of Turkish Pistachio (*Pistacia vera* L.). *J. Agric.Food Chem.* 52 (12): 3911-3914.
- Van de Braak, S.A.A.J., Leijten, G.C.J.J., 1999. Essential Oils and Oleoresins: A Survey in the Netherlands and other Major Markets in the European Union. CBI, Centre for the Promotion of Imports from Developing Countries, Rotterdam, p. 116.
- Sara Burt (2004). Essential oils: their antibacterial properties and potential applications in foods—a review. *International Journal of Food Microbiology* (94) 223–253
- Woolf A. (1999): Essential oil poisoning. *Journal of Toxicology- Clinical Toxicology*, 37: 721–727.
- NCCLS (1997): Performance standards for antimicrobial disk susceptibility test. 6th Ed. Approved Standard, M2-A6. National Committee for Clinical Laboratory Standards. Wayne.
- Cheesbrough, M (2000). District Laboratory Practice Manual in Tropical Countries Part 2. Cambridge University Press, Cambridge, 136-137. 158,165, 180.
- Collins, C.H., Lyne, P.M., Grange, J. M. and Falkinham III, J.O. (2004) *Mirobiological Methods*. 8th Edition. *Butterworth and Co. Ltd.* pp 168- 186.
- Khan, M. R.; Kihara, M. and Omoloso, A.D. (2001) Antimicrobial activity of *Cassia alata*. *Fitoterapia*, 72(5): 561-564.
- Rios J.L., Recio M.C. (2005): Medicinal plants and antimicrobial activity. *Journal of Ethnopharmacology*, 100:80–84.
- Trivedi NA, Hotchandani SC (2004). A study of the antimicrobial activity of oil of Eucalyptus. *Indian J. Pharmacol.* 36: 93-94.
- Farah A, Satrani B, Fechtal M, Chaouch A, Talbi M (2001). Composition ch essentielles extraites des feuilles d'*Eucalyptus camaldulensis* et de imique et activités antibactérienne et antifongique des huiles son hybride naturel (clone 583). *Acta Bot. Gallica.* 148 (3): 183-190
- Gamal AM, Sabrin RMI (2007). Eucalyptone G, a new phloroglucinol derivative and other constituents from



- Eucalyptus globulus* Labill. ARKIVOC Inter. J. Org. Chem. October. pp. 281-291.
- Nair R, Vaghasiya Y, Chanda S (2008). Antibacterial activity of *Eucalyptus citriodora* Hk. oil on few clinically important bacteria. Afr.J. Biotechnol. 7: 25-26.
- Iserin P (1997). Encyclopédie des plantes traditionnelles, identification, préparation, soin. Ed. Lavoisier.Paris.
- Inouye S, Takizawa T, Yamaguchi H (2001). Antibacterial activity of essential oils and their major constituents against respiratory tract pathogens by gaseous contact. J. Antimicrobial Chemother. 47: 565-573.
- Cimanga K, Kambu K, Tona L, Apers S, De Bruyne T, Hermans N, Totté J, Pieters L, Vlietinck AJ (2002). Correlation between chemical composition and antibacterial activity of essential oils of some aromatic medicinal plants growing in the Democratic Republic of Congo. J. Ethnopharmacol. 2(79): 213-220.
- Braca A, Siciliano T, D'Arrigo M, Germanò MP (2008). Chemical composition and antimicrobial activity of *Momordica charantia* seed essential oil. Fitoterapia. Vol 79. Issue 2. February:123-125
- Sartorelli P, Marquioreto AD, Amaral-Baroli A, Lima MEL, Moreno P RH (2006). Chemical composition and antimicrobial activity of the essential oils from two species of *Eucalyptus*. Phytother. Res. 21(3): 231-233.
- Mohammadreza VR (2008). Chemical composition and antimicrobial activity of *Pimpinella affinis* Ledeb. Essential oil growing in Iran. Int. J. Green Pharm. 12 (3): 138-140.
- Maksimovi_ Z, Milenkovi_ M, Vu_i_evi_ D, Risti_ M (2008). Chemical composition and antimicrobial activity of *Thymus pannonicus* All. (*Lamiaceae*) essential oil Central Eur. J. Biol. 3(2): 149-154.

**ABSTRACT CCT-: 065**

A. R. Isa^{1*}, O. O. Fasanya¹, S. Gbadamasi¹, A. O. Umar¹, Z. S. Gano¹, A. Y. Atta¹, B. Y. Jibril², B. Mukhtar², B. O. Aderemi².

¹ National Research Institute for Chemical Technology, Zaria

² Department of Chemical Engineering, Ahmadu Bello University, Zaria

Email: rbed.abdul@narict.gov.ng; rbed.abdul@gmail.com

AROMATIZATION OF LPG OVER ZNO/ZSM-5 CATALYSTS: A STATISTICAL OPTIMIZATION OF PROCESS VARIABLES

ABSTRACT: Research efforts being made regarding one-step production of petrochemical feedstocks from natural gas, liquefied petroleum gas (LPG) and natural gas liquids (NGLs) will guarantee the continuous supply of these petrochemical feedstocks. In this regard, a statistical approach for optimizing the process variables (reaction temperature, catalyst weight and ZnO wt% loading on ZSM-5) in LPG aromatization over ZnO/ZSM-5 catalysts was carried in this work. Three different ZnO loaded ZSM-5 (50) catalysts were prepared and characterized by BET, XRD, FTIR, UV-Vis, SEM, and IR spectra of pyridine adsorption. Response surface methodology (RSM) was employed in optimizing the process variables in the aromatization process. D-optima experimental design was used to establish the interaction effects of the variables towards LPG conversion and aromatic selectivity. Coefficient of determination (R^2) was determined to be 95.61% and a second order regression model was developed. Optimum LPG conversion of 94.79% was achieved at 550°C for 0.15g catalyst weight and 0.5wt% ZnO loading with a corresponding aromatic selectivity of 21.46%.

Keywords: LPG; Aromatization; RSM; Aromatics; ZnO; ZSM-5.

1. Introduction

Recent developments in zeolite processes have dramatically increased the demand for aromatic hydrocarbons (Vosmerikova et al., 2014). To meet this demand, aromatization of light hydrocarbons, the components found in natural gas (NG), LPG and natural gas liquids (NGLs), over zeolite catalysts have evolved. Various commercial processes such as cyclar from British Petroleum, aroforming from Salutec, z-forming from Mitsubishi and Chiyoda, have been established for LPG transformation into benzene, toluene, ethylbenzene and xylene (BTEX) hydrocarbons with simultaneous formation of a large amount of hydrogen which is also a valuable product (Caeiro, et al., 2006). A lot of interest has been paid to gallium or zinc-based ZSM-5 catalysts because of their selectivity towards aromatic hydrocarbon selectivity (Niu, et al., 2014; Frey et al., 2011). As a result of their high dehydrogenating abilities, the presence of these metal ions (gallium and zinc) in the ZSM-5 catalyst helps in the hydrogen recombination and desorption with consequent improvement in the BTEX selectivity (Viswanadham et al., 2004).

RSM is a statistical tool that is being employed to optimize any process where a number of independent variables affect the output of the desired product. This method easily allows for the study of interactions between two or more process variables unlike the conventional approach, where one variable is studied while keeping the others constant, thereby making it impossible for the overall effects of all the variables to be studied at a time. A number of studies have shown that RSM could be used as an effective optimization tool in experimental process. Sachchit, *et al.* (2013) employed RSM central composite design in optimizing methane conversion over Zn-Mo/H-ZSM-5 catalyst in the presence of methanol. The group reported a second order regression model for

the methane conversion and obtained 0.96 coefficient of determination. Similarly, optimization of operational parameters for adsorption of heavy metals from industrial effluent on nano-adsorbents has been reported using the Box–Behnken design matrix. Dubey, *et al.* (2016) demonstrated the use of RSM Box-Behnken design in determining the effects of process variables in the high uptake of Cr(VI) on the nano-particles. To the best of our knowledge, no literature exists for the process optimization of LPG conversion to aromatics using the RSM D-optimal design.

To this effect, we report on the optimization studies of LPG aromatization process over ZnO supported ZSM-5 using RSM D-optimal design. The study was performed at different reaction temperatures, varying catalyst:diluent ratios, and constant flowrates of LPG and nitrogen to optimize the LPG conversion and BTEX selectivity. Three catalysts with different zinc loadings were prepared via the impregnation method with ZSM-5 ($\text{SiO}_2/\text{Al}_2\text{O}_3=50$) as support. As-prepared catalysts were characterized and their performances investigated in a fixed bed microactivity reactor.

2. Materials and methods

Three catalysts containing 0.5, 2 and 5 wt% zinc oxide, supported on ZSM-5 ($\text{SiO}_2/\text{Al}_2\text{O}_3=50$) were prepared via the incipient wet impregnation method with an aqueous solution of $\text{Zn}(\text{NO}_3)_2 \cdot 6\text{H}_2\text{O}$. The prepared catalysts were calcined under air at 550°C for 6 h.

The calcined samples were characterized by UV-Vis spectroscopy, SEM, and X-ray diffractometry (XRD). Nitrogen sorption isotherms were performed at liquid nitrogen temperature (-196°C) on an F-Sorp 2400 surface area analyzer to determine the specific surface areas for the three catalysts. Prior to the sorption measurements, about 200 mg of each



of the prepared catalyst was degassed at 200°C until constant pressure was achieved.

Statistical experiment design was prepared using three independent process variables: reaction temperature, catalyst weight, and ZnO wt% loading on ZSM-5 (50). Reaction temperature and catalyst weight are grouped as numeric factors with range between 520°C to 580°C and 0.0-0.5 g respectively. ZnO wt% loading on ZSM-5 is taken as a categorical factor with 3 levels depicting the 0.2, 0.5 and 2 wt% respectively. The design obtained was used in the study of LPG aromatization over ZnO/ZSM-5 catalysts at different temperatures and catalyst weights. The responses (conversion and selectivity) obtained after experimentation were analysed using ANOVA and coefficient of determination (R^2).

The activities of the prepared catalysts were tested in a continuous flow vertical fixed bed microactivity reactor with 11 mm internal diameter and 55 cm in length based on the design of experiment (DOE). In a typical run, 1 g of catalyst diluted with glass beads is charged into the reactor and supported at the centre with the aid of glass wool. Reactant streams consisted of LPG and Nitrogen at 20 ml/min and 80 ml/min respectively and regulated by calibrated mass flow controllers. Reactor exit stream was conducted by a line maintained at 150°C and the analyses of the reaction mixtures was online with a gas chromatography (BUCK Scientific, model 910) equipped with a TCD and an FID detector. Peak areas were converted into concentrations by means of response factors determined

through calibrations. LPG conversions ($\%X_{iC_4}$) and BTEX selectivity ($\%S_{BTEX}$) are defined as expressed in the following equations (1) and (2) respectively:

$$X_{iC_4}(\%) = \frac{\text{concentration of } iC_4 \text{ in feed} - \text{concentration of } iC_4 \text{ in product}}{\text{concentration of } iC_4 \text{ in feed}} \times 100 \dots\dots\dots (1)$$

$$S_{BTEX}(\%) = \frac{\text{concentration of BTEX}}{\text{concentration of } iC_4 \text{ in feed} - \text{concentration of } iC_4 \text{ in product}} \times 100 \dots\dots\dots (2)$$

3. Results and discussions

Catalysts characterization

A noticeable decrease in the BET surface area of the catalysts as ZnO was impregnated was observed. ZnO impregnation resulted into possible surface coverage of the mesoporous section of the catalysts as evident from Table 1 and the decrease in surface area increases with increase in ZnO loading. Furthermore, there was also decrease in the average pore volume and average pore size of the catalysts upon impregnation. Expectedly, this decrease increases with increase in the ZnO loading and could be associated to partial pore blockage by the impregnated ZnO. Though there was a decrease in the average pore size, the final pore size still falls within the mesoporous region as per IUPAC classification. This is a desirable property as it would enhance diffusivity during the aromatization reaction.

Table 1: Physicochemical properties of the synthesized catalysts

Catalysts	BET (m ² /g)	Micropore area (m ² /g)	Mesopore area (m ² /g)	Average pore volume ^a (cm ³ /g)	Average pore size ^b (Å)	ZnO crystallite size ^c (Å)
ZSM-5 (50)	358.7	225.1	133.6	0.1919	34	–
0.5wt% ZnO	360.6	244.3	116.3	0.1750	29	460
2wt% ZnO	339.7	248.7	91.0	0.1615	29	537
5wt% ZnO	299.6	227.8	71.8	0.1429	26	403

^aBJH adsorption average pore diameter. ^bBJH adsorption pore volume. ^cCalculated by using Scherrer equation based on XRD results

Plate 1 shows the SEM images and the corresponding EDX of the support, ZSM-5 (50) and the catalysts, 0.5 wt%, 2 wt% and 5 wt% ZnO loadings. The images revealed highly crystalline ZSM-5(50) with hexagonal morphology. Upon impregnating ZnO, there was no observable change in the morphology of the parent ZSM-5(50), as the hexagonal structure was maintained.

Though the presence of ZnO could not be clearly seen from the SEM images, the EDX

results confirmed its presence. In addition, ZnO could not be detected in the catalyst with 0.5 wt% ZnO loading and this could be associated with the concentration of the zinc in the catalyst which might be below the detection limit of the machine used.

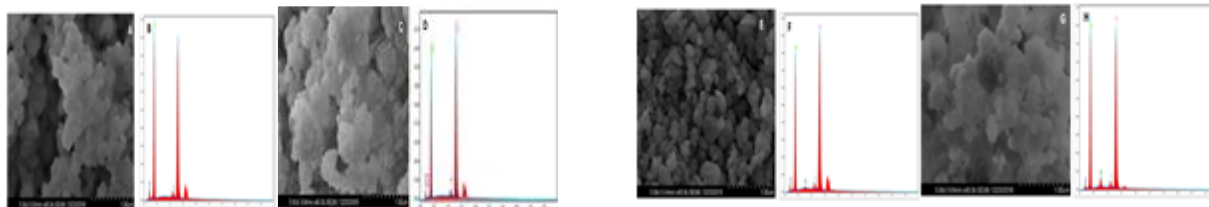


Plate 1: SEM and EDX images of images of (A/B) ZSM-5 (Si/Al=50) (C/D) 0.5 wt% Zn loading on ZSM-5 (E/F) 2 wt% Zn loading on ZSM-5, (G/H) 5 wt% Zn loading on ZSM-5

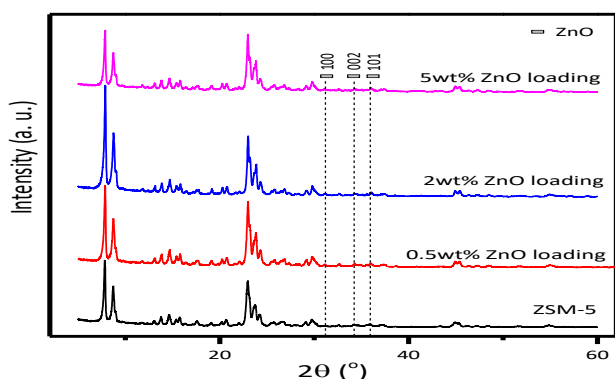


Fig. 1: XRD patterns ZSM-5 (Si/Al=50) and the different ZnO wt% loadings on ZSM-5

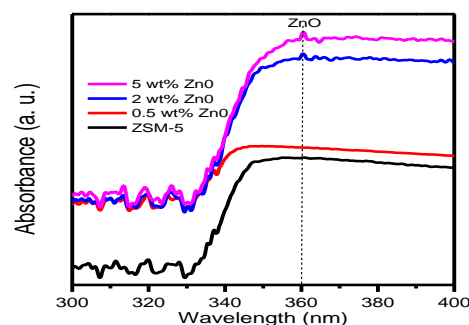


Fig. 2: UV-Vis spectra of the catalysts, with ZSM-5 (50) as reference

Figure 1 shows the XRD patterns for the support (ZSM-5) and the corresponding catalysts (0.5-5 wt% ZnO loadings). The results show that the crystalline nature of the ZSM-5(50) was maintained upon calcination. The patterns for 0.5, 2, and 5 wt% ZnO loadings showed similar diffraction peaks as the parent ZSM-5 (50), except for slight increment of the peak at $2\theta = 31.1^\circ$, 34.3° , and 36° . These peaks corresponded to the (100), (002), and (101) hexagonal structure of ZnO respectively (JCPDS 01-079-0208). The ZnO crystallite sizes of the catalysts, calculated by Scherrer equation, using the peak d(100) are presented in Table 1.

In Figure 2, the UV-Vis spectra of the catalysts, with ZSM-5 (50) as the reference point is depicted. Catalysts with 2 and 5 wt% loadings show the presence of a peak at about 360 nm which is due to the presence of ZnO nanoparticle (Premanathan M. et al., 2011; Goh, X., & McCormick, 2014). On the other hand, there was no noticeable peak on the catalyst with 0.5 wt% ZnO loading and it was identical to the parent ZSM-5 (50). The absence of peak on this catalyst is attributed to its low quantity of ZnO loading and the low detection limit of the UV-Vis analyzer.

3.2 Optimization of LPG aromatization using regression analysis

Aromatization experiments using the design matrix obtained from D-optimal design of RSM were carried out to obtain responses from the independent process variables itemized in the experimental design matrix using the

quadratic model. The empirical model equation for LPG conversion relating the independent process variables and the corresponding responses is expressed in the following equation (3):

$$\%LPG_{Conv} = +111.65 + 0.87A + 44.68B + 3.93C_1 - 4.98C_2 + 1.61AB + 0.18AC_1 + 0.68AC_2 - 9.65BC_1 + 7.31BC_2 - 24.21A^2 - 40.08B^2 \quad (3)$$

Where A, B, $C_{(1/2)}$ are reaction temperature, catalyst weight, and $ZnO_{(0.5/2)}$ wt% loading on ZSM-5 respectively. This equation could be employed in the prediction of responses for each factor at a given level. However, it could not be used to determine the relative influence of each factor because of the scaling of the coefficients to accommodate the individual unit of each factor.

Testing the goodness of fit of the LPG conversion model, response surface quadratic model was employed because of its suitability. The coefficient of determination (R^2) was determined to be 95.61%. Adjusted and predicted R^2 were obtained as 90.78% and 56.69% respectively. These values are not as close as one may reasonably expect because the difference between them is >0.2 . This might be attributed to large block effects or a possible problem with the model and/or data. Model corrections, transformation of responses, outliers etc are some measures that should be considered to improve the R^2 agreement. The F-value (lack-of-fit) of 19.80

indicates that the model is significant, and shows that there is only a 0.01% chance that this value could be as a result of error. As a result, the model could be used in navigating the design space.

The effect of interactions between process variables such as reaction temperature, catalyst weight, and ZnO wt% loading on ZSM-5(50) was studied by employing the RSM 3D surface plot diagrams. Interpretation of the ANOVA results indicates that the regression model is significant because of the large F-value and a small p-value. Catalyst weight was seen as the dominant variable in the linear effect amongst others with sum of square values of 34307.00. This was followed by ZnO wt% loading on ZSM-5 (50) and reaction temperature. This is attributed to the increase in the number of active sites on the catalyst surface with increase in catalyst weight and vice versa. Combined effect of catalyst weight and temperature at different ZnO wt% loading is shown in Figure 3. Temperature affects LPG conversion to a large extent. The energy

requirement for the activation of butanes (the predominant component in LPG) is relatively low. Increasing the temperature enhances the decomposition of LPG to smaller molecules, thereby greatly improving the conversion. Furthermore, at higher catalyst weight conversion is improved, which can also be attributed to increase in the number of active sites.

The combined effects of reaction temperature and ZnO wt% loading are shown in Figure 3. LPG conversion is increased with temperature. At the lower design limit (520°C reaction temperature, 0.5 g catalyst weight and 5 wt% ZnO loading), a conversion of 97.76% was achieved. Increasing the process conditions to upper design limit resulted in a decrease in conversion to 94.07%. This could be attributed to the blockage of ZSM-5 (50) pores and channels by coke and volatilization of zinc at higher temperatures. Figure 4 indicates the process requires 0.22 g catalyst weight and 5 wt% ZnO loading for optimum LPG conversion of 99.14% at

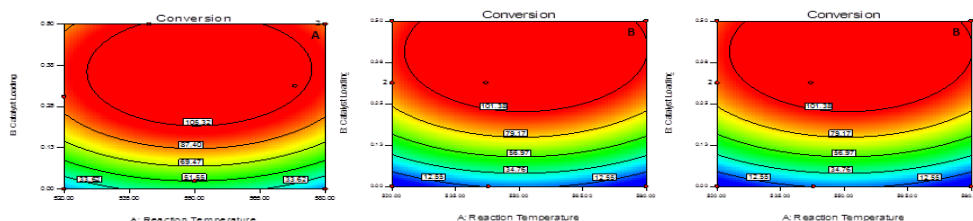


Fig. 3: Combined effects of reaction temperature, catalyst weight and ZnO wt% loadings on LPG conversion

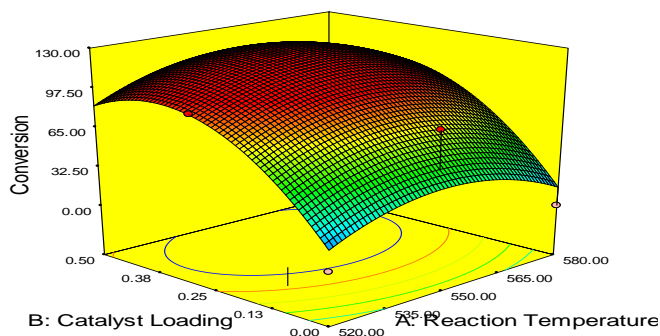


Fig. 4: 3D curve of the optimum LPG conversion for the developed model

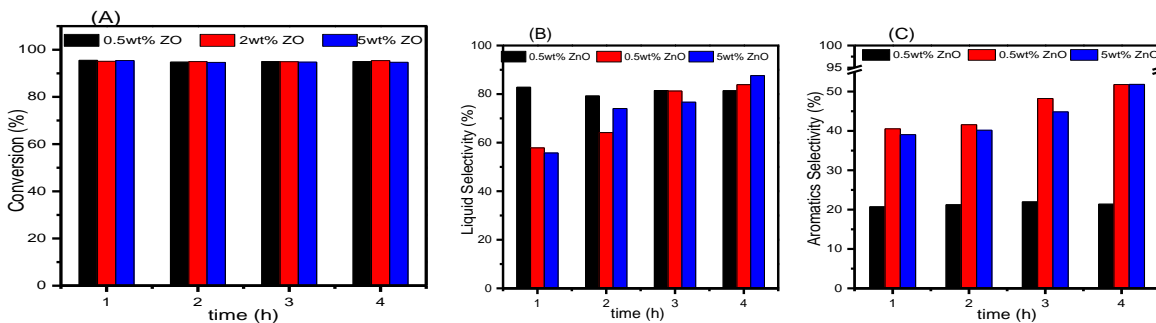


Fig. 5: Aromatic selectivity for the three different ZnO wt% loadings



Aromatic selectivity for the three different ZnO wt% loadings is depicted in Figure 5. An improvement in the selectivity towards aromatic than aliphatic compounds was observed. This underscored the role of zinc in dehydrogenating and subsequent conversion of small cracked olefins to aromatics (Tshabalala & Scurrall, 2015). Selectivity towards alkylated benzenes were also profound. Similarly, the three catalysts have demonstrated that aromatic formation hinders the formation of light alkenes and olefins (Niu, et al., 2014).

Here also, RSM was used to determine the influence of process variables on product selectivity. The Zn/ZSM-5 catalysts studied initially exhibited high conversions close to 100% with BTEX selectivities around ~45%. A rapid decrease in activity after few hours on stream of the catalysts was linked to coke formation and zinc volatilization at the reaction temperatures. Zinc has been reported to exhibit low vapor pressure at the conversion temperature and in the presence of strong reducing agents like hydrogen and carbon, the zinc in the catalysts elutes resulting in the decline in aromatic selectivity (Seddon, 1990). Increase in reaction temperature slightly affects product selectivity and aromatic distribution for 0.5 and 2 wt% Zn loading. A slight decrease in BTEX selectivity was noticed while the selectivity for naphthalenes and C₉₊ aromatics increased. At reaction temperature of 520°C, the catalysts displayed a conversion of 94.41-97.76% with BTEX selectivity of 13.99-34.45% for ZnO wt% loadings of 0.5-5. Increasing the temperature however, results in increased conversion but selectivity suffers a decline because of dominance of LPG cracking at higher temperatures.

4. Conclusion

Optimization of LPG aromatization process conditions over three different ZnO loaded ZSM-5 catalysts were conducted by developing a model equation. The optimization process involved these independent process variables: reaction temperature; catalyst weight; and ZnO wt% loading on ZSM-5. From the design of experiment, the interaction between these variables affected considerably the conversion of LPG over the catalysts. The combined effects of these variables

on the conversion were determined based on the D-optima design of RSM. Experimental results obtained were relatively in good agreement with predictions from the model. Quadratic and linear models were employed in optimizing the conversion and selectivity respectively. An optimum LPG conversion of 94.79% could be achieved at 550°C, 0.15 g catalyst weight and 0.5 wt% Zn loading.

Acknowledgement

The authors are thankful to the Petroleum Technology Development Fund (PTDF) for funding the research.

References

- Cairo, G., Carvalho, R., Wang, X., Lemos, M., Lemos, L., Guisnet, M., et al. (2006). Activation of C₂-C₄ alkanes over acid and bifunctional zeolite catalysts. *Journal of Molecular Catalysis A, Chemical*(255), 131-158.
- Dubey, S., Upadhyay, S. N., & Sharma, Y. C. (2016). Optimization of removal of Cr by γ -alumina nano-adsorbent using response surface methodology. *Ecological Engineering*, 97, 272–283.
- Frey, K., Lubango, L. M., Scurrall, M. S., & Guzzi, L. (2011). Light alkane aromatization over modified Zn-ZSM-5 catalysts: characterization of the catalysts by hydrogen/deuterium isotope exchange. *Reac Kinet Mech Cat*, 303-309.
- Goh, E., X., X., & McCormick, P. (2014). Effect of particle size on the UV absorbance of zinc oxide nanoparticles. *Scripta Materialia*, 78, 49-52.
- Niu, Xianjun; Gao, Jie; Miao, Qing; Dong, Mei; Wang, Guofu; Fan, Weibin; Qin, Zhangfeng; Wang, Jianguo (2014). Influence of preparation method on the performance of Zn-containing HZSM-5 catalysts in methanol-to-aromatics. *Microporous and Mesoporous Materials*, 197, 252-261.
- Premanathan M. et al. (2011). Selective toxicity of ZnO nanoparticles toward Gram-positive bacteria and cancer cells by apoptosis through lipid peroxidation. *Nanomedicine: Nanotechnology, Biology and Medicine*, 7(2), 184-192.
- Sachchit, M., Pravakar, M., Ajay, D. K., & Kamal, P. K. (2013). Statistical Optimization of Process Variables for Methane Conversion over Zn-Mo/H-ZSM-5 Catalysts in the Presence of Methanol. *Energy Technology*, 1, 157-165.
- Scurrall, M. S. (1988). Factors Affecting the Selectivity of the Aromatization of Light Alkanes on Modified ZSM-5 Catalysts. *Applied Catalysis*, 41, 89-98.
- Seddon, D. (1990). Paraffin Oligomerisation to Aromatics. *Catalysis Today*, 6(3), 351-372.
- Tshabalala, T. E., & Scurrall, M. S. (2015). Aromatization of n-hexane over Ga, Mo and Zn modified H-ZSM-5 zeolite catalysts. *Catalysis Communications*(72), 49–52.
- Viswanadham, N., Muralidhar, G., & Rao, T. P. (2004). Cracking and aromatization properties of some metal modified ZSM-5 catalysts for light alkane conversions. *Journal of Molecular Catalysis A: Chemical*, 223, 269–274.
- Vosmerikova, L. N., Barbashin, Y. E., & Vosmerikov, A. V. (2014). *Petroleum Chemistry*, 54(6), 420–425.

**ABSTRACT CCT-: 004**

Ukwubile Cletus Anes, Nettey Henry

Department of Science Laboratory Technology, School of Science and Technology,
Federal Polytechnic, Bali, Nigeria.Department of Pharmaceutics and Microbiology, University of Ghana School of
Pharmacy, University of Ghana, Legon-Accra, Ghana.Email: doccletus@yahoo.com**EXOSOME-LOADED PLANT EXTRACT AS AN ANTI-OVARIAN CANCER DRUG
DELIVERY SYSTEM**

ABSTRACT: Exosomes are nanoparticles that play a crucial role in intercellular communication. This research investigated the role of exosome as drug carrier in ovarian cancer therapy. Exosomes were isolated by ultracentrifugation of blood from the liver. Morphology of exosome-plant complex was studied using scanning electron and atomic force microscopes. Under optimal conditions for cancer therapy, exosome-loaded plant extract showed higher anti-ovarian cancer efficacy such as reduced viable cell, high inhibitory concentration, induced apoptosis, and prevention of metastasis of cancer cells than doxorubicin anticancer drug. Our results showed that exosome-loaded anti-ovarian cancer plant extract is a promising nanosized drug formulation for ovarian cancer therapy.

Keywords: Exosome, nanoparticles, anti-ovarian cancer, plant extract.

1. Introduction

Exosome are cell-derived vesicles that are present in many and perhaps all biological fluids including blood, urine and cultured medium of cell cultures. They are a class of membrane secreted lipid vesicles formed intracellularly by invaginations of the multi-vesicular body limiting membrane and then fused out of the cell plasma membrane [1]. These small vesicles range from 30-100 nm and are of endocytic origin that were first proposed to function as a way for reticulocytes to eradicate the transferrin receptor while maturing into erythrocytes, were later named exosomes. As intercellular communicators, exosomes have received much attention as not only a basic natural characteristic, transporting mRNA and proteins among cells, but also a possible alternative to traditional nanoparticle approaches as drug delivery vehicles with certain advantages: **a.** biological and small drugs can be loaded into exosomes due to the natural presence of proteins and genetic materials; **b.** exosome derived drug delivery vehicles have broader distribution in biological fluids, likely producing longer circulating time and possibly better efficacy; **c.** Exosomes derived from tissue-specific cells can cross the physiological barrier and target the tissue via their natural surface proteins [2-4]. Exosomes potentially have advantages over polymer and liposome based nano-particle delivery systems, with a better safety profile and better selectivity [5].

The plant *Camelia sinensis* is a taxon of dicotyledonous flowering plants found in the tropics. In Nigeria, the plant is found in Ngoruje (Sarduana Local Government Area) Taraba State, where it is locally called "Tea" by the Fulanis, and used to produce the famous green tea by The Mambila Beverages Company Ltd, Kakara, Taraba State. This study was carried out to investigate the application of exosomes-loaded plant extract of *C. sinensis* as a carrier of anti-cancer drug in

cancer drug delivery system.

2. Materials and Methods**2.1 Materials**

The materials used in this study were: air-dried leaves of *Camelia sinensis*, ovarian cancer cell line, centrifuges model 800D, oven, buffer solution, Scanning Electron microscope, X-ray diffractometer, Bovine serum albumin, penicillin plus streptomycin solution GC-MS (Agilent 7820A), methanol (analytical grades), PBS solution, MTT reagent, CO₂ incubator, filter paper, scanning biological microscope, magnetic stirrer, among others.

2.2 Methods**2.2.1 Collection, identification, preparation and extraction of plant**

Fresh leaves of *C. sinensis* (Theaceae), were collected from Kankara, Sarduana Local Government Area, Taraba State, and was authenticated by a biologist Mr. C.A Ukwubile of Biology Unit, Department of Science Laboratory Technology, Federal Polytechnic Bali where a voucher number *THEA001* was deposited for the plant. The leaves were air-dried and reduced into fine powder using electronic blender. 2000 g of the powder was defatted in 2500 mL petroleum ether and then extracted with 5 Liters of methanol by Soxhlet apparatus. The filtrate was concentrated *in vacuo* using rotary evaporator at room temperature and further fractionated successively using solvents in increasing order of their polarities from the elutropic series. Final weight of methanol leaf extract was calculated. Fractions of extracts were bio-guided by anti-ovarian cancer activity *in vitro*. Fraction with best biological activity (anti-ovarian cancer) was used for the study. Purification of the compound was done using a 60 cm long glass column and 60-120 mesh size silica gel by step-wise gradient elution.

2.2.2 Isolation of exosome from whole blood

Serum was obtained from a freshly procured liver by squeezing the liver to release blood.



The blood was subjected to ultracentrifugation at 3000xg over night at 4⁰C to obtain serum containing exosomes [6].

2.2.3 Preparation of exosome- loaded plant extract (CE)

Exosome was dissolved in DEPC (diethylpyrocarbonate)-treated water to a final concentration of 0.88 mg/mL (stock solution). Purified plant extract from the construction reaction was diluted to 2 µm in DEPC treated water (pH 4.6). The Isolated extract solution was added to exosome solution to obtain the weight ratios of 4, 8, 16, and 32. The mixture was gently pipetted and vortexed for 3–5 s to initiate EX/PE complex formation and left for 30 min at room temperature. Complex formation was confirmed by gel electrophoresis [6].

2.2.4 Morphological studies of exosome-loaded plant extract

The morphology of exosome-plant complex was determined by an atomic force microscope (AFM) using tapping-mode AFM in air and scanning electron microscope [7-8].

2.2.5 Complex formation

Exosome was dissolved in DEPC (diethylpyrocarbonate) -treated water to a final concentration of 0.88 mg/mL (stock solution). Purified plant extract from the construction reaction was diluted to 2 µm in DEPC treated water (pH 4.6). The solution was added to exosome solution to obtain the weight ratios of 4, 8, 16, and 32. The mixture is gently pipetted and vortexed for 3–5 s to initiate complex formation and left for 30 min at room temperature. The complex formation was confirmed by electrophoresis.

2.2.6 Size and zeta potential measurement

The particle sizes and surface charge of the complexes was measured by photon correlation spectroscopy (PCS) using the Zeta sizer at room temperature. The complexes were diluted with phosphate buffer saline (PBS) pH 7.2 which was passed through 0.22 µm membrane filter prior used. All samples were measured in triplicate.

2.2.7 Morphology study of exosome

The morphology of exosome was determined by an atomic force microscope (AFM) using tapping-mode AFM in air. The complexes were diluted with distilled water which was passed through 0.22 µm membrane filter prior used. These samples were dropped immediately onto freshly cleaved mica and air-dried. Ovarian cancer cell line OV1063 was obtained. The cell line was maintained in suitable medium supplemented with 10 % fetal bovine serum and antibiotics (100 unit / mL penicillin and 100 mg / mL streptomycin), then incubated at 37 °C in a 5 % CO₂ incubator. At 24 hours

before transfection, the cells were added to a 96 well plate at a concentration of 2×10⁵ cells / well, then transfected with the complexes. Fresh medium was changed after transfection for 24 h and continued to culture for another 48 h.

2.2.8 Cytotoxicity

Evaluation of exosome complexes and standard anticancer drug doxorubicin cytotoxicity were performed by MTT assay, and using tadpoles. Tadpoles were scooped from ponds at Daniya Bali Local Government Area of Taraba State and was properly identified by Mr. Ukwubile Cletus Anes of Biology Unit. Ten tadpoles of similar sizes were selected with the aid of a broken Pasteur pipette into different beakers containing 30 mL of the natural water from the habitat of tadpoles. This was made up to 49 mL with distilled water. The mixture was made up to 50 mL with 20, 40, 100, 200 and 400 µg/mL of the leaf extract in 5% DMSO. The assay was performed in triplicate and a control assay was performed using 50 mL containing 1mL of 5% DMSO in distilled water. This procedure was repeated for three times [8].

2.2.9 Determination of antiproliferative effects on *Sorghum bicolor* (guinea corn) radicle length

Seeds of *S. bicolor* (Guinea corn) was purchased from Bali market in Taraba State. A simple viability test carried out by placing the seeds in distilled water. The viable seeds sank because of their denser embryonic tissues, unlike the non-viable seeds which floated and were therefore discarded. The floating seeds were decanted and separated from the viable ones. The viable seeds were washed with 95% ethanol for sterilization for 1 minute and were finally rinsed with distilled water. Ten (10) mL different concentrations of the leaf methanol extract (1-30 mg/mL) containing 5% DMSO was poured into the Petri-dish of about 9 cm wide containing filter (Whatman No.1) underlay with cotton wool, after which twenty (20) of the sterile Petri-dishes was incubated in a dark cupboard at room temperature and the lengths of the radicle emerging from the seeds was measured at 24, 48, 72 and 96 hours. The control seeds were treated with 10 mL distilled water containing 5% DMSO. The experiment was carried out in triplicates for all concentrations and controls while the radicle lengths was measured to the nearest millimeter. The procedure was carried out for both the leaf extract and the complexes.

2.2.10 Statistical analysis

The data obtained were expressed as mean ± SEM. Significant difference between means were determine at p≤0.05 (one-way ANOVA).

3. Results and Discussion

In Table 1, exosome-complex formulation showed percentage entrapment efficiency in dose dependent manner. This showed that the higher the percentage of entrapment efficiency of exosome, the better the therapeutic measures in the cell. In Table 2, the various kinetic equations used in order to understand the kinetic and mechanism of drug release from the in vitro studies showed that exosome-loaded drug exhibited a slow drug release at 0.8-1.0 and entrapment between 45.88 ± 0.1^a and 62.93 ± 0.01^b in concentration dependent fashion. This revealed that exosome as a nano-carrier for anticancer drugs does not show exponential release of its content thereby exposing potent drugs to enzymatic actions [9-10]. It then means that exosome offers distinct advantages that uniquely positioned them as high effective drug carriers composed of cellular membranes with multiple adhesive proteins on their surface, specialized in cell-to-

cell communication and provide an exclusive approach for the delivery of various therapeutic agents to target cells. In Table 3, exosome-loaded plant extract showed strong inhibitory efficacy on ovarian cancer cell line in concentration dependent manner, with CE I having the least IC_{50} value of 322.50 $\mu\text{g/mL}$ while CE V showed the highest inhibitory concentration of 550.12 $\mu\text{g/mL}$ on the growth of ovarian cancer cell. It is possible therefore, that exosome-loaded *C. sinensis* leaf methanol extract inhibited the growth of ovarian granulosa cells by correcting defective gene like FOXL2 and promoting apoptosis of the cell (Table 3). Therefore, the cell is devoid of metastasis of any kind [11]; showing the potential of exosome as a strong drug delivery system in cancer therapy. This result was comparable to the inhibitory effect showed by a first line anti-cancer drug doxorubicin at $p \leq 0.05$ (one-way ANOVA) that was delivered ordinarily (i.e. not in exosome)

Table 1. Formulation of exosome- loaded extract complexes (CEC)

Batch Code	Drug carrier ratio (mL)	Experimental weight (g)	% EE
CE I	1:1	161.5	45.88 ± 0.1^a
CE II	1:2	191.5	54.40 ± 0.1^a
CE III	1:3	201.5	57.24 ± 0.01^b
CE IV	1:4	211.5	60.1 ± 0.1^a
CE V	1:5	221.55	62.93 ± 0.01^b

Results are mean \pm SEM, n =3, numbers followed by the same alphabet are statistically significant at $p \leq 0.05$, CE (*C. sinensis*- exosome complex), EE (entrapment efficiency), % EE = (Experiment drug weight/ Theoretical drug weight) X 100.

Table 2. Correlation coefficients according to different kinetic equations

Formulation	Cumulative drug released (%)	Zero order	First order
FM1	84.31	0.8	1.0
FM2	82.7	0.9	1.0
FM3	75.30	0.8	1.0
FM4	73.01	0.8	1.0
FM5	70.02	0.8	1.0

FM1 – 5= formulation, zero order (cum drug released Vs time), first order (log % drug remaining Vs time)

Table 3 Growth inhibition assay of human ovarian cancer cell line OV1063

Sample code	Concentration ($\mu\text{g/mL}$)						IC_{50} ($\mu\text{g/mL}$)
	6.25	12.5	25.0	50.0	100.0	200.0	
CE I	2.11	2.51	4.12	17.20	24.20	30.11	322.50
CE II	3.13	5.00	6.17	22.00	30.11	42.10	400.10
CE III	4.22	8.12	10.00	25.00	32.01	45.02	405.12
CE IV	6.12	12.02	10.50	28.12	38.14	51.04	500.45
CE V	8.10	14.45	12.88	32.00	41.12	57.10	550.12
Do RuB	1.22	1.88	2.11	16.00	20.12	22.00	108.04

n = 3, Do RuB (doxorubicin anticancer drug), CE 1-V (*C. sinensis* – exosome formulations)

4. Conclusion

Cancer nanotechnology is on its way to accelerating early detection of ovarian cancer and improving therapy of resistant and recurrent cases. In order to enhance this further, training of bio-researchers is a must, and this will create additional interdisciplinary collaborative opportunities with their non-bio-researchers or

engineering colleagues to advance the field further into a direction of research that is disease oriented, and thus accelerate specific disease needed solutions. The study therefore, showed that exosome nanoparticles serve as effective and safe therapeutics in cancer therapy as drug carrier, and this research aspect should be sustained for cancer treatment.



Acknowledgement

The authors are grateful to Mr. Clement of the Department of Pharmaceutics and Microbiology, University of Ghana School of Pharmacy, College of Health Sciences, Accra, Ghana.

References

- Li, E, Zeringer, T., Barta, J., Schageman, A., Cheng, and Vlassov, A.V. (2016). Analysis of the RNA content of the exosomes derived from blood serum and urine and its potential as bio-maker. *Philosophical transactions of the Royal Society Biological Science*: 3-33.
- Basu, J., BLudlow, J.W. (2016). Exosomes for repair, Regeneration and Rejuvenation *Expert opinion on Biologic therapy*;3:34-40.
- Leiserowitz, G.S., Lebrilla, C., Miyamoto, S., An, H.J., Duong, H., Kirmiz, C., *et al.* (2008). Glycomics analysis of serum: a potential new biomarker for ovarian cancer? *International Journal of Gynecologic Cancer*; 18:470–475.
- Park, J.E., Tan, H.S., Datta, A., Lai, R.C., Zhang, H., Meng, W., Lim, S.K., Size, S.K. (2010). Hypoxic Tumor Cell Modulates its micro environment to enhance Angiogenic and metastatic potentials by secretion of proteins and exosomes. *Molecular and cellular proteomics*; 9(6): 56-67.
- Qin, J., Q.xu. Function and application of exosomes. *Acta Pol Phar.*2014: 71
- Shabbir, A., Cox, A., Rodriguez-menocal L., Salgodom. And Badiavas E. V. (2015). Mesenchymal stem cell exosomes induce proliferation and migration of normal and chronic wound fibroblast and enhance development; 24(14): 1635-1647.
- Alvarez-Erviti, L., Seow, Y., Yin, H., Betts, C., Lakhali, S., and Wood, M.S. (2011). Delivery of siRNA to the mouse brain by systemic injection of targeted exosomes. *Nat. Biotechnology*; 29(4):341-5.
- Vanderpole, E., Boing, A.N., Harrison P., Sturk A., and Nieuwland, R. (2012). Classification, function and clinical relevance of extracellular, vesicles. *Journal of Pharmacology*; 64(3): 676-705.
- Yeo, R., Lim, W.Y., and Lim, S.K. (2010). Exosomes and their therapeutic application in advances in pharmaceutical cell therapy: principle of cell-based; *Biopharmceutic*; 3(5):477-501.
- Kahlert, C., Kalluri, R. (2012). Exosomes in tumor microenvironment influence cancer progression and metastasis. *Journal of Molecular Medicine (Berl)*; 91: 431–437.
- Batrakova, E.V., Kim, M.S. (2015). Using exosomes, naturally-equipped nano-carriers for drug delivery. *Journal of controlled release*; 219:396-405.

**ABSTRACT CCT-: 009**

Lawal O. M.¹, Nwokem N. C.², Ukpong M.K.¹, Suleiman I.A.¹, Ozogu A.N.¹, Anyim P.B.¹, Daniel D.¹, Anakorchibuzor N.C.¹, Ibrahim S.U.¹, Suleimon M.A.

¹Department of Textile Technology, National Research Institute for Chemical Technology, Zaria

²Department of Chemistry, Ahmadu Bello University, Zaria

Email: olamilekanlawal17@yahoo.com

REMOVAL OF OIL FROM CRUDE OIL POLLUTED WATER USING MANGO SEED BARK AS SORBENT IN A PACKED COLUMN

ABSTRACT: A column study was conducted to evaluate efficiency of mango seed bark as a sorbent material in the removal of crude oil from crude oil polluted water. The study was carried out in a packed continuous column with initial oil concentration of 200 mg/L. The result showed that increasing the bed height of the packing from 5 – 25 cm resulted to an increase in percentage removal of the oil from 47.69 - 95.38 % at a constant contact time of 30 min and flow rate of 26.52 cm³/min and correlation coefficient of $R^2 = 0.92$. The study identifies mango seed bark as a suitable sorbent that can be used for continuous remediation of oil from crude oil polluted water. The maximum uptake of 190.77 mg/L oil was recorded at 25 cm bed height.

Keywords:

1. Introduction

Since the advent of crude oil exploration, spillage from oil fields has created serious environmental concern due to its hazardous nature and its eventual contamination of both the aquatic and terrestrial ecosystems. Oil is a naturally occurring substance. The organic residue from the decay of plant and animals are converted by heat and pressure into petroleum, migrating upwards, sometimes over extensive areas, either to reach the surface or be occasionally trapped in to become oil reservoirs. Oil is one of the most important sources of energy and is also used as raw material for synthetic polymers and chemicals worldwide. Oil has been a part of the natural environment for millions of years (Karan *et al.*, 2010). The methods commonly used to remove oil involve oil booms, dispersants, skimmers, oil pumping in-situ burning, bioremediation, solidifier and sorb

ents (Aliyu *et al.*, 2015). The main limitations of some of these techniques are their high cost and inefficient trace level adsorption. Also most of the dispersants are often inflammable and cause health hazards to the operators and potential damage to fish, and marine mammals. They can also lead to fouling of shorelines and contamination of drinking water sources. Removal of oil by sorption has been observed to be one of the most effective techniques for complete removal of spilled oil under ambient conditions. The use of sorbents is of great interest, as it allows the collection and complete removal of oil by achieving a change from liquid to semi-solid phase. The efficiency of an oil sorbent material is determined by properties, such as hydrophobicity, high uptake capacity, high rate of uptake, retention over time, oil recovery, reusability and biodegradability (Aliyu *et al.*, 2015). The sorbent materials in use for oil spill clean-up include organic natural ones and agro wastes, such as egg shell (Aliyu *et al.*, 2016), cassava peel activated carbon (Oghenejoboh *et al.*, 2016), mango seed kernel powder (El-Nafaty *et al.*, 2014), oil removal using banana peel

(Aliyu *et al.*, 2015), low grade raw cotton fibres (Hussein *et al.*, 2011), coconut fibre carbon (Egwaikhide *et al.*, 2007), hybrid peel waste of *Musa balbisiana* and *Citrus sinensis* preliminary study (Abdullah *et al.*, 2016) have already investigated. Since most oil products are biodegradable, oil could be disposed of for example by composting. A biodegradable material with excellent adsorption properties would be advantageous in this respect (Hussein *et al.*, 2011). In practice, clean up oil spill is a difficult economic problem. It is uneconomical to store large quantities of sorbent materials that are used to clean up oil spills and their disposal. The use of sorbents made from organic materials does not cause additional problems in the disposal of the spilled oil (Karan *et al.*, 2010).

This consideration therefore underlines the significance of establishing sorbent properties of locally available agro waste. Global production of mangoes is concentrated mainly in Asia and more precisely in India (number one producer in the world). Mangoes are grown in 85 countries and 63 countries provide more than 1000 metric tonnes a year. Total world production was 24,420,116 metric tonnes in 1999 with developing countries accounting for about 98% of total production (Yusuf and Salau, 2007). Despite lack of encouragement as to large scale production of tropical fruits in the country, Nigeria still occupies the 8th position in the world ranking of mango producing countries as at 2002. This is instructive as it suggests the potential of tropical fruit in Nigeria. The main producing states in the country include Benue, Jigawa, Plateau, Yobe, Kebbi, Niger, Kaduna, Kano, Bauchi, Sokoto, Adamawa, Taraba, and FCT (Yusuf and Salau, 2007). Therefore, there is need for an effective remediation process that will remove the oil spills from the water surface.



2. Materials and Method

2.1 Reagents

All reagents used were of analar grade and distilled water was used throughout the work

2.2 Apparatus and Equipment

Meter rule, Long glass column, pH meter (Jenway 3505, UK), Milling machine, Analytical balance (JD 400-3, UK), Hot oven (Mettler, Germany), Spectrophotometer (HACH DR/2400, USA), FTIR (SCHIMADZU 8400S, Japan), BET (V-sorb 2800P, China).

2.3 Sample Collection

The waste samples (mango seeds) were obtained in Basawa community, Zaria, Kaduna State. The crude oil was obtained from Kaduna refinery and petrochemicals, Kaduna State, Nigeria.

2.4 Sample Preparation

Preparation of Simulated Crude Oil Polluted Water

The simulated oil polluted water was prepared by adding 5 g of the crude oil into 25 L of distilled water in a 50 L plastic gallon and was shaken vigorously and stored for the sorption experiment.

2.5 Preparation of Sorbent Material

The waste samples (mango seeds) barks were removed manually and the bark was oven dried at 105 °C. It was then pulverized to finer particles, passed through a mesh of 300 µm particle size. The powdered bark was washed with distilled water severally to rid the sample of traces of impurities and dried in an oven at a temperature of 105 °C until constant weight. The dried powdered then was stored in glass bottle labelled as mango seed bark (MSB) sample.

2.6 Characterization of Sorbent Material

The functional groups present at the surface of

the mango seed bark (sorbent material) was determined using FTIR (SCHIMADZU 8400S, Japan) ranging from 4000-400 cm⁻¹, and surface area of the sorbent was determined using BET (Brunauer-Emmett-Teller) V-Sorb 2800P Surface Area Analyzer, China).

2.7 Sorption Experiment

The glass column was clamped vertically and a meter rule was also clamped beside it. The base of the meter rule and the column were at the same level. A perforated rubber cork was inserted at the bottom of the column. A plastic aspiration bottle containing the produced polluted water was placed above the column with a rubber tube connected to a valve and dropped into the column continuously (at rate previously determined). A beaker was placed below the column to collect the treated water. The column was packed with the sorbent material (mango seed bark) to a height of 5 cm. A control valve was slightly opened to allow the oil polluted water to flow into the bed and treated water was collected below the column using a beaker. The experiment was repeated for different bed heights of 10, 15, 20 and 25 cm respectively at a constant flow that was determined during the experiment. Each of the samples with respect to their bed heights was collected separately in a plastic sample bottle and labelled appropriately. The concentration of polluted oil adsorbed was then determined using a spectrophotometer (HACH DR/2400, USA).

3. Results and Discussion

Characterization of the Sorbent Material

The results of sorbent material characterization using FTIR and BET are presented in the figures 1 and 2 respectively

3.1 Characterization using FTIR

FTIR spectroscopy method was used to show the functional groups present on the surface of the sorbent material.

Wavenumber (cm ⁻¹)	Functional group
925	C-H bend aromatic
1030	C-O stretch
1200	C-O-C symmetric & ass stretch
1525	C=C-NO ₂ stretch
1625	C=C stretch aromatic
1700	C=O stretch
1707	C=O stretch
1725	C=O stretch
1750	C=O stretch
2075	C≡C stretch

From table 1 different functional groups were present on the material surface. The MSB was observed to have shift at 925 cm⁻¹ which was attributed to aromatic C-H bend, at 1030cm⁻¹ C-O stretch. At 1200 cm⁻¹ the peak was

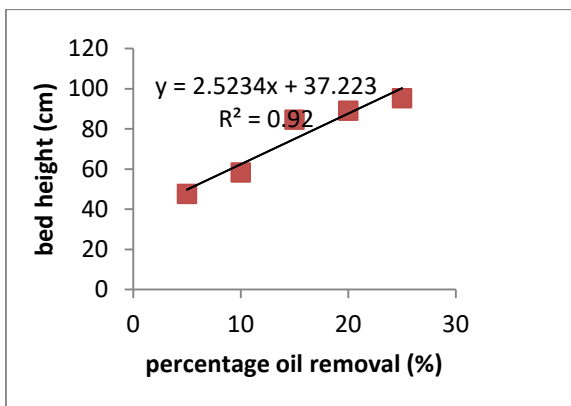
assigned to C-O-C symmetric and asymmetric stretch, while at peak 1525 cm⁻¹ was assigned to C=C-NO₂ symmetric. At 1625 cm⁻¹ was assigned to aromatic C=C stretch and at the MBS was observed to have shift between

1700-1750 cm^{-1} which was attributed to C=O stretch, while at 2075 cm^{-1} was as a result of C≡C stretching.

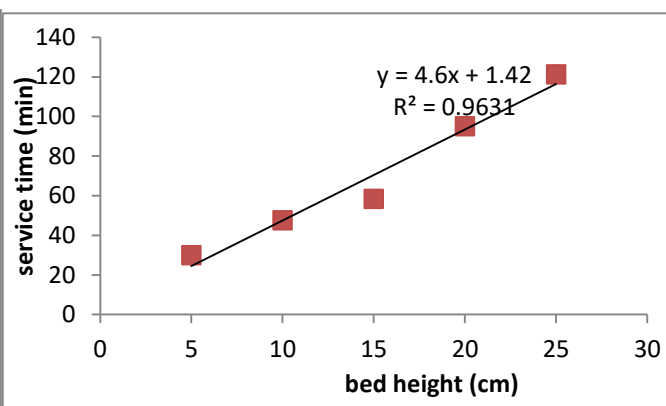
3.2 Characterization using BET

The surface area of MSB was measured using Brunauer Emmett Teller method.

The surface area of MSB was found to be 30.387848 m^2/g surface area measurement by Langmuir method revealed the area to be 62.201848 m^2/g with pore volume 0.008853 cm^3/g and a pore size of 1.165314 nm which was better than the values reported for egg shell by (Muhammad *et al.*, 2015).



Graph of Bed height against Percentage oil removal



Graph of Service Time against Bed Height

The breakthrough curves obtained for oil sorption on to adsorbent at different bed heights (5, 10, 15, 20 and 25 cm), at a constant flow rate of 26.52 cm^3/min and pH of 8.1 are shown in fig. 3. The results indicated that when bed height increased from 5 to 10 cm there was an increase in percentage removal of the adsorbent. The increase in the uptake of oil with the bed height was due to an increase in sorption sites for the oil removal. The optimum uptake which was 190.77 mg/L was found at the bed height of 25 cm. The plot of bed height against percentage oil removal is presented in fig. 3 which shows there is linearity between bed height and percentage oil removal which also supported that as bed height increases, percentage oil removal also increases. The correlation coefficient ($R^2 = 0.92$) from the plot also indicated linearity which is approximate to unity 1.

From the results obtained, it was observed that as the bed height increases the bed service time increases. This was due to the availability of sorbent sites for sorption to occur. The plot of service time against bed height in fig. 4 was used to calculate the values of sorption capacity of the bed No using equation (2) and bed depth service constant K_a was also calculated using equation (3). The values of N_o and K_a were found to be 920 mg/L and 0.0107 $\text{L}/\text{mg}/\text{min}$ respectively. The critical bed depth Z_o value was found to be 0.3086 cm.

4. Conclusion

Mango seed bark was used to remediate crude oil polluted water in a continuous manner. Effect of bed height was investigated from 5 to 25 cm, which revealed that oil removal and service time were increased with increase in bed height at 30 min contact time and flow rate of 26.52 cm^3/min . the mango seed bark sorption capacity was found to be 190.77 mg/L at 25 cm bed height, which shows that with increase in height of column also increased the quantity of the MSB thereby increasing sorption capacity because of the increased sorption sites. BDST model was used to predict the relationship between bed height and service time, which is essential in column process design and experimental data gave a fit to the BDST model.

References

- Abdullah M., Muhamad S.H., Sanusi S.N., Jamaludin S.I., Mohamad N.F. Rusil M.A. (2016) Preliminary study of oil removal using hybrid peel waste: musa balbisiana and citrus sinensis. Journal of Applied Environmental and Biological Sciences, Vol.6 (8S), pp.59-63.
- Aliyu U.M., El-Nafaty U.A., Muhammad I.M. (2015) Oil removal from crude oil polluted water using banana peel as sorbent in a packed column. Journal of Natural Sciences Research, Vol.5 (2), pp.157-162.
- Mohammed M.A., Shitu A., Tadda M.A., Ngabura M. (2014) Utilization of various agricultural waste materials in the treatment of industrial waste containing heavy metals: A review. International Research Journal of Environment Sciences, Vol.3 (3), pp.62-71.

**ABSTRACT CCT-: 043**

Oyegoke Toyese, Fadimatu Dabai, Jaju Abubakar Muhammed, and Baba El-Yakubu
Jibiril

Department of Chemical Engineering, Ahmadu Bello University Zaria, Nigeria

Email: oyegoketoyese@gmail.com

Process Modelling and Economic Analysis for Cellulosic Bioethanol Production in Nigeria

ABSTRACT: Waste, which includes the residue from agriculture, tends to be burnt or left in a form that amounts to an environmental nuisance, rather than converted into useful raw materials or products. The profitability of the conversion of agricultural waste into products is the essence of this research. In particular, this research examines the profitability of establishing a bioethanol plant in Nigeria, using waste (sugar cane bagasse) as feedstock. The proposed plant is to produce 143 million liters of fuel grade ethanol per annum from 402 metric tonnes of sugarcane bagasse. The research was undertaken with the aid of a process simulator (Aspen HYSYS) and computational software (MATLAB and Ms-Excel). The study showed the benefit/cost ratio, Net Present Worth (NPW), Pay Back Period (PBP) and Return on Investment (ROI) value(s) of 1.84, NGN 37.48 million, 6.90 years and 12.83 % respectively, which suggests that the plant will be feasible, based on the project parameters and assumptions adopted. Sensitivity analysis confirmed that the investment criteria were highly sensitive to change(s) in the cost of sugarcane and Government subsidy, and not very sensitive to change(s) in minimum wages and taxation

1. Introduction

Nigeria is a developing economy, with a land mass of 923,768 sq.km, and it is located in West Africa in the tropical region with latitude 10.0N and longitude 8.00E (Nwofe, 2014). In 2014, total primary energy consumption in Nigeria was about 4.8 quadrillion British thermal unit (Btu), as reported by the U.S. Energy Information Administration (EIA). Of this amount, traditional biomass and waste (typically consisting of wood, charcoal, manure, and crop residues) accounted for 74%, while oil, natural gas and hydropower accounted for 13%, 12% and 1% respectively. Thus Nigeria requires a huge amount of energy, which is mainly derived from biomass and waste.

Nwofe (2014) reported that the volume of wastes generated in Nigeria, on a daily basis, is quite enormous. These wastes, which include municipal wastes, organic wastes, and agricultural wastes, are usually disposed of using crude or primitive ways, such as open dumping. However, it is possible to convert these wastes into useful energy or products. One of such products is Bioethanol.

Bioethanol, a liquid biofuel, is known to be an oxygenated fuel that contains 35 % oxygen, which reduces particulates and NO_x emissions from combustion (Balat, 2007). It can be produced from sugary or starchy crops such as corn, sugarcane and sweet sorghum or from non-food sources, such as trees, grasses, bagasse, straws, groundnut shell, and maize cob (Cardona & Sánchez, 2007; Prasad, *et al.*, 2007). Its properties include a higher octane number, broader flammability limits, higher flame speeds and higher heats of vaporization (Balat, 2007) than gasoline. Therefore,

bioethanol fuel is an attractive alternative to gasoline (Hansen, *et al.*, 2005; Rebel, 2015).

This research focuses on establishing an economically viable way of converting Nigeria's agricultural waste, specifically sugarcane bagasse, into renewable liquid fuel known as Bioethanol. The research examines the material and energy requirement, plant capital cost, as well as the techno-economic viability of establishing the bioethanol production plant. A cellulosic biochemical process, with the aid of a process simulator (Aspen HYSYS V8.0) and computational software (Matlab 7.11.0), is employed for the research.

2. Method and Materials**2.1 Process Descriptions**

The production of bioethanol begins with a crushed and pretreated sugarcane feed, which is composed of cellulose, hemicellulose, lignin, sucrose, dextrose and water, as shown in Table 1. This composition is fed into a modelled plant. For the purpose of this research, it is assumed that the extracted sugar juice from the hydro-cyclones is sold off for sugar production, while the remaining bagasse is further processed, by hydrolysis in the presence of cellulase and xylanase (enzymes). After hydrolysis, the fermentable sugar produced were pretreated to meet the fermentation operating conditions and then passed to the fermenter, where the sugars were converted into bioethanol and carbon dioxide, in the presence of yeast (enzymes). The product was then purified in a flash, absorber and distillation columns.

Table 1: Feedstock Composition & Operating Conditions

Component Name	Value
Cellulose*	0.049
Hemicellulose*	0.046
Lignin*	0.026
H ₂ O	0.700
Sucrose	0.145
Dextrose	0.034
Temperature [C]	25.000
Pressure [atm]	2.000
Mass Flow [kg/h]	50,000.00

Adopted from: Juliana *et al.*, (2014), Felipe *et al.*, (2012) and Carolina *et al.*, (2012).

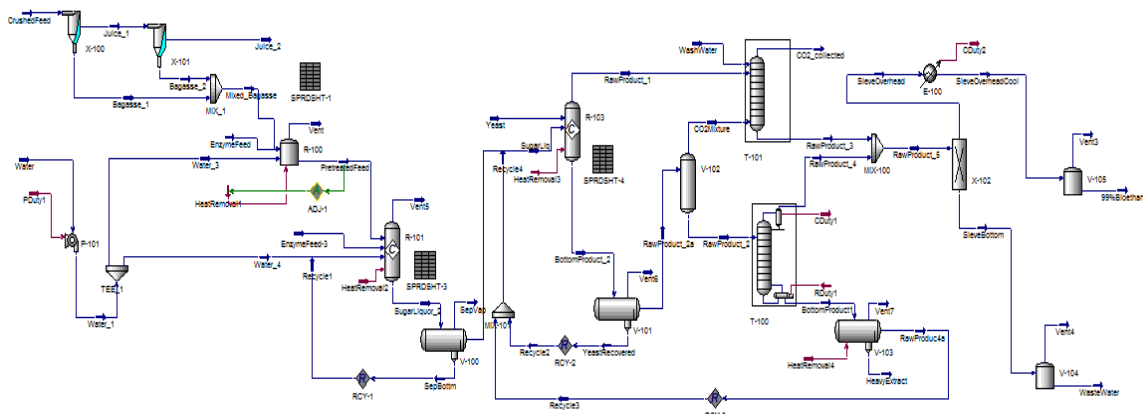


Fig 1: Process Flow Diagram for Bioethanol from Sugarcane Bagasse

2.2 Model Development

This research adopted a process simulation approach in modelling and simulating process flow (on Figure 1) for the production of bioethanol from sugarcane bagasse. Aspen HYSYS, being an efficient simulator with reasonable accuracy, was adopted. In modelling the process plant technology, the Non-Random Two-Liquid (NRTL) thermodynamic model was adopted as the fluid package. This model fits best to equilibrium because the components involved in the process have characteristics of polarity (like water and ethanol) and the vapour phase behaviour can be assimilated to that of an ideal gas due to the low operating pressures (1 – 5 atm) (Ruhul, et al., 2013; ProSim, 2009). The required binary interaction parameters that were not available in Aspen HYSYS were estimated with a predictive model found in the Aspen HYSYS fluid package (Oyegoke, 2016).

2.3 Process Economics

In order to evaluate the profitability of establishing a bioethanol plant in Nigeria, the proposed model and simulated process technology was subjected to economic assessment(s), using different economic cases, with the aid of Matlab 7.11.0 and Microsoft Excel 2016. The sensitivity of sugarcane price and exchange rate on the investment criteria for the production, were examined using One-Factor-At-Time (OFAT) design approach.

2.4 Cost Optimization Studies

The objective of this optimization studies is to minimize the cost of manufacturing. Some important variables, such as minimum wages, tax, sugarcane price and subsidy were selected, and a 2 by 5-1 fractional-factorial design of experiment was employed for the analysis.

3. Results & Discussion

3.1 Material and Energy balance

The material balance analysis, as shown in Table 2, shows that 14,163 kg/h (equivalent to 143 million liters per annum) of fuel grade bioethanol can be produced from 50,000 kg/h pretreated crushed feed of sugarcane, using 6,852 kg of enzymes per hour (to aid the breaking down of large molecules of sugar such as cellulose, hemicellulose and sucrose to monosaccharides) and 693 kg of yeast per hour (to convert the monosaccharides to bioethanol) at a moderate temperature of 303 K. The energy balance analysis, also shown in Table 2, confirms that hydrolysis reaction(s) of hemicellulose and cellulose, and fermentation reaction of monosaccharides are highly exothermic reactions, which release large amount(s) of heat.



Table 2: Results of Overall Plant Material & Energy Balance for the Flowsheet Summary

Inlet Material Streams	Mass Flow kg/h	Outlet Material Streams	Mass Flow kg/h	Inlet Streams	Energy Flow kJ/h	Outlet Streams	Energy Flow kJ/h
Yeast	693	Juice	793	Yeast	2.90E+03	CO ₂ collected	-4.54E+07
Enzyme Feed-3	3,538	CO ₂ collected	5,213	Heat Removal3	-1.70E+07	99%	-8.56E+07
Enzyme Feed	3,314	99% Bioethanol	14,163	Heat Removal2	-1.09E+08	Bioethanol Waste Water	-1.22E+06
Water	50	Waste Water	79	Heat Removal1	-5.20E+06	CDuty1	1.15E+09
Crushed Feed	50,000	Recycle1	35,121	PDuty1	4.43E+00	CDuty2	1.44E+07
Wash Water	72	Recycle4	2,297	Crushed Feed	-1.18E+07	Recycle1	3.69E+06
				Wash Water	-1.14E+06	Recycle4	-9.43E+06
				Heat Removal4	-8.93E+05	Juice_2	-6.27E+06
				RDuty1	1.16E+09		
Total Flow of Inlet Streams	57,666	Total Flow of Outlet Streams	57,666	Total Flow of Inlet Streams	1.02E+09	Total Flow of Outlet Streams	1.02E+09
		Error (%)	0.00			Error (%)	0.01

3.2 Economic Analysis

From the investment analysis carried out, it can be deduced that if the product sells for \$ 0.71 per liter at the exchange rate of 305 NGN per \$ and tax rate of 20% per annum, the revenue, gross income, net profit and return on investment will be \$ 103.99 million per annum, \$ 8.10 million per annum, \$ 6.48 million per annum and 12.83 % respectively. These values confirm that the project is feasible and profitable.

3.3 Cost Optimization Studies

Results show that the cost of production is

significantly dependent on the cost of sugar cane. Further statistical analysis, as shown in Table 3, shows that sugarcane (SG) and subsidy (SD) will contribute by 31% and 66% to the effects of optimizing the selling price of bioethanol, while factors such as wages and tax have insignificant effects.

Table 4 shows the optimum conditions for minimizing both the selling and cost price. The optimization studies show that it will be possible to sell bioethanol at 0.36 \$/L to 0.45 \$/L, provided the conditions stated in Table 4 are taken into consideration.

Table 3: Contribution of Different Factors on Selling Price (SP) and Cost of Manufacturing (CoM) per Liter

Term	Selling Price (SP)		Cost of Manufacturing (CoM)	
	Effect	% Contribution	Effect	% Contribution
A (SG)	0.22	31.06	0.26	100.00
B (WG)	0.00	0.00	0.00	0.00
C (SD)	-0.33	66.36	0.00	0.00
D (PF)	0.03	0.58	0.00	0.00
E (TX)	0.00	0.00	0.00	0.00

Table 4: Results of Optimization Studies for SP and CoM

SG	WG	SD	PF	TX	SP	CoM
12	18000	35	10	20	0.3578	0.5005



4. Conclusion

The simulation of the bioethanol plant shows that 143 million liters of fuel grade bioethanol requires 402 metric tonnes of crushed sugarcane bagasse. The economic analysis of the plant shows ROI of 12.8%, NPW at 10 % r of \$ 37.5 million, IRR of 12.1 %, B/C of 5.2, DBC of 1.8, PBP of 4.8 years and DPBP of 6.9

years. These suggests that the plant will be economically feasible and profitable. The study also shows under the following conditions, cost of sugarcane being as low as 12 to 15 NGN/kg, Government subsidy in the range of 20 % to 40 %, and a moderate tax rate of 20 % (maximum) on the Bioethanol being sold as fuel, Bioethanol can be sold for \$ 0.36 to \$ 0.45 per liter in Nigeria.

Abbreviations

n	= Project life	costs	NPW	= Net present worth	
NCF	= Negative cash flows	Ct	= Net cash inflow	NP	= Net profit
PCF	= Positive cash flows	r	= Discount rate	COM	= Total cost of manufacturing
PBP	= Payback Period	WG	= Minimum wages	IRR	= Internal rate of return
TCI	= Total capital investment	SG	= Sugarcane farm-gate price	B/C	= Benefit-cost ratio
DPBP	= Discounted payback period	SB	= Subsidy approval	DBC	= Discounted benefit-cost ratio
Co	= Total initial investment	TX	= Tax	NGN	= Nigeria naira
		PF	= Profit per sale		
		t	= number of time periods		
		ROI	= Return on investment		

References

- Atta A.Y., Aminu, M., Yusuf N., Gano Z.S., Ahmed O.U. and Fasanya O.O., 2016. *Potentials of Waste to Energy in Nigeria*, *J. of Applied Sc. Res.* 12(2):1-6.
- Christiana, O., and Eric, C.O., 2013. Economic Feasibility of On-farm Fuel Ethanol Production from Cassava, *Afri. Journal of Biotechnology*, 12(37):5618-5626.
- Diep, N.Q., Fujimoto, S., Yanagida, T., Minowa, T., Sakanishi, K., Nakagoshi N., and Tran X.D. (2012). Comparison of the Potential for Ethanol Production from Rice Straw in Vietnam and Japan via Techno-economic Evaluation, *International Energy Journal*, 13(2012):113-122.
- Felipe F.F., Renato T.F., Fabio H.P., Caliane B.C., Antonio J.G., Raquel C.G., Roberto C.G., 2013. Bioelectricity versus Bioethanol from Sugarcane: Is it worth being flexible, *Biotechnology for Biofuel*, 6:142(1-2).
- Gavin T., Ray S., 2008. *Chemical Engineering Design: Principles, Practice and Economic of Plant and Process Design*, Butterworth-Heinemann, London, UK, p.297-392.
- Hahn-Hägerdal B., Galbe M., Gorwa G.M.F., Lidén G., Zacchi G., 2006. Bioethanol - the fuel of tomorrow from the residues of today, *Trends Biotechnology* 24, 549-556.
- MBG, 2013. *Proposal Report on Production of Bioethanol from Sugarcane Bagasse*, Australian Renewable Energy Agency.
- Nwofe, P.A., 2014. Utilization of Solar and Biomass Energy, *Int'l J. of Energy & Env. Res.*, 2(3):10-19.
- Outlaw, J.L., Luis, A.R., James, W.R., Jorge, S., Henry, B., and Steven, L.K. 2007. Economic of Sugar-based Ethanol Production and Related Policy Issues, *Journal of Agricultural and Applied Economics*, 39(02):357-363.
- Oyegoke, T., 2016. *Techno-economic of Bioethanol Production in Nigeria*, Unpublished MSc Dissertation, Chemical Engineering Department, ABU Zaria.
- Prasad S., Singh A., Joshi H.C., 2007. Ethanol as an alternative fuel from agricultural, industrial and urban residues, *Resource Conservation Recycle* 50:1-39.
- Richard T., Richard C.B., Wallace B.W., Joseph A.S., Debansu B., 2012. *Analysis, Synthesis and Design of Chemical Processes*, Prentice Hall International, Pearson Education, Inc., New Jersey, Fourth Edition.
- Ruhul Amin M., Saquib H.M., Sarker M., 2013. Simulation of Ethanol Production by Fermentation of Molasses, *Journal of Engineering (JOE)*, 1(4):69-73.
- US Energy Information Administration (EIA), (2014). Nigeria's total primary energy consumption, 2014. Traditional solid biomass and waste data: International Energy Agency, *World Energy Statistics*, <http://www.eia.gov/beta/international/analysis.cfm?iso=NGA>, Accessed on 23 June, 2017

**ABSTRACT CCT-: 056**

Usman D. Hamza, Jibril Mohammed, Idris Muhammad Misau and Yakubu Dauda

Department of Chemical Engineering, AbubakarTafawa Balewa University, PMB 0248 Bauchi, Bauchi State, Nigeria.

Email: dhusman@atbu.edu.ng**Methylene Blue Removal from Wastewater Using Orange Peel Adsorbent**

ABSTRACT: Various industries use dyes to colour their products. Wastewater release from the dye associated industries has negative consequences on the ecosystem. In this study, orange peel was modified with sodium hydroxide for use as an adsorbent for the removal of methylene blue dye from prepared wastewater. Effect of contact time and initial dye concentration were studied. Equilibrium Batch adsorption studies was carried out using dye initial concentration of 100 to 500 mg/L. The adsorption capacity and efficiency of the NaOH modified orange peel was obtained for the various samples prepared. The experiment was carried out at pH = 7 at time between 30 to 90 min. The results showed that modified orange peel adsorbent has the methylene blue MB removal efficiency of 80 % at pH = 7 and 90 minutes.

Keywords: Adsorption, Orange Peel, Methylene blue, Wastewater, Dye

1. Introduction

Dyes are used by various industries such as paint, textile, leather, paper and plastics industries in order to colour their products. Most of the dyes are recalcitrant and completely resistant to biodegradation processes (Demirbas, 2009). The presence of even little amounts of dyes in water (less than 1ppm for some dyes) is highly visible and undesirable (Crini, 2006). Most of the methods employed in dye removal from wastewater are costly, ineffective or very slow. However, adsorption is inexpensive, very effective and versatile in dyes removal from wastewater (Velmurugan et al. 2011). Activated carbon is the most commonly used adsorbent material used for contaminants removal due to its versatility and high adsorption efficiency, but its cost and difficulty in regeneration prompted researches to look for alternatives. Low-cost adsorbents (LCAs) materials have proven to be effective and a number of them offer promise for the future. LCAs from agro-waste are renewable and abundant natural resources, which are currently under-utilized (Gupta et al. 2009). In this research work, orange peel was used as low cost adsorbent material for adsorption of methylene blue.

2. Methodology**2.1 Adsorbent Preparation**

Waste orange peel was obtained from a local orange seller in Bauchi. The peels were washed with water followed by cleaning with distilled water to remove dust particles and water-soluble impurities. After that, they were cut into small pieces, dried in sunlight for two days and further dried in an oven at 105°C for 24 h. The dried peels were crushed into smaller particles and then packed in airtight container. For the modified adsorbent, the crushed orange peel was treated with 20% (w/v) sodium hydroxide solution for 5 minutes, then filtered and dried before use.

2.2 Dye Wastewater Preparation

The dye was dissolved in distilled water to prepare the stock solution (1000 ppm). The resulting solution required were obtained by successive dilutions. The pH and ionic strength of the working solutions were adjusted to the required pH and ionic strength by adding appropriate amounts of acetic acid solution and NaOH solution. A pH meter was used for all pH measurements. Dye concentration was determined by using absorbance values measured before and after the treatment, at 650 nm with UV Visible Spectrometer.

2.3 Equilibrium Adsorption

Batch adsorption was used to study the adsorption equilibrium of the dye adsorption. For each set, 100 mL of dye solution of known concentration and pH was added to 0.2 g of the adsorbent material and then transferred to 250 ml flask. The solution was stirred in a rotary orbital shaker at 150 rpm. Samples solutions were withdrawn from the flask at predetermined time intervals. Solution were filtered out, optical density measurement was carried out using UV Visible Spectrometer at maximum wavelength of 650 nm. The final dye concentration of dye was obtained using the calibrated absorbance data. The adsorption experiments were performed at different time intervals (15, 30, 45, 60, 75 and 90 min).

The amount of dye adsorbed per gram of adsorbent (qe) is given by Eqn. 1:

$$q_e = \frac{V}{m} (C_0 - C_e) \quad (1)$$

The percentage of dye removal (R) was calculated using Eqn. 2.

$$\%R = \frac{(C_0 - C_e)}{C_0} \quad (2)$$

Where, C_0 and C_e are the initial and final equilibrium concentration, V is the volume of the dye solution and, m , is the mass of the adsorbent (g).

3. Results and Discussion

The percentage of dye removal is highly dependent on the initial amount of dye concentration. Figure 1 shows the percentage of MB removal at different initial concentration and time. Initial Concentrations of 100, 200, 300, 400 and 500 mg/L were used in the experiment at various times. The percentage of MB removal was in the range of about 20 to 80%. There is decrease in percentage dye removal with increase in initial dye concentration. The low removal percentage at high concentrations is due to the saturation of adsorption sites (Kaouah et al., 2013). This is similar to what was observed previously by other researchers (Kaouah et al., 2013).

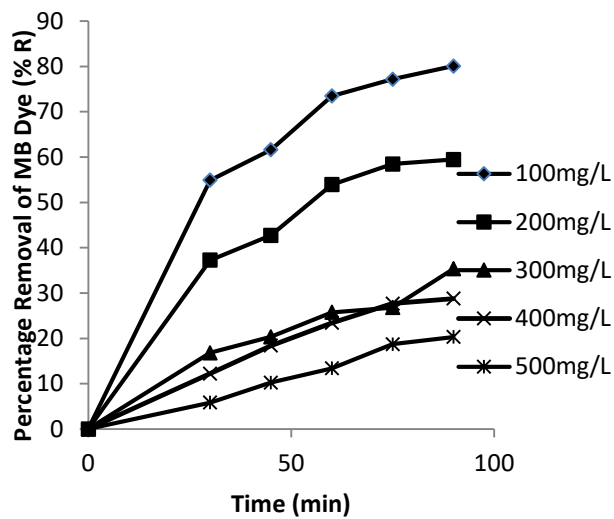


Figure 1: Effect of initial Dye Concentration on Percentage Removal of MB at Different Times

4. Conclusions

From this study, the removal of methylene blue dye from aqueous solution of modeled wastewater by adsorption using orange peels was studied. The uptake of methylene blue increased with increase in contact time. Adsorption equilibrium was reached in about 60 min. There was increase in percentage methylene blue removal with decrease in initial dye concentration. The percentage of MB removal was about 80% for initial dye concentration of 100 mg/L. This work shows that low cost adsorbent such as orange peel adsorbent is an alternative material for dye removal from wastewater.

References

- Demirbas, A. Agricultural based activated carbons for the removal of dyes from aqueous solutions: A review. *Journal of Hazardous Materials*, 167 (2009), 1–9.
- Gupta, V.K., Carrott, P.J.M., Ribeiro, M.M.L., Carrott & Suhas. Low-Cost Adsorbents: Growing Approach to Wastewater Treatment—a Review. *Critical Reviews in Environmental Science and Technology*, 39:10, (2009), 783-842.
- Kaouah, F., Boumaza, S., Berrama, T., Trari, M. and Bendjam, Z. Preparation and characterization of activated carbon from wild olive cores (oleaster) by H₃PO₄ for the removal of Basic Red 46. *Journal of Cleaner Production*, 54 (2013), 296-306.
- Lata, H., Gark, V.K. and Gupta, R.K. Removal of a basic dye from aqueous solution by adsorption using *Partheniumhysterophorus*: An agricultural waste. *Dyes and Pigments*, 74 (2007), 653-658.
- Velmurugan P., Rathinakumar.V, Dhinakaran G. Dye removal from aqueous solution using low cost adsorbent. *International Journal of Environmental Sciences*, 1:7, (2011), 1492-1503.

**ABSTRACT CCT-: 046**

Apampa, Sulaiman Ayodeji

Department of Chemistry, Federal College of Education, Zaria.

Email: ayodejialal2000@gmail.com**REDUCE, REUSE AND RECYCLING OF WASTE FOR SUSTAINABLE ECONOMY:
A CASE OF ALUM FROM ALUMINUM CANS.**

ABSTRACT: Reduce, Reuse and Recycling of unwanted materials is a key component of environmental sustainability, economic diversification and self-reliance. Reducing the amount of items bought is the most significant of all the options to manage waste. The numerous environmental and economic advantages from recycling process is overwhelming as it creates more jobs than the landfilling industry, saves energy, reduces pollution, greenhouse gas emissions and conserves virgin resources. Aluminium recycling is the process through which scrap aluminum is reprocessed to be used in products after its initial production. Modern beverage containers are usually composed of Aluminium in the form of aluminium cans which can be recycled. This paper describes a chemical process that would be used to transform scrap aluminium cans into a useful chemical compound, potassium aluminium sulphate dodecahydrate, $KAl(SO_4)_2 \cdot 12H_2O$, usually called alum. Alum is widely used in the dyeing of fabrics, in the manufacture of pickles, as a coagulant in water purification and waste-water treatment plant and in the paper industry, just to mention a few. The growing concern about the depletion of aluminium from its ores has necessitated this study vis-à-vis the major concern on the amount of energy needed to extract aluminium. The protection of our environment and the stability of our nation's economy through the application of the three R'S is highly recommended

Keywords: Reduce, Reuse, Recycling, Aluminium can and Alum

1. Introduction

Reduce, Reuse and Recycling of materials that would otherwise be discarded is a key component of environmental sustainability, economic diversification and self-reliance. Reducing the amount of items bought is the most significant of all the options to manage waste, and a careful look at things we are throwing away (Fahzy Abdul-Rahman, 2014) will definitely reinvigorate an idea that they are materials that can be reused to solve everyday problems and satisfy everyday needs. The numerous environmental and economic advantages from recycling create more jobs than the landfilling industry, save energy and reduce pollution (Dara, 2000). Also, it greatly reduces greenhouse gas emissions, including harmful methane thereby conserving resources for future generations. Aluminium recycling is the process through which scrap aluminum is reprocessed to be used in products after its initial production (Ugwekar and Lakhawat, 2012). Modern beverage containers are usually made from aluminium cans which can be recycled. This paper describes a chemical process that would be used to transform scrap aluminium cans into a useful chemical compound, potassium aluminium sulphate dodecahydrate, $KAl(SO_4)_2 \cdot 12H_2O$, usually called alum with 25% recovery. Alum is widely used in dyeing, manufacture of pickles, as a coagulant in water purification and waste-water treatment plant etc. The growing concern about the depletion of aluminium from its ores has necessitated this study vis-à-vis the major concern on the amount of energy needed to extract aluminium.

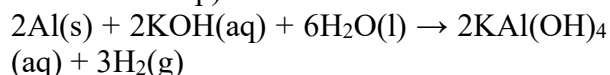
2. Materials and Method

The first part of this experiment was to cut the cans into pieces and then dissolve the cans in 1.5 M of potassium hydroxide by placing both in a beaker and placing it on a hot plate heated

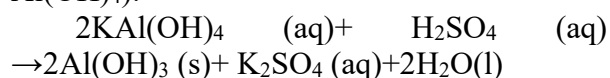
to a temperature of 250° C. Once the solution started to bubble vigorously, it was removed from the hot plate and continually stirred to dissolve all of the aluminum can. The solution turned a grey/black color. During this process, hydrogen gas is released (Ugwekar and Lakhawat, 2012). Once the aluminum was fully dissolved, the solution was filtered through a Buchner funnel lined with filter paper, which removed the undissolved plastic lining and paint that was present from the aluminum can. The filtrate was then transferred into a beaker and 20 mL of 9M sulfuric acid was added to it. This solution was then placed in an ice bath for about 15 minutes, to allow the solution to produce white crystals, which are the alum.

While the crystals were forming, the filter paper from the draining was rinsed through the Buchner funnel using water, to collect the paint and undissolved plastic in a pile and weigh using an analytical balance. From the stoichiometry of the reaction, one mole of Aluminium metal will give one mole of Alum. Hence, from the number of moles of product, the mass of product (also known as the theoretical yield) is given as number of moles of alum x molar mass of alum (g/mol). The percentage yield is obtained by dividing the actual yield of the alum (g) by the theoretical yield and multiply by 100. The equations below show the complete sequence of reactions involved in the experiment.

Reaction of aluminum with KOH (the dissolution step):

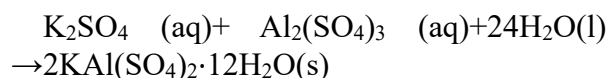
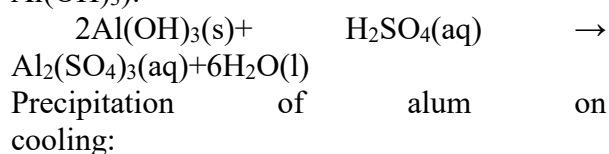


Initial addition of sulfuric acid (precipitation of $Al(OH)_4$):





Further addition of sulfuric acid (dissolving of $\text{Al}(\text{OH})_3$):



3. Results & Discussion

Reusing saves money, conserves resources and gives an assurance of a sustainable environment. Less energy is required to process alum from recycled aluminium cans than to process alum from aluminium ores. Saving energy has its own benefits as it decreases pollution, creates less environmental hazards and encourages economic diversification for better output (Sharma and Sharma, 2007). The method used for the recycling of the aluminium cans was found to be suitable for using the waste material and turning it into useful chemical, alum. The

process can be integrated with the plant where lot of Aluminum scrap gets generated or as the use of aluminum cans for soft drinks are increasing, the subsequent waste can be handled effectively by this process.

4. Conclusion

Aluminum recycling is important to the environment and the people all over the world as it opens window for diversifying the economy and produces an avenue for job opportunities.

References

- Dara S.S., (2000). "A textbook of Environmental chemistry and Pollution Control". S. Chand Publication, pp 97-164.
- David A. Katz (2000). Alum from Waste Aluminum Cans. www.chymist.com
- Fahzy Abdul-Rahman (2014): Reduce, Reuse, Recycle: Alternatives for Waste Management. Retrieved from www.aces.nmsu.edu on 23/06/17. pp1-3
- Sharma. A, Sharma C, and Sharma A.K. (2007). Characteristics and Management of Medical Solid Waste. *Indian Journal of Environmental Protection*. 27(10): 897-904
- Uqwekar, R.P and Lakhawat, G.P (2012). Potash Alum from Waste Aluminum Cans and Medicinal Foil. *IOSR Journal of Engineering (IOSRJEN)*. 2(7), 62-64. www.isosrjen.org.

**ABSTRACT CCT-: 059**¹OSIGBESAN A. A., ²ABUBAKAR Y. W., ¹FASANYA O., ¹ATTA A.Y., ²DABAI F.N. AND ²JIBRIL B.Y.¹Petrochemicals and Allied Department, National Research Institute of Chemical Technology, Zaria²Department of Chemical Engineering, Ahmadu Bello University Zaria, NigeriaEmail: aishatosigbesan2011@gmail.com**A PROMISING CONCEPT OF WASTE MANAGEMENT THROUGH PYROLYSIS OF LOW DENSITY POLYETHYLENE**

ABSTRACT: Waste management has been a topic of concern among researchers and this has led to the research into various methods of managing them. Pyrolysis otherwise known as thermal decomposition of waste polymeric materials is a renowned technology that is gaining popularity among researchers. This process helps to reduce the environmental menace caused by the conventional methods of waste disposal which include incineration and land filling. Waste low density polyethylene in the form of water sachets was collected from households over time, dried and shredded in preparation for pyrolysis. A measured weight of the waste Low Density Polyethylene (LDPE) was fed into the reactor for the pyrolysis to take place at temperatures above 350°C. The products of the pyrolysed waste LDPE which include the condensable gases and the non condensable gases were collected in their different collectors. The residue otherwise known as char was also collected. The liquid product also known as pyrolysis oil was analysed using analytical instruments such as GC-MS and FTIR. The analysis shows that the hydrocarbon components present in the oil are C9 to C25 which are in forms of aliphatics, aromatics, esters and alkanolic acids.

1. Introduction:

Global population growth is eminent to inspire high energy demands and waste generation [1, 2]. Though researches are ongoing to scale up energy source to meet this demand, promising concepts dedicated to reducing specific waste implication of population growth are scarce. The available ones are rather not adequate to profile waste management for specific waste generated. On the account of Nigerian waste generation context, about 32 million tons of solid wastes are been generated annually [3, 4]. These include plastics, Municipal Solid Wastes, etc. [5]. Plastics which amount to 33.3% unlike other classifications have very stringent impact on environmental health; it can clog underground water pipe, suffocate useful organism, etc [1]. While allowing plastics to roam in the environment is not a good option, most research proliferations are still at their infancy stage. So, at this moment one cannot broadly say that waste management concept is fully implementable.

Many approaches have been used for waste management process. This include anaerobic digestion, pyrolysis, etc [6, 7]. The former is concerned with a fermentation process [8] while the latter employs thermal decomposition techniques [9].

This work is limited to the pyrolysis of waste water sachets and analysis of the liquid product

otherwise known as pyrolysis oil.

2. Materials and Method**2.1 Materials:**

Water sachets, glass wool, 1000ml three necked round bottom flasks (RB flask), rubber corks, condenser, chiller, nitrogen gas, 250ml three necked round bottom flask for liquid collection and gas bags for gas collection. The set up was arranged as shown in figure.

Weighing balance, heating mantle, drying oven, sample bottles are required equipment. Analytical equipment required include the GC-MS and FTIR for the analysis of the products.

2.2 Methodology:

Waste LDPE in form of water sachets were collected from households, dried and shredded. 50g of the waste LDPE was measured using the Shimadzu UW2200H model weighing balance and fed into the 1000ml RB flask. The system was purged using nitrogen gas for about 1 minute to create inertness for the pyrolysis process. The LDPE was heated up as shown in the set up in figure at a heating rate of approximately 4°C to a temperature of 450°C being the limit of the heating mantle with respect to the feedstock. The temperature of the reaction was monitored using a K type thermocouple. The evolving gases which included the condensable and the non condensable gases were collected in a 250ml RB flask and gas bags

3. Results and Discussion:
Table 1: GC – MS analysis of the pyrolysis oil.

S/No.	Structural Formula	Molecular Formula	Nomenclature	Remark
1		C ₉ H ₂₀	nonane	alkane
2		C ₉ H ₁₈	nonylene	alkene
3		C ₁₀ H ₂₀	octene	aromatic
4		C ₁₀ H ₂₂	octane	aromatic
5		C ₁₂ H ₂₄	dodecene	aromatic
7				aromatic
8		C ₁₃ H ₂₆	Tridecene	aromatic
9		C ₁₄ H ₂₈	tetradecene	aliphatic
10		C ₁₁ H ₂₂	cyclopropane	aromatic
11		C ₁₂ H ₂₄	cyclododecane	aromatic
12		C ₁₃ H ₂₆	cyclotridecane	aromatic
13		C ₁₄ H ₂₈	cyclotetradecane	aromatic
14		C ₁₅ H ₃₀	cyclopentadecane	aromatic
15		C ₁₇ H ₃₄ O ₂	Pentadecanoic acid	Alkanoic acid
16		C ₈ H ₆ O ₂	P-formylbenzoic acid	Aromatic acid
17		C ₂₀ H ₂₆ O ₄	Phthalic acid	Alkanoic acid
18		C ₂₅ H ₄₈ O ₂	15-tetracosenoic acid, methyl ester	ester
19		C ₂₃ H ₄₄ O ₂	13-docosenoic acid, methyl ester	ester

20		9- octadecenoic acid, methyl ester	C19H36O2	ester
21		10-dodecenol	C12H24	alkanol
22		1-Docosene	C22H44	aliphatic

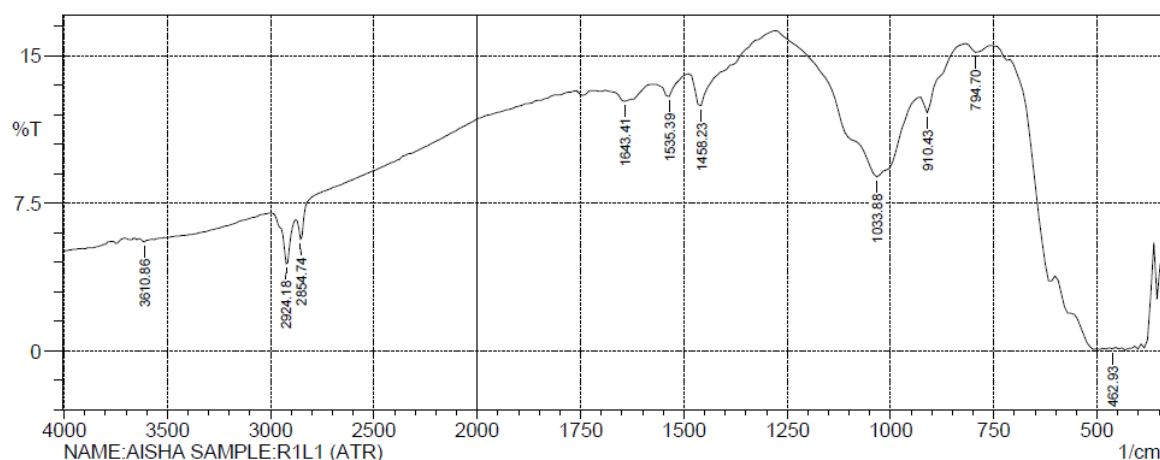


Figure 1: FTIR spectra of the pyrolysis oil sample.

Table 2: Wavebands with corresponding peak assignments from the FTIR spectra.

S/No	Wavebands (/cm)	Type of vibration	Associated functional group
1	910	C – H bending	Alkane
2	1033.88	C – H bending	Alkane
3	1458.23	C = C stretching	Aromatic fingerprint
4	1535.39	C = C stretching	Aromatic fingerprint
5	1643.41	C = C stretching	Aromatic ring
6	2854.74	C – H stretching	Alkyls, Aliphatics
7	2924.18	C – H stretching	Alkyls, Aliphatics
8	3610.86	O – H stretching	hydroxyl

Table 1 shows the various components detected by the GC – MS analysis ranging from few aromatics [C9 – C12], aliphatics [C13 – C25], esters and alkanolic acids. This is in conformity with the FTIR analysis described by table 2 and figure 1.

4. Conclusion:

In this study, the concept of waste management using pyrolysis of waste water sachets was investigated. 50grams of the waste water sachets was pyrolysed and approximately 43grams of the oil was produced which is 86%w/w yield. The pyrolysis oil was analysed and it was evident from the result that it consists of aliphatics, aromatics, esters and alkanolic acids. This oil can be treated to produce usable fuel which can help in reducing the increasing energy demand by the growing population.

References:

Hasanuzzaman, M., et al., *Global electricity demand, generation, grid system, and renewable energy polices: a review*. Wiley Interdisciplinary Reviews: Energy and Environment, 2017. **6**(3).
 Wiens, J.A., *Population growth. Ecological Challenges and Conservation Conundrums: Essays and Reflections for a Changing World*, 2016: p. 105-108.
 Coker, A., et al., *Solid Waste Management Practices at a Private Institution of Higher Learning in*

Nigeria. Procedia Environmental Sciences, 2016. **35**: p. 28-39.

Pour Rahimian, F., et al., *Review of motivations, success factors, and barriers to the adoption of offsite manufacturing in Nigeria*. Procedia Engineering, 2017.

Maya, D.M.Y., et al., *Gasification of Municipal Solid Waste for Power Generation in Brazil, a Review of Available Technologies and Their Environmental Benefits*. J. Chem, 2016. **10**: p. 249-255.

Kamali, M., et al., *Anaerobic digestion of pulp and paper mill wastes—An overview of the developments and improvement opportunities*. Chemical Engineering Journal, 2016. **298**: p. 162-182.

Baeyens, J., et al., *The production of bio-energy by microbial (biogas through anaerobic digestion) or thermal (pyrolysis) processes*. Renewable Energy: An International Journal, 2016. **96**: p. 1055-1055.

Gubicza, K., et al., *Techno-economic analysis of ethanol production from sugarcane bagasse using a Liquefaction plus Simultaneous Saccharification and co-Fermentation process*. Bioresource technology, 2016. **208**: p. 42-48.

Hamidi, N. et al., 2013. Pyrolysis of Household Plastic Wastes. *British Journal of Applied Science & Technology*, 3(3), pp.417–439.

**ABSTRACT CCT-: 069**

EDOKPAYI O.; FADILAT S. A.; OGBEIDE S. E.

Department of Chemical Engineering, Faculty of Engineering, University of Benin

Email: edokpayi.osariemen@uniben.edu**ADSORPTION OF METHYLENE BLUE FROM A SYNTHESIZED INDUSTRIAL WASTEWATER IN A BATCH SYSTEM USING ACTIVATED CARBON FROM COCONUT SHELL**

ABSTRACT: The use of synthetic chemical dyes in industries have increased considerably over the years resulting in dye contaminating aquatic ecosystems and industrial effluent. This research is aimed at using coconut shell in the adsorption of methylene blue from a synthesized industrial wastewater in a batch system. Azo dyes are known to cause serious irritation to the eye, skin and respiratory system. Coconut shell was processed into activated carbon by carbonizing at 600°C and activated with 3.0 M H₃PO₄ at 80°C for 3 hours. Synthetic solutions of methylene blue were prepared and the adsorption process was carried out by varying initial dye concentration; adsorbent dosage and contact time. The final solution in all the samples were analyzed using the visible spectrophotometer. The results showed the best removal efficiency of 83.53% for 2g of coconut shell and this occurred at an initial dye concentration of 50mg/L at 120 minutes. The adsorption of coconut shell which followed Langmuir isotherm model with R² value of 0.9772, while the adsorption kinetics study was best described by Lagergren pseudo first-order kinetics. It was concluded that, coconut shell is a good adsorbent in the adsorption of methylene blue, therefore coconut shell can be used as a low cost adsorbent in waste water treatment.

1. Introduction

This study was conducted to determine the adsorption of dispersed Azo Dye using activated carbon of coconut shell. Due to their chemical structures, dyes are resistant to fading on exposure to light, water and many chemicals, therefore, are difficult to be decolorized, once released into the aquatic environment. (Mckay et al., 1979; Poots and McKay, 1996). Azo Dyes are dyes with -N=N- azo structure. They are commonly used in Textile Industries. Since most dyes are toxic in nature, their presence in industrial effluent causes Environmental pollution, as they are very recalcitrant to microbial degradation (Pagga et al, 1986). Due to this, Industrial waste water needs to be treated before sending it to water bodies in order to minimize Environmental Pollution, this can be done using Activated Carbon (charcoal), which can be obtained from carbonaceous source materials by Adsorption.

2. Materials and Methods

Coconut shell was obtained from a Local Coconut candy seller at Oba market, Ring Road Benin City. Orbital shaker, Stuart SSLIS at rotating 250rpm; GallenKemp furnace made in Japan; Tyler series Mesh sieve; Gellenkamp Oven; Pyrex Calibrated pipette B.S. 604 Made in England; Digital Weight Balance make Adventure OHAUS, Corporation AR2130. All reagents used in this experiment were of Analytical grade.

2.1 Preparation of Activated Carbon from coconut shell.

The coconut shell was washed with portable water to remove dust, colour, and impurities. Rinsed with distilled water, then oven dried at 110°C for 3hrs. The sample was carbonized and activated. The pretreated

coconut shell sample was kept in a crucible, which was placed at the center of a 40 mm tubular furnace. The pretreated Coconut Shell sample was heated from ambient temperature to the carbonization temperature of 600°C for one hour and these was repeated for subsequent carbonation of this sample. The sample was then allowed to cool to ambient temperature in presence of N₂ flow. The carbonized samples were sieved using a 30mesh sized sieve to obtain a particle size of 0.6mm and stored in sealable air-tight plastics. The carbonized sample of coconut shell was activated using 200g of coconut shell in 400ml of 3.0M of H₃PO₄ for 4 hours. Then it was filtered and pH was checked, to obtain a slightly acidic pH of 6.2. The washed sample was dried at 120°C for 4hrs. The crushing process is required to crush or refine the activated carbon produced. The carbonized samples were sieved using a 35mesh sized to obtain a particle size of 0.45mm and stored separately in sealable air-tight plastics.

2.2 Preparation of Synthetic Industrial Wastewater

A cationic dye, methylene blue (MB), having molecular formula C₁₆H₁₈CLN₃S was chosen as adsorbate. The MB was chosen in this study because of its known strong adsorption onto solids. A stock solution of methylene blue of concentration 50 ppm (50 mg/L) was prepared by dissolving 0.5g of methylene blue in a 1000 mL volumetric flask, and completed with distilled water up to the mark. This solution was again stirred for some minutes to obtain homogeneity. Solutions of various concentrations were obtained by dilution. Dye final concentration was determined by using



absorbance values measured before and after the treatment, at 668 nm with Visible Spectrometer (J. T. Nwabanne and M. I. Mordi; 2009).

2.3 Experimental Data and Analysis

The amount of MB absorbed by a unit mass of an adsorbent at equilibrium (Q_e), also the amount of MB absorbed at any time and the adsorption percentage (% R) at an instant were calculated using the relations (Abechi et al, 2011);

$$Q_e = \frac{c_o - c_e}{m} V \quad (1)$$

$$Q_t = \frac{c_o - c_t}{m} V \quad (2)$$

$$\text{Percent removal} = \frac{c_o - c_t}{c_o} 100 \quad (3)$$

3. Results and Discussion

3.1 Effect of Initial Dye Concentration.

The influence of the initial dye concentration of methylene blue (50, 100, 150, 200, 250, 300) mg/L on the adsorption rate using coconut shell. The experiment was carried out at a constant adsorbent dosage of 2 g, at a room temperature ($26 \pm 1^\circ\text{C}$). It was observed that the percentage removal decreases as the concentration increases. The trend observed could be attributed to the fact that increase in concentration increases the number of dye molecules with limited adsorbent particle to attach to; and therefore the rate at which dye molecule pass from the bulk solution to the

3.4 Isothermal Studies

Langmuir and freudlich Isotherm

Table 1 gives values of Langmuir and Freundlich Isotherm Parameters for the Adsorption of Methylene Blue Using Rice Husk and Coconut Shell.

adsorbents	Langmuir constants			Freundlich constants		
	Q_o (mg/g)	K (L/mg)	R^2	K_f (mg/g)	n	R^2
Coconut shell	-1.1134	-0.7949	0.9772	4.0514	2.4969	0.9365

From the results of the isotherm studies shown in table 1 based on the R^2 values the Langmuir isotherm model best describe the adsorption isotherm of methylene blue from industrial waste water.

3.5 Adsorption kinetics

The data from the experiment were also analysed using lagergren pseudo first-order and pseudo second-order. Based on the R^2 values obtained from the adsorption kinetics it was evident that the adsorption of methylene blue from industrial wastewater was best described by lagergren Pseudo First-order.

4. Conclusion

adsorbent surface is highly reduced.

3.2 Effect of Contact Time and Initial Dye

The effect of contact time of methylene blue on the adsorption rate using coconut shell was carried out at a fixed dosage of adsorbent (2 g), at a temperature ($26 \pm 1^\circ\text{C}$). It was observed that the mixing time had a great impact on the reduction of methylene blue. The adsorption of methylene blue by coconut shell increased steadily throughout the study, and the adsorption was generally rapid within the first 80 minutes then it becomes fairly constant. The fast kinetics process observed at the initial stage can be attributed to the abundant availability of active binding site on the adsorbent which are later occupied as the process proceeds (Mavi et al., 2004).

3.3 Effect of Adsorbent Dosage

The effect of the adsorbent dosage (0.5, 1, 1.5, 2, 2.5, 3g) on the adsorption of methylene blue on adsorption rate using coconut shell. The experiment was carried out at an initial concentration of 50mg/l at room temperature ($26 \pm 1^\circ\text{C}$). The effect of adsorbent dosage was used to determine the capacity of adsorbent for a given initial adsorbate concentration and binding site available for adsorption. It was observed that increasing the adsorbent dosage increases the dye uptake as a result of the increase in the population of active site (Ho et al., 1995). The maximum removal of methylene blue was observed at an adsorbent dosage of 2 g

From the research carried out, activated carbon from coconut shell proved a good adsorbent for removal of methylene blue. The adsorption isotherms for coconut shell was described by Langmuir isotherm model with R^2 value of 0.9772, while the adsorption kinetics was best described by lagergren Pseudo First-order. Finally, this study has revealed that the low cost adsorbent from coconut shell can be used efficiently for the



removal of methylene blue from industrial wastewater.

NOMENCLATURE

Symbols

C = Concentration of adsorbent, mg/ml

Q = Amount of methylene blue adsorbed, ml

V = volume, L

K = constant, dimensionless

R = coefficient of regression, dimensionless

m = mass, g

n = intensity of adsorption, dimensionless

Subscript

O = refers to initial

e = refers to equilibrium

t = refers to at a given time

References

- Abechi E. S., C. E. Gimba, A. Uzairu, and J. A. Kagbu, (2011) "Kinetics of the adsorption of methylene blue onto activated carbon prepared from palm kernel shell" Scholar Research Library, vol. 3, no. 1, pp. 154–164
- Aksu, Z. (2005) Application of Biosorption for the Removal Organic Pollutants: a review process. *biochem.* pp40, 997-1026.
- Ho, Y.S.; John Wase, D.A. and Forster, C.F. (1995) Batch nickel removal from aqueous solution by sphagnum moss peat. *Water Research*, vol. 29, no. 5, p. 1327-1332
- Lagergren, S. (1898) About the Theory of So-Called Adsorption of Soluble Substance. *KungligaSvenskaVetenskapsakademiensHandling ar*, 24, 1-39.
- Mavi A., Terzi Z., Ozgen U., Yildirim A., Coskun M., "Antioxidant properties of some medical plants: prangosferulacea (Apiaceae), sedum sempervivoides(crassulaceae), malvaneglecta (malvaceae)Cruciatataurica (Rubiaceae), Rosa pimpinefolia (rosaceae), Galiumversubps. Varum (Rubiaceae)." *Boil. pharm. Bull.* 27(5) 702-705pp.
- Nwabanne J. T., and Mordi M. I., (2009). "Equilibrium uptake and sorption dynamics for the removal of a basic dye using bamboo". *African Journal of Biotechnology*, Vol. 8, no.8, pp. 1555-1559
- Olgun, A. N. Atar, (2009.) "Equilibrium and kinetic adsorption study of Basic Yellow 28 and Basic Red 46 by a boron industry waste", *Journal of Hazardous Materials*, vol. 161, pp. 148-156
- Pagga, U; Brown, d. (1986) the degradation of dye stuffs. *Chemosphere*. Pp. 15, 479-491

**ABSTRACT CCT-: 039**

Muibat A. Obianke¹, Lawal Gusau Hassan¹, Adamu A. Aliero², Lubabatu Mu'azu Jodi¹ and Aminu Bayawa Muhammad¹

¹Department of Pure & Applied Chemistry, Usmanu Danfodiyo University, Sokoto, Nigeria.

²Department of Biological Sciences, Usmanu Danfodiyo University, Sokoto, Nigeria.

Email: muhammad.aminu@udusok.edu.ng

OPTIMIZATION OF *IN SITU* OF TRANSESTERIFICATION OF OIL FROM MIXED-FEEDSTOCK OF RUBBER, CASSAVA, AND JATROPHA OIL SEEDS.

ABSTRACT: In this work Simple lattice mixture design was used to investigate effect of blending oilseeds of rubber, cassava and *Jatropha* in biodiesel production by *in situ* acid-catalysed transesterification. The results displayed a quadratic relationship between the proportions of the oilseeds and biodiesel yield. In general, slightly higher than average proportions of rubber and *Jatropha* oilseeds are associated with relatively high biodiesel yields. Increased in the amount of methanol and reaction time were also observed increase biodiesel yield. Response optimizer predicted an optimal yield of 90% when the relative proportions of rubber, cassava and *Jatropha* oilseeds are 33.33%, 29.98% and 36.69%, respectively at reaction time and amount of methanol of 360 minutes and 4.0 cm³/g of the oilseeds mixture, respectively. The predictions were found to be in agreement with experimental results. The biodiesel obtained from the optimal blend has specific gravity of 0.888, viscosity of 6.12 Cst @ 40°C, cetane number of 62.47, flash point of 158°C, cloud point of 16.63°C as well as pour point of 11.23°C which are in agreement with Biodiesel Guidelines provided by the Worldwide Fuel Charter Committee there by making it suitable for use as fuel in diesel engines.

Keywords: Rubber, Cassava, *Jatropha*, biodiesel, mixture design, *in situ* transesterification, optimization.

1. Introduction

Arguably the most important and promising biofuel is biodiesel - a mixture of monoalkyl esters derived from vegetable oils or animal fats. It has properties that are similar to petrodiesel and can thus be used in diesel engines with no engine modification [1]. It is biodegradable, non-toxic and produces much less harmful emissions than conventional petrodiesel [2,3]. However, it has slightly lower calorific value than petrodiesel and cost about 1.5 to 3 times higher due to the high cost of raw materials as well as high cost of production [4].

The cost of production can be reduced by careful design of the production process including; taking advantage of novel technologies, such as *in situ* transesterification, which lowers cost of production from reduced number of unit operations. On the other hand, the cost of raw materials can be reduced by utilizing non-edible oils as well as processing mixed feedstock [5,6], which could also provide biodiesel with improved physical properties [7]. Mixed feedstock processing may also be economically advantageous in that it could extend the lifetime of a comparatively more expensive feedstock through blending with less expensive ones.

In this work, we report results from an investigation of the effect of blending pulverized oilseeds of rubber (*H. brasilienses*), cassava (*M. esculenta*) and *Jatropha* (*J. curcas*) in biodiesel production by *in situ* acid-catalysed transesterification. The experimental design was based on simple lattice mixture design aimed to investigate and optimize the effect of the three mixture components and two process variables (reaction time and the amount of methanol) on biodiesel yield.

Catalyst (H₂SO₄ in methanol) concentration and reaction temperature were held constant at 0.88M and 50°C, respectively.

In each trial, the oilseeds blend (5g) was refluxed with acidic methanol and n-hexane (5.0 cm³) as co-solvent at the temperature of interest for the specific periods as in the design matrix. The residue was then removed by filtration and the filtrated was treated with water (10 cm³) and n-Hexane (10 cm³) facilitate the separation. The aqueous phase was discarded and the organic phase containing the biodiesel was recovered, evaporated, washed and dried over anhydrous Na₂SO₄ to obtain the biodiesel. The percentage biodiesel yield was calculated relative to the weight of oil in 5.0 g of the blended seed [8].

The molecular profile of the biodiesel produced from the optimally mixed feedstock was determined on scan mode using an Agilent 7890A GC coupled to 5973 MSD. And physicochemical properties of the biodiesel were determined according to standard procedures as described in [9].

ANOVA and regression analysis of the results revealed that 7 out of the 16 terms of the model are significant. The model accounts for about 94% of the experimental observation with the predictive power of 92%. The model displayed a quadratic relationship between the proportions of the oilseeds and biodiesel yield (Fig. 1a)

Biodiesel yields greater than 90% are obtained when the proportion of the cassava oilseed is below 30% and greater than 10% proportion of either of *Jatropha* and rubber oilseeds. In general, slightly higher than the average proportions of rubber and *Jatropha* oilseeds are associated with relatively high biodiesel yields.

Although the best yields are obtained when the amount of methanol and reaction time were at their highest levels (Fig. 1b2), the amount of methanol showed the most influence on the biodiesel yield (Fig. 1b3 and Fig. 1b4) such that when it was at its lowest level, the yields are generally less than 60% (mostly below 40%). However, when the amount of methanol levels of biodiesel yields (Fig. 1b1).

Response optimizer predicted an optimal yield of 90% when the relative proportions of rubber, cassava, and Jatropha oilseeds are 33.33%, 29.98%, and 36.69%, respectively at reaction time and the amount of methanol of 360 minutes and 4.0 cm³/g of the oilseeds mixture, respectively. The predictions agreed well with experimental results from validation. Physicochemical analyses of the biodiesel

is at its highest level, the yields are mostly between 40 and 60% even when the reaction time was at its lowest level (Fig. 1b1). It is noteworthy that at provided the amount of methanol is at its highest level, at low reaction time high proportions of cassava oilseeds tend to give the highest

obtained from the optimal conditions revealed that it has specific gravity of 0.888, viscosity of 6.12 Cst @ 40°C, cetane number of 62.47, flash point of 158°C, cloud point of 16.63°C as well as pour point of 11.23°C. All the quality parameters are in agreement with ASTM D6751-08 specifications for B100 biodiesel [10] and Biodiesel Guidelines provided by the Worldwide Fuel Charter Committee [11] thereby making it suitable for use in diesel engine

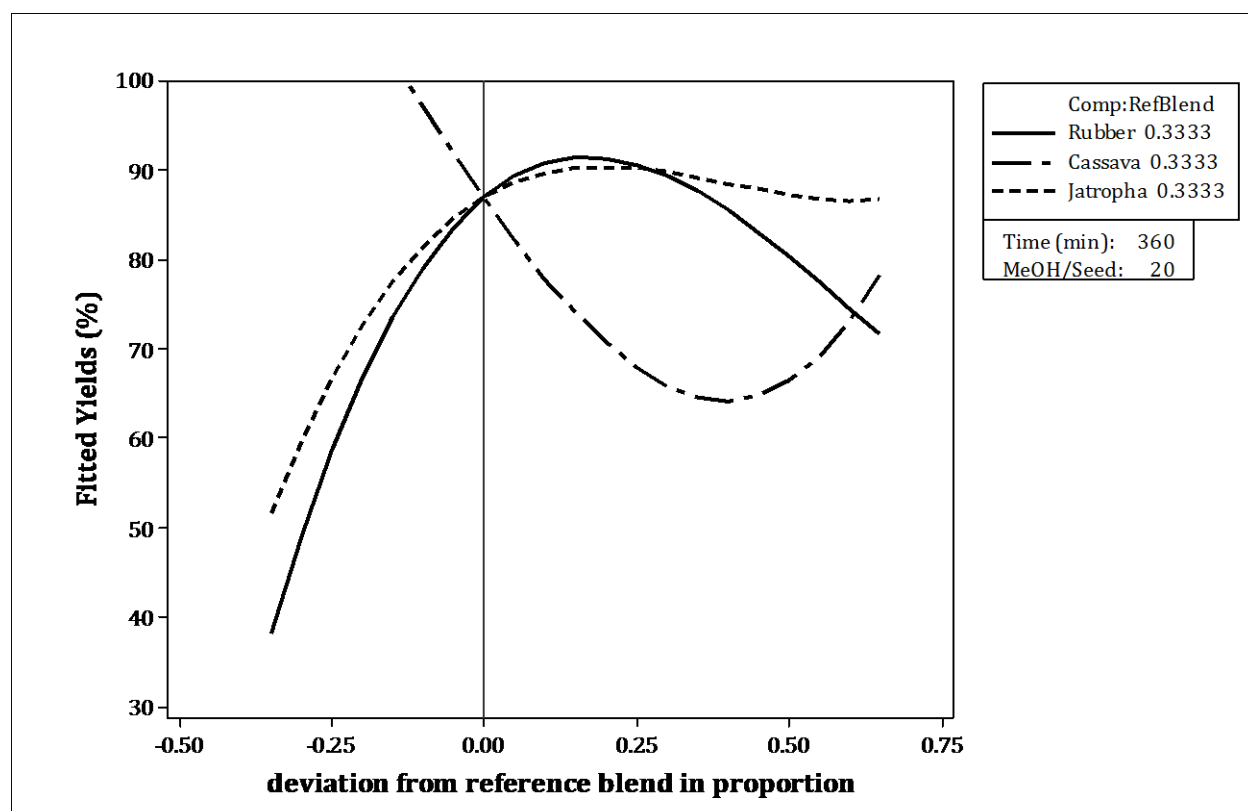


Fig. 1a. Cox plot showing the effect of the relative amounts of the mixture components on the biodiesel yield relative to the reference blend.

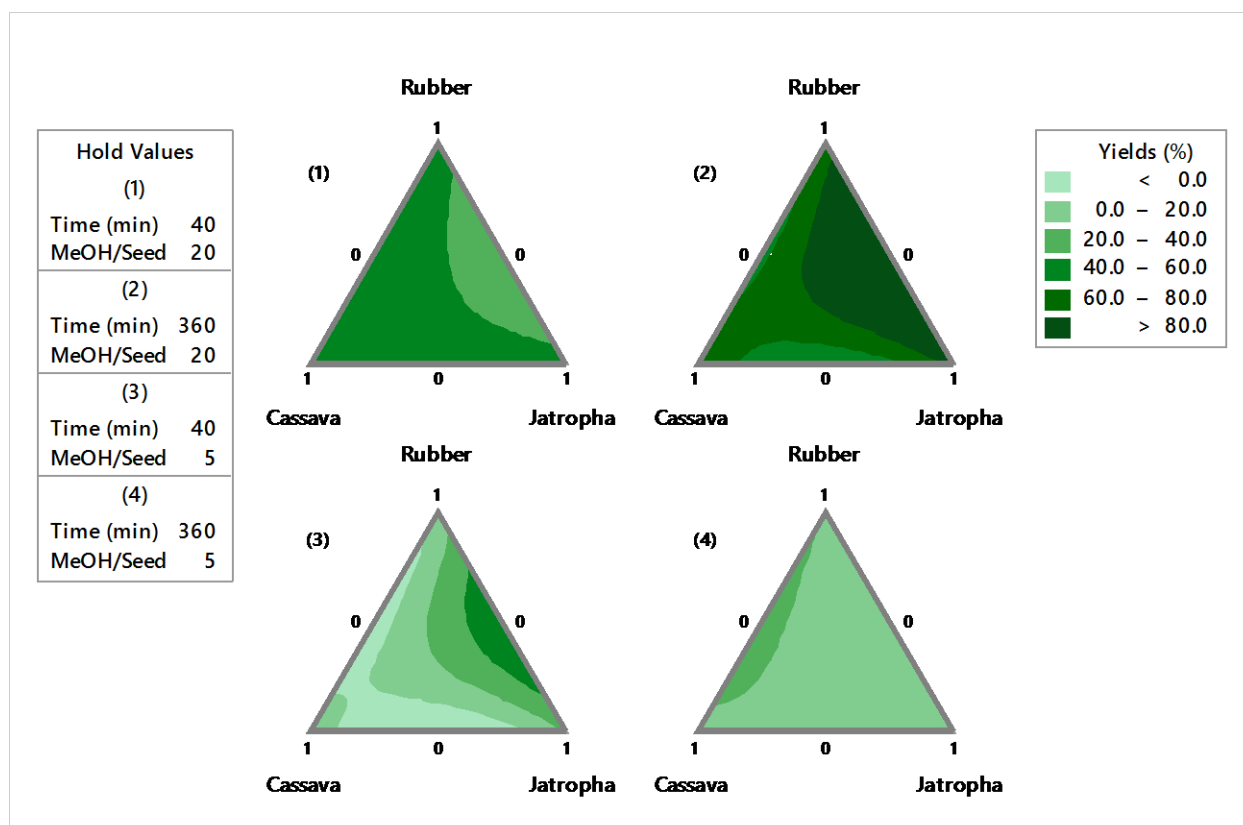


Fig. 1b. Contour plots showing the effect of the mixture components are process variables on biodiesel yield.

References

- Atadashi IM, Aroua MK, Aziz AA. High quality biodiesel and its diesel engine application: A review. *Renewable and Sustainable Energy Reviews*. 2010; 14: 1999-2008.
- Antolin G, Tinaut FV, Briceno Y, Castano V, Pirez C, Ramirez AI. Calcium oxide as a solid base catalyst for transesterification of soybean oil. *Bioresour. Technol.* 2002; 83: 111 - 114.
- Issariyakul T, Kulkarni MG, Meher LC, A.K. D, N.N. B. Heterogeneous catalysts for biodiesel production. *Chem. Engineering J.* 2008; 140: 77-85.
- Abbaszaadeh A, Ghobadian B, Omidkhan MR, Najafi G. Current biodiesel production technologies: A comparative review. *Energy Conversion and Management*. 2012; 63: 138-148.
- Meneghetti SMP, Meneghetti MR, Serra TM, Barbosa DC, Wolf CR. Biodiesel production from vegetable oil mixtures: Cottonseed, soybean, and castor oils. *Energy Fuels*. 2007; 21: 3746-3747.
- Moser BR. Influence of blending canola, palm, soybean, and sunflower oil methyl esters on fuel properties of biodiesel. *Energy & Fuels*. 2008; 22: 4301-4306.
- Bora DK, Baruah DC, Das LM, Babu MKG. Performance of diesel engine using biodiesel obtained from mixed feedstocks. *Renewable and Sustainable Energy Reviews*. 2012; 16: 5479-5484.
- Zakaria R, Havey AP. Direct production of biodiesel from rape seed by reactive extraction/in situ transesterification. *Fuel*. 2012; 102: 53-60.
- Muhammad AB, Obianke M, Gusau LH, Aliero AA. Optimization of process variables in acid catalysed in situ transesterification of hevea brasiliensis (rubber tree) seed oil into biodiesel. *Biofuels*. 2016: 1-10.
- Hoekmana SK, Broch A, Robbins C, Ceniceros E, Natarajanb M. Review of biodiesel composition, properties, and specifications. *Renewable and Sustainable Energy Reviews*. 2012; 16: 143 - 169.
- WWFCC (2009) *Guidelines for biodiesel*, Worldwide Fuel Charter Committee.

**ABSTRACT CCT-: 075**A. A. MUHAMMAD^{A*}, B.Y. JIBRIL^a, F. MJALLI^b, J. NASER^b.^aDepartment of Chemical Engineering, Ahmadu Bello University Zaria, Nigeria^b Petroleum and Chemical Engineering Department, Sultan Qaboos University, Muscat, 123 Oman.Email: aminuam@yahoo.com**IONIC LIQUID BASED DEEP EUTECTIC SOLVENT FOR THE REMOVAL OF AROMATICS FROM ALIPHATIC HYDROCARBONS**

ABSTRACT: Removal of aromatics from aliphatic hydrocarbon is important due to requirement for high purity aliphatic. There is a need for more efficient method for the removal. A new class Ionic Liquid-based Deep Eutectic Solvents (DES) was synthesized and tested in separation of Toluene from Octane using liquid-liquid extraction. The DESs were formed from Tetrabutylphosphonium methanesulphonate (TM) as an organic salt with either Polyethylene Glycol 200 (PEG200) or Polyethylene Glycol 600 (PEG600) as Hydrogen Bond Donors (HBD). The DESs formed are referred to as TM-PEG200 and TM-PEG600 respectively. The extraction was done under atmospheric pressure at 30, 40 and 50 °C. Solute distribution coefficient and selectivity were calculated and used to evaluate the performance of the DESs. Analysis of the raffinate phase showed negligible DES composition in the raffinate. The performance test shows distribution coefficient and selectivity of TM-PEG600 as 1.52, 9.33 and TM-PEG200 as 0.71, 9.17 respectively.

Keywords: Deep Eutectic Solvent, Ionic Liquids, Aromatic Separation, Liquid-Liquid equilibrium

1. Introduction

The separation of aromatic compounds from the aliphatic poses a lot of challenge to the petrochemical industry due to the formation of azeotropes and close boiling point components. The commonly employed solvents in these process are sulfolane, ethylene glycols, dimethylsulfoxide, N-formylmorpholine which are organic based. The sulfolane process is currently the most common and is design for higher aromatic feed composition greater than 20 wt. % and its recovery is by extractive distillation which is energy intensive. [3,7]

Ionic liquids are organic salts that are liquid at low temperatures (<100 °C) and consist of large organic cations based on methylimidazolium [Rmim], N-butylpyridinium [RN-bupy], quaternary ammonium or phosphonium ions and others, and anions such as hexafluorophosphate, tetrafluoroborate, alkylsulfates, alkylsulfonates, chloride, bromide, nitrate, sulfate, aluminium chloride etc.[12]. The application of some ILs for the removal of aromatic from aliphatic hydrocarbons has been reported [3]

Deep Eutectic solvents are mixtures of one or more hydrogen bond acceptors (HBA) and one or more hydrogen bond donors (HBD) that when mixed together in the proper molar ratio, show a big decrease in the melting point compared to the initial compounds [7,8].

Currently, there is no feasible process for the separation of aromatic content less than 20 wt.%. [3] Liquid-liquid extraction process has been proposed by many researchers to be feasible due to its low energy requirements [1,7,8]. Recently, a new generation solvent, called deep eutectic solvents (DESs) have been reported as a potential alternatives to organic solvents. The aim of this work is to evaluate the potential applications of two Ionic Liquid based DESs as extracting agents in liquid-liquid extraction of aromatic and aliphatic

hydrocarbon.

2. Materials and Methods

Polyethylene glycol (PEG-200) and Polyethylene glycol (PEG-600) for synthesis was supplied by Merck (Germany). Acetonitrile (99.9%, HPLC grade) was also supplied by Merck. Octane and (99%) were supplied by BDH (England). Toluene was supplied by Fischer scientific and Honeywell. The Ionic liquids tetrabutylphosphonium methanesulfonate (TBPMS) (98%) was supplied by Sigma Aldrich (Austria). All chemicals were used as supplied without further purification.

Methods

DESs were prepared by measuring and mixing the ionic liquids with the hydrogen bond donor HBD to form the solvent. The salts to HBD molar ratio for all the solvents were 1:2. .

The mixture was heated up to 80 °C and 600rpm inside screw capped bottles until a clear liquid is formed. Mixtures of toluene and n – octane were prepared in five different concentrations (2.5, 5.0, 10.0, 15.0, and 20.0 wt. % toluene.) to form the feed. DESs as solvent were added to the feed samples at a feed: solvent mass ratio of 1: 1. Each set of experiment was conducted at 30, 40 and 50 °C. The mixtures of the solvent and the feed were put in a screw capped vials. The vials were put inside a thermoshaker capable of controlling the temperature and the speed. The mixture was agitated for 6 hours at 600 rpm and allowed to settle for 12 hours to attain equilibrium. Micropipette was used to separate the top raffinate layer and the bottom layers which were analyzed using High performance liquid chromatography (Agilent 1260) infinity series equipped with variable wave length detector and a reversed column.

3. Results and Discussions

Ternary liquid-liquid equilibrium data

The solute distribution coefficients and selectivity are two important parameters that were evaluated from experimental data in order to study the potential applications of the synthesized DESs for the removal of toluene from octane.

The results of the analysis of the raffinate layer by the HPLC after the liquid-liquid experiments shows that components of TM-PEG200 as DES1 and TM-PEG600 as DES2 were not found in the raffinate. This shows that the interaction between the salt and the HBD is very strong which prevents the solvent from being released into the raffinate layer a process called “solvent loss”. This is a very important industrial property that is desired of a solvent in liquid-liquid extraction.

These parameters can be calculated from the experimental data for the extraction aromatic and n-octane hydrocarbon mixture with DES using the following expressions:

$$\beta_{\text{aro}} = \frac{x_{\text{Tol}}^{\text{E}}}{x_{\text{Tol}}^{\text{R}}} \quad \text{Equ. 1}$$

$$s = \frac{x_{\text{Tol}}^{\text{E}} \cdot x_{\text{Oct}}^{\text{R}}}{x_{\text{Tol}}^{\text{R}} \cdot x_{\text{Oct}}^{\text{E}}} \quad \text{Equ. 2}$$

Where x is the mole fraction of aromatic and aliphatic in the raffinate and extract phase respectively.

The measured composition at equilibrium in both liquid phases and for each DES are plotted in the ternary diagrams given in fig. 1.0 – 2.0

The effect of temperature on the separation based on solute distribution coefficient and selectivity can be analyzed in fig. 1.0 – 2.0. The effect of temperature in both the systems is rather small this shows the separation can be done at low temperatures. The selectivity of the studies systems were found to be greater than one, indicating that the separations with these DESs is feasible. [11] the solute distribution coefficient of DES2 were found to be greater than one implying lower solvent to feed ratio and therefore, small amount of solvents to be recovered and though lower energy requirements.

Table 2. Values of distribution coefficient (D) and selectivity (S) reported in literature compared

systems	solvents	T(K)	D	S	Reference
Tol/Oct	DES1	303	0.71	9.17	This work
Tol/Oct	DES2	303	1.52	9.33	This work
Tol/Oct	TBAB:SF	298	0.50	25.7	[4]
Tol/Oct	[EMPY][EtSO4]	298	0.25	55.2	[9]
Tol/Oct	[EMIM][EtSO4]	298	0.23	68.1	[10]
Tol/Hep	EPI:SF	313	0.50	80.22	[7]

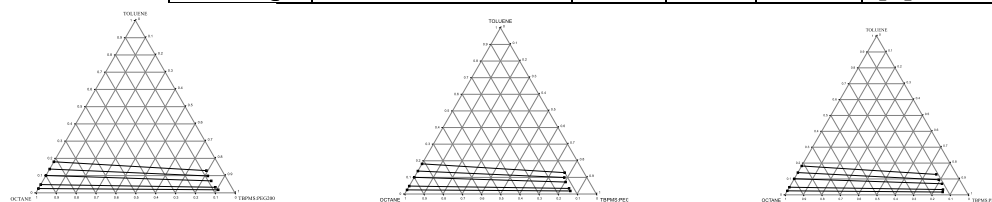


Figure 1.0 Ternary diagram for TM-PEG200 at 30,40 and 50 oC

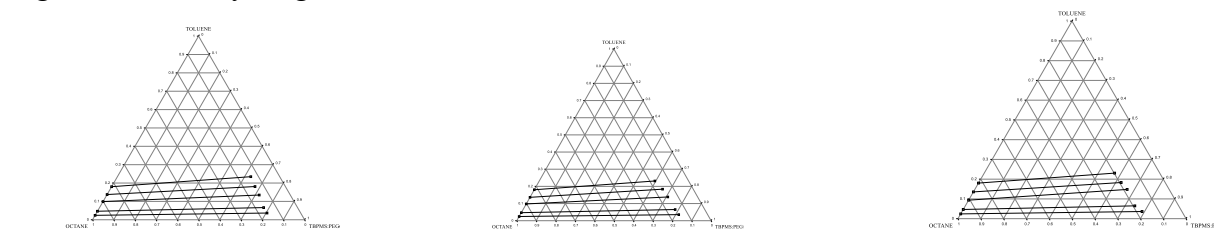


Figure 2.0 Ternary diagram for TM-PEG600 at 30,40 and 50 oC

4. Conclusion

In this work two different DESs were prepared from tetrabutylphosphonium methanesulfonate as salt and polyethelene glycol 600 and polyethelene glycol 200 as hydrogen bond donors. They were evaluated for their potential application as extracting agents for the separation of toluene and n-octane. Liquid liquid equilibrium experiments were performed and the performance of the DESs were evaluated in terms of selectivity and solute distribution coefficients. Analysis of the raffinate shows no traces of DESs components and this is one of the most important industrial properties. The performance of the DESs in terms of distribution

coefficients was found surpass some of the previously reported DESs in the literature.

Reference

- E. L. Smith, A. P. Abbott, and K. S. Ryder. Deep Eutectic Solvents (DESs) and their applications. ACS Publications. 2014.
- Q. Zhang. KDO Vigier, S. Royer, f. Jerome. Deep eutectic solvents: synthesis, properties and applications. Chem. Soc. Rev. 2012, 41, 7108.
- G. W. Meindersma, A. Podt, A. B. de Haan. Ternary liquid-liquid equilibria for mixtures of an aromatic and aliphatic hydrocarbon + 4- methyl-n-butylpyridinium tetrafluorate. J. Chem. Eng. Data 51 (2006) 1814-1819.
- M. S. Selvan, M. D. McKinley, R.H. Dubios, J. L.



- Atwood, Liquid-Liquid extraction, Chem. Comm. 16 (1998) 1765 – 1766
- W. Arlt, M. Seilar, C. Jork, T. Schneider, Ionic Liquids as selective additives for the separation of close boiling or azeotropic mixtures. PCT Int. Appl. WO 2002/074718 A2 September 2006.
- I. Dominguez, N. Calvar, E. Gomez, A. Dominguez. Separation of Benzene from heptane using three ionic liquids: BMimMSO₄, BMimNTf₂, PMimNTf₂. 20th International Congress of Chemical and Process Engineering CHISA 2012.
- Kareem M.A. et.al. Phase equilibria of toluene/heptane with deep eutectic solvents based on ethylphenyl phosphonium iodide for the potential use in the separation of aromatics from naphtha properties.. J. Mol. Liq. 178 (2013) 137-141.
- Emilio J. González Noelia Calvar Irene Domínguez Ángeles Domínguez J. Separation of toluene from alkanes using 1-ethyl-3-methylpyridinium ethylsulfate ionic liquid at T=298.15 K and atmospheric pressure Chem. Thermodynamics 43 (2011) 562–568
- Emilio J. González Noelia Calvar Begoña González Ángeles Domínguez J. Chem. Thermodynamics 42 (2010) 752–757
- Rodríguez, N.R. Requejo P.F. and Kroon M.C. Aliphatic-aromatic separation using deep eutectic solvents as extracting agents. I & EC research S 2015.
- J.F. Brennecke, E.J. Maginn, Ionic liquids: innovative fluids for chemical processing, AIChE J. 47 (11) (2001) 2384–2389.
- A. Hayyan, F. S. Mjalli, I. M. Inas, Y. M. Al-Wahaibi. Glucose-based deep eutectic solvents: Physical

**ABSTRACT CCT-: 079**

Dangoggo S.M., Yusuf A.U.

¹Department of Pure & Applied Chemistry, Usmanu Danfodiyo University, Sokoto, Nigeria.Email: aykaura0@gmail.com**COMPARATIVE STUDY OF BIOGAS PRODUCTION FROM SELECTED AGROWASTES**

ABSTRACT: This research compared biogas production from poultry and orange peel wastes, and evaluates the economic feasibility. The parameters studied included the physicochemical characteristics of the substrates and the inorganic content of the digested poultry and orange peel waste. Three substrates slurries of poultry waste (sample A), orange peel waste (sample B), and the mixture of both poultry and orange peel waste (sample C) were fed into 3 digesters and fermented anaerobically over a period of 6 weeks. It was discovered that the mixture of the poultry and orange peel waste (sample C) produced the highest volume of biogas and the undigested poultry waste has higher mineral content.

KEYWORDS: Biogas, Poultry waste, Orange peel, Slurry.

1. Introduction

The consumption of energy all over the world has increased, which have led to a drastic increase in the rates of usage of the hydrocarbon based fuels which has limited source that will not be able to meet the increasing fuel needs. (Ogbuagu, *et al.*, 2004). Biogas typically refers to a mixture of different gases produced by the breakdown of organic matter in the absence of oxygen. Biogas is a renewable energy source and in many cases exerts a very small carbon footprint. (NNFCC, 2016).

Biogas which can be produced mainly from raw materials such as agricultural waste, manure, municipal (foreground), natural gas and waste, plant materials, sewage, food waste and other domestic waste can be carried through pipes. Biogas is primarily methane (CH₄) and carbon dioxide (CO₂) and may have small amounts of Hydrogen sulphide (H₂S), moisture and siloxanes. The gases methane, H₂S and carbon monoxide (CO) can be combusted or oxidized with Oxygen. This energy release allows biogas to be used as fuel. It can be used for any heating purpose such as cooking. (Biogas and Energy, 2011)

Biogas production has been tried with many substrates and at the same time, a number of factors affecting the production process have been studied and the effect of such parameter such as pH, C-N ratio, catalyst, and poultry cooping was reported. (Fernando and Dangoggo, 1986).

Nigeria lies within the equatorial axis where sunlight intensity is very high, receiving about 35 to 7kw/m²/day from the coastal latitude to the north. The average annual temperature is about 36⁰c which is favorable for biogas production. (Emeka, 2010).

This research work looked into the gas yield patterns of different kind of wastes that can be fed into a prototype household digester unit for optimum yield of biogas. The specific objectives of this research were to: (1) Assess the potential of orange and poultry waste and

their mixture for biogas production. (2) Assess and analyze the inorganic mineral content of the selected agro waste for fertilizer application.

2. Materials and Method

Source: The orange peel was obtained from Sokoto Central Market, Sokoto State while, the poultry waste was collected from Poultry Farm at Arkilla Federal Lowcost, Sokoto State. The wastes were sundried, grounded and then stored in a black polyethane bag for subsequent use.

Chemicals: Conc. H₂SO₄, Boric acid (H₃BO₃), NaOH, Conc. HCl and Ethanol from May and Baker Manufacturer.

Chemical Analysis: The chemical analysis of the fermenting slurries was done at Usmanu Danfodiyo University Sokoto Agricultural laboratory. Various parameters included in the analysis were; pH, nitrogen, phosphorus, potassium, temperature, moisture content, ash content and organic matter content. The parameters mentioned above were determined using the AOC method (2006).

According to the analytical results, the pH value obtained was 6.2 average which is not optimum for the methanogenesis process thereby affecting production of methane. The wastes were then diluted with water at 1:4 ratio of the total solids content for feeding into the biodigester. (Karki and Dixit, 1984).

3. Results and Discussions

The result showed that the mixture hydrolyzes much more easily than any of the individual substrates and therefore are fermented faster to produce biogas. Temperature in the laboratory ranged from 27-34⁰c. The mean temperature was 31⁰c. This low mean temperature could affect the volume of biogas generated since temperature influences the action of methanogenic bacteria and the rate of hydrolysis. (Fernando and Dangoggo, 1986). Therefore, the use of organic waste for biogas generation will encourage the use of biogas as an alternative source of energy in Nigeria.

**Table 1.** Average biogas generated from each digester

S/NO.	DIGESTERS	AVERAGE BIOGAS (cm ³)
1.	A	3,038.00cm ³
2.	B	1,725.00cm ³
3.	C	4,060.00cm ³

Table 2. Physicochemical Analysis of the Digested Samples

S/NO.	PARAMETERS	SAMPLE A	SAMPLE B	SAMPLE C
1.	Ash content %	57.50.00	16.00	31.00
2.	Moisture content %	15.00	37.00	10.00
3.	Organic matter %	27.50	47.00	59.00
4.	Nitrogen %	0.95	0.35	0.602
5.	Phosphorus (mg/kg)	7.45	5.56	6.33
6.	Potassium (mg/kg)	1400.00	2900.00	2000.00
7.	pH	4.51	4.20	4.48

Table 3. Physicochemical analysis of the undigested samples

S/NO.	PARAMETERS	SAMPLE A	SAMPLE B	SAMPLE C
1.	Ash content %	46.00	8.50	32.5
2.	Moisture content %	1.00	2.00	1.50
3.	Organic matter %	53.00	89.50	66.00
4.	Nitrogen %	2.21	0.94	1.08
5.	Phosphorus (mg/kg)	4.01	3.69	3.71
6.	Potassium (mg/kg)	1450.00	4000.00	3900.00
7.	pH	7.48	4.86	5.83

The percentage nitrogen of the digested samples is less than that of the undigested sample. Sample A of the undigested sample has nitrogen percentage of 2.12% greater than any of the substrates samples, this also shows that, the sample A of the undigested sample is a better choice for fertilizer production. The percentage nitrogen for sample (A) obtained by Singh, *et al.* (2008) is 1.79% which is higher than 0.952% (for sample A of the digested sample) making the later poor substrate for the fertilizer production.

The phosphorus content for the undigested samples is 4.09, 3.69, & 3.71mg/kg for sample A, B, & C respectively. For the digested samples are 7.45, 5.56, & 6.33mg/kg for sample A, B, & C respectively. The phosphorus content for sample A of the digested sample is greater than any of the samples. It has also a higher content as compared to that of Singh, *et al.* (2008) which is 5.85mg/kg using the same substrate, making it a better source of phosphate fertilizer.

The potassium content of the undigested samples is 1450.0, 4000.0, & 3900.0mg/kg for sample A, B, & C respectively; making sample B a better source of potassium. The potassium content of the digested samples is 1400.0, 2900.0, & 2000.0mg/kg for sample A, B, & C respectively, making sample B a better source for potassium. In general, the potassium content of the undigested samples is greater than that of the digested samples. In conclusion, the potassium content determined by Singh, *et al.* (2008) with value of 5.51% is less than

either of the two Bs' samples, thereby making sample B a better source of potash fertilizer.

4. Conclusions

From the results above it showed that biogas yields produced from combination of orange peel and poultry waste better than use of either orange peel or poultry waste alone. Furthermore, proximate analysis confirms the utilisation of organic mineral content in the undigested samples as compared to the digested samples at the end of the fermentation.

Recommendations

Further research should be geared to the determination of parameters of the composite substrates to achieve an optimum biogas yield. The organic mineral content of slurries after the fermentation is sufficient for it to be used as bio-fertilizer which will improve the soil fertility.

Acknowledgements

My immense gratitude to one of the Noble Professors of Chemistry on earth, and also a father, in which his tremendous contribution to the field of Chemistry has been recognized in person of Prof. S.M. Dangoggo, who gave me the idea to carry out this research work and his expert guidance and encouragement was a key factor in the accomplishment of this study. I am equally indebted to Dr. A.M. Bayawa, Dr. Ezennia Okoh.

I am immensely obliged to Dr. S.A. Ibrahim, Basic Research Dept. National Research Institute for Chemical Technology (NARICT). Basawa - Zaria.



REFERENCES

- American Official Chemists, (2006). Official Method of Analysis of the Used of the Official Analytic Chemists. Washington DC-20044. 15th edition. Pp.33-41.
- Biogas and Energy, (2011). www.clarke-energy.com/
- Emeka EE, (2010). "Casualty Analysis of Nigerian Electricity Consumption and Economic Growth." *Journal of Economics and Engineering*, 4:80-85. ISSN:2078-0346.
- Fernando and S.M. Dangoggo, (1986). "Some Factors Affecting Biogas Production". *Nigerian Journal of Solar Energy*. 4, 111-114.
- Karki A.B. and K. Dixit (1984). "Biogas Fieldbook" Sahayogi Prakashan, Kathamandu.
- National Non-Food Crops Centre, (2016). NNFC. "Renewable Fuels and Energy Facts Heat: Anaerobic Digestion. Retrieved: 5:15-21.
- Ogbuagu J.O., Nwokoye A.O.C., Nwosu M.C., and Okoye M.I., (2004). "Biogas Availability from Organic Waste Deposits in Anambra State, Nigeria". *Nigerian Journal of Renewable Energy*. 11(1 and 2): 23-32.
- Rajendra S., Amrit B., and Jagan N. S., (2008). "International Journal of Renewable Energy". Vol. 3, No. 1.

**ABSTRACT CCT-: 078**Gauje, B.,¹ Chia, M. A.,² Okoduwa, S.I.R.,³ Adudu, A. J.,¹ Inuwa, B.,¹ Muazu, K.¹

1. Industrial Environmental Technology Dept. National Research Institute for Chemical Technology
2. Botany Department, Ahmadu Bello University
3. Research and development Department, National Institute of leather and Science Technology

Email: write2bally@gmail.com**TREATMENT OF TANNERY EFFLUENT WITH CHLORELLA VULGARIS.**

ABSTRACT: Leather tannery effluents are ranked as the highest pollutants among all the industrial wastes, which leads to an introduction of novel chemicals into the ecosystem. Tannery effluent was collected from an effluent stream from Tanneries in Challawa Industrial Estate, Kano. The effluent was sterilised and inoculated with 10 % volume of algal inoculums. Total dissolved solids were determined using Hanna combo pH/EC meter HI 98129. Sulphate was determined using HACH DR 2400 spectrophotometer. Standard methods were used to determine dissolved oxygen, biological oxygen demand and chemical oxygen demand titrimetrically. There were significant reductions in most physicochemical parameters but there was no significant reduction in concentrations of biological oxygen demand and chemical oxygen demand hence treatment of tannery effluent should be in combination of *Chlorella vulgaris* with either bacteria or fungi. *Chlorella vulgaris* treats tannery effluent effectively in high dilution especially 25% dilution.

KEYWORDS: Tannery effluent, *Chlorella vulgaris*, physicochemical parameter, Treatment dilutions

1. Introduction.

Tannery effluent is a by - product of the manufacturing and transformation of hides and skin to leather products. It constitutes an environmental concern as it increases the pollution status of rivers (Midha et al., 2008). Leather tannery effluents are ranked as the highest pollutants among all the industrial wastes, which leads to an introduction of novel chemicals into the ecosystem. The released pollutants such as organic compounds and heavy metals exercise negative impact on environment causing toxicity to flora and fauna. In every step of tanning process, a considerable amount of waste water is released containing huge amount of chemicals. Most of the industries have effluent treatment plants but there is no complete removal of chemicals even in treated samples. Because of high cost implication, less than 5% of the industries in the world have adopted a sufficient measure for treatment of effluent while most have ignored it (Khopkia, 2009; Precathi et al., 2009). The problems associated with tannery effluents are their undesirable influence on the biological processes in receiving environmental media, undesirable taste and odour in addition to the high volume of effluent waste generated, which is usually released into the environment usually untreated or with minimal treatment (Rajasulochana et al., 2009). This exposes every consumer to unknown quantities of pollutants in the water they consume. It is therefore imperative to seek alternative cheap means of treating tannery effluent before it is released to the environment.

2. Materials and Methods

Tannery effluent from Mario – Jose, Mahaza, Mahmuda Tanneries in Challawa Industrial Estate, Kano. A dilute acid pre – rinsed plastic container was used to collect the tannery effluent and was preserved with ice packs. It was transported to National Research Institute for Chemical Technology, Zaria to determine physicochemical parameters. *Chlorella vulgaris* UTEX 2714 cultured in modified

Bold Basal Medium (Andersen, 2005) with 10ml 2.5g/l Na₂CO₃ as carbon source (Chia, 2015). Effluent sample was diluted into 0%, 5%, 10%, 25%, 50%, 75%, 100% concentration sample (Ajayan, 2012) The batch experiment was carried out in triplicate using 1 litre conical flasks containing 500 ml of standardized medium and a 10 % volume i.e. 50ml of algal inoculums in the exponential growth phase with cells to a concentration of about 1×10^6 cell mL⁻¹ with a photoperiod of 12:12 h light and dark cycles.

2.1 Determination of Total dissolved solid (TDS)

The total dissolved solid was determined using (Hanna combo pH/EC meter HI 98129. Total dissolved solid was measured in milligram per litre (mg/l) (APHA, 2005).

2.2 Determination of Sulphate

The sulfaver 4 method as described by APHA, (2005) was used to measure sulphate (SO₄²⁻) concentration in mg/l, at a wavelength of 450nm using HACH DR2400 portable spectrophotometer.

2.3 Determination of Dissolved Oxygen and Biochemical Oxygen Demand

The dissolved oxygen (DO) and biochemical oxygen demand (BOD) of tannery effluent was determined using the Alkaline – Azide modification of Winkler's method as described by Ademoroti (1996).

2.4 Determination of Chemical Oxygen Demand

This was determined using the titrimetric method described by Ademoroti (1996) One-way analysis of variance (ANOVA) with Tukey's HSD post hoc test was used to test for significant differences among the physicochemical parameter. Two-way analysis of variance was used to test for significant difference among the dilutions. SPSS version 20 for windows was used for the analysis of variance.



3. Result and Discussion

The Total Dissolved Solids measured is an indication of the concentration of dissolved ions in it (Azarpira *et al.*, 2014). TDS in Table 1 increased in low concentration of tannery dilutions in the 4th day is due to the addition of BBM and *Chlorella vulgaris*. These findings agree with Rao *et al.*, (2011) where *Chlorella*

vulgaris with a reduction efficiency for TDS 21%. The decrease of TDS based on a unique mechanism of bio-absorption/adsorption of different types of dissolved ions including various nutrients from wastewater which is utilised by microalgae for growth (Nanda *et al.*, 2010).

Table 1. Effect of *Chlorella vulgaris* on Total Dissolved Solid (mg/l) at different dilutions treated tannery effluent

Dilution	DAYS			
	Initial	4	8	12
BBM	875.00±0.58 ^a	410.33±20.18 ^b	376.33±10.20 ^b	357.33±9.24 ^b
0%	0.00±0.00 ^b	106.33±10.87 ^a	97.67±5.24 ^a	92.00±10.79 ^a
5%	233.67±1.20 ^a	164.00±4.16 ^b	160.67±2.03 ^b	138.33±11.17 ^b
10%	443.33±3.48 ^a	222.33±1.76 ^b	217.00±0.58 ^b	206.00±8.19 ^b
25%	937.67±5.84 ^a	426.67±45.43 ^b	400.00±29.05 ^b	373.00±49.24 ^b
50%	1599.00±17.52 ^a	692.67±17.90 ^b	675.00±14.42 ^b	653.67±11.10 ^b
75%	5073.33±29.63 ^a	965.33±5.24 ^b	940.67±8.99 ^{bc}	845.00±35.25 ^c
100%	7233.33±73.11 ^a	1153.33±8.41 ^b	1136.67±30.75 ^b	1089.67±36.15 ^b

Table 2. Effect of *Chlorella vulgaris* on Sulphate (mg/l) at different dilutions treated tannery effluent

Dilution	DAYS			
	Initial	4	8	12
BBM	100.00±10.00 ^a	170.00±20.82 ^a	150.00±11.55 ^a	103.33±31.80 ^a
0%	0.33±0.33 ^b	190.00±70.00 ^a	120.00±0.00 ^{ab}	70.00±11.55 ^{ab}
5%	60.00±5.77 ^b	126.67±23.33 ^a	63.33±8.82 ^{ab}	60.00±11.55 ^b
10%	106.67±17.64 ^a	123.33±8.82 ^a	103.33±33.33 ^a	96.67±17.84 ^a
25%	250.00±11.55 ^a	190.00±10.00 ^{ab}	163.33±23.33 ^b	123.33±14.53 ^b
50%	410.00±15.28 ^a	256.67±6.67 ^b	250.00±17.32 ^b	246.67±20.28 ^b
75%	656.67±40.96 ^a	310.00±20.82 ^b	303.33±14.53 ^b	300.33±0.33 ^b
100%	886.67±46.67 ^a	393.33±18.56 ^b	386.67±13.33 ^b	373.33±17.64 ^b

Table 3. Effect of *Chlorella vulgaris* on Dissolved Oxygen (mg/l) at different dilutions treated tannery effluent

Dilution	DAYS			
	Initial	4	8	12
BBM	4.14±0.48 ^{ab}	1.57±0.64 ^{bc}	1.24±0.30 ^c	4.57±0.34 ^a
0%	7.65±0.05 ^a	2.02±0.41 ^c	1.31±0.03 ^c	4.60±0.10 ^b
5%	4.50±0.10 ^a	1.41±0.34 ^a	1.51±0.30 ^a	4.20±0.11 ^a
10%	3.45±0.45 ^{ab}	2.25±0.71 ^{ab}	1.44±0.10 ^b	4.47±20.25 ^a
25%	3.78±0.03 ^a	1.51±0.03 ^b	1.41±0.13 ^b	4.33±20.25 ^a
50%	2.38±0.31 ^b	1.35±0.07 ^b	1.58±0.30 ^b	4.20±0.17 ^a
75%	2.05±0.04 ^b	1.61±0.07 ^b	1.61±0.07 ^b	4.50±0.14 ^a
100%	3.86±0.10 ^a	1.51±0.10 ^b	1.51±0.10 ^b	4.43±0.13 ^a

(1) Data is represented in mean ± S.E.
 (2) Means with the same alphabet superscript across row are not significant at (P > 0.05)

The significant reduction of sulphate in Table 2 was observed in day 4 in tannery dilution of 25%, 50%, 75% and 100% while in dilution of 10% and control there was no significant reduction and 0% and 5% dilution, there was significant increase because of addition of algae and medium. Most of the sulphate ion culminate are the major source of anion in industrial effluents discharged in receiving water bodies. In highly polluted wastewater when dissolved oxygen is low, sulphate serves as a substitute as electron acceptor to breakdown organic matter which produces

hydrogen sulphide (Alaguprathana *et al.*, 2015) whereas microalga tannery treatment, sulphate reduction is used as nutrient for algal growth (Azarpira *et al.*, 2014).

Table 3 shows decrease in dissolved oxygen in day 4 and day 8 can be attributed to active cellular respiration, nutrients are converted to biochemical energy such as ATP and oxygen serves as an electron acceptor (Perry *et al.*, 2007) while increased biomass and active photosynthesis is responsible for the increase of oxygen on day 12. This agrees with Promya (2008) which reports photosynthesis of the

algae may be the reason for increase in DO of municipal wastewater.

Tannery effluent are characterised with high BOD due to the presence of organic matter contributed by skin and hides of animal (Nanda, 2010). In Fig. 1, BOD reduction was not significant during the period of treatment which can be due to the time for the treatment whereas Sahu (2014) reports *Chlorella vulgaris* in waste water was able to reduce BOD by 70 % in a 21 days treatment period. Metabolism of organic matter by algae is possibly responsible for the BOD reduction. (Azarpira *et al*, 2014). The COD concentration as shown in Fig. 2 increased significantly in day 0 from initial to day 4 in 0% and 5% dilutions because of the addition of medium and algae at inoculation and a significant decrease was observed only in 75% and 100% dilutions. COD reduction is largely not

significant because it is accomplished exclusively by *C. vulgaris* whereas Kshirsagar (2014) findings of a mixed culture *Aspergillus niger* + *Chlorella vulgaris* removed COD at 72.26% or bacterial in vitro cultures reduced COD by 72.25% after a period of 72hours from sewage (Joshi and Sharma, 2002).

Comparative effect of *Chlorella vulgaris* on physicochemical parameters among treated tannery effluent (mg/L) in Table 4, TDS gives an indication that 25% dilution is not significantly different from BBM, the Sulphate concentration of 25% dilution was not significantly different from BBM and also associated with samples from 0% to 10% dilution. DO and BOD in all the dilutions were not significantly different but COD in BBM was comparable to 0% dilution and other dilution of tannery

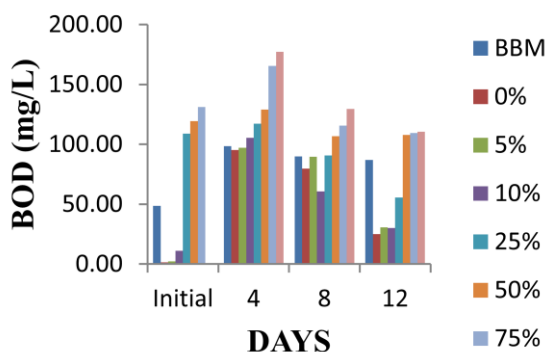


Fig. 1 Effect of *Chlorella vulgaris* on Biological Oxygen Demand (mg/l) at different dilutions treated tannery effluent

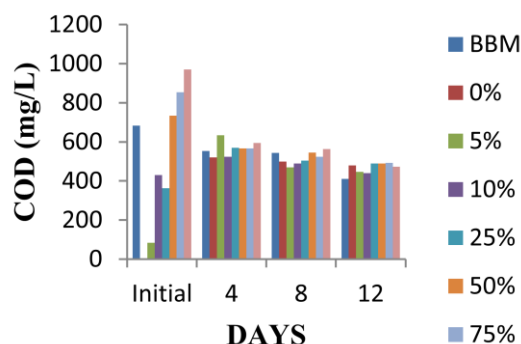


Fig. 2 Effect of *Chlorella vulgaris* on Chemical Oxygen Demand (mg/l) at different dilutions treated tannery

Table 4. Comparative effect of *Chlorella vulgaris* on physicochemical parameters among treated tannery effluent

	BBM	0%	5%	10%	25%	50%	75%	100%
TDS	510.50 ^d	76.38 ^f	173.88 ^e	246.57 ^e	559.14 ^d	879.40 ^c	2095.57 ^b	2649.00 ^a
Sulphate	131.25 ^{de}	108.88 ^e	82.50 ^e	100.00 ^e	194.29 ^d	278.00 ^c	417.14 ^b	506.25 ^a
DO	2.88 ^{ab}	3.89 ^a	2.26 ^b	2.76 ^{ab}	2.51 ^b	2.20 ^b	2.57 ^b	2.83 ^{ab}
BOD	80.99 ^a	50.34 ^a	54.94 ^a	57.83 ^a	95.04 ^a	114.60 ^a	131.93 ^a	104.31 ^a
COD	592.50 ^{abc}	366.25 ^d	422.50 ^{cd}	470.00 ^{bcd}	458.57 ^{bcd}	626.00 ^{ab}	614.29 ^{ab}	696.25 ^a

4. Conclusion

The use of *Chlorella vulgaris* in the treatment of tannery effluent has been shown to reduce TDS and sulphate significantly and significantly increase the dissolved oxygen content in the tannery effluent which will support other organism in the effluent. *Chlorella vulgaris* was not able to reduce BOD and COD which are important pollution indices in waste water owing to the complex nature of the effluent, hence treatment of tannery effluent should be in combination of

Chlorella vulgaris with either bacteria or fungi. *Chlorella vulgaris* treats tannery effluent effectively in high dilution especially 25% dilution as compared in low dilution such as 50% to 100%.

References

- Chia, M. A., Araujo, M. K. C. and Oliveira, M. C. B. (2015). Growth and antioxidant response of *Microcystis aeruginosa* (cyanobacteria) exposed to anatoxin – a. Harmful Algae, 49:135 – 146
- Midha, V. and Dey, A. (2008). Biological treatment of tannery wastewater for sulfide removal. International Journal of Chemical Sciences, 6(2):472-486.



Khopkia, S.M. (2009). Environmental Pollution monitoring and control. New Delhi India: New Age International (P) Limited. 299p.
Rajasulochana, P., Dhamotharan, R., Murugesan, S. and

Rama C. M. A. (2009). Bioremediation of Oil Refinery Effluent by Using *Scenedesmus obliquus*. Journal of American Science, 5(4):17-22.

**ABSTRACT CCT-: 019**Egere, B. C. ¹, Momoh, O.R. ² and Aderemi, B.O. ²¹ Department of Polymer and Textile Science, Ahmadu Bello University Zaria, Nigeria² Department of Chemical Engineering, Ahmadu Bello University Zaria, NigeriaEmail: idiche@yahoo.com**STUDYING THE OPTIMAL CONDITIONS FOR THE PRODUCTION OF GLUCOSE FROM HYDROLYSIS OF SPIROGYRA AFRICANA**

ABSTRACT: Various species of *Spirogyra* are being currently investigated for the production of biofuels but little attention has so far been paid to *Spirogyra africana* specie, a more abundant specie under Nigeria climate. Prior to hydrolysis, the samples were sun dried, sized to $\leq 125 \mu\text{m}$, and analyzed for carbohydrate content. Subsequently following the conventional unifactorial approach, attempt was made to determine the best conditions for the production of glucose from hydrolysis of *Spirogyra africana*. Proximate analysis showed that *Spirogyra africana* contains 39.72% carbohydrate. The reaction temperature, 25-30 °C, pH, 4.5, residence time of 48 hrs., substrate concentration, 50g/l and *A. niger* concentration of 0.6 % (w/v) were found to be the optimal conditions for the production of glucose from *Spirogyra africana* and a glucose yield of 31.47(w/w %) dry basis was achieved.

Keywords: Glucose, Algae biomass, optimal conditions, Hydrolysis, *Spirogyra Africana*

1. Introduction

Renewable and sustainable fuels development has been a major venture owing to the anticipated shortage of fossil fuels and climate change. Bio-ethanol has been proposed as a viable alternative to gasoline. Established biomass for bioethanol production could come from different sources such as grains, tubers and fibres, of these, fibers (lignocellulose) are the most abundant, sustainable, cheapest, and less competing with human food chain (Salvi, *et al.*, 2010 and Dias *et al.*, 2009). The conversion technology of fibres are challenging due to the crystalline nature of cellulose, the resistance of lignin to degradation and multiple products due to hemicellulose lignin degradation making substrate pretreatment and indispensable step in lignocellulosic utilization in glucose production (Guo *et al.*, 2015). The enzymatic hydrolysis of cellulose equally requires the synergistic action of multiple enzyme components having different mechanisms of action (Cannella *et al.*, 2014). These enzymes are found commonly in fungal species like *Aspergillus niger* (Steffien *et al.*, 2014 and Holzapple *et al.*, 1990). The exoglucanases bind to the reducing and non-reducing ends of the cellooligomers converting the same to cellobiose and the final component that acts is the β -glucosidase, which converts cellobiose to glucose (Bravo *et al.*, 2000 and Margaritus and Creese 2001). In addition to the quantity and quality of enzymes, maintaining optimal operating conditions like temperature and pH is also important (Juturu and Wu 2014, Kostylev and Wilson 2012). The typical operating temperature for cellulose hydrolysis ranges between 40 and 55 °C, and pH 4.5 and 5.0 (Guo *et al.*, 2015, Cannella *et al.*, 2014). Algae offer many advantages that approve its utilisation for glucose production: They grow easily without soil, hence do not compete with agricultural food production, capture CO₂ for photosynthesis to reduce greenhouse gas

emissions (Razif and Michael 2011, Chiti 2008) and possess a very short harvesting cycle (1–10 days) compared to other bio-ethanol feedstock (Razif and Michael 2011). These and other advantages bequeath algae with a sufficient capacity to replace existing bioethanol modalities (Chiti 2007 and Eshaq *et al.*, 2010). This work focuses on the optimal conditions for glucose production (being a necessary intermediate in bioethanol production) from *Spirogyra africana* to save cost, time, and energy as well as improve the efficiency of glucose production form *Spirogyra africana*.

2. Methodology:

The algae, *Spirogyra africana* was collected from Ahmadu Bello University (A.B.U.) Zaria's Dam. The samples were collected in sterile containers and transferred to the laboratory.

The substrates were hydrolyzed to fermentable sugar (glucose) by treatment with *Aspergillus niger* of concentration between 0-1.3 % (w/v), these were done after pH adjustment of the mash. The pH, substrate concentration, temperature, contact time, *Aspergillus niger* concentration were varied during the saccharification of *Spirogyra africana* substrate in order to determine the optimum conditions for glucose production. The results of the research work were observed, recorded and analysed. The optimal contact time was studied by keeping other parameters constant thus; temperature at 30 °C, pH at 4.5 substrate concentration at 50 g/L, and *A. niger* concentration at 0.6 % (w/v). The initial sugar concentration was observed and the subsequently sugar concentrations were recorded after every 24 hours for 6 days. The optimal substrate concentration was studied at different *Spirogyra africana* concentrations between 1.0 - 8.0 % (w/v), at 2.0 % (w/v) interval and at constant temperature of 30 °C, pH of 4.5, substrate concentration of 50 g/L,

residence time of 2 days and *A. niger* concentration of 0.6 % (w/v). In order to determine the optimal cell loading for glucose production, saccharification was carried out at different *Aspergillus niger* concentrations between 0.2 – 1.0 % (w/v) at 0.2 % (w/v) interval, and at constant temperature of 30 °C, pH of 4.5, 2 days residence time and 50 g/L substrate concentration. The optimal temperature study was carried out at different temperature of 25-45 °C at 5 °C interval using the incubator at constant pH of 4.5, substrate concentration of 50 g/L, residence time of 2 days and *A. niger* concentration of 0.6 % (w/v). The optimal pH was investigated by carrying out the saccharification at pH of 3.5-6.0 at 0.5 interval using sodium acetate buffer at constant temperature of 30 °C, 50 g/L substrate concentration, 2 days residence time and *A. niger* concentration of 0.6 % (w/v).

2.1 Glucose Determination

Table 1: Proximate Analysis of the *Spirogyra africana*

Sample Name	% Moisture	% Ash	% Lipid	% Protein	% fibre	% CHO
<i>Spirogyra africana</i>	1.05	31.03	3.00	5.05	20.05	39.72

3.2. Effect of substrate concentration on saccharification

According to the result shown in Figure 1, the glucose concentration was increasing gradually as substrate concentration increased from 10 g/l to 40 g/l. The highest glucose concentration of 12820 mg/l was achieved at substrate concentration of 50 g/l. However, at concentrations beyond 50 g/l, a decline in

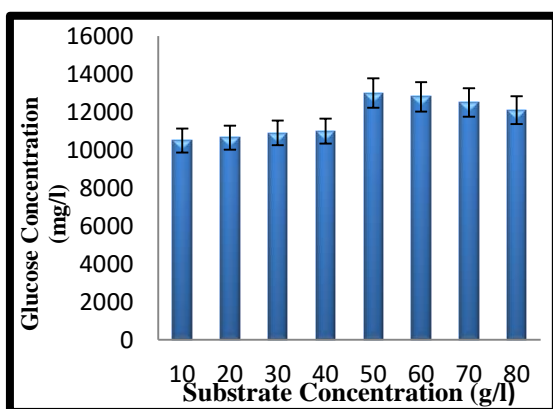


Figure 1: Effect of substrate concentration on saccharification at a fixed *A. niger* concentration 0.6 % (w/v), pH 4.5, particle size $\leq 125 \mu\text{m}$, temperature 30 °C and contact time of two (2) days.

The quantitative determination of glucose was done using the UV-spectrophotometer at constant wavelength of 550 nm using distilled water as blank and calibration curve prepared in conjunction with Beer Lambert Law was used to estimate the amount of glucose.

3. Results and Discussion

The results of this research work on studying the optimal conditions for production of glucose for bioethanol production from *Spirogyra africana* are:

3.1 Proximate analysis of the *spirogyra africana*

The result gotten from proximate analysis of *Spirogyra africana* on dry basis shows that it contains 39.72 wt % carbohydrates, which makes it a good candidate for glucose production and a further break down of the carbohydrates shows it contains starch and cellulose, which makes the choice of *A.niger* appropriate (Carvalho *et al.*, 2013).

amount of glucose produced was observed signify substrate inhibition. Eshaq *et al.*, (2010) also reported 50 g/l as the optimum substrate concentration for *Spirogyra singularis* saccharification whereas (Razif and Michael (2011) reported 10 g/l as the optimum substrate concentration for glucose production from microalgal.

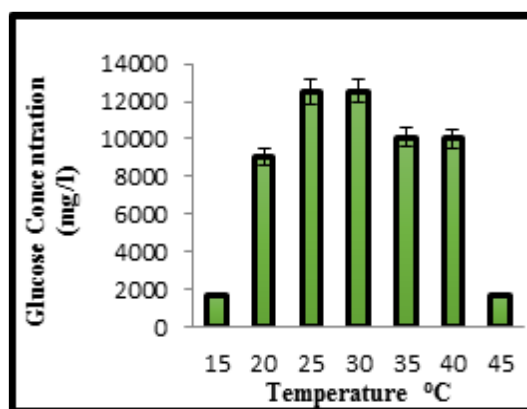


Figure 2: Effect of temperature on saccharification at *A. niger* concentration of 0.6 % (w/v), pH of 4.5, particle size of $\leq 125 \mu\text{m}$, substrate concentration of 50 g/l, and residence time of two (2) days.

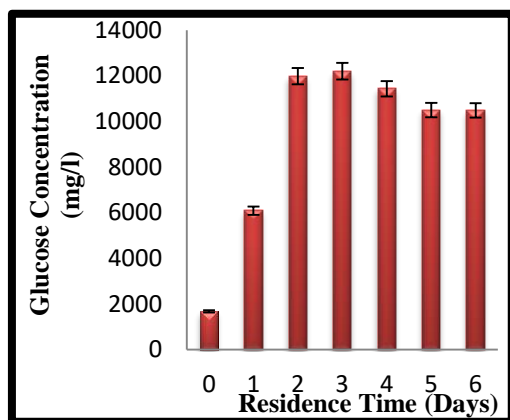


Figure 3: Effect of contact time on saccharification at a fixed *A. niger* concentration of 0.6 % (w/v), pH of 4.5, particle size of $\geq 125\mu\text{m}$, substrate concentration of 50 g/l, and temperature of 30 °C.

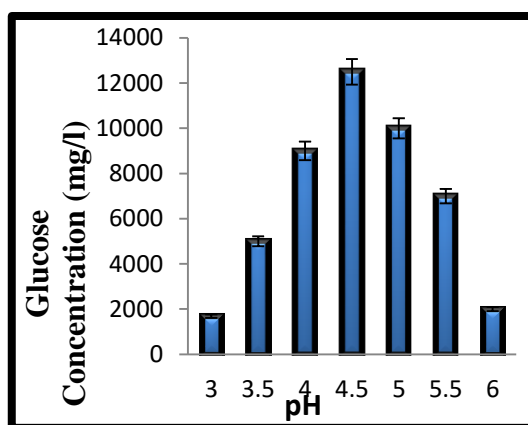


Figure 4: Effect of pH on saccharification at a fixed *A. niger* concentration of 0.6 % (w/v), contact time of two (2) days, particle size $\leq 125\mu\text{m}$, substrate concentration of 50g/l, and temperature of 30 °C

3.3 Effect of temperature on saccharification

Figure 2 shows that at 15 °C the concentration of glucose production was 1680 mg/l, the glucose production increased gradually from 15°C to 25°C, highest production was recorded between 25 °C to 30 °C, which witnessed a decline at temperature above 30 °C. This shows that *A. Niger* performs best at temperature range between 25-30 °C when used to hydrolyse *Spirogyra africana* biomass. It implies that hydrolysis can be done at room temperature, hence reduced energy requirement. This compares favourably with other works (Eshaq *et al.*, 2010 and Kadam *et al.*, 2004) that reported 30 °C as the optimum temperature for *Spirogyra singularis* saccharification. However, 45 °C was reported as the optimum temperature for elephant grass, maize and rice straw hydrolysis (Aiyejagbara *et al.*, 2016, Cannella *et al.*, and Aderemi *et al.*, 2008) using the same fungus. This discrepancy is likely due to high lignin in elephant grass, maize and rice straw, which needs a higher temperature for unbundling. This finding underscores the fact that optima temperature is a function of the substrate texture and the cell specie involved in hydrolysis.

3.4 Effect of contact time on saccharification

It was observed as shown in Figure 3 that the initial free sugar was about 1680 mg/l which increased after 1 day to 6090 mg/l and further rapidly to 11680 mg/l after 2 days. After 3 days, there was only a slight increase in the concentration of glucose produced which is statistically insignificant ($P > 0.05$) when compared with the glucose produced after 48 hrs saccharification. Hence, contact time of 2 days was taken as the optimum hydrolysis duration. At residence time of 4, 5 and 6 days there is a decline in the concentration of

glucose produced which may be due to the glucose formed being consumed or the process being inhibited. Similar result was reported by Eshaq *et al.*, (2010) while hydrolysing *Spirogyra singularis* whereas witnessed a steady increase in the amount of sugar released for over were reported 72 hrs while hydrolyzing sugarcane, elephant grass and maize (Dias *et al.*, 2009, Aiyejagbara *et al.*, and Jorgensen *et al.*, 2007), which may not be unconnected with the differences in the temperatures of the substrates involved.

3.5 Effect of pH on Saccharification

The effect of pH on saccharification was studied and its result in Figure 4 shows that at pH of 3.0 the glucose produced was 1690mg/l, between pH of 3.0 and 4.0 there was a gradual increase in the concentration of glucose produced. At pH 4.5, the maximum concentration of glucose was produced but a decline in glucose concentration was observed at 5.0 pH and beyond. This shows that *A. Niger* cells perform best at pH 4.5. Likewise, the work of (Dias *et al.*, 2009, Aiyejagbara *et al.*, and Jorgensen *et al.*, 2007) reported pH of 4.5 as the best saccharification pH for various lignocellulosic biomasses (sugarcane, elephant grass and maize) using *A. niger*.

3.6 Effect of Aspergillus Niger Concentration on Saccharification

The effect of *Aspergillus niger* concentration was studied. The result presented in Figure 5 shows that the sample contained initial glucose (free sugar) concentration of 1680 (w/v) %. At cell loading of 0.2 (w/v) %, 4000 (mg/l) of glucose was produced. There was gradual increase in the concentration of glucose produced as cell loading increased from 0.2 (w/v) % to 0.4 (w/v) %, whereas glucose production was very rapid at cell loading of 0.4

(w/v) % and 0.6 (w/v) %, maximum production was observed at a cell loading of 0.6 (w/v). Thus 0.6 (w/v) % was taken as the optimal cell loading. Cell loading beyond 0.6 (w/v) % produced a slight decline in the glucose concentration. This may be because of

cells activity inhibition due to high toxicity of glucose in the media (Dias *et al.*, 2009, Aiyejagbara *et al.*, and Jorgensen *et al.*, 2007) Reported 0.6 (w/v) % as the best cell loading for elephant grass and sugarcane baggers respectively using *A.niger*.

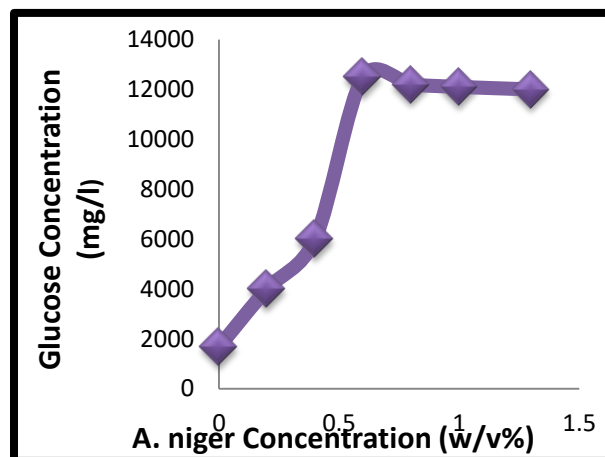


Figure 5: Effect of *A. Niger* Concentration on Saccharification at a fixed pH of 4.5, residence time of two (2) days, particle size of $\leq 125\mu\text{m}$, substrate concentration of 50 g/l, and temperature of 30 °C

Conclusion

1. The untreated biomass sample at two (2) days hydrolysis period with glucose yield value of 31.47 wt/wt % was chosen as ideal for saccharification in this study on economic considerations.
2. The optimal processing conditions for the hydrolysis are: Soaking temperature = 25-30 °C; pH = 4.5, Contact time = Two (2) days, Substrate Concentration = 50 g/l, *A. niger* concentration = 0.6 % (w/v).

References

A. Margaritus, E. Creese, (2001). Thermal stability characteristics of cellulase produced by *Sporotrichum Thermophile*, *Biotechnol. Lett.* 3 471–476.

B.O. Aderemi, E. Abu and B. K. Highina (2008) The kinetics of glucose production from rice straw by *Aspergillus niger* Vol.7 (11), pp. 1745-1752, June 2008 DOI: 10.5897/AJB08.109 ISSN: 1684-5315.

D. Cannella, H. Jørgensen, (2014). Do new cellulolytic enzyme preparations affect the industrial strategies for high solids lignocellulosic ethanol production? *Biotechnol. Bioeng.* 111 59–68.

D. Cannella, H. Jørgensen, (2014). Do new cellulolytic enzyme preparations affect the industrial strategies for high solids lignocellulosic ethanol production? *Biotechnol. Bioeng.* 111 59–68.

D. Steffien, I. Aubel, M. Bertau, (2014). Enzymatic hydrolysis of pre-treated lignocellulose with *Penicillium verruculosum* cellulases, *J. Mol. Catal. B-Enzym.* 103 29–35.

D.A., Salvi, G.M., Aita, D., Robert and V., Bazzan (2010) Ethanol production from sorghum by dilute ammonia pre-treatment. *Jind microbial Biotechnol*; 37:27-34.

F, S. Eshaq, N. A. Mir, and K. M. Mazharuddi, (2010). *Spirogyra* biomass a renewable source for biofuel (bioethanol) Production. *International Journal of Engineering Science and Technology* Vol. 2(12), 2010, 7045-7054

F. S. Eshaq, N. A. Mir, and K. M. Mazharuddi, (2010). *Spirogyra* biomass a renewable source for biofuel (bioethanol) Production.

H. Guo, S. Zou, B. Liu, R. Su, R. Huang, W. Qi, et al., (2015). Reducing β -glucosidase supplementation during cellulase recovery using engineered strain for successive lignocellulose bioconversion, *Bioresour.Technol.* 187 362–368.

H. Jørgensen, J.B. Kristensen, C. Felby, (2007) Enzymatic conversion of lignocellulose into fermentable sugars: challenges and opportunities, *Biofuels. Bioprod. Biorefin.* 1 119–134.

H., Razif and K.D., Michael (2011) Influence of acid pre-treatment on microalgal biomass for bioethanol production. *Process Biochemistry* 46 (2011) 304–309.

**ABSTRACT CCT-: 077**Ibraheem, A. S¹., Danmallam, A. A^{1*}., Salisu M²., Musa M¹., Igunnu, A³., and Malomo, S. O³.¹Department of Basic Research, National Research Institute for Chemical Technology, Zaria²Department of Industrial and Environmental Technology, National Research Institute for Chemical Technology, Zaria³Department of Biochemistry, Faculty of Life Sciences, University of Ilorin, Ilorin, NigeriaEmail: daddinanna@gmail.com**PRELIMINARY STUDIES OF PECTIN FROM *Adansonia digitata* L. PULP**

ABSTRACT: Pectin was extracted from the pulp of *Adansonia digitata* L. at 60°C using acidified water for 120 minutes. The physicochemical properties of the extracted pectin were evaluated and its FTIR spectra analysis and was compared with citrus pectin. The extract contained 3.21% protein with percentage yield of 13.13g. The water holding capacity (solubility) and oil holding capacity were 82.93% and 7.10g/g respectively. Functional groups such as -OH, C=O and methyl groups were also detected from the FTIR spectra analysis. The findings from this study suggest that the extract from *Adansonia digitata* L. pulp may be useful in food industry where high oil retention capacity is required to improve the quality of their baked products.

Keywords: Extraction, Pectin, Physicochemical properties

1. Introduction

Plants are an integral part of human life. They fulfill basic needs such as food, shelter, fuel, medicine (Bukar, 2014). One of the plants that have been reported to provide these services is *Adansonia digitata* L. It is commonly known as baobab and is a native deciduous tree from the African savanna. (UNCTAD 2005). Every part of this plant has been reported to be useful (Kabore et.al, 2011). Increasing demands for novel additives from natural sources in the food industry have stimulated research activities in this direction especially from agro wastes. This is because plant materials have been proven to be versatile functional ingredients and biologically active components in food. They have broad applications in the areas of foods as thickener, gelling agent, emulsifier, coating, fat substitute and radical-scavenging agent (Castro, Tirapegui, & Benedicto, 2003; Ebringerova, et al., 2008). One of the plant-derived materials that has been found to be useful in these areas is pectin and its derivatives.

Pectin plays an important role in food processing as food additives and as a source of dietary fiber. Its important in the modification of texture in jams, jellies, confectionery and low fat dairy products (Rain, 1998). Pectin is a class of complex polysaccharides found in the cell walls of higher plants, where they function as hydrating agent and cementing material for the cellulosic network (Beli, 2009). It is also used as ingredients in pharmaceutical preparations such as antidiarrheal, detoxicant and demulcent formulations (Voragen, Pilnik, Thibault, Axelos, & Renard, 1995). It is considered a safe additive with no limits on acceptable daily intake (FAO, 1969).

Pectin isolated from *Adansonia digitata* L. was evaluated as a substitute in jam preparation but its physicochemical properties have not been reported in open scientific literature. This

study therefore aims to determine the functional/physicochemical properties of pectin isolated from *Adansonia digitata* L pulp.

2. Materials and Methods

2.1 Materials

The baobab fruits were obtained from Basawa village, of Sabon Gari LGA, Kaduna State Nigeria. The pulp was separated from the seeds pulverized. All chemicals used in the experiment were analytical grade.

2.2 Isolation of Pectin from Baobab Pulp

50g of the Baobab pulp was weighed and blended with 300ml distilled water. The water to be used for extraction was acidified using 40% nitric acid and pH was maintained at 2.0. The acidified mixture blended with the baobab pulp was then heated at 60°C for about 120mins. After the heating period was over, the mixture was passed through two-fold muslin cloth and cooled at room temperature. Ethyl alcohol was used as a precipitating agent for pectin.

2.3 Gel Preparation

Gels (0.5% w/w) were prepared by dry-mixing 0.2g of the extracts with 32.5g of sucrose. 50ml of citrate buffers at pH 2 were then added to the mixtures and heated at 100°C/360RPM using a magnetic stirrer until the mixture dissolved. The gel was allowed to stand at 4°C for 18 hours prior to analysis.

2.4 Flow Analysis

The flow behaviors in the gels were examined using Brookfield Rheometer (DV3T) machine to measure the viscosity at different temperature and time.

2.5 Solubility Test

Samples (0.1g) were suspended with 15ml buffer solution at pH 2. The suspensions were incubated at room temperature with constant shaking (200rpm) for 9 hours. The suspensions were then centrifuged at 5000g for 15mins. The supernatant was dried at 50°C in the oven until constant weight is achieved. Percentage of solubility was calculated as follows:

$$\% \text{ solubility} = (W_s/W_i) \times 100$$

Where W_i = initial weight

Ws = weight of dried supernatant.

3. Results and Discussion

The result of the physicochemical properties of the extracted pectin is shown in Table 1. The percentage yield of the pectin was 13.13% which indicates that *Adansonia digitata L.* pulp is a rich source of pectin as reported by the previous researchers. Solubility and oil holding capacity of the extract were 82.93% and 7.10g/g respectively. These properties depend on the amount and the nature of the fiber present in a sample. High oil holding capacity in this study indicates that the pulp of *Adansonia digitata L.* has high content of soluble fiber which allows the extract to retain oil due to its hydrophobic nature and particle sizes. High oil holding capacity of the extract may encourage its incorporation in baked products in order to impart freshness and softness in them. However, non-greasy sensation in fried product requires low oil holding capacity additives.

The FTIR analysis was performed in order to

identify the major functional groups in the extract (Figure 1). In order to confirm the identity of *Adansonia digitata L.* extracts, these spectra were compared with CP (Figure not shown). It was apparent that the FTIR spectra of extract exhibited similarities of the % transmittance (%T) patterns to that of CP. It was suggested that the extract was pectin-like polysaccharides. Further analysis of each b. and was also conducted. A broad band of %T between 2500 and 3600 cm⁻¹ which is due to OH stretching was exhibited. This band might be due to the inter/intra-molecular hydrogen bonding of the galacturonic acid backbone (Singthong et al., 2004). An O-CH₃ stretching band would be expected between 2950 and 2750 cm⁻¹ as observed in all samples which usually refers as C-H adsorption which include CH, CH₂, and CH₃ stretching and bending vibrations. This might be due to the presence of methyl ester group of galacturonic acid (Singthong et al., 2004)

Table 1. Physicochemical properties of pectin from *Adansonia digitata L.* pulp

Parameters	% yield	Protein content	Solubility (%)	Oil Holding Capacity (g/g)
Sample	13.13%	3.21%	82.93	7.10

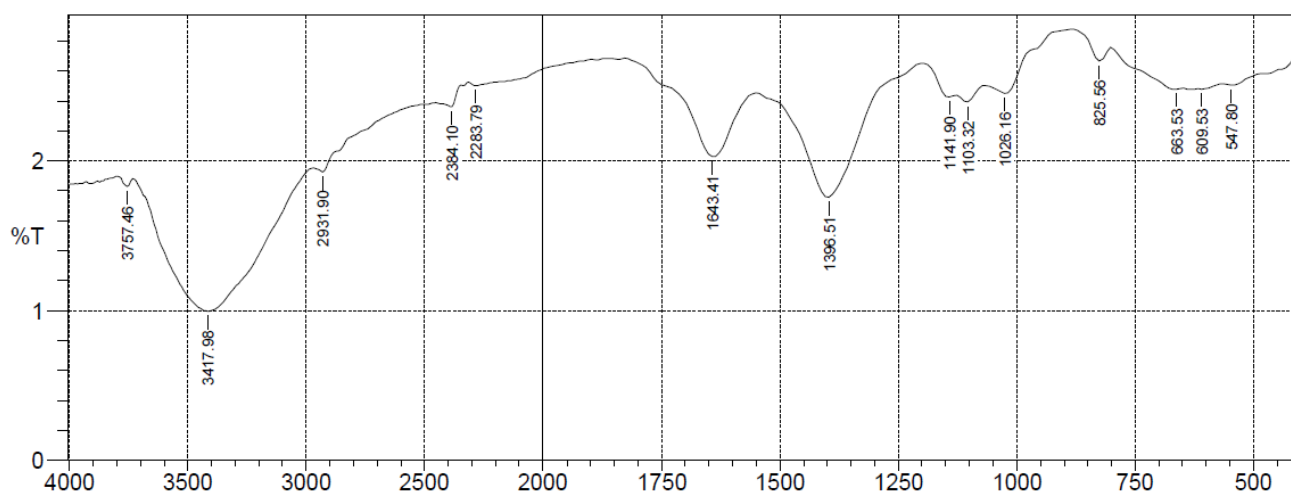


Figure 1: FTIR analysis of the pectin extracted from *Adansonia digitata L.* pulp.

Conclusion

Pectin was extracted from the pulp of Adansonia digitata L. and the extract analyzed for the physicochemical analysis. The results obtained from the study indicate that value-added products could be developed from the pulp of Adansonia digitata L. which may be useful in the food industry.

References

Beli et al, B. R. (2009). Critical reviews in food science and Nutrition.
 Bukar et al. (2015). Evaluation of phytochemical and potential antibacterial. *Journal of pharmacognosy and phytochemistry*.
 Castro, I. T. (2003). Effects of diet supplementation with three soluble polysaccharides on serum lipid levels of hypercholesterolemia rats. *Food Chemistry*, 323-330.

FAO. (1969). Nutrition Meetings, rep. ser. No. 46A. 133.
 Singthong et al. (2004). structural characterization, degree of esterification and some gelling properties of pectin. *carbohydrate polymers*, 58, 391-400.
 Thibault, J. F., & Ralet, M. C. (2001). In Advanced Dietary Fibre Technology. *Blackwell Science*, 369-378.
 Voregen, A. e. (1995). food polysaccharides and their applications. *Mercel Dekker*, 287-340.

**ABSTRACT CCT-: 054**A.Y. Waziri¹, A.A. Osigbesan², F.N. Dabai¹, A.Y. Atta² and B.Y. Jibril¹

Chemical Engineering Department, Ahmadu Bello University, Zaria

2 Petrochemicals and Allied Department, National Research Institute of Chemical Technology, Zaria

Email: abubakaryusufwaziri@gmail.com**CATALYTIC REFORMING OF GASEOUS PRODUCT FROM PYROLYSIS OF LOW DENSITY POLYETHYLENE: CATALYSTS PREPARATION AND CHARACTERIZATION**

ABSTRACT: Plastic wastes are now a scourge to the environment (air, land and water). These materials exhaust the landfills, and endanger wild and civil life. It is predicted that petroleum resources are decreasing, while demands for petrochemicals are increasing for both industrial uses and energy production. Therefore, it is important to provide an alternative to petroleum resources as well as an alternative solution for eliminating waste plastics by recycling methods (thermal or catalytic decomposition) that convert these wastes to fuels. Therefore, a two-stage catalytic degradation process of low density polyethylene using ZSM-5 (loaded with iron) was carried out in this work. Four types of ZSM-5 were prepared and characterized using X-ray diffraction (XRD), Fourier transform infrared spectroscopy (FTIR) and Brunauer-Emmett-Teller (BET). The commercial ZSM-5 was calcined at 500°C to obtain H-ZSM-5, which was acid treated at room temperature and then modified by metal (iron) impregnation with loading of 0.3, 0.6 and 1 wt% on the ZSM-5 zeolite support respectively. The XRD patterns showed that the structure of the ZSM-5 catalysts remained intact for the four samples. The FTIR spectra also showed that there was no structural deformation of the catalysts even after modification, while the BET surface area of all the four catalysts showed a trend of improvement in the physicochemical properties of the ZSM-5 zeolite as the iron loading increased. The surface area was highest for the acid treated ZSM-5 (518.6168 mm²/g), and the pore sizes ranged from 1.8106 - 1.9810 nm for all four catalysts.

Keywords:**1. Introduction**

Many varieties of materials used on a daily basis are made from petroleum derivatives called plastics. Plastics have revolutionized the quality of life, and increasingly many new life-saving devices are and will be made of them. They are so dependable nowadays that it seems without plastics, human being would have a hard time managing normal living. However, enormous volumes of plastics composed of bags, dishes, packing materials, etc., after daily use, generate billions of tons of non-degradable wastes. Plastics have unique properties because of strong chemical bonds which make them adequate for many applications; however, these bonds are not biodegradable. Thus plastic waste quickly become pollutant to the environment (air, land and water), exhaust the landfills, and endanger wild and civil life (Hamidi et al. 2013). It is predicted that petroleum resources are decreasing, while demands for petrochemicals are increasing by hours for both industrial uses and energy production (Gumula et al. 2009). Therefore, it is important to provide an alternative to petroleum resources. It has been suggested that the portion of petroleum used to fabricate household materials could be recovered by thermal or catalytic decomposition of these plastic wastes. Therefore, the conversion of waste plastics to fuel has several benefits. First, it steps up a new cycle of consumption to nonrenewable energy sources. Second, it also provides a considerable source of petrochemicals that reduces the expenditure of nonrenewable energy resources. Third it establishes an effective, innovative, and alternative solution for eliminating waste plastics, consequently,

preventing them from polluting the environment either through incineration or filling up landfills and waterways (Sarker, Rashid, et al. 2012; Sarker, Mamunor Rashid, et al. 2012, Kumar et al. 2011).

Thermo-catalytic pyrolysis of refuse derived fuels using different catalysts was conducted in a two stages process by Miskolczi et al. (2010). The first stage was a pure thermal pyrolysis in a horizontal tubular reactor with feed rate of 0.5 kg/h. In the second stage, a semi-batch process in the presence of ZSM-5 and zeolite Y catalysts was used. Results showed that the tested catalysts significantly affected the quantity of products. E.g. gas yield could be increased by 350% when ZSM-5 catalyst was used, and the pyrolytic oil could be increased by 115% when zeolite Y was used.

2. Materials and Methodology**2.1 Materials:**

The materials used for this study include: Commercial NH₄-ZSM-5(Si/Al=50), Iron III nitrate nanohydrate, distilled water, spatula, filter paper, funnel, retort stand, beakers, conical flask, measuring cylinder, digital thermometer and crucibles.

2.2 Preparation of the catalysts

Fe₂O₃-ZSM-5 zeolite sample was prepared using ion exchange method following the procedure of Sun et al. (2006). Commercial NH₄-ZSM-5 (supplied from Zeolyst CBV 55246, with Si/Al = 50 and surface area = 425 m²/g was dissolved in 500 ml of distilled water. The resulting solution was treated with 500 ml of 1 molar solution of HCl under reflux condition at a pressure of 1 atm for 1 hour, to activate the catalyst (H- ZSM-5). The sample was filtered, washed with distilled water, dried

at 80°C for 10 hours, crushed and then calcined in air for 3 hours at 500°C to activate the acidity of the catalysts (H-ZSM-5). 20 g of the H-ZSM-5 and a required amount of precursor ($\text{Fe}(\text{NO}_3)_3 \cdot 9\text{H}_2\text{O}$) was also dissolved in 500 ml and 100 ml of distilled water respectively. The two resulting solution was mixed in a drop wise manner under the reflux condition at 1 atm for 3 hours to have a uniform dispersion of the active site. The sample was dried at 80 °C for 10 hours, crushed and then calcined in air for 3 hours at 500 °C. The samples were labeled A1, A2, A3, A4 and A5, for the commercial ZSM-5, acid treated ZSM-5, iron loaded on ZSM-5 (Fe_2O_3 -ZSM-5) with 0.3, 0.6, 1 %wt. loading of iron and Si/Al =50

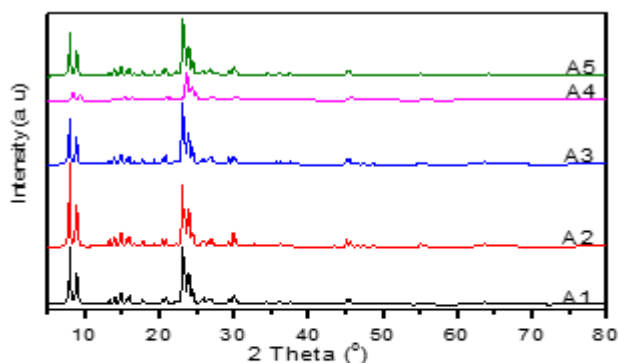


Figure 1: XRD pattern of ZSM-5 Si/Al =50; (A1) conventional ZSM-5, (A2) acid treated ZSM-5, (A3) 0.3wt% iron loading on ZSM-5, (A4) 0.6 iron loading on ZSM-5, and (A5) 1wt% iron loading on ZSM-5

The figure also shows that there is a minor decrease in the intensity of the diffraction peak after iron inclusion in A4. This is probably as a result of uneven dispersion of iron oxide sample in the ZSM-5 channels. The typical diffraction lines for iron oxide were not visible in the diffractograms of all the samples. This lack of X-ray diffraction pattern for iron oxide may be because iron oxide was not uniformly dispersed in the material or as a result of the small amount(s) of iron loaded (Aziz et al. 2016). Thus the diffraction patterns of the Fe_2O_3 -ZSM-5 samples resemble that of the H-ZSM-5 parent material with no extra peak(s) belonging to the other phases present which is similar to that reported in literature (Zhao et al. 2005). In particular, there are no increase in the intensity(ies) of the peaks at 2 θ value(s) of

respectively.

3. Result and Discussion

3.1 Catalysts Characterization

Figure 1 shows the X-ray diffraction pattern of the different Fe-ZSM-5 samples prepared by impregnation method. The results show that there were reflection peaks at 2 θ value(s) of 7.99°, 9.14°, 23.21°, 23.64°, and 24.38°, which corresponds to the framework structure of ZSM-5 (Khoshbin & Karimzadeh 2017). The sharpness of the peak(s) suggests that all solids are characterized by a good crystallinity. The results indicate that the zeolite structure of ZSM-5 was maintained even after treatment and modification.

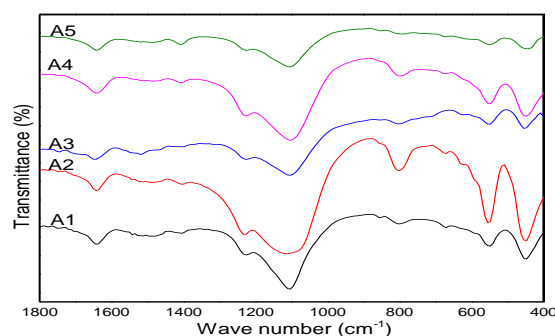


Figure 2: FTIR spectra of ZSM-5 Si/Al=50; (A1) conventional ZSM-5, (A2) acid treated ZSM-5, (A3) 0.3wt% iron loading on ZSM-5, (A4) 0.6 iron loading on ZSM-5 and (A5) 1wt% iron loading on ZSM-5.

33.15° and 35.65° (which indicate the presence of iron oxide). This may be because the loading of the iron is less than 5 wt. %, as reported in literature (Calsavara & Luciano 2008).

The most important physicochemical properties of the ZSM-5 and the modified catalysts (Fe_2O_3 -ZSM-5) used in the catalytic upgrading of pyrolytic gaseous product of low density poly ethylene are presented in Table 1. The results show that following the initial acid treatment, the surface area of the catalyst increased slightly. When the acid treated catalyst was then impregnated with Iron, the surface area decreased significantly. However, subsequent increase in the iron loading (impregnation) resulted in increase in the surface area. This could be attributed to dealumination of zeolite by the acid treatment.

**Table 1.** Physicochemical properties of ZSM-5 Si/Al=50; (A1) conventional ZSM-5, (A2) acid treated ZSM-5, (A3) 0.3wt% iron loading on ZSM-5, (A4) 0.6wt% iron loading on ZSM-5, and (A5) 1wt% iron loading on ZSM-5

Sample	BET area (m ² /g)	Surface Langmuir surface area (m ² /g)	Micro pore volume (cm ³ /g)	Average pore size (nm)
A1	342.5240	459.5942	0.1655	1.9326
A2	348.0381	467.2876	0.1724	1.9810
A3	152.7611	208.2078	0.1875	1.9643
A4	247.7233	326.7099	0.1121	1.8106
A5	391.9352	518.6168	0.0750	1.9151

BET Surface area and the Langmuir Surface area show that A5, which represents the highest (1wt.%) iron loading on ZSM-5, has the highest surface area compared to the other catalysts, including the conventional ZSM-5 zeolite. Table 1 also shows that the micro pore volume(s) of the modified catalysts A4 and A5 were significantly lower compared to that of the conventional ZSM-5 zeolite while A2 and A3 were higher. The results correspond with the expectation of an increase in pore volume after the acid treatment and a decrease on iron loading (Aziz et al. 2016). Nevertheless, the micro pore volume(s) and the average pore size(s) of all of the samples (A1-A5) are within the range of the standard values (less than 2 nm) (Agullo et al. 2007).

The confirmation of the XRD result was done by FTIR measurement. Figure 2 shows the FTIR spectra (400-1800 cm⁻¹) of all the catalysts (samples).

In Figure 2, the first two characteristic bands observed are; one at 1220 cm⁻¹, which denotes the T-O-T asymmetric stretching mode (between TO4 tetrahedral), typical of well crystallized zeolites, and another at 550 cm⁻¹, which denotes the asymmetric stretching mode of the five-membered rings of the pentasil ZSM-5 zeolite structure, which is absent in amorphous materials (Figueiredo et al. 2016). The symmetric stretching vibration of Si-O-Al framework can also be seen at wavenumber(s) of 550cm⁻¹, 450 cm⁻¹, 1050cm⁻¹ and 1200cm⁻¹. These wavebands increase to higher values for A2 (due to the effect of the acid treatment) and decreases for A3, A4 and A5 (due to the Fe₂O₃ impregnation). In addition, the stretching vibration(s) at 1350cm⁻¹, 1500cm⁻¹, 1600cm⁻¹ and 1700cm⁻¹ indicate the bending vibration of O-H-O. The intensities reduce and broaden for A3, A4 and A5, as a result of Fe₂O₃ impregnation. While it becomes sharper for A2 (acid treated ZSM-5) implying pores were opened more, hence the metal impregnation inside the inner pores of the catalyst was achieved, as reported in literature (Aziz et al. 2016). These show that there is no structural damage, and the ZSM-5 samples catalyst have their distinct properties.

4. Conclusions

It can be concluded that the four catalysts prepared and characterized have physicochemical properties (such as microspore sizes of less than 2 nm) required for catalytic upgrading and reforming of liquid fuels.

References

- Agullo, J. et al., 2007. Catalytic pyrolysis of low density polyethylene over H-β, H-Y, H-Mordenite, and H-Ferrierite zeolite catalysts: Influence of acidity and structures. *Kinetics and Catalysis*, 48(4), pp.535–540.
- Aziz, A., Kim, S. & Kim, K.S., 2016. Fe/ZSM-5 zeolites for organic-pollutant removal in the gas phase: Effect of the iron source and loading. *Journal of Environmental Chemical Engineering*, 4(3), pp.3033–3040. Available at: <http://dx.doi.org/10.1016/j.jece.2016.06.021>.
- Calsavara, V. & Luciano, M., 2008. Transformation of ethanol into hydrocarbons on ZSM-5 zeolites modified with iron in different ways., 87, pp.1628–1636.
- Figueiredo, A.L. et al., 2016. Catalytic cracking of LDPE over nanocrystalline HZSM-5 zeolite prepared by seed-assisted synthesis from an organic-template-free system. *Journal of Analytical and Applied Pyrolysis*, 117, pp.132–140.
- Gumula, T., Paluszkiwicz, C. & Blazewicz, S., 2009. Study on thermal decomposition processes of polysiloxane polymers-From polymer to nanosized silicon carbide. *Journal of Analytical and Applied Pyrolysis*, 86(2), pp.375–380.
- Hamidi, N. et al., 2013. Pyrolysis of Household Plastic Wastes. *British Journal of Applied Science & Technology*, 3(3), pp.417–439.
- Khoshbin, R. & Karimzadeh, R., 2017. The beneficial use of ultrasound in free template synthesis of nanostructured ZSM-5 zeolite from rice husk ash used in catalytic cracking of light naphtha: Effect of irradiation power. *Advanced Powder Technology*. Available at: <http://dx.doi.org/10.1016/j.appt.2017.01.001>.
- Kumar, S., Panda, A.K. & Singh, R.K., 2011. A review on tertiary recycling of high-density polyethylene to fuel. *Resources, Conservation and Recycling*, 55(11), pp.893–910. Available at: <http://dx.doi.org/10.1016/j.resconrec.2011.05.005>.
- Miskolczi, N. et al., 2010. Two stages catalytic pyrolysis of refuse derived fuel: Production of biofuel via syncrude. *Bioresource Technology*, 101(22), pp.8881–8890. Available at: <http://dx.doi.org/10.1016/j.biortech.2010.06.103>.
- Sarker, M., Rashid, M.M., et al., 2012. Conversion of Low Density Polyethylene (LDPE) and Polypropylene (PP) Waste Plastics into Liquid Fuel Using Thermal Cracking Process., 2(1), pp.1–11.
- Sarker, M., Mamunor Rashid, M. & Molla, M., 2012.



First Waste Plastic Conversion into Liquid Fuel by using Muffle Furnace through Reactor. International Journal of Energy Engineering, 2(6), pp.293–303. Available at: <http://article.sapub.org/10.5923.j.ijee.20120206.04.html>.

Sun, K. et al., 2006. Chemistry of N₂O decomposition on active sites with different nature: Effect of high-temperature treatment of Fe / ZSM-5. , 238, pp.186–195.
Zhao, T. et al., 2005. Synthesis and Characterization of ZSM-5 / β Co-Crystalline Zeolite. , 14, pp.95–100.

**ABSTRACT CCT-: 047**

Imeh Etim Onukak^{*1,2}, Ibrahim A. Mohammed-Dabo¹, A.O. Ameh¹, Stanley I.R. Okoduwa², Opeoluwa O. Fasanya⁴, Isuwa K. Adamu³ and Amali Ejila²

¹Department of Chemical Engineering, Ahmadu Bello University, Zaria- Nigeria

² Directorate of Research and Development, Nigerian Institute of Leather and Science Technology, Zaria-Nigeria

³ Directorate of Academics, Nigerian Institute of Leather and Science Technology, Zaria-Nigeria

⁴National Research Institute for Chemical Technology, Zaria – Nigeria

Email: imykk224@gmail.com

DEVELOPMENT OF BIOMASS BRIQUETTES FROM TANNERY SOLID WASTE: CHARACTERIZATION OF BRIQUETTES

ABSTRACT: The tannery industry is renowned for the huge amount of toxic solid and liquid waste it produces. Waste is generated from cleaning, fleshing, splitting, tanning, shaving and buffing of raw materials. Different ways to utilize tannery solid wastes (TSW) are being investigated. Biomass briquettes are a well proven way of generating energy from waste. Using TSW collected from a tannery in Kano, Nigeria, six briquettes were formulated and characterized. The TSW comprised of hair, fleshings, chrome shavings and buffing dust. Scanning electron microscopy and proximate analysis was carried out on the samples. Briquettes developed had calorific values between 18632 and 24101 kJ/kg depending on their composition.

1. Introduction

Waste disposal or utilization from various sectors including both large and small industries and households is a major challenge in developing countries. The exact quantity of waste generated is difficult to come by as there are lots of inconsistencies in data collection methods, definitions and seasonal variations (Atta *et al.*, 2016). The tannery industry is renowned for the huge amount of toxic solid and liquid waste it produces. This trait is exhibited in tannery industries all over the world. As of 2009, six million tons of solid waste was generated from tanning industries all over the world (Masilamani *et al.*, 2017). Waste is generated from cleaning, fleshing, splitting, tanning, shaving and buffing of raw materials. Environmental pollution thrives around these industries due to the inefficient use or in some cases lack of use of these waste materials (Ravindran, Wong, Selvam, Thirunavukarasu, & Sekaran, 2016).

Different efforts are on the way to find ways to utilize tannery solid wastes (TSW). Masilamani *et al.*, 2017 where able to develop biodegradable packing materials from gelatin extracted from TSW. Using *C. limosum* (Ravindran *et al.*, 2016), were able to successfully produce the enzyme metalloprotease from TSW.

Biomass briquettes are a well proven way of generating energy from waste. The advantage of being able to transform biomass which traditionally have low density, low heating value and high moisture content to efficient fuel briquettes is a commendable research in briquette development. A variety of sources have been used and newer ones are being explored. Interests are tailored towards using locally available materials as raw materials for briquette production. In Uganda, Luwanba and Yiga (Lubwama & Yiga, 2017) demonstrated the use of groundnut shell and bagasse briquettes for cooking use. The team of Merete *et al* (Merete, Haddis, Alemayehu, & Ambelu,

2014) in Ethiopia made use of coffee husks and pulp. While in Nigeria, Nwabue *et al.*, 2017 where able to produce a multi component briquette comprising of coal, plastics and biomass. In this paper we study the production and characterization of briquettes produced from TSW.

2. Materials and Methods

Feedstock was gotten from Unique Finishing Leather, Sharada, Phase I, Kano State. Materials and equipment used include; Cassava starch, roll of Aluminum foil, Leather shaving, lime fleshing, distilled water, Oxygen bomb calorimeter, Oven (OV-010 (9A-122-B), Milling Machine, Briquette mold, Nabertherm furnace (30-30000°C).

The methodology was categorized into five stages; sample collection, sample pre-treatment, preliminary analysis, briquetting and characterization. Characterisation involved calorific value and proximate analysis using European Committee for standard Technical specification (Hans *et. al.*, (2012). Energy evaluation to determine the ignition time, water boiling time and burning rate was evaluated using the Thermal Energy Efficiency formula according to Rathore (2010).

Solid waste samples from pre-fleshing, lime fleshing, shaving, buffing and trimming, randomly selected among piles from the various leather operation units in Unique Leather Finishing Company in Sharada-Phase II, Kano State Nigeria, were examined within the scope of this study. In all, 600 kg of the waste were collected for the study.

Briquetting of the pretreated sample was done using a biomass briquette mold fabricated with the following specifications: capacity- 150g per die consisting of eight dies arranged in two rows. Each die was 40mm by 120mm dimension. Six different formulations were used to produce six briquette samples by pressing the mold in a compression molding machine at a pressure of 38.61kPa and at a

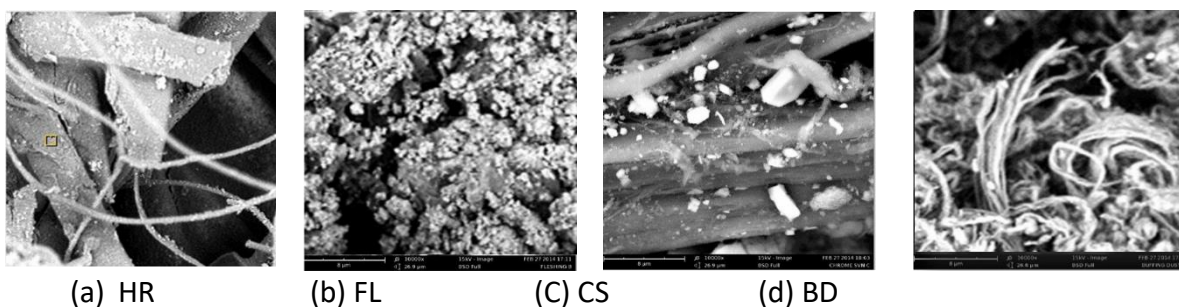
temperature of 150°C for 2 hours. The briquette was allowed to cool and dry for 2 weeks before carrying out proximate, mechanical and energy evaluation analysis.

3. Results and Discussion

3.1 Scanning Electron Microscopic (SEM)

The SEM result of raw samples as shown in Plate 1 reveals the fine collagen fibre network of the processed skin. The fibre of hair is vertically arranged while that of chrome shaving is horizontally arranged and more tightly packed than buffing dust due to the pre-tanning operations. Fleshings has shorter strands since it is more of adipose fats. The particle sizes ranges from 1.64 μm to 39.73 μm in diameter and the results were observed at 1.50 μm^2 to 8,797.58 μm^2 pore areas within

flash point/area. Plate 2 shows the size and surface morphology of the carbonised residue obtained after pyrolysis of the pretreated waste sample. 500g of each of the dried samples were put in a crucible and placed in an oven at a temperature of 450°C for 30min for pyrolysis. The fine collagen fibre network was seen to have been distorted after pyrolysis. The surface area of chrome shavings and buffing dust were finer than fleshing while the hair was coarser than others. The finer the particle size, the easier the compaction process during densification. Fine particles give a larger surface area for bonding. The particle sizes ranges from 277.30 nm to 2.64 μm in diameter and results were gotten from 6433.98 nm^2 to 19.92 nm^2 pore areas within flash point/area



Legend: HR- hair, FL- fleshings, CS- chrome shavings and BD- buffing dust

Plate 1: SEM Analysis Result of Pretreated Waste Samples at 15 kV X 10,000 Magnification

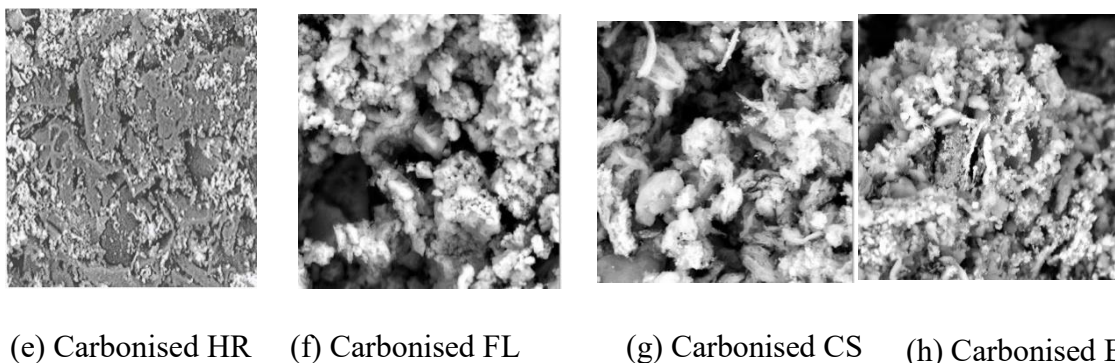


Plate 2: SEM Analysis Result of Carbonised Pretreated Waste Samples at 15kV X 8,000 Magnification.

Table 1: Formulations for Briquette Molding

SAMPLES	HR(g)	FL(g)	CS(g)	BD(g)	ST(g)
1	10	10	10	10	60
2	15	10	5	10	60
3	5	15	15	5	60
4	15	25	5	5	50
5	20	50	15	15	0
6	10	10	10	10	60

HR= Hair, FL = Fleshing, CS = Chrome Shavings, BD = Buffing Dust, ST = Starch

**Table 2:** Proximate Analysis of Briquettes Samples Result

SAMPLE	MC (wt%)	VM (wt%)	AC (wt%)	FC (wt%)	CV (kJ/kg)
1	0.6844	2.1695	3.0555	94.09	20140.2
2	0.5317	2.2716	3.1402	92.38	19821.4
3	0.9521	2.7610	3.9031	93.23	18632.1
4	1.0767	1.8438	2.9349	94.13	22141.3
5	1.2615	2.1411	3.3714	93.22	24101.3
6	0.3807	1.8978	3.1105	94.61	21461.8

MC= Moisture content, VM = Volatile Matter, AC = Ash Content, FC = Fixed Carbon, CV = Calorific Value

Table 1 shows the formulations for the six briquette molds. Each having varying concentrations of the various components of tannery solid waste. Proximate analysis of the prepared briquettes showed sample 3 would require more energy to burn off its relatively high volatile matter when compared with the other samples. The highest ash content was also observed in sample 3. The higher the ash content, the lesser the burning rate and also lesser heating value of the fuel. The high ash content and high volatile matter seem to be responsible for the low calorific value in the formulation. The calorific value determines the amount of heat energy present in a material. From Table 2, Sample 5 was observed to have the highest calorific value of 24,101.3 kJ/kg which is probably due to the high carbon content and the presence of high FL and CS in their formulation. The particle sizes of the raw materials and the uniform formulation favours attrition and a high degree of conditioning due to its ability to absorb moisture. Sample 1, 6 and 4 also have high calorific values of

20,140.2 kJ/kg, 21,461.8 kJ/kg and 22,141.3 kJ/kg respectively. Coal from Odagbo (Kogi State) and Ezimo (Enugu State) both in Nigeria, have calorific values of 22,600kJ/kg and 19,100kJ/kg respectively (Chukwu, Folayan, Pam, & Obada, 2016), showing that tannery derived briquettes can compete favourably with these coal. Manufacturing conditions such as temperature and pressure also influences calorific value (Adapa, Schoe, Tabil, Sokhanasanj, & Crerar, 2003; Tumuru et al., 2010). Samples 2 and 3 had the lowest calorific value of 19,821.4 kJ/kg and 18,632.1 kJ/kg respectively. This may be due to the fact that it has low composition of FL even though high amount of the binder. Cassava starch used as binder also influences the properties of the briquette. Cassava starch has a moisture content of 13.09 % on dry basis, ash content of 0.24 %, a pH of 5.34 and a calorific value of 159.48 kJ/kg or 381 cal/110g (Chitedze, Monzerezi, Kalenga-Saka, & Steenkamp, 2012).

Table 3: Energy Evaluation Analysis of Briquettes

Sample	Weight of Briquette (g)	Volume of Water (l)	Ignition Time (min)	Water Boiling Time (min)	Burning Rate (g/min)	Thermal Efficiency %
1	100	100	15	29.35	0.126	21.091
2	100	100	15	32.18	0.122	20.229
3	100	100	17	32.36	0.155	20.707
4	100	100	12	31.00	0.175	20.784
5	100	100	13	29.32	0.169	23.126
6	100	100	9	28.20	0.132	26.376

Water boiling time is a function of the volatile matter, calorific value and TFE. Sample 6 has the least water boiling time at 28.20 minutes followed by sample 5 at 29.32 minutes as shown in Table 3. According to Onuegbu *et al.*, (2010), it took 26 minutes to boil 100cm³ of water with 100kg of coal. Samples 2 and 3 have the longest water boiling time at 32.18 minutes and 32.36 minutes respectively.

4. Conclusions

Tannery derived briquette was formulated using tannery solid waste (fleshings, hair, chrome shavings and buffing dust). The briquette properties such as particle size, presence of binder, moisture content, volatile matter, ash content and calorific value were found to affect the quality of the briquettes. Briquettes with high moisture content such as 0.6844%, 1.0767% and 1.2615% had the



highest calorific values of 20,140.2 kJ/kg, 22,141.3 kJ/kg and 24,101.3 kJ/kg respectively. These briquettes had in their composition high content of fleshing with a calorific value of 14,570 kJ/kg. Cassava starch used as binder had a calorific value of 159.48 kJ/kg and was observed to have affected the briquette calorific value and compressive strength. The ratio of solid waste to binder were 40:60, 50:50 and 100:0. Briquettes with varying particle sizes of waste were found to be of better quality than those with uniform particle sizes. It took a minimum of 28.2 minutes to boil 100 litres of water with 100g of briquette at the rate of 0.132g/mim. In the end the briquette produced meet up with the standard sub-bitmus coal in terms of calorific value and water boiling time.

Refernces

- Adapa, P. K., Schoe, G. J., Tabil, L. G., Sokhanasnj, S., & Crerar, B. (2003). Pelleting of Fractionated Alfalfa Products. *American Society of Associated Executives (ASAE) paper 036069*, 104-115.
- Atta, A. Y., Aminu, M., Yusuf, N., Gano, Z. S., Ahmed, O. U., & Fasanya, O. O. (2016). Potentials of Waste to Energy in Nigeria. *Journal of Applied Sciences Research*, 12, 1-6.
- Chitedze, J., Monzerezi, M., Kalenga-Saka, J. D., & Steenkamp, J. (2012). Binding Effect of Cassava Starch on the Compression and Mechanical Properties of Ibruprofen Tablets. *Journal of Applied Pharmaceutical Sciences*, 02(04), 31-37.
- Chukwu, M., Folayan, C. O., Pam, G. Y., & Obada, D. O. (2016). Characterization of Some Nigerian Coals for Power Generation. *Journal of Combustion*, 2016, 11. doi: 10.1155/2016/9728278
- Hans, H. and Markku, H. (2012). *Physical and Mechanical Fuel Properties-Significance and Standard Determination Methods*
- Lubwama, M., & Yiga, V. A. (2017). Development of groundnut shells and bagasse briquettes as sustainable fuel sources for domestic cooking applications in Uganda. *Renewable Energy*, 111, 532-542. doi: <https://doi.org/10.1016/j.renene.2017.04.041>
- Masilamani, D., Srinivasan, V., Ramachandran K, R., Gopinath, A., Madhan, B., & Palanivel, S. (2017). Sustainable packaging materials from tannery trimming solid waste: A new paradigm in wealth from waste approaches. *Journal of Cleaner Production*. doi: <https://doi.org/10.1016/j.jclepro.2017.06.200>
- Merete, W., Haddis, A., Alemayehu, E., & Ambelu, A. (2014). The Potential of Coffee Husk and Pulp as an Alternative Source of Environmentally Friendly Energy. *East African Journal of Sciences*, 8(1), 29-36.
- Nwabue, F. I., Unah, U., & Itumoh, E. J. Production and characterisation of smokeless bio-coal briquettes incorporating plastic waste materials. *Environmental Technology & Innovation*. doi: <https://doi.org/10.1016/j.eti.2017.02.008>
- Rathore, M. M. (2010). *Thermal Engineering*. Tata McGraw-Hill Education private limited. New Dehli. Pg. 539. ISBN 13 978-0-07-068113-2.
- Ravindran, B., Wong, J. W. C., Selvam, A., Thirunavukarasu, K., & Sekaran, G. (2016). Microbial biodegradation of proteinaceous tannery solid waste and production of a novel value added product – Metalloprotease. *Bioresource Technology*, 217, 150-156. doi: <https://doi.org/10.1016/j.biortech.2016.03.033>
- Tumuru, J. S., Sokhanasnj, S., Lim, C. J., Bi, T., Lau, A., Melin, S., . . . Oveisi, E. (2010). Quality of Wood Pellet Produced in British Columbia for Export. *Applied Engineering in Agriculture*, 26(6), 1013-1020.

**ABSTRACT CCT-: 014**

Mbonu, I. J. and Mebitaghan, B.

1,2Department of Chemistry, College of Science, Federal University of Petroleum Resources, Effurun, Delta State, Nigeria

Email: idongesitmbonu@yahoo.com**IRON (II) METAL-ORGANIC FRAMEWORK FOR SUSTAINABLE ENERGY STORAGE APPLICATION**

ABSTRACT: The trend for sustainable energy globally has drawn international attention. Nigeria is blessed with fossil-fuel, but the consumption rate is high due to population growth and increased in standard of living. To enhance industrial break through, reduce poverty, and enable sustainable development, an energy storage facility has to be sort. Metal-organic frameworks, a new class of porous crystalline materials could act as an outstanding tool in this field based on their high surface areas, controllable structures and excellent electrochemical properties for various energy storage and conversion technologies.

Key words: Iron(II), Metal-organic Framework, Sustainable Energy Storage

1. Introduction

Metal-organic frameworks have diverse structures, tunable chemical composition, high surface areas, excellent electrochemical properties with highly porous framework suitable for energy storage and conversion (Zhou and Tian, 2013). Metal-organic frameworks as photovoltaic cells are electrical devices for direct conversion of solar energy to electricity, which is another intriguing application of MOFs as electrochemical devices in converting fuels (e.g., hydrogen, natural gas, and methanol) to electricity for powering vehicles, stationary facilities, and portable appliances (Kuppler et al., 2009, Beidaghi and Gogotsi, 2014).

2. Materials and Methods

All chemical reagents used for the synthesis of the complex were of analytical grade and were used without further purification, they include iron (II) chloride tetrahydrate ($\text{FeCl}_2 \cdot 4\text{H}_2\text{O}$), 8-hydroxyquinoline and Benzoic acid. The IR-spectrum of the Fe(II) complex was taken on a (Shimadzu, FTI R- 8400S) Fourier Transform Infrared Spectrophotometer (4000- 400) cm^{-1} as KBr disc, electronic spectrum in the range of 200-700 nm at room temperature with M501 Single beam UV-Visible spectrophotometer. The morphology of the complex was examined by scanning electron microscopy using Joel JEM-5200 operating at an acceleration voltage of 20 Kv in a magnification range of 300-80 μm . The particle properties data were calculated based on weigh and by count. The powder X-ray diffraction pattern for the complex was collected using a PANanalytical X'PERT pro automatic diffractometer operating at 40 kV and 30 mA. Iron (II) complex was synthesized under

solvent evaporation conditions. 1.22 g (10 mmol) of benzoic acid, 1.9981 g (10 mmol) of $\text{FeCl}_2 \cdot 4\text{H}_2\text{O}$, and 1.45 g (10 mmol) of 8-hydroxyquinoline were dissolved in a mixture of distilled water (5 mL) and ethanol (10 mL). The solution was stirred for 2 hours (Mbonu, 2015).

3. Results and Discussion

The physical properties analyses of the complex show that the Fe(II) complex was isolated as needle like crystals, stable in air, has a melting point in the range of 120 -130 °C and insoluble in water, partially soluble in hot water and ammonia, but completely soluble in methanol and ethanol. The molar conductance for the mixed ligand complex of Fe(II) was 1905 μf which signifies that the complex was non electrolytic in nature and the pH value of 2.01 which shows an acidic nature of the iron(II) complex.

The diffractogram for the Fe (II) complex in Figure 1 shows a crystalline single phase system.

The particle size D of the Fe (II) complex was determined using the Debye - Scherrer equation (Hussain and Shabeeb, 2014):

$$D = \frac{k\lambda}{\beta \cos\theta}$$

Where, K is a constant equal to 0.9, β is the full width at half maximum of the most intense diffraction peak at Bragg angle θ and $\lambda = 1.5406 \text{ \AA}$. A dimensional particle size of 34.25 nm was determined from the Debye-Scherrer equation for the synthesized Fe (II) complex. The other crystallographic data and structure refinement for the Fe (II) complex is given in Table 1

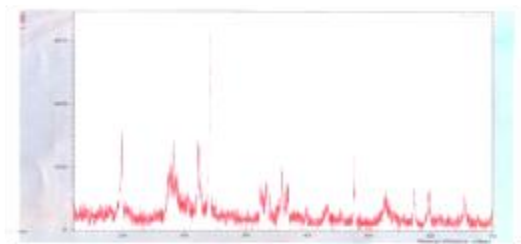


Fig.1: Powder X-ray Diffractogram of Fe(II) Complex

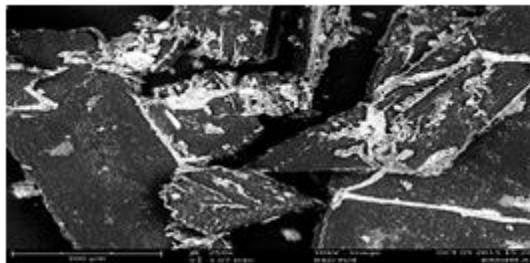


Fig. 2: SEM micrograph of Fe(II) Complex at 300 μm magnification

Table 1: Particle size (D) for Fe(II) complex from the first three strongest peaks.

Complexes	D1 (nm)	D2 (nm)	D3 (nm)	Average (nm)
Fe(II)	3219.80	2781.08	4275.10	3425.86

The SEM micrograph in Figure 2 at a magnification of 300 μm revealed a plate like structure with particle properties presented in Table 1. Highlighted regions show metal organic frameworks locations in the image.

The IR spectrum of the Fe(II) complex in Fig. 3 shows bands with an appropriate shift due to

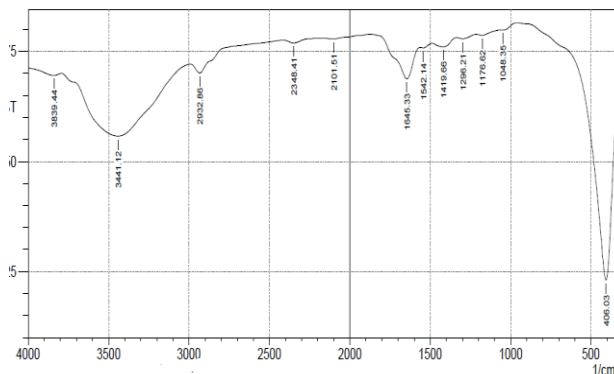


Fig. 3: FT-IR Spectrum of Fe(II) Complex

complex formation. The following vibrational bands were observed: at 1419, 1296, 1645, 1542, 3441, and 406 assigned to $\nu_{\text{asCOO-}}$, $\nu_{\text{sCOO-}}$, $\nu(\text{C-O})$, $\nu(\text{C=C})$, $\nu(\text{C=N})$, and $\nu(\text{M-O})$ respectively. This observation is in agreement with that reported in the literature (Ren et al., 2006, Nakamoto, 2009)

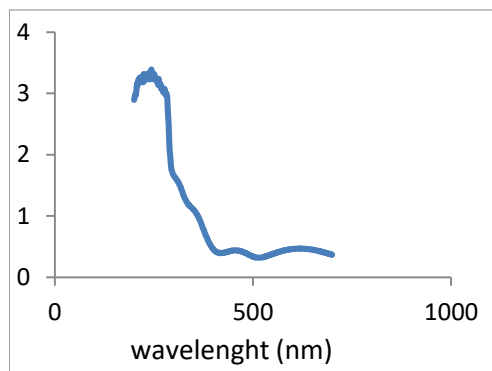


Figure 4: UV spectrum for Fe(II) complex

The UV-visible spectrum of Fe(II) complex in Fig. 4 gave three absorption bands at 240, 460, 610 nm. The first two bands were attributed as inter-molecular charge transfer while the third was attributed to metal ligand interaction (Jarad et al., 2011). The absorption in the ultraviolet region shows the potency of the synthesized complex to be used in photovoltaic devices for the conversion of solar energy to electricity (Fultz and Howe, 2013, Pandian and Anbusrinivasan, 2014, Biplab et al., 2014)). This analysis further confirms an octahedral structure for the iron(II) complex.

Conclusion

The preliminary investigations on the Fe(II) metal organic framework properties have yielded promising results. The synthesized complex exhibits high surface area, porosity, crystallinity, nanoparticle size, optical properties that are unique to the storage of energy and this implies they can be used as fuel cells. The research will integrate the support, design and development of high rate

performance novel, advanced energy storage technologies to enable the transformative energy solutions.

Acknowledgements

We are grateful to the National Research Institute for Chemical Technology, Zaria for the kind invitation to her 1st National Conference on Chemical Technology. We acknowledge colleagues who have worked with us in this area and whose names can be found in the references.

References

- Beidaghi, M. & Gogotsi, Y. (2014). Capacitive Energy Storage in Micro-Scale Devices: Recent Advances in Design and Fabrication of Micro-Super capacitors, *Energy & Environment Society*; 7(3), 867.
- Biplab, M.; Shweta, S. & Sujit K, G. (2014). Guest driven Structural Transformation Studies of a Luminescent Metal-organic Framework, *Journal of Chemical Sci*;126 (5), 1417-1422
- Hussain M. and Shabeeb, G. M. (2014). Synthesis and Optical Properties of a Biphenyl Compound. *Walailak Journal of Science & Technology*, 11(9):



- 769-776.
- Jarad, A. J., Kadhim M. A. and Jabrallah S. A. (2012). Synthesis and spectral studies of Zn(II), Cd(II) and Hg(II) complexes with 5-(2-Benzoic acid azo)-8-hydroxyquinoline ligand. *Baghdad Science Journal*, 9 (1), 178-184
- Kuppler R. J., Timmons D. J, Fang Q. R. (2009) Potential applications of metal-organic frameworks. *Coord Chem Rev* 253:3042–3066
- Mbonu, I. J. (2015). Synthesis and optical properties of self-assembled coordination polymer of Zn(II) ions with phenylmalonic acid and 4-1H-Amino-1,2,4- Triazole. *Ife Journal of Science*. 17, 525-532.
- Nakamoto, K. (2009). *Infrared and Raman spectra of inorganic and coordination compounds* (6th ed.). New York: John Wiley and Sons, 112-143.
- Zhou, Y. H. and Tian Y. P. (2013). Synthesis, crystal structure and photoluminescent property of Cd(II) metal-organic framework with mixed carboxylate and Bis (imidazole) ligand. *Korean Chemical Society*, 34 (9), 2800-2802.

**ABSTRACT CCT-: 020**Egere, B. C. ¹, Momoh, O.R. ² and Aderemi, B.O. ².¹Department of Polymer and Textile Science, Ahmadu Bello University Zaria, Nigeria² Department of Chemical Engineering, Ahmadu Bello University Zaria, NigeriaEmail: idiche@yahoo.com**INFLUENCE OF THERMAL AND CHEMICAL PRE-TREATMENT ON SPIROGYRA AFRICANA BIOMASS FOR GLUCOSE PRODUCTION**

ABSTRACT: The utilization of some species of algae biomass for biofuel production has been documented in literatures, but little attention has been paid to *Spirogyra africana* species. Hence, this study espoused the influence of pre-treatment of *Spirogyra africana* biomass on glucose yield. The effects of thermal and chemical pre-treatment and soaking time as they affect glucose yield was monitored in presence of *Aspergillus niger* being source of hydrolysing enzyme. On the first day of hydrolysis, the thermal pre-treated sample gave a relatively superior glucose yield 15.94 (wt/wt %) in comparison to the values of 14.33 and 12.03 (wt/wt %) for NaOH treated sample and the control respectively. On the second day, the glucose yield from the three setups (blanched, NaOH treated and the control) all gave a comparative glucose yield of 29.15, 29.41 and 29.13 respectively while on the third day the corresponding yields of 30.72, 32.28 and 30.66 wt/wt % respectively were obtained, showing marginal advantage of NaOH pre-treatment over others.

Keywords: Glucose, Algae biomass, Biofuel, Pre-treatment, Hydrolysis, *Spirogyra africana*

1. Introduction

Bioethanol is a fuel used as gasoline substitute. It is either produced by sugar fermentation process, or by the process of reacting ethylene with steam (Matthew, 2013). The main source of sugar for bioethanol production comes from energy crops, which are normally grown specifically for energy or food; and these include maize, reed canary grass, cord grasses, Jerusalem artichoke, miscanthus, sorghum plants, elephant grass and wheat (Salvi *et al.*, 2010, Dias *et al.*, 2009 and Aiyegbara *et al.*, 2016). Ethanol can also be produced from algae by converting its starch and cellulose, but unlike energy crops, algae can be grown on water bodies and therefore, there is no competition for land space with food crops (Somma *et al.*, 2010).

Researches on how to efficiently convert some algae species to bio-ethanol have been conducted. Razif and Michael (2011) studied the influence of acid pre-treatment on microalgal biomass for bioethanol production. Hirano *et al.*, (2012) investigated a particularly interesting method of micro algae bio-ethanol production. They demonstrated that under anaerobic conditions, even in the dark, the starches within the cells of micro algae were fermented. The potentials for simple, low cost bio-ethanol production are apparent. Furthermore, Kurakake *et al.*, (2007) studied

the effect of biological pre-treatment with two bacterial strains for enzymatic hydrolysis of office paper. Lee *et al.*, (2007) investigated the effect of biological pre-treatment of softwood *Pinus densiflora* by three white rot fungi and Singh *et al.*, (2008) studied the biological pre-treatment of sugarcane trash for its conversion to fermentable sugars.

Works on bio-fuel production from *Spirogyra africana* a common specie in Nigeria are very scarce and there is a need to investigate the influence of pre-treatment of the biomass prior to its exploitation, thus being conventional route for cellulosic substrate utilisation. Thus, pre-treatment is expected to lead to higher yield of glucose for bio-ethanol production from *Spirogyra africana* as have been the case for 1st and 2nd generation biomass (Agbodike 2009 and Nirmala and Sivamani 2011).

2. Materials and Methods**2.1 Spirogyra Africana**

The algae, *Spirogyra africana* sample was collected from the water dam at Ahmadu Bello University Zaria, Nigeria. The sample collected was transferred to the laboratory in sterile containers. Summary of the methods as shown in figure 1



Plate 1: *Spirogyra africana* bloom at the water dam, Ahmadu Bello University, Zaria

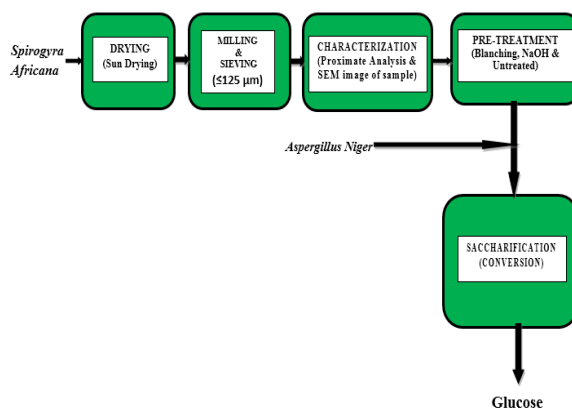


Figure 1: Block Diagram Showing the Method for Glucose Production from *Spirogyra africana*

2.3 Pre-treatment of the *Spirogyra africana*

i. Physical Pre-treatment (Drying, Milling and Sieving)

The *Spirogyra africana* sample was sun dried to reduce the water content and to make it millable. The dried sample was then milled and sieved to $\leq 125 \mu\text{m}$, these were done to increase the surface area and to make the cellulose extraction more effective. The milled feedstock is called mash. The biomass was grinded and sieved to $\leq 125 \mu\text{m}$ according to Eshaq, *et al.*, (2010).

ii. Chemical and Thermal Pre-treatment

A portion of the sample was pre-treated with NaOH of 0.5 (w/v) %, 1.0 (w/v) % and 2.0 (w/v) %. This was done to study the effect of chemical pre-treatment on the glucose yield. Another portion of the sample was blanched with hot water of various temperatures (30-100 °C) for five minutes. This was done to study how thermal pre-treatment will affect the amount of glucose produced. The untreated sample was used as control in both cases.

iii. Enzymic Conversion / Saccharification

The above pre-treated samples and control sample were converted to fermentable sugar (glucose) by treatment with *Aspergillus niger* of concentration between 0-1.3 % wt/wt. This was done after pH adjustment of the mash.

iv. Fungal Culturing

The fungal cultures (*Aspergillus niger*) were sourced from the Department of Microbiology, Ahmadu Bello University Zaria, Nigeria. The fungi was cultured and maintained on a potato

dextrose agar medium at 30 °C.

v. Uv-Spectrophotometer

The quantitative determination of glucose in this study was done using the UV-spectrophotometer at constant wavelength of 550 nm, with distilled water as a blank sample. A pre-calibrated absorbance versus glucose concentration chart was prepared to determine the glucose concentration in various samples.

3. Results and Discussion

3.1. Proximate Analysis of the *Spirogyra africana*

Table 1 shows the results gotten from proximate analysis of *Spirogyra africana* on dry basis. It contains 39.72 % carbohydrates, which makes it a good candidate for glucose production.

3.2 Morphology

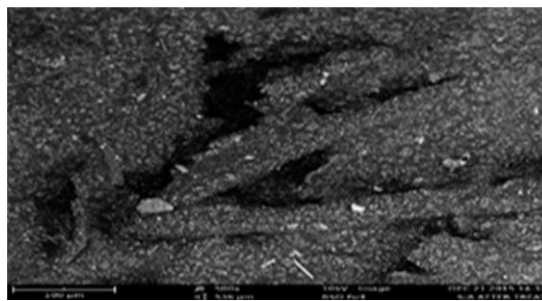
Plate II (a & b) shows the images of sample before and after blanching at 80 °C. From the images, the blanched samples have more active sites for interaction with the hydrolyzing agent *Aspergillus niger*. This is because of the unbundling after blanching which makes the particles become tender.

Table 1: Proximate Analysis of the *Spirogyra africana*

Sample Name	% Moisture	% Ash	% Lipid	% Protein	% fibre	% CHO
<i>Spirogyra africana</i>	1.05	31.03	3.00	5.05	20.05	39.72



(A)



(B)

Plate I: SEM image of *Spirogyra africana* Sample (a) before and (b) after thermal pre-treatment (blanching)

3.3. The effect of thermal pre-treatment on glucose produced.

The effect of thermal pre-treatment on glucose production was carried out to determine the best blanching temperature. Figure 2 shows that a rapid increase in the concentration of glucose produced was observed from 30 °C to 80 °C and witnessed a decline at temperature beyond 80 °C. The maximum concentration of glucose was observed at 80 °C and this conformed to the SEM analysis in Plate I which shows that more particles were exposed for hydrolysis in blanching sample than in the unblanching sample. Thus samples blanching at 80 °C were used for further studies in this work.

3.4 Effect of NaOH Pre-treatment on Glucose Production

The effect of NaOH concentration on glucose production was carried out as can be seen in NaOH, blanching at 80 °C and the untreated sample serving as control. The results of the tests showed that there was a rapid increase in the glucose production from day one (1) to day two (2) for each of the setups. The blanching

Figure 3, 1.0 % (w/v) NaOH pre-treated sample gave the highest concentration of glucose produced when compared with 0.5 and 2.0 % (w/v) NaOH pre-treated, thus samples pre-treated with 1.0 % (w/v) NaOH were used for further experiments.

3.5 Saccharification

In this experiment the carbohydrate content of the substrate *Spirogyra africana* were hydrolysed to reducing sugar using *Aspergillus niger* cells. The optimal conditions for glucose production were adopted from Egere et al., (2017) under review.

3.6 Comparism of the Various Pre-treatment Methods on Saccharification.

At fixed conditions of: temperature 30 °C, pH 4.5, substrate concentration 50 g/l, *A. niger* concentration 0.65 % (w/v), and particle size ≤ 125 µm. Figure 4 shows the effect of pre-treatment on saccharification using 0.1 (w/v)

at 80 °C produced more glucose than the untreated and 0.1 (w/v) NaOH pre-treated in day one (1), as there was statistical significance ($P < 0.05$) between glucose produced from it when compared to others.

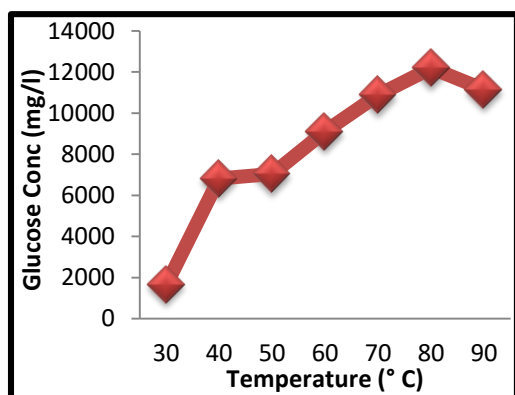


Figure 2: Effect of Blanching Temperature on Glucose Production at the following hydrolysis conditions: temperature 30 °C, pH 4.5, substrate concentration 50 g/L, *A. niger* concentration 0.65 % (w/v), and particle size $\leq 125 \mu\text{m}$.

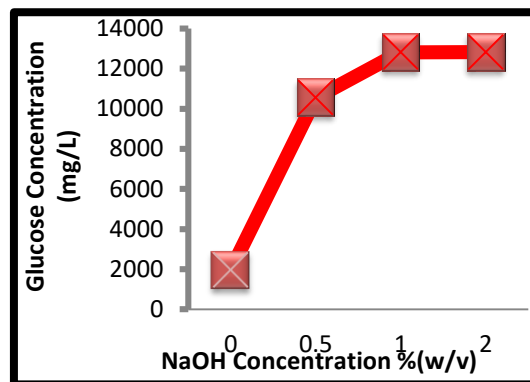


Figure 3: Effect of NaOH Concentration on Glucose Production at following hydrolysis conditions: temperature 30 °C, pH 4.5, substrate concentration 50 g/L, *A. niger* concentration 0.65 % (w/v), and particle size $\leq 125 \mu\text{m}$.

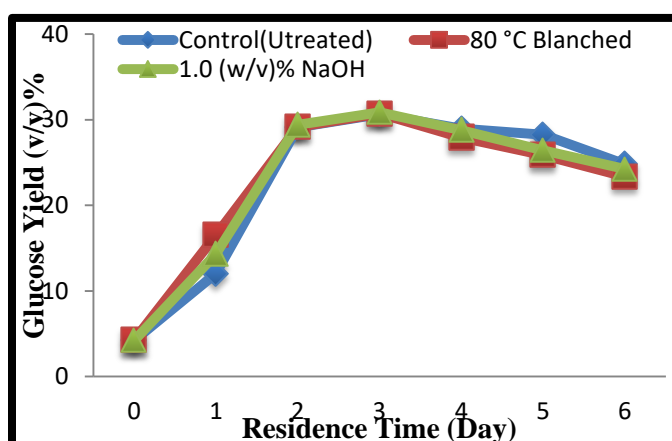


Figure 4: Effect of pre-treatment on saccharification at following hydrolysis conditions: temperature 30 °C, pH 4.5, substrate concentration 50 g/L, *A. niger* concentration 0.65 % (w/v), and particle size $\leq 125 \mu\text{m}$.

This observation may be connected with the ability of water at that temperature to swell up the starch present in the substrate, making it assessable to the hydrolyzing enzymes, when compared to the untreated sample. The same is likely true of the sample pre-treated with NaOH, although to a slightly lesser extent. However, after the day two, the results show that there was no statistical significant difference ($P > 0.05$) between glucose produced from NaOH pre-treatment, blanching and untreated substrates. This finding is of importance because; the economic difficulties on commercialization of 2nd generation biofuel substrates linger on the biomass pre-treatment step. Hence, avoiding this step (pre-treatment) in the 3rd generation biomass conversion to fuel is an added advantage to its commercialization.

4. Conclusion

From the above studies, the following conclusions are drawn.

- The proximate analysis of *Spirogyra*

africana biomass showed that it contains 39.79 % carbohydrate, which makes it suitable for glucose production.

- This research also confirms that there is no significant effect of the thermal and chemical pre-treatment of *Spirogyra africana* biomass before on saccharification.

References

- Aderemi, B.O., Abu, E., and Highina, B.K., (2008) The kinetics of glucose production from rice straw by *Aspergillus niger* Vol.7(11), pp. 1745-1752 , June 2008 DOI: 10.5897/AJB08.109 ISSN: 1684-5315
- Agbodike, T.C. (2009). *Evaluation of Elephant Grass (Pennisetum Purpureum) as Substrate for bioethanol Production using Co-culture of Aspergillus niger and Saccharomyces Cerevisiae*; MSc Thesis, Department of Microbiology Ahmadu Bello University Zaria. P 10-35.
- Aiyejagbara, M.O., Aderemi, B.O., Ameh, A.O., Ishidi, E., Aiyejagbara, E..F., Ibeneme, U., Olakunle M. S.(2016). *Production of Bioethanol from elephant grass*. International Journal of Innovative Mathematics, Statistics & Energy Policies 4(1):1-9, Jan-Mar. 2016



- Dias, M.O.S., Ensinas A.V., Nebra S.A., Maciel, F.R., Rossell C.E.V., and Maciel, M.R.W. (2009). Production of bio-ethanol and other bio-base materials from sugarcane bagasse: integration of conventional bio-ethanol production process. *Chem.EngResDes*: 87:1206-16.
- Egere, B.C., Momoh, O.R. and Aderemi B. O. (2017) Studying the optimal conditions for glucose production from the hydrolysis of *Spirogyra africana* (under review).
- Eshaq, F. S., Mir, N. A., and Mazharuddin, K. M. (2010). Spirogyra biomass a renewable source for biofuel (bioethanol) Production. *International Journal of Engineering Science and Technology* Vol. 2(12), 2010, 7045-7054
- Hirano, A., Ueda, R., Hirayama, S., Ogushi, Y., (2012). CO₂ fixation and ethanol production with microalgal photosynthesis and intracellular anaerobic fermentation. *Energy* 22, 137–142.
- Hwang S.S, Lee S.J., Kim H.K.,(2008) *Biodegradation and saccharification of wood chips of Pinus strobus and Liriodendron tulipifera by white rot fungi*. *J Microbiol Biotechnol*, 18: 1819 – 1825.
- Kurakake M, Ide N, Komaki T. (2007) Biological pretreatment with two bacterial strains for enzymatic hydrolysis of office paper. *Curr Microbiol*, 2007; 54: 424 – 428.
- Lee J.W, Gwak K.S, Park J.Y. (2007) Biological pretreatment of softwood *Pinus densiflora* by three white rot fungi. *J Microbiol*, 2007; 45: 485 – 491.
- Mathew, A. K. (2013). Dilute acid pre-treatment of oilseed rape straw for bioethanol production. *Renewable Energy* 36, 2424–2432.
- Nirmala, C. and Sivamani, S. (2011). Effect of Pre-treatment Methods on Bioethanol Yield from Cassava waste: A Comparative Study, *Advanced Biotechnology* 11(5) : 46-47
- Razif. H. and Michael, K. D. (2011). Influence of acid pre-treatment on microalgal biomass for bioethanol production. *Process Biochemistry*, 46 (2011): 304–309.
- Salvi, D.A., Aita, G.M., Robert, D., and Bazzan, V. (2010). Ethanol production from sorghum by dilute ammonia pre-treatment. *Jind microbial Biotechnol*; 37:27-34.
- Singh P, Suman A, Tiwari P. (2008) Biological pretreatment of sugarcane trash for its conversion to fermentable sugars. *World J Microbiol Biotechnol*, 2008; 24: 667 – 673.
- Somma, M. I., and Al-Shyoukh, A. O. (2010) Experimental evaluation of the transesterification of waste palm oil into biodiesel; *Journal of Bioresource Technology*, 85:253–6.
- Yang B, Wyman C E. (2008) Pre-treatment: the key to unlocking low-cost cellulosic ethanol. *Biofuels Bioprod Bioref*, 2:26 – 40.
- Yi, Z., Zhongli, P., Ruihong Z,(2009) Overview of biomass pretreatment for cellulosic ethanol production September, 2009 *Int J Agric & Biol Eng* Open Access at <http://www.ijabe.org> Vol. 2 No.3 51

ABSTRACT CCT-: 060Abba, H¹., Adamu, I.K²., Musa, A¹., and Iji, M³¹Department of Chemistry, Ahmadu Bello University, P.M.B.1045, Zaria-810006, Nigeria.²Nigerian Institute of Leather Science and Technology, P.M.B. 1034, Zaria, Nigeria.³Department of Chemistry, Abubakar Tafawa Balewa University, P.M.B. 0248, Bauchi, Nigeria. *Email:*idongesitmbonu@yahoo.com**EFFECT OF NATURAL ZEOLITE ON INTUMESCENT AMMONIUM POLYPHOSPHATE-PENTAERYTHRITOL-MELAMINE SYSTEM IN FLAME RETARDATION OF POLY (VINYL CHLORIDE) (PVC)**

ABSTRACT: An intumescent flame retardant (IFR) composite comprising PVC, ammonium polyphosphate (APP), melamine (MEL) and pentaerythritol (PER) was prepared by compression moulding method to serve as control. Nine sheets of the same dimension were also prepared by the same method after addition of varying amount of natural zeolite (NZ). The 10 composite samples were subjected to limiting oxygen index (LOI) and vertical burn (UL-94V) tests. Fire performance index (FPI), heat of combustion (H_c), total heat release (THR) and peak heat release rate (PHRR) and mass loss rate (MLR) were also determined. The results showed that addition of NZ to the IFR has drastically enhanced the flame retardation performance of the PVC sheets. The LOI was increased by 35.95% for the 4.5g NZ-containing compared to the pure sample. While both the pure PVC and the IFR-containing PVC samples belong to the V-2, V-0 was attained by the 2.5 to 4.5g NZ-containing samples. The FPI had increased from 4.12sm²kW⁻¹ for the pure PVC to 29.97sm²kW⁻¹ for the sample containing 4.5g NZ. All the four parameters studied (H_c, THR, PHRR and MLR) decreased to different extents with increase in concentration of NZ. The results were attributed to the formation of a charred layer of carbon on the surface of the PVC sheets that blocks out heat transfer via conduction, convection and radiation. The heated APP decomposed to yield poly(phosphoric acid) catalyzed the dehydration of PER and the inert ammonia gas generated extinguished the burning PVC sheets.

Keywords: Flame retardant, intumescence, limiting oxygen index, synergy, zeolite

1. Introduction

PVC is the most versatile plastic and its variety of uses comes from its ability to be formulated with different additives and with different molecular masses, giving plastics that range from rigid to pliable (Lyon *et al.*, 2009; Unar *et al.*, 2010). Industrially, PVC is made by free-radical polymerization mechanism in suspension (80%), emulsion (12%) and bulk (8%) polymerization techniques:

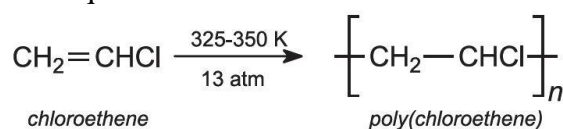


Fig. 1: Polymerization of chloroethene to PVC

(Chanda and Roy, 2006)

Although PVC is inherently fire resistant, there is need to add flame retardants to suppress or delay the appearance of flame and reduce its propagation in PVC or its products meant for use where fire hazard is a critical issue (Weil and Levchik, 2009).

2. Materials And Methods**2.1 Sample**

Preparation: A 130 × 65 × 13mm³ sheet of an intumescent flame retardant (IFR) composite comprising 2.5 g each of PVC, APP, MEL and PER was prepared by compression moulding method. Nine sheets of the same dimension were also prepared by the same method after addition of 0.5, 1.0, 1.5, 2.0, 2.5, 3.0, 3.5, 4.0 and 4.5 g of NZ to the formulation used in the control composite.

Limiting oxygen index (LOI) Test: ASTM-2683 method was used to test the LOI of the 10 samples.

UL-94 Vertical Burn Test: The method employed by Hull and Kandola (2009) was used to test the 10 samples for UL-94V.

Cone Calorimeter Test: FPI, H_c, THR, PHRR and MLR tests were carried out for the 10 samples according to the procedure of Brohez (2005)

RESULTS AND DISCUSSION

Results of the LOI, UL-94V and cone calorimeter tests for the 10 samples under study are shown Tables 1 and 2 and Figure 1. From the experimental results obtained, it was observed that addition of NZ to the IFR has drastically enhanced the flame retardation performance of the PVC sheets, for example, LOI increased by 35.95% for the 4.5gNZ-containing compared to the pure sample. While both the pure PVC and the IFR-containing PVC samples belong to the V-2 (poor) class, V-1 (good) rating was achieved by the 0.5 to 2.0g NZ-containing samples belong to class V-1. The best rating (V-0) was attained by the 2.5 to 4.5g NZ-containing samples. The fire performance index (FPI) of the samples has improved with increase in concentration of NZ. The FPI had increased from 4.12sm²kW⁻¹ for the pure PVC to 29.97sm²kW⁻¹ for the sample containing 4.5g NZ. The results obtained from the cone calorimeter test showed that all the four parameters studied (H_c, THR, PHRR and MLR) decreased, although to different extents, with increase in concentration of NZ.

Table 1: Limiting oxygen index (LOI) and UL-94 vertical burn rating and classification of the pure PVC, intumescent flame retardant PVC and natural zeolite-containing intumescent flame retardant PVC sheets.

Sample	LOI (%)	UL-94V rating
Pure PVC	46.57	V-2
PVC + IFR	48.06	V-2
PVC + IFR + 0.5g NZ	53.33	V-1
PVC + IFR + 1.0g NZ	57.52	V-1
PVC + IFR + 1.5g NZ	61.15	V-1
PVC + IFR + 2.0g NZ	64.27	V-1
PVC + IFR + 2.5g NZ	66.98	V-0
PVC + IFR + 3.0g NZ	69.11	V-0
PVC + IFR + 3.5g NZ	70.88	V-0
PVC + IFR + 4.0g NZ	72.02	V-0
PVC + IFR + 4.5g NZ	72.71	V-0

Table 2: Mass loss rate (MLR), heat of combustion (H_c), total heat released (THR) and peak heat release (PHRR) of the pure PVC, intumescent flame retardant PVC and natural zeolite-containing intumescent flame retardant PVC sheets.

Sample	H_c (MJkg ⁻¹)	THR (MJm ⁻²)	PHRR (kWm ⁻²)	MLR (gs ⁻¹ m ²)
Pure PVC	18.23	17.87	63.38	13.72
PVC + IFR	17.57	16.83	61.16	13.21
PVC + IFR + 0.5g NZ	16.05	14.04	56.68	12.03
PVC + IFR + 1.0g NZ	14.69	13.02	53.63	10.96
PVC + IFR + 1.5g NZ	13.51	12.01	50.66	9.01
PVC + IFR + 2.0g NZ	12.49	10.98	48.04	8.15
PVC + IFR + 2.5g NZ	11.51	10.15	45.62	7.37
PVC + IFR + 3.0g NZ	10.63	9.38	43.51	6.71
PVC + IFR + 3.5g NZ	9.86	8.73	41.56	6.13
PVC + IFR + 4.0g NZ	9.21	8.16	39.82	5.64
PVC + IFR + 4.5g NZ	8.66	7.67	38.59	5.25

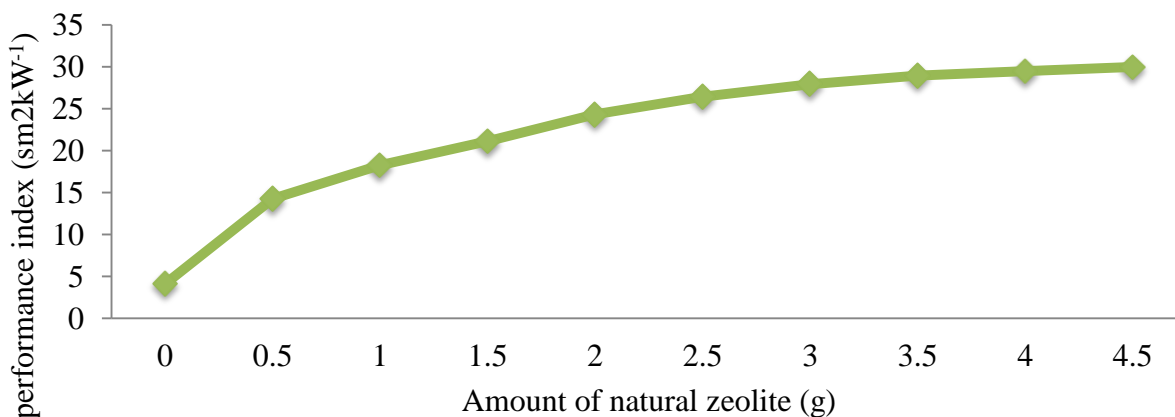


Fig. 1: Effect of concentration of natural zeolite on fire performance index (FPI) of the intumescent flame retardant PVC sheets

Compared to the pure sample, the decrease in value for the 4.5g NZ-containing sample was 50.71% for H_c , 54.43% for THR, 36.90% for PHRR and 60.26% for MLR. It was concluded that since NZ and IFR is a synergistic mixture (the two compounds multiply their inherent individual flame-retarding properties) in the PVC sheets. The results were attributed to the formation of a charred layer of carbon on the surface of the PVC sheets that blocks out heat transfer via conduction, convection and radiation. The heated APP decomposed to yield poly(phosphoric acid) and ammonia and the poly(phosphoric acid) formed catalyzed the

dehydration of PER. Being inert, the ammonia gas generated extinguished the burning PVC sheets, in agreement with what Chen and Wang (2010) reported. The array of channels within the three-dimensional and microporous structure of the NZ provides the large surface area needed for the chemical reaction (intumescence) to take place and the honeycomb framework of the ducts, cavities and channels in NZ enable it to adsorb and absorb the IFR components, in accord with the findings of Demir *et al* (2005). Being environment friendly, NZ was recommended for inclusion in intumescent flame



retardant formulations for PVC products meant for use where fire hazard is high.

References

Brohez, S. (2005). Uncertainty analysis of heat release rate measurement by oxygen consumption calorimetry. *Fire and Materials* 29(6): 383-394.

Chanda, M. and Roy, S. K. (2006). *Plastics technology handbook*. CRC Press, Boca Raton, pp. 1–6.

Chen, L. and Wang, Y.Z. (2010). A review on flame retardant technology in China. Part I: development of flame retardants. *Polymers for Advanced Technologies* 21: 2-7.

Demir, H., Arks, E., Balkose, D. and Ulku, S. (2005). Synergistic effect of natural zeolites on flame

retardant additives. *Polymer Degradation and Stability* 89: 478-482.

Hull, R. and Kandola, B. (2009). Fire

retardancy of polymers, New strategies and mechanisms, Jones

and Bartlett Publishers, London, pp.2-10.

Lyon, R.E., Takemori, M.T., Safronawa, N., Stoliarov, S.I. and Walters, R.N. (2009). A molecular

basis for polymer flammability. *Polymer* 50(12): 2608-2617.

Unar, I.M., Soomro, S.A. and Aziz, S. (2010). Effect of Various Additives on the Physical Properties of Poly (vinyl chloride) Resin.

Pakistani Journal of Analytical and Environmental Chemistry 11 (2): 44-50.

Weil, E.D. and Levchik, S.V. (2009). *Flame retardants for plastics and textiles*, Hanser Publishers, Munich, pp.16-25.

**ABSTRACT CCT-: 076**¹M. Yusuf*, ²A. Y. Atta, ¹B. Y. Jibril, ¹B. O. Aderemi and ¹B. Mukhtar¹Department of Chemistry, Ahmadu Bello University, P.M.B.1045, Zaria-810006, Nigeria.²National Research Institute for Chemical Technology, P.M.B 1052, Basawa Zaria, Nigeria.Email: mustaphayusuf@abu.edu.ng**IMPROVING THE STABILITY OF PROPANE AROMATIZATION CATALYST VIA ISOMORPHOUS SUBSTITUTION OF ZINC IN ZSM-5**

ABSTRACT: Zinc-ZSM-5 catalyst (isomorphously substituted with 2wt.% Zn) was successfully synthesized by hydrothermal crystallization method. The synthesized catalyst and commercial ZSM-5 zeolite impregnated with 2wt.% zinc were characterized by XRD, BET, XRF, FTIR and the catalytic activity tested for propane aromatization in a fixed bed reactor at 1atm, 540 °C, WHSV of 1200 ml/g.h and N₂ to C₃H₈ molar ratio of 2. The results revealed that the isomorphously substituted Zn-ZSM-5 has a stable BTX selectivity of about 44 – 43 % between the 2 hour to 8-hour time on stream test which was higher than that of the impregnated catalyst, 30 – 19 % between the 2 hour to 8 hour time on stream test. Thus, isomorphous substitution of zinc in ZSM-5 improved greatly the stability of the catalyst in propane aromatization.

Key words: Stability, propane, aromatization, isomorphous-substitution, zinc-ZSM-5.

1. Introduction

Propane aromatization plays an important role in economic and strategic fields and has been extensively studied in recent years (Xiao *et al.*, 2015). The field has attracted interest of many research groups as it allows the direct use of these cheap and readily available raw materials to provide an alternative to current aromatics production processes that largely depend on oil. The main reason for the production of aromatics is their application as high octane blending components for gasoline as an excellent solvent and a base chemical in a number of petrochemical processes, (Asaftei *et al.*, 2015). Many types of zeolites structures have been studied for the aromatization of lower saturated and unsaturated hydrocarbons, (Liu *et al.*, 2009), but the most frequently used catalyst is ZSM-5. Zinc modified ZSM-5 is one of the most frequently used catalyst for propane aromatization based on its superior catalytic performance, (Xiao *et al.*, 2015). Zinc has very good dehydrogenating activity, high aromatic selectivity and it is very cheap, (Tshabalala and Scurrrell 2015; Asaftei *et al.*, 2013). Unlike the conventional impregnation method that produces unstable metal species that are mostly located on the outer surface of the zeolite, which may reduce and elude in the reactor bed, (Bayense and van Hooff 1991; Berndt *et al.*, 1996; Biscardi *et al.*, 1998), catalysts prepared via isomorphous substitution of metal in the zeolite frame work exhibited better stability, (Bayense and van Hooff, 1991; Akhtar and Al-khattaf, 2010). At present, the main problem with zinc-ZSM-5 catalyst is its inadequate stability (Nicolaidis *et al.*, 2002), that is, zinc easily vaporizes at aromatization temperatures of 500 to 600 °C, (Tshabalala and Scurrrell 2015). Therefore, this work was aimed at investigating the effect of isomorphous substitution of zinc in ZSM-5 zeolite for propane aromatization.

2. Experimental**2.1 Raw Materials**

Commercial ZSM-5 zeolite (Zeolyst international) with 2.0 wt.% zinc oxide (ZnO) loading was obtained from basic research laboratory of the National Research Institute for Chemical Technology, Zaria. Sodium hydroxide (Sigma Aldrich, reagent grade, 98%, anhydrous pellets), NH₄Cl, propane, tetrapropyl ammonium bromide (Sigma Aldrich, 99.5%), active alumina (Sigma Aldrich, 98%), colloidal silica (silica sol, Sigma Aldrich 30 wt.%), sulphuric acid (Sigma Aldrich, 98) and Zn(NO₃)₂, were used as reagents.

2.2 Synthesis of Zn-ZSM-5

Zn-ZSM-5 was synthesized using the hydrothermal procedure as reported by Lisensky, *et al.*, 2010 with some modifications. The solid product was dried in an oven at 100 °C for 12 hour. Finally, the dried sample was calcined at 550 °C for 5 hour to remove the template and obtain the NaZn-ZSM-5.

2.3 Conversion of Na-ZnZSM-5 to H-ZnZSM-5

The conversion procedure used is as follows; 5g of sodium form of ZnZSM-5 was ion exchanged two times with 500 ml of 1.0 M NH₄Cl solution for 7 hour at room temperature. The resulting mixture was filtered using a vacuum pump. The residue was thoroughly washed with deionized water and dried in an oven at 80 °C for 8 hour. The dried sample was calcined in a furnace at 550 °C in air for 5 hour.

2.4 Catalyst characterization

Powder X-ray diffraction (XRD) patterns of the prepared samples were recorded on a Bruker advance diffractometer using Cu K α ($\lambda=1.5404 \text{ \AA}$), irradiation at 40 mA and 45 kV, with Lynx eye detector in the 2θ range of 5° – 55°. X-ray fluorescence spectrometer experiments were conducted on a X-Supreme-

8000 Oxford Instrument, X-ray tubes with W, Pd or Ti target, high resolution large area silicon drift (SDD) and proportional detector, and SMARTCHECK software package was employed for the analysis. The Fourier transform infrared spectrophotometer analysis was conducted on SHIMADZU FTIR-8400S. The textural properties of catalyst were measured by nitrogen physical sorption using a V-Sorb 2800P Surface area and porosimetry analyzer. Surface areas were calculated by the BET method and micro-meso- and macropore volumes by the t-plot method.

2.5 Catalyst evaluation

The catalysts test for propane aromatization was carried out in a fixed-bed reactor at temperature of 540 °C, pressure of 1atm. WHSV of 1200 ml/g.h and with a N₂ to C₃H₈ molar ratio of 2. Outlet gas was analyzed after 2 – 12 hour reaction time. The products were analyzed by online gas chromatograph 25 (MACK-10) equipped with a flame ionization detector (FID) and a thermal conductivity detector (TCD), respectively. The propane

conversion and aromatics selectivity were determined.

3. Results and Discussion

The XRD patterns of the commercial Zn/ZSM-5 and the synthesized (isomorphously substituted) Zn-ZSM-5 are shown in Figure 1. Every sample showed the characteristic patterns of MFI topological structures. The intensity of the peaks of the zeolites decreased in the synthesized sample. Diffraction peaks of ZnO crystallites in the synthesized Zn-ZSM-5 were not observed, which may indicate that the Zn species in the samples were highly dispersed. Figure 2 presents the FTIR results of both samples. Characteristic vibrations in MFI type zeolites are those bands at about 455, 555, 800, 1095 and 1225 cm⁻¹. The presence of a band at 550 cm⁻¹ in addition to the one at 450 cm⁻¹ shows that ZSM-5 zeolite has been formed even if the material is X-ray amorphous, (Vafaeian, Haghghi, and Aghamohammadi 2013). However, it is obvious that there is decrease in the intensity of the peaks in the synthesized sample due to the addition of zinc into the zeolite frame work.

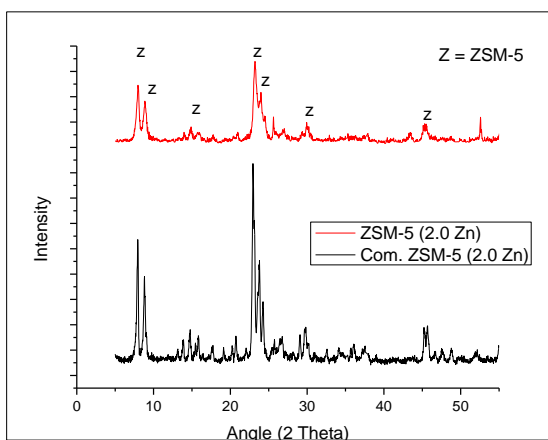


Figure 1: XRD diffraction patterns of commercial and synthesized samples

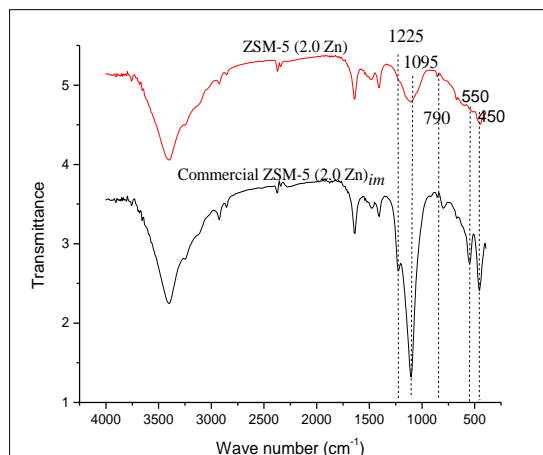


Figure 2: FTIR diffraction the patterns of samples

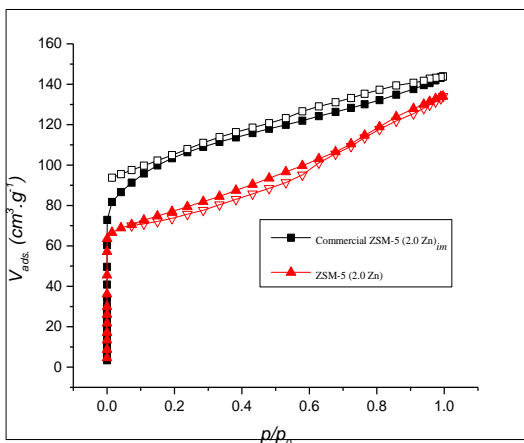


Figure 3: N₂ adsorption-desorption isotherms of Zn/ZSM-5 commercial and Zn-ZSM-5 synthesized samples

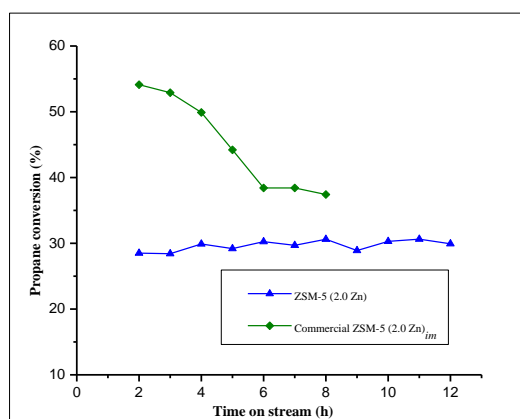


Figure 4: Propane conversion as a function of time on stream. Reaction conditions: 1atm, 540 °C, WHSV of 1200 ml/g.h and N₂ to C₃H₈ molar ratio of 2.

Figure 3 presents the N₂ adsorption–desorption isotherms of the two samples, for the samples isomorphously substituted by Zn and the commercial Zn-supported by impregnation methods at relative pressure (p/p_0) between 0 and 1.0. The incorporation of Zn by isomorphous substitution method reduced the amount of N₂ adsorption, the micro-pore volume of ZSM-5 zeolite was also reduced as revealed in Table 1. The micro-pore volume decreased and the BET surface area of the commercial sample is higher, 330 m²/g than that of the synthesized sample, Zn-ZSM-5, 264 m²/g. The XRF result, present also in table 1, revealed that the commercial Zn/ZSM-5 has the following elemental compositions; 87.78 SiO₂, 3.39 Al₂O₃ and 6.56 ZnO respectively,

whereas, the synthesized sample has 91.32 SiO₂, 5.71 Al₂O₃ and 1.66 ZnO. From the viewpoint of catalytic performance, it is clear, from figure 4, that the impregnated sample has the higher percentage propane conversion of 54%, the conversion collapsed rapidly to 37% within the first 6 hour. The synthesized sample shows lower but stable conversion trend of about 30% for the entire period of time on stream test. Figure 5 presents results for the Benzene, Toluene, and Xylene (BTX) selectivity. The Zn/ZSM-5 commercial sample exhibit lower BTX selectivity than Zn-ZSM-5 synthesized. In addition, a stable BTX selectivity was observed from the synthesized catalyst under the conditions used in this work.

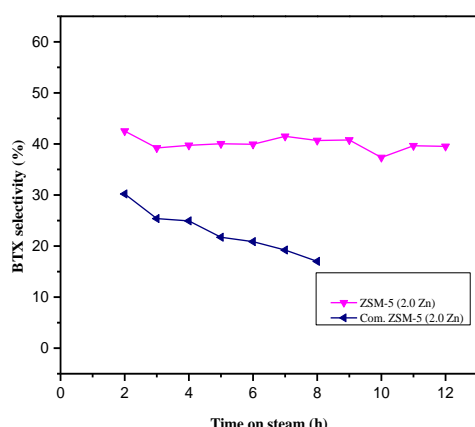


Figure 5 Selectivity of BTX as a function of time on stream.. Reaction conditions: P = 1atm, T = 540 °C, WHSV = 1200 ml/g.h and N₂/C₃H₈ molar ratio = 2.

Table 1: Chemical composition and textural properties of the catalysts.

Sample	Elemental analysis			Textural properties		
	SiO ₂	Al ₂ O ₃	ZnO	S _{tot} ^a (m ² /g)	V _{mes} ^b (m ³ /g)	V _{mic} ^c (m ³ /g)
Zn-ZSM-5 synthesized	91.32	5.71	1.66	264	121	143
Zn/ZSM-5 Commercial	87.78	3.39	6.56	349	151	199

Conclusion

Zinc-ZSM-5 catalyst was successfully synthesized using hydrothermal procedure via isomorphous substitution of 2 wt. % zinc and characterized using XRD, BET, XRF and FTIR techniques. The results clearly indicated the formation of MFI type zeolite with reduced degree of crystallinity when compared with the commercial ZSM-5 impregnated with 2wt. % zinc. Performance test at 1atm, 540 °C, WHSV of 1200 ml/g.h and N₂ to C₃H₈ molar ratio of 2, revealed a stable BTX selectivity of about 43% which is higher than that of the impregnated catalyst, 30% at the expense of propane conversion.

Acknowledgements

The authors appreciate the support of the Petroleum Technology Development Fund (PTDF), Abuja, Nigeria for funding the research.

REFERENCES

Akhtar, M Naseem, and Sulaiman S Al-khattaf. 2010.

“Catalytic Aromatization of Alkanes.” In *Catalysts in Petroleum Refining & Petrochemicals*.

Asaftei, Iuliean Vasile, Kamel Earar, Lucian Mihail Birsa, Ioan Gabriel Sandu, Neculai Catalin Lungu, and Ion. Sandu. 2015. “Conversion of Light Hydrocarbons with Butanes and Butenes from Petroleum Refining Processes over Zn-HZSM-5 and ZnO/HZSM-5 Catalysts.” *Revista de Chimie (Bucharest, Romania)* 66 (7): 963–71.

Asaftei, Iuliean V., Nicolae Bilba, and Ion Sandu. 2013. “Synthesis, Characterization and Catalytic Activity of Gallium-Modified ZSM-5 (MFI) Zeolites in N-Heptane Aromatization.” *Revista De Chimie* 64 (5): 509–15.

Bayense, C. R., and J. H C van Hooff. 1991. “Aromatization of Propane over Gallium-Containing H-ZSM-5 Zeolites. Influence of the Preparation Method on the Product Selectivity and the Catalytic Stability.” *Applied Catalysis A, General* 79 (1): 127–40.

Berndt, H., G. Lietz, B. Lücke, and J. Völter. 1996. “Zinc Promoted H-ZSM-5 Catalysts for Conversion of Propane to Aromatics: I. Acidity and Activity.” *Applied Catalysis A: General* 146 (2): 351–63.



- Biscardi, Joseph A, George D Meitzner, and Enrique Iglesia. 1998. "Structure and Density of Active Zn Species in Zn/H-ZSM5 Propane Aromatization Catalysts." *Journal of Catalysis* 179 (1): 192–202.
- Vafaeian, Yaser, Mohammad Haghighi, and Sogand Aghamohammadi. 2013. "Ultrasound Assisted Dispersion of Different Amount of Ni over ZSM-5 Used as Nanostructured Catalyst for Hydrogen Production via CO₂ Reforming of Methane." *Energy Conversion and Management* 76. Elsevier Ltd: 1093–1103.



ABSTRACT CCT-: 034

Sule, A.M., Inuwa, B. and Gero, M.

1National Research Institute for Chemical Technology, P.M.B 1052, Basawa Zaria, Nigeria.

Email: asmaikano8319@gmail.com

**BIOREMEDIATION POTENTIAL OF HEAVY METALS RESISTANT
ASPERGILLUS VERSICOLOR ISOLATED FROM TANNERY EFFLUENT,
CHALLAWA INDUSTRIAL ESTATE, KANO STATE, NIGERIA.**

ABSTRACT: Heavy metals and physico-chemical properties of tannery effluent from Challawa industrial estate of Kano state, Nigeria were analyzed in this study and most of the parameters were found to be beyond the permissible standards stipulated by the Nigerian Environmental Standards and Regulations Enforcement Agency (NESREA) and this call for serious concern and attention. Heavy metal resistant *Aspergillus versicolor* was isolated and screened in the presence of chromium, cadmium, copper, manganese and lead. The most heavy metals resistant *Aspergillus versicolor* fungal isolate was used to bioaugment a fabricated pilot scale trickle biofilter in order to produce the desired biofilm for the bioremediation of some selected heavy metals present in the tannery effluent (chromium, cadmium, copper, manganese and lead). The optimal uptake of the heavy metals per unit biomass by the *Aspergillus versicolor* fungal isolate were 0.148mg/g, 0.027 mg/g, 0.094mg/g, 0.098mg/g and 0.014mg/g for chromium, cadmium, copper, manganese and lead respectively while the optimal percentage removal efficiency for the removal of chromium, cadmium, copper, manganese and lead were 65%, 38%, 75%, 59% and 50% respectively. Hence the high percentage removal of these heavy metals recorded in this study is an indication that this technology may offer a feasible solution to the serious environmental pollution problems associated with the presence of heavy metals in industrial effluent.

Keywords: Tannery effluent, Heavy metals, Bioaccumulation, *Aspergillus versicolor*.

1. Introduction

There has been a tremendous growth of industries worldwide in the last few decades and the associated anthropogenic activities have often resulted in environmental pollution. Heavy metals are prominent components of industrial effluents which are discharged into the environment and consequently pollute the ecosystem (Olatunji *et al.*, 2009).

The present study attempts to elucidate the potential of heavy metal resistant *Aspergillus versicolor* isolated from tannery effluent and also to assess its efficiency to bioaccumulate and remove chromium, cadmium, copper, manganese and lead present in tannery effluent

2. Materials and Methods

2.1 Sample Area and Sample Collection

The sample area used for this study was a tannery industry located at Challawa industrial estate of Kano state. A total of 50 tannery effluent samples from five sampling points were collected for this study according to the method described by Ezike *et al.* (2012).

2.3 Assessment of Heavy Metals and Physicochemical Parameters of the Tannery Effluent

Physico-chemical and heavy metals contents of the tannery effluent samples were assessed according to standard methods described by APHA, (1992).

2.4 Isolation and Preservation of Fungal Isolates from Tannery Effluent

Isolation and identification of *Aspergillus versicolor* isolates was carried out according to the method described by Ijah (1998) Barnett and Hunter, (1999); Larone, (2002).

2.5 Bioaccumulation Experiment

The bioaccumulation experiment was carried according to the method described by Abida *et al.* (2009).

2.6 Estimation of Heavy Metals Uptake by *Aspergillus versicolor* per Unit Mycelium Biomass

The heavy metal uptake of each of the heavy metals by the *Aspergillus versicolor* was



calculated in accordance with the methods described by Viraghavan *et al.* (1999).

2.7 Estimation of Percentage Removal Efficiency of Heavy Metals by the Selected Fungal Biomass

The percentage removal efficiency of each of the *Aspergillus versicolor* was according to the method by Kumar *et al.* (2011).

2.8 Statistical Analysis

The student F-test was used to analyze the data that were obtained with the aid of statistical package for social sciences (SPSS) version 20 (Using ANOVA ≤ 0.05)

3. Results and Discussion

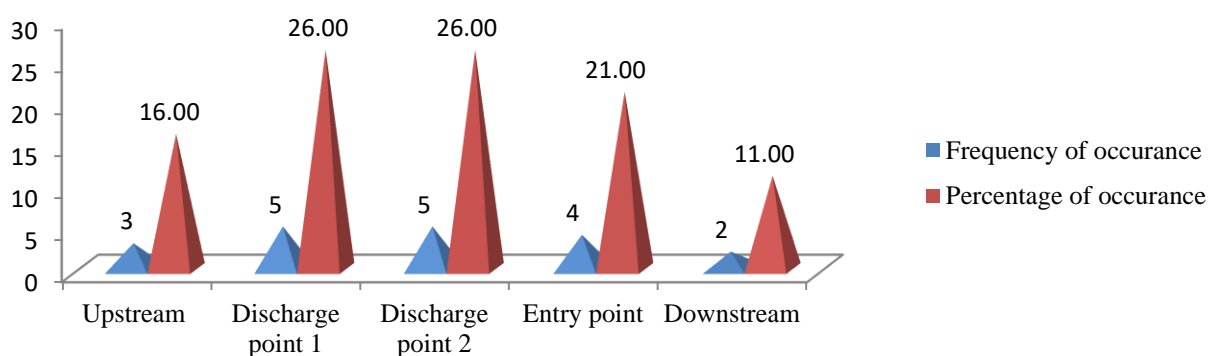


Figure 3.1 Frequency and Percentage Occurrences of *Aspergillus versicolor* across Sampling Points

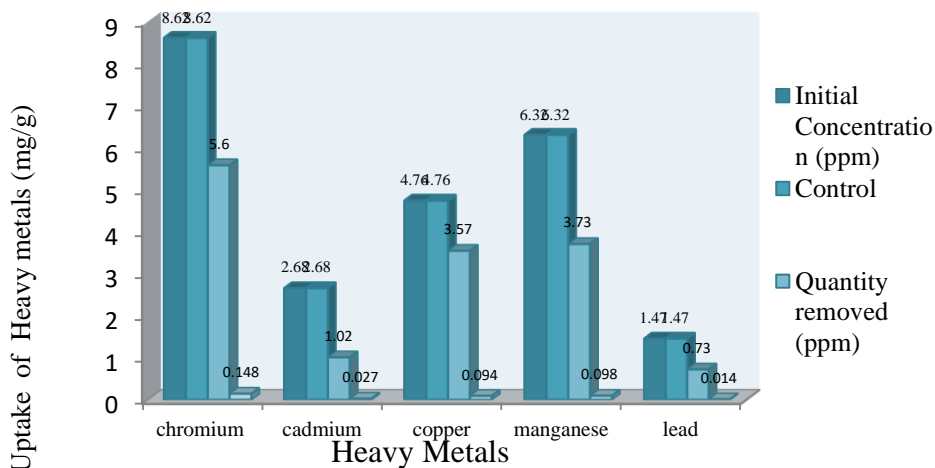


Figure 3.2: Mean Uptake of some Heavy from Tannery...



Table 3.1: Physicochemical Analysis and Heavy Metal Contents of the Tannery Effluent and Challawa River

Physicochemical Parameter and Heavy Metal Contents	<u>Mean Values ± SD</u>					P value	Permissible Standard (NESREA)
	Sampling Sites						
	A	B	C	D	E		
pH	7.5±0.17 ^d	11.0±0.10 ^a	10.4±0.20 ^b	8.3±0.30 ^c	7.5±0.40 ^d	0.000	6.0-9.0
Temp (°C)	29.0±0.35 ^b	30.1±0.10 ^a	29.8±0.12 ^a	29.2±0.15 ^b	29.3±0.34 ^b	0.720	<40
EC (µs/cm)	5.1±0.36 ^b	6.5±0.93 ^a	6.9±0.16 ^a	7.3±0.90 ^a	7.2±0.25 ^a	0.008	2.0
Turbidity (NTU)	6.8±0.85 ^b	9.1±4.57 ^b	14.7±0.56 ^a	16.7±0.91 ^a	14.7±0.35 ^a	0.000	5*
TDS (mg/l)	444.7±6.1 ^c	640.0±8.0 ^b	652.0±2.0 ^a	612.0±4.0 ^c	560.0±6.0 ^d	0.000	500
TS (mg/l)	471.3±3.05 ^d	681.3±7.02 ^a	690.0±9.00 ^a	646.0±6.00 ^b	585.3±4.73 ^c	0.000	2000
TSS (mg/l)	24.0±2.0 ^c	42.0±5.0 ^a	38.0±6.0 ^a	34.0±3.0 ^{ab}	29.0±5.0 ^{bc}	0.000	30
BOD (mg/l)	28.0±4.001 ^c	71.3±5.0 ^a	68.0±7.0 ^a	56.0±6.0 ^b	48.0±8.0 ^b	0.000	30
DO (mg/l)	15.0±1.53 ^a	7.0±6.0 ^b	7.7±2.65 ^b	7.0±4.00 ^b	6.1±1.53 ^c	0.000	10
Nitrate (mg/l)	24±3.0 ^c	48±7.0 ^a	52±4.58 ^a	36±5.00 ^b	31±4.00 ^{bc}	0.000	20
Sulphate (mg/l)	250.7±5.0 ^c	610±5.0 ^b	652±2.0 ^a	543±4.0 ^c	450±6.0 ^d	0.000	500
Phosphate (mg/l)	2.0±0.4 ^d	11.0±3.0 ^{ab}	14.0±2.0 ^a	9.0±2.0 ^{bc}	6.0±1.9 ^c	0.000	5.0
Chromium (ppm)	1.2±0.15 ^c	9.2±0.50 ^a	6.8±0.60 ^b	4.6±0.50 ^c	3.7±0.15 ^d	0.000	0.50
Cadmium (ppm)	0.43±0.25 ^{a^c}	0.63±0.25 ^a	0.73±0.15 ^a	0.53±0.12 ^{ab}	0.27±0.12 ^{bc}	0.000	0.02
Copper (ppm)	1.37±0.25 ^c	4.80±0.70 ^a	5.60±0.30 ^a	3.27±0.71 ^b	2.53±0.40 ^b	0.000	0.10
Manganese (ppm)	3.40±0.50 ^c	6.13±0.31 ^a	5.60±0.44 ^{ab}	4.80±0.70 ^b	3.60±0.50 ^c	0.000	1.00
Lead (ppm)	1.20±0.26 ^a	0.60±0.20 ^{bc}	0.80±0.40 ^{ab}	0.40±0.20 ^{bd}	0.27±0.21 ^{cd}	0.010	0.50

Means with different superscript across the row are significant ($P > 0.05$). Means with the same superscript across the rows are not significant ($P \leq 0.050$) using ANOVA. EC= Electrical conductivity, TDS= Total dissolved solids, TS= Total solids, TSS= Total suspended solids, BOD= Biological oxygen demand, DO= Dissolved oxygen. A= Upstream, B= Discharge point 1, C= Discharge point 2, D= Entry point E= Downstream. NESREA= Nigerian Environmental Standards and Regulations Enforcement Agency. *=World health organization (WHO) Permissible standard. SD= Standard Deviation Means with different superscript across the row are significant ($P > 0.05$), Conc.= Concentration, ppm= part per million.

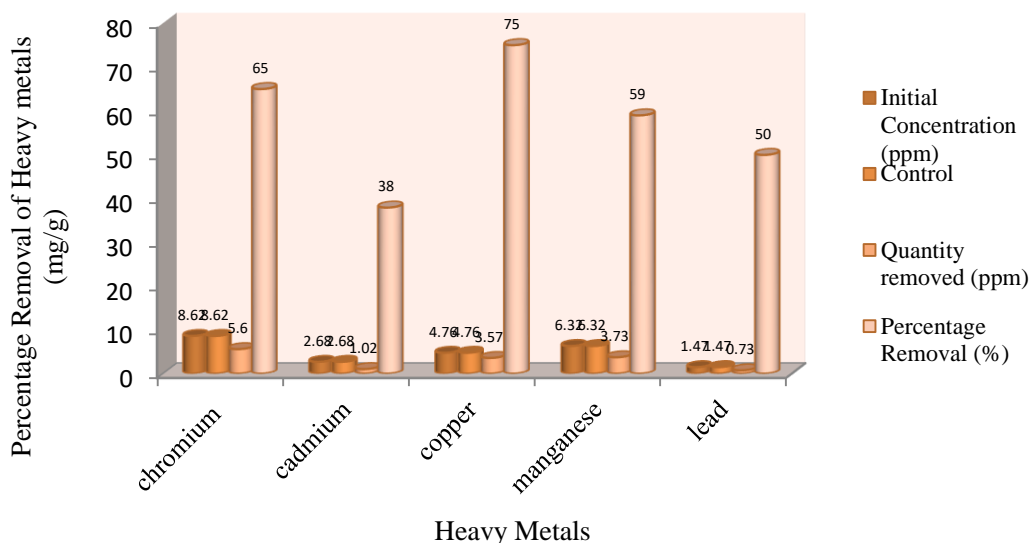


Figure 3.2: Mean Uptake of some Heavy Metals from Tannery Effluent...

4.0 Conclusion

Physicochemical and heavy metals analyzed in this study were found to be beyond the permissible limits stipulated by Nigerian Environmental Standards and Regulations Enforcement Agency (NESREA) which call for serious concern and attention.

Total of 19 *Aspergillus versicolor* fungal isolates were and screened for their ability to tolerate and bioaccumulate the five heavy metals used in this study with the following percentage removal efficiencies chromium 65%, cadmium 38%, copper 75%, manganese 59% and lead 50%.

References

Abida, B., Ramaiah, H.M., Khan, I. and Veena, K. (2009). Analysis of Heavy Metals Concentration in Soil and Lichens from Various Localities of Hosur Road, Bangalore, India, *E- Journal of Chemistry*, 6(1):13-22.

Ademoroti, C.M.A. (1996). *Standard Method for Water and Effluents Analysis*. Foludex press Ltd, Ibadan pp.22-23, 44-54, 111-112.

Barnett, H.I. and Hunter, B.B. (1999). *Illustration Genera of Imperfect Fungi*. Fourth edition. The American Phytopathological Society St. Paul, Minnesota, U.S.A., pp. 62-218.

Ezike, N.N., Udiba, U.U., Ogabiela, E.E., Akpan, N.S., Odey, M.O., Inuwa, B., Sule, A.M. and Gauje, B. (2012). Assessment of the Performance of Primary Effluent Treatment Plant of Major Tanneries in Kano, Nigeria. *Trends in Advanced Science and Engineering*, 5(1): 58-45.

Kumar, A., Bisht, B.S. and Joshi, V.D. (2011). Zinc and Cadmium Removal by Acclimated *Aspergillus niger*: Trained Fungus for Biosorption. *International Journal of Environmental Sciences and Research*, 1(1):27-30.

Viraghawan, T., Kapoor, A. and Cullimor, D.R. (1999). Removal of Heavy Metals Using the Fungus *Aspergillus niger*. *Journal of Bioreources Technology*, 70:95-104



ABSTRACT CCT-: 071

H. Ibrahim*, S. Ayilara, K. O. Nwanya, A. S. Zanna, O. B. Adegbola, and D. C. Nwakuba
Renewable Energy Division, National Research Institute for chemical Technology, Zaria-Nigeria
Email: asmaikano8319@gmail.com

EXPLORING GMELINA ARBOREA LEAVES FOR BIOFUELS, PETROCHEMICAL AND PHARMACEUTICAL FEEDSTOCKS

ABSTRACT: An investigation was carried on the chemical constituents of *Gmelina arborea* leaves by hydrolyzing the pulverized dry leaves with 3 % sulphuric acid solution at 100 oC for 30 minutes. The extract on analysis with GCMS yielded 31 compounds. The major components of the extract include; 5-methyl furfural 13.024%, 5-hydroxyl methyl furfural 7.548 %, 2-furan methanol 22.728 %, 6-methyl-3-pyridazinone 3.256 %, o-hydroxyphenol 2.704 %, p-hydroxyphenol 4.4 %, m-hydroxyphenol 3.048 %, levoglucosenone 7.576 %, levoglucosan 3.26 %, 4-Altrosan 1.63 %, 1,6-Anhydro-beta-d-talopyranose 1.63 % and D-Allose 1.63 %. Biorefinary processes of *Gmelina arborea* leaves products can be capable of replacing petroleum products in future. The plant leaves have feedstocks for pharmaceutical, agro-industries and others.

Keywords: biofuels,, *Gmelina arborea* leaves, petrochemical, pharmaceutical

1.

Introduction

Gmelina arborea is a very important medicinal plant belongs to the family of verbenaceae [1]. It is a fast growing deciduous tree with a wide spread canopy [2] and straight trunk [4]. It is commonly known as white teak and Kashmir [3]. It grows from 3 to 30 m tall [2:3], thrives better at 22-34oC, survive from 16-46oC but get killed at 1oC and below [2]. It has life span of 40 years [2] borne flowers 3-4 years after planting [4]. The leaves are 10-23 cm long 6.3 cm broad used as demulcent to throat gonorrhoea and cough and also applied to wounds and ulcer [2]. The flowers are abundant scented reddish brown or yellow terminals and axillary 1-3 flowered cymes on the panicle branches about 8-40 cm long [4]. The flowers are said to bisexual in nature [1] and have been used to treat leprosy and blood diseases [2]. The fruits are edible sweet taste and its flowers can be used with rice to make delicious cake like festive dish [2]. The roots and barks contain oil, resins, alkaloids, benzoic acid, butyric acid and tartaric acid used for stomachic, laxative and anthelmintic good for remedy of pile, improve appetite and inflammation [3:2]. The root also used for blood purifier and antidote for snake bite and scorpion sting [2:3]. The fruits and barks have medicine for bilious fever [2]. Both the wood ash and fruits yield very persistent yellow dye [2].

The wood is light, soft to hard, very susceptible to fungi, dry wood borer and termites. The natural durability is about 15 years [2]. The wood is good for furniture, plywood cores stock, mine prop, matches and timber for construction of dug canoes, musical instruments and carving images [2:3]. The wood produces good quality pulp suitable for cardboard and low grade writing papers.

Adisa and Olurunsoju [5] reported to have isolated para-hydroxyphenol from leaves of *Cnestis ferruginea* (D.C). Chakraborty et al., [6], have extracted furfural from leaves of decorative plants and also Ibrahim et al., [7],

have extracted furfural, 2-furan methanol and hosts of other useful chemicals from the leaves of earleaf acacia using 3 % sulphuric acid. In this work, we delight to investigate the chemical components of *Gmelina* leaves by hydrolyzing it with 3 % sulphuric acid for 30 minutes at 100°C. The chemical components of the resulting extract were analyzed with GCMS.

2. Materials and Methods

The materials used in this study include; pulverized *Gmelina arborea* leaves, GC-MS and Hot plate magnetic stirrer. The following laboratory equipment were also used; mortar and pestle, 1000 ml conical flask, 1000 ml beaker, filter paper, separating funnel, burette and thermometer. The chemical used include; sulphuric acid and analytical grade methanol. Dried leaves of *Gmelina arborea* were collected from around the premises of NARICT, Zaria. These leaves were pulverized using mortar and pestle. 3% sulphuric acid solution was prepared and 500 ml of it was mixed with 50 g of the pulverized leaves and heated to 100oC for 30 minutes [7]. The hydrolyzed mixture was filtered and part of it was neutralized with hydrated lime to pH of 7. The neutral filtrate was analyzed with GC-MS to determine its chemical constituents.

3. Results and Discussion

The hydrolyzed product of *gmelina arborea* leaves contain was found to 31 compounds as presented in Table 1. It has 20.576% furfural derivatives, 22.728% furan methanol, 3.256 % 6-methyl-3-pyridazinone, 7.58 % Levoglucosenone, 3.26 % Levoglucosan, 15.022 % benzene derivatives, 7.548 % borane halides, 1.228 % alkynes and 17.958 % others as presented in Table 1. The benzene derivatives found in the product including; toluenes, phenols, styrene and amines. Hydroxyphenols consist of 10.152 % which include ortho-hydroxyphenol, para-hydroxyphenol and meta-hydroxyphenol. It



had only 7.576 % fatty acid which was 2, 4-pentadienoic acid.

3.1 Furfural Derivatives

Figure 1 depicted the structural formula of three furfural derivatives found in the hydrolysis product which were; 5-methyl furfural 13.024 %, 5-hydroxymethyl furfural 7.548 % and 2-furan methanol 22.728 % as presented in Table 1. 1. 5-methyl furfural is a very expensive compound. 98% concentration of this compound is selling at the rate of 23.50 euro for 25.0 g [8]. It boils at 186-188 oC, relative density of 1.106, refractive index 1.5310, flash point 72 oC soluble in alcohols and water. It is used in perfuming agent and a smoking essence [8]. 5-Methylfurfural is a volatile compound present in *Lavandula stoechas*, *Lavandula angustifolia* and

Lavandula angustifolia x *latifolia* unifloral honeys and formed during the photo exposition of ranitidine hydrochloride. It is employed as potential age marker for Madeira wine [9]. 5-Hydroxymethyl furfural abbreviated as HMF is known to be produced from hexose and cellulose [10:11]. It is used for production of polyurethane [10] and nylon 6,6 monomers [11]. It has been reported by Rosatella et al., [12] that HMF can be useful in the production of important molecules such as levulinic acid, 2,5-furandicarboxylic acid (FDA), 2,5-diformylfuran (DFF), dihydroxymethyl furan and 5-hydroxy-4-keto-2-pentenoic acid. 2-furan methanol has been found useful in Furan polymers, in making Sealants and Cements, Urea-formadehyde and Phenolic Resins, as a Solvent, Foundry cores, Flavorings [7].

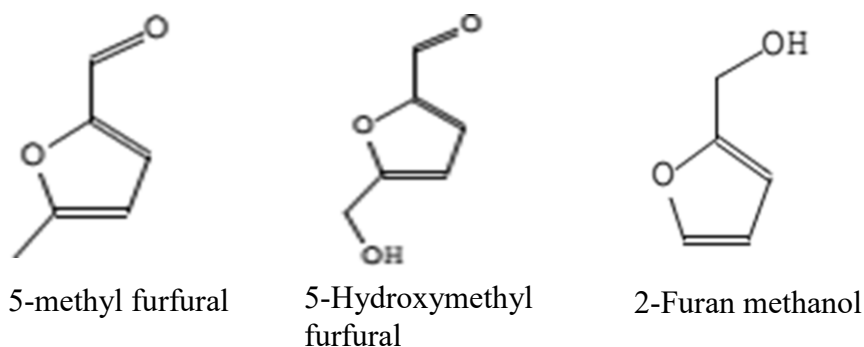


Figure 1: Structural formulae of furfural derivatives extracted from *gmelina arborea* leaves

3.2 Nitrogen Compounds

The structural formula of some nitrogen compounds extracted from *gmelina arborea* is depicted in Figure 2. They include; 6-Methyl-3-pyridazinone 3.256 %, o-Nitrobenzylalcohol 0.912 %, N-(1-Cyanopropenyl) formamide 0.848 %, Ethinamat (Valamin) 0.614 % among others as presented in Table 1. 6-methyl-3-pyridazinone is a derivative of pyridazine which has been found to be active in antimicrobial, antitubercular, analgesic and anti-inflammatory, antipyretic, antifeedant, herbicidal, antiplatelet, anticancer, cardiovascular and neurological disorder and

other anticipated biological and pharmacological activities [7]. According to Phamacodes [13], Valamin is a very important pharmaceutical product for treatment for ascariasis caused by *Ascaris lumbricoides* (roundworm) and enterobiasis (oxyuriasis) caused by *Enterobius vermicularis* (pinworm). It is also used to treat partial intestinal obstruction by the common roundworm, a condition primarily occurring in children. Unfortunately, there was no information on uses of the other two compounds, o-Nitrobenzyl alcohol and N-(1-Cyanopropenyl) formamide.

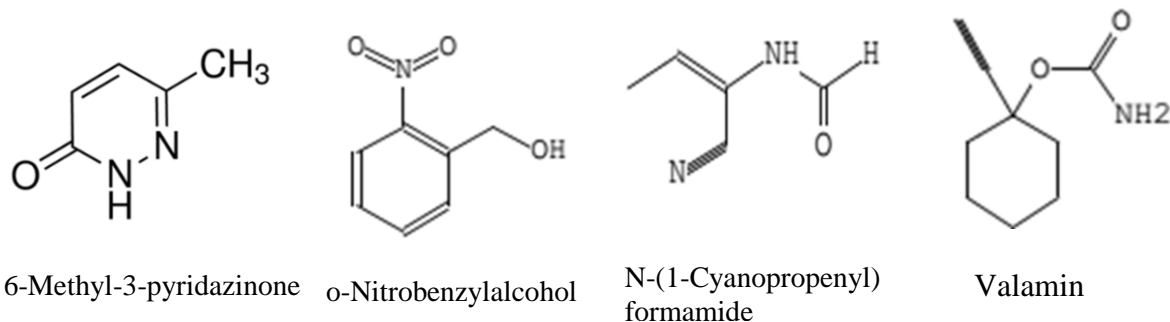


Figure 2: Structural formulae of nitrogen compounds extracted from *gmelina arborea* leaves

3.3 Hydroxyphenols

Figure 3 depicted the structural formula of three major benzene derivatives extracted from

Gmelina arborea leaves. The hydrolytic product had a lot of benzene derivatives, but hydroxyphenols in Figure 3 have higher



concentration than others. They include; o-hydroxyphenol (pyrocatechol) 2.704 %, p-hydroxyphenol (hydroquinone) 4.4 % and m-hydroxyphenol (resorcinol) 3.048 %. According to GPS-2011 [14] pyrocatechol or simply catechol is used as precursor to various flavorings such as vanillin or eugenol, used in food industry, perfumery, home and personal product. Adisa and Olurunsogu [5] reported that p-hydroxyphenol possesses very powerful

antioxidant property. According to Drugs.com [15], the hydroquinone cream is used in lightening freckles, age spots and other skin discoloration associated with pregnancy, skin trauma, birth control pills or hormone. It has been reported by Xueyanghu [15] that resorcinol is used in antiseptic, disinfectant, as ointment in the treatment of skin diseases such as eczema and psoriasis and also antidandruff.

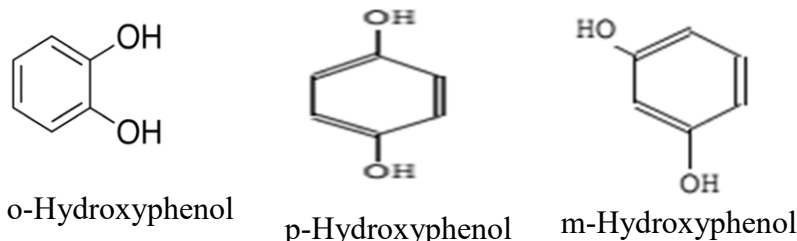


Figure 3: Structural formula of Hydroxyphenols extracted from *gmelina arborea* leaves.

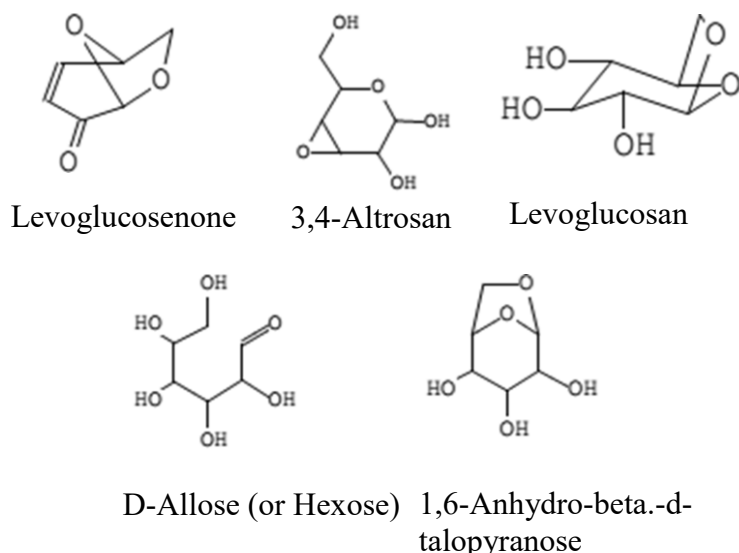


Figure 4: Structural formulae of simple sugars extracted from *gmelina arborea* leaves.

3.4 Sugars

Five simple sugars were identified from the hydrolytic extraction of *gmelina arborea* leaves which are; levoglucosenone 7.576 %, Levoglucosan, 3.26 % 3,4-Altrosan, 1.63 %, 1,6-Anhydro-beta.-d-talopyranose, 1.63 %, and D-Allose (or Hexose) 1.63 %. The structural formulas of the five sugars are shown in Figure 4. Levoglucosenone is produced from cellulose which has been used for the synthesis of natural products such as tetrodotoxin [17]. According to Perez [18], levoglucosan can be hydrolyzed and converted to a multitude of chemical species, including alcohols and lipids and that the use of levoglucosan for the production of polymers was extensively studied in the 1980s and early 1990s. 3,4-Altrosan is a Bacteriostat and fungicide [19:20]. 1,6-Anhydro-beta.-d-talopyranose also called 1,6-anhydro-beta-D-mannopyranose is found used as a marker of toasted oak wood used for ageing wines and

distillates [21]. Cayman [22] described it as a major organic tracer used to evaluate in atmospheric samples of burning of wood. It is reported that β -D-Allose a rare sugar member of the aldohexose family and a C3 of glucose is used as an inhibitor of fruiting body formation and sporulation in *myxococcus xanthus* [23]. The extract of *gmelina arborea* leaves is rich in pharmaceutical, biofuel and plastic feedstocks. 2-furan methanol (furfuryl alcohol) which has the highest quantity in the extract is described as the most important furfural derivative due to its numerous applications. It has been used in reinforced carbon-carbon composite materials, developed to protect the shuttle around its nose and wing leading edge from extremely high and cold temperatures (-121-1,649°C) encountered during there-entry of shuttles into space [24]. It has ingredient for wood modification processes that convert soft woods to products that like and have properties that are similar to



tropical hard woods [24]. It was reported by Elbert [25] that the blend of hydroxymethyl furfural fossil gave smooth engine

performance with significant reduction in sooth emissions from vehicles.

Table 1: Product components of *Gmelina arborea* leaves extract

Compound	MF	% Composition	Group composition %
1 5-methyl-Furfural	C ₆ H ₆ O ₂	13.024	Furfural derivatives
2 5-Hydrxomethylfurfural	C ₆ H ₆ O ₃	7.548	
3 2-Furanmethanol	C ₅ H ₆ O ₂	22.728	43.300
4 6-Methyl-3-pyridazinone	C ₅ H ₆ N ₂ O	3.256	Methyl pyridazinone, 3.256
5 2,4-Pentadienoic acid	C ₅ H ₆ O ₂	7.576	Fatty acid 7.576
6 3,4-Altrosan	C ₆ H ₁₀ O ₅	1.63	
7 .beta.-D-Allose	C ₆ H ₁₂ O ₆	1.63	
8 1,6-Anhydro-.beta.-d-talopyranose	C ₆ H ₁₀ O ₅	1.63	
9 Levoglucosan	C ₆ H ₁₀ O ₅	3.26	Sugar
10 Levoglucosenone	C ₆ H ₆ O ₃	7.576	15.726
11 o-Hydroxyphenol	C ₆ H ₆ O ₂	2.704	
12 p-Hydroxyphenol	C ₆ H ₆ O ₂	4.4	
13 m-Hydroxyphenol	C ₆ H ₆ O ₂	3.048	
14 2-Hydroxy-4-methylphenol	C ₇ H ₈ O ₂	0.456	
15 p-(Hydroxymethyl)phenol	C ₇ H ₈ O ₂	0.912	
16 3-Nitro-4-methylaniline	C ₇ H ₈ N ₂ O ₂	0.494	
17 (2-Nitrophenyl)methanol	C ₇ H ₇ NO ₃	0.494	
18 1,2,3,6-Tetrahydrobenzaldehyde	C ₇ H ₁₀ O	0.614	
19 Toluene-2,6-diol	C ₇ H ₈ O ₂	0.456	
20 2,6,2',6'-Tetramethylazobenzene	C ₁₆ H ₁₈ N ₂ O ₂	0.494	
21 2,3-Dihydroxytoluene	C ₇ H ₈ O ₂	0.456	Benzene derivatives
22 4-Hydroxy-3-methoxystyrene	C ₉ H ₁₀ O ₂	0.494	15.022
23 N-(1-Cyanopropenyl)formamide	C ₅ H ₆ N ₂ O	0.848	0.848
24 -4-Methyl-4-hepten-3-one	C ₈ H ₁₄ O	3.774	
25 Isopropyl(dipropyl)borane	C ₉ H ₂₁ B	3.774	Borane halides
26 Tripropylborane	C ₉ H ₂₁ B	3.774	7.548
27 2,7-Dioxa-tricyclo[4.4.0.0(3,8)]deca-4,9-diene	C ₈ H ₈ O ₂	0.494	
28 3a,6-Methano-3aH-inden-4-ol, octahydro-, (3a.alpha.,4.alpha.,6.alpha.,7a.beta.)-	C ₁₀ H ₁₆ O	0.614	
29 Ethinamat (Valamin)	C ₉ H ₁₃ NO ₂	0.614	
30 1-Undecen-3-yne	C ₁₁ H ₁₈	0.614	Alkynes
31 1-Decen-3-yne	C ₁₀ H ₁₆	0.614	1.228
Total		100	

Therefore furfural and its derivatives are transportation fuels for the future. Eseyin and Steele [24] also reported that hydrocarbon fuels can also be produced from furfural and its derivatives by their hydrogenolysis. Hence, biorefinary can be established with *Gmelina arborea* leaves as feedstock for the production of biofuels. The benzene derivatives have wide range of applications in petrochemicals, fuels, pharmaceutical, agrochemicals and food. Among the nitrogen compounds found in the extract methyl pyridazinone is most useful with wide range of applications. The sugar content of the extract all have important applications, this makes the leaves of the *Gmelina arborea* as important as other parts of it. The exploration of *Gmelina arborea* will provide good alternative for petroleum base

products for industrial applications. *Gmelina arborea* leaves is renewable and sustainable and that can have the capacity to replace fossil fuel for transportation fuels and plastic chemicals.

4. Conclusion

Extraction of *Gmelina arborea* leaves extract with 3 % sulphuric acid yielded 43.3 % furfural derivatives made up of 13.028, 7.548 and 22.728 % 5-methyl furfural, 5-hydroxyl methyl furfural and 2-furan methanol. Also 3.256 % 6-methyl-3-pyridazinone, 15.726 % sugars and 15.022 % benzene derivatives were found in the extract. The sugars comprises of Levoglucosenone, 3,4-Altrosan, Levoglucosan, 1,6-Anhydro-.Beta.-D-talopyranose and D-Allose with compositions of 7.576, 1.63, 3.26, 1.63 and 1.63 % respectively. Pyrocactechol (o-hydroxyphenol), hydroquinone (p-hydroxyphenol) and resorcinol (m-



hydroxyphenol) had 2.704, 4.4 and 3.048 % respectively were the major benzene derivatives in the extract. Exploration of *Gmelina arborea* as a renewable source, transportation fuels, chemicals for petrochemical, plastic, pharmaceutical and food industries can be found in abundance to replace fossil fuel sources.

Acknowledgment

The materials and facilities used in this study belong to National Research Institute for Chemical Technology (NARICT), Zaria and we the authors highly appreciate it.

References

1. Pahala D., Harini A. and Hegde P. L. (2015). Review on Gambhari (*Gmelia arborea* Roxb), Journal of Pharmacognosy and Phytochemistry.
2. Hawaii K. H. (Accessed 28/12/2016). *Gmelina arborea*, Useful Tropical Plants. Available at: tropical.theferns.info/viewtropic
3. The Bosch Power Box (Accessed 28/12/2016). *Gmelina arborea*, Spices and Medicinal Herbs. Available at: www.spicesmedicinalherbs.com
4. yemane Gumhar (2009). *Gmelina arborea*, Agroforestry Database
5. Adisa R. A. and Olorunsogo O. O. (2013). Robustaside B and *para*-hydroxyphenol: Phenolic and antioxidant compounds purified from *Cnestis ferruginea* D.C induced membrane permeability transition in rat liver mitochondria, Molecular Medicine Reports 8: 1493-1498, 2013
6. Sattar M.A., Chakraborty A.K., Al-Reza S.M and Islam M. S. (2007). Extraction and Estimation of furfural from Decorative Plants Grown in Bangladesh, *Bangladesh J. Sci. Ind. Res.* 42(4), 495-498, 2007
7. Ibrahim H., Nwanya K. O., Ayilara S., Adegbola O., Nwakuba D. C., Tyoor A. D., Ba'are A.M. and Shuaibu H. (2015). Potential of Earleaf *Acacia (Acacia auriculiformis)* Leaves for Industrial Raw Materials, International Journal of Scientific Engineering and Applied Science (IJSEAS) - Volume-1, Issue-4, July 2015 ISSN: 2395-3470 www.ijseas.co
8. Aldehydes, A13264 5-Methyl-2-furaldehyde, 98%, Accessed 22/12/2016. At available at: <https://www.alfa.com/en/catalog/A13264/>
9. Aldrich (Accessed 22/12/2016). 5-methylfurfural. Available at: <http://www.sigmaaldrich.com/catalog/product/aldrich/137316?lang=en®ion=NG>
10. Lewkowski J. (2001). Synthesis, chemistry and applications of 5-hydroxymethylfurfural and its derivatives, general paper, ARKIVOC 2001 (i) 17-54
11. Tianfu W. "(2014)." Catalytic conversion of glucose to 5-hydroxymethylfurfural as a potential biorenewable platform chemical *Graduate Theses and Dissertations*. Paper 13721.



ABSTRACT CCT-: 074

S. Muktari and B.M. Mahmuda

Department of Polymer and Textile Science, Ahmadu Bello University, Zaria, Nigeria

Email: smuktari@abu.edu.ng

SYNTHESIS AND CHARACTERIZATION OF ENVIRONMENTALLY SAFE SOAPY AND SOAP-LESS DETERGENTS FROM PURE CARAWAY

ABSTRACT: Soapy detergents (53.50g), soap-less detergent (100ml), were synthesized from caraway oil. Chemical Analysis of them showed a satisfactory comparison with a medicated (Dettol) soapy detergent bought from the market (Samaru-Zaria, Nigeria) used as control. Antimicrobial Test with three organisms (*Staphylococcus aureus*, *Pseudomonas aeruginosa*, and *Candida albican*) showed that the soapy detergent and the control had sensitivity to only one (*Staph. aureus*) of the three organisms. Hence the soapy detergent confirmed antiseptic. The soapy and 'soap-less' detergents also reduced the surface tension of water from 0.0735Nm-1 to 0.0399Nm-1 and 0.0294Nm-1 respectively hence could be used as excellent wetting and cleansing agent

Keywords: Soapy detergent, soap-less detergents, micro-organisms.

1. Introduction

Generally, detergent is a substance used to enhance the cleansing action of water. It serves as an emulsifier, which penetrates and breaks up the oily film that binds dirt particles and a wetting agent which helps them to float off [4]. These emulsifier molecules have an oil like non polar portion which is drawn into the oil, and a polar group that is water soluble; by bridging the oil-water interface, they break the oil into dispersible droplets (emulsion). Hence on this account soap can be seen as a detergent [6].

The basic function of a detergent is to remove dirt [14]. In Nigeria most people wash clothes with their hands. The detergent which removes the dirt and grime from the clothes also degreases the skin while washing the clothes. Thus natural oils from the skin are removed which may lead to certain skin diseases [12]. Linear Alkyl Benzene Sulphonate (LABS) - a primary ingredient of modern day detergents, can penetrate the epidermis causing irritation of the skin. More over the alkaline builders and fillers added to the detergents are also harmful to the sensitive skin. If the clothes are not washed very well with water, the residual detergent sticking to the cloth also may irritate the skin [12, 13].

Phosphates used as detergent builders cause eutrophication. Another active ingredient in laundry detergent is household bleach, or sodium hypochlorite. Responsible for the majority of the household poisonings, this chemical is a forerunner to chlorine. When it reacts with other organic materials, the results are even more harmful. Carcinogenic and toxic compounds are created. These can cause damage or disorder to the reproductive system, endocrine and immune system [18].

From fragrance to whiteners, detergents have become increasingly dangerous to use, especially on a regular basis. Hence the Mother to this Research Work; to Synthesize Detergent from Caraway oil - an essential oil with health benefits attributed to its properties as a galactagogue, anti-histaminic, antiseptic, cardiac, anti-spasmodic, carminative, digestive,

stomachic, disinfectant, diuretic, emagogue, expectorant, aperitif, astringent, insecticide, stimulant, tonic and vermifuge substance.

2. Materials and Methods

2.1 Materials

Caraway oil, Sodium hydroxide pellets (NaOH), Potassium hydroxide pellets (KOH), Conc. Sulphuric acid (H₂SO₄), Sodium carbonate (Na₂CO₃), Ethanol (C₂H₅OH), Neutral alcohol, Phenolphthalein indicator, Distilled water.

2.2 Equipment.

Beakers, Soap pot, Wooden stirrer, Electric balance, Glass rod, Heating mantle, Thermometer, pH meter, Mould, Burette, Pipette, Conical flask, Volumetric flask.

2.3 Synthesis

Caraway oil of the Kano Origin was sourced from Kano, Nigeria and subjected to the processes of making soapy and soap-less detergents.

2.4 Soapy detergent

50g of caraway oil was weighed into a 500 ml beaker, lye water prepared by dissolving 9.1g of NaOH in 10 ml of water was gradually added over 5mins to the oil with continuous stirring for 2 hrs. Time after which the mixture became thick and then transferred into a mould. It was left for 7 days for complete curing.

2.5 Soap-less detergent

50g caraway oil was placed in a stainless beaker and the temperature raised and kept constant at 50°C. 10.4g KOH dissolved in 29.952ml distilled water was gradually added with stirring and immediately followed with gradual addition of 5ml conc. H₂SO₄ with stirring. The cooking and stirring continued for 30mins. The mixture separated into two layers. It was decanted and the detergent (lower layer) collected. It was diluted with 50ml of boiled distilled water.

2.6 Characterization

Chemical analyses of the detergents were made according to ASTM D455-69 (2006) specifications for milled toilet soap.



2.7 pH Determination

1.00g of the various samples were weighed and dissolved in 10ml of distilled water. The pH was determined with a pH meter and recorded in Table 1.

Table 1: pH of the Detergent Samples.

SAMPLES	pH
A	9.00
B	9.50
C	10.00

KEY: A = Cold process soap, B = Liquid detergent, C = control

2.8 Determination of Surface Tension (Capillary Rise Method).

20ml of the prepared liquid detergent was measured into a 250ml beaker (washed with dilute NaOH and rinsed thoroughly with distilled water) and filled up with distilled water. For solid detergent 5g was used.

A clean capillary tube of diameter 1mm (washed with dilute NaOH and rinsed thoroughly with water) was pushed into the beaker containing the soap solution. The capillary tube was removed and clamped gently so that the tip just touches the surface of the liquid. When the liquid inside the capillary tube has fallen to a constant position the height of this liquid from the surface of the soap solution was measured with a transparent rule and recorded as liquid height in metres (h). The surface tension was calculated with the formula = $\frac{r h \rho g}{2}$ where; = surface tension, r = radius of capillary tube in metres, h = liquid height in metres, ρ = density of water = 1000kgm^{-3} , g = acceleration due to gravity = 9.8ms^{-2} . Results obtained are shown in Table 2.

2.9 Anti Microbial Test

A Fungus and two bacteria were used. All been clinical isolates from the Department of Microbiology, Ahmadu Bello University Zaria. These isolates were: *Candida albican* (fungus), *Pseudomonas aeruginosa* (bacteria), *Staphylococcus aureus* (bacteria)

2.10 Culture Media

The culture media used for the analysis include Mueller Hinton Agar (MHA), Nutrient Agar (NA) and Mueller Hinton Broth (MHB). They were all used for the sensitivity test, determination of minimum inhibitory concentration (MIC) and minimum bactericidal concentration (MBC) respectively. All the media were prepared according to manufacturer's instructions.

2.11 Sensitivity Test of the Detergent Using Agar Well Diffusion Method.

The bacterial isolates were standardized and streaked uniformly onto freshly prepared Mueller Hinton Agar plates using a sterile swab stick. Four wells were punched on the agar plates with the aid of a sterile cork borer (8mm) in diameter. The well was properly labeled according to different concentrations of the soap prepared (50, 25, 12.5 & 6.25mg/ml). The wells were then filled up with 0.2ml of different concentration of the soap respectively. The plates were left on the bench for 1hr for the soap to diffuse in the agar, after which they were incubated at 37^oc for 24hrs. After the incubation period, the plates were observed for any evidence of inhibition, which will appear as a clear zone that was completely devoid of growth around the wells (zone of inhibition). The diameter of the zones were measured using a transparent rule calibrated in millimeter (mm) as shown in Table 3.

2.12 Determination of Minimum Inhibitory Concentration.

The minimum inhibitory concentration (MIC) of the detergents were determined using the tube dilution method. Serial dilution of the soap was carried out in well labeled test tubes using Mueller Hinton Broth as a diluent. The lowest concentration of the soap showing inhibition for each organism when the soaps were tested using agar well diffusion method was serially diluted in the test tubes containing Mueller Hinton Broth. Each organism was inoculated into each tube containing the diluted detergent. The tubes were then incubated at 37^oC for 24hrs.

After the incubation period, the tubes were examined for the presence or absence of growth using turbidity as criterion. The lowest dilution (concentration) in the serial without visible signs of growth (turbidity) was considered to be the minimum inhibitory concentration (MIC). Results are shown in Table 4.

2.13 Determination of Minimum Bactericidal Concentration (MBC)

The results from the minimum inhibitory concentration were used to determine the minimum bactericidal concentration of the detergent. A sterile wire loop was dipped into the test tubes that did not show turbidity in the MIC test, it was then streaked on a freshly prepared nutrient agar plates. The plates were incubated at 37^oC for 24hrs. After the incubation period, the plate was examined for the presence or absence of growth. This was done to determine if the antibacterial effect of the detergent is bactericidal or bacteriostatic.



Table 2: Surface Tension of Distilled Water, and Detergent Solutions.

Sample	r (m)	h (m)	ρ (kgm ⁻³)	g (ms ⁻¹)	γ (Nm ⁻¹)
Distilled water	0.0005	0.0300	1000	9.8	0.0735
A	0.0005	0.0163	1000	9.8	0.0399
B	0.0005	0.0120	1000	9.8	0.0294
C	0.0005	0.0120	1000	9.8	0.0294

where; γ = surface tension, r = radius of capillary tube in metres, h = liquid height in metres, ρ = density of water = 1000kgm⁻³, and g = acceleration due to gravity = 9.8ms⁻².

Table 3: Sensitivity Test

Test Organisms	Zones on Inhibition (mm) at Varying Concentrations of the Soap (mg/ml)											
	A			B			C					
<i>Candida albican</i>	R	R	R	R	R	R	R	R	R	R	R	R
<i>Pseudomonas aeruginosa</i>	R	R	R	R	R	R	R	R	R	R	R	R
<i>S. aureus</i>	15	13	12	R	R	R	R	R	23	20	18	16

where R = Resistant.

Table 4: MBC and MIC Test.

Test Organism	MIC (mg/ml)		MBC (mg/ml)	
	A	C	A	C
<u>Staph. aureus:</u>	3.125	1.562	6.25	3.125

3. Results and Discussion

From the result, all the detergents have pH within the normal pH range for soap 8-10.5 [14] and compete well with the control 10.00. This indicate that the prepared detergents are not corrosive to the skin. This alkalinity favours detergency [10].

Soap A reduced the surface tension of distilled water from 0.0735 to 0.0399 which is comparable to that of the control 0.0294. The control is more effective due to additional builders. The liquid detergent (B) had a value 0.0294 exactly the same with the control irrespective of the builder due to the presence of sulphate (-O-SO₃⁻) group. The lower the surface tension the more efficient the detergent and vice versa.

MBC and MIC are limited to A and C because they were the only samples *Staph. aureus* was sensitive to. The soap-less detergent B was resistant to all the test organisms (*Candida albican*, *Pseudomonas aeruginosa*, *Staphylococcus aureus*). Soap A and C had sensitivity for *Staph. aureus* only and resistant to *Candida abican* and *Pseudomonas*

aeruginosa. This sensitivity indicates inhibition to the bacterium and resistant; no inhibition. The zones of inhibition of A at concentrations 50, 25, 12.5, and 6.25mg/ml are 15, 13, 12mm, and Resistant respectively. The control (C): 23, 20, 18 and 16mm respectively. The wider the zone on inhibition the more antibacterial effect of the detergent. Hence even though A showed sensitivity to *S. aureus* the control is more effective due to added antibacterial agents. The minimum Inhibitory Concentration (MIC) values of A and C are 3.12mg/ml & 1.562mg/ml respectively. The lower this value the more effective. The Minimum Bacteriocidal Concentration (MIC) values of A and C are 6.25mg/ml and 3.125mg/ml respectively. Also, the lower the value the more effective the detergent. C having more effect due to added antibacterial agents. The soap as well as the control had activity only for the *Staph. aureus* out of the three organisms tested. Hence can be said to be Bactericidal and Bacteriostatic to some but not all organisms.



4. Conclusion

The soapy and soap-less detergents were successfully prepared from caraway oil. Chemical analysis showed that the soap and soap-less detergents conform to standard- ASTM D455-69 (2006) and could be used as Toilet soaps. Antimicrobial Test revealed that the soapy detergent could be used as a bactericidal and bacteriostatic soap against some harmful organisms particularly Staphylococcus aureus without any external builder. The soapy and soap-less detergents can be used excellently for stain removal because of their ability to lower the surface tension of wash water.

References

1. ASTM D455 – 69 (2006): Standard Specifications for Milled Toilet Soap. American National Standards Institute.
2. David, T. (2005). Experimental Organic Chemistry. New Jersey: Prentice-Hall, Inc. pp 400.
3. Detergent,(2002). Encyclopedia of Science and Technology, vol. 5. London: MC Graw Hill, Inc. pp 411-412.
4. Essential Oils (2012). Encyclopedia Britannica, vol. 4. Chicago: Encyclopedia Britannica. pp 563
5. James, K.A (1997). Riegel's Handbook of Industrial Chemistry, 9th Ed. India: CBS publishers. pp1040
6. Janardhanan, K. (2012). [/http://issstindian.or../art.6.pdf/soaps and detergent](http://issstindian.or../art.6.pdf/soaps%20and%20detergent).
7. Jubb, A.H and Nechvatal, A. (1998). Organic Chemistry". London: John Wiley & Sons. pp 453, 457, 462-466.
8. Kirschenbauer, H.G. (2011). Fats and Oil; an outline of their chemistry and technology, 6th Ed. New York: Chapman & Hall, Ltd. pp 5, 24, 27-34.
9. Lewkowitsch, M.A. (1997). Chemical Technology and Analysis of Oils, Fats and Waxes, 9th Ed, vol. 3. London: Macmillan & Col Ltd. pp 237, 313.
10. Mak-Mensah, E.E and Firempong C.K (2011) Chemical characteristics of toilet soap prepared from neem (Azadirachta indica A. Juss) seed oil". Asian Journal of Plant Science and Research, 1(4):1-7.
11. Martin, G. (2010). The Modern Soap and Detergent Industry, vol. 2. London: Elsevier Applied Science. pp 4-7, 10.
12. Mercola, E.D (2010). Laundry Soap Detergent; Harmful Side Effects for Humans. Green Health Technologies. Annual publication, pp 40.
13. Nicholson, N.L (1994). Detergents are Bad for Health and Environment. Green Health Technologies. Annual publication, pp 25.
14. Nkeonye, P.O (2009). Textile Preparatory Processes and Waste Liquor Treatment. Zaria: Asekome & Co. pp 22-34.
15. Pandey, G. (1994). A Textbook of Chemical Technology, vol. 2. New Delhi: Vikas Publishing House Ltd. pp 7.1-7.47
16. Perry, Anthony, et al (2005): Surface Active Agents and Detergents. New York: MC Graw-Hill, Inc. pp 32, 40, 55.
17. Pritchard, J.L.R and Rossell, J.B. (1991). Analysis of Oilseeds, Fats, and Fatty Foods. London: Elsevier Applied Science. pp 227-230.
18. Soap and detergent (2012). The New Encyclopedia Britannica, vol. 21. Chicago: Encyclopedia Britannica. pp 352-357.
19. Soap and Detergent (2001). Chemical and Process Technology Encyclopedia. New York: MC Graw-Hill, Inc. pp 345-352.
20. Woolatt, E. (2000). The Manufacture of Soaps, other Detergents and Glycerine. England: Ellis Horwood Ltd. pp 1-10.

Other comments:

The source of the control detergent was not mention in the body of work and why it was chosen



ABSTRACT CCT-: 023

Aliyu N., Shafiu M. and Lawal H.

Department of Science Laboratory Technology, Nuhu Bamalli Polytechnic, Zaria.

Email: nafnaf4U@gmail.com

COMPARATIVE ANTIOXIDANT EFFECT OF CUCUMBER AND CARROT USING DIFFERENT METHODS

ABSTRACT: This study was aimed at comparing the antioxidant effect of aqueous and methanolic extracts of cucumber and carrot using Reducing power, phosphomolybdenum and hydrogen peroxide methods. Samples were collected around irrigated farms located along River Galma, air dried, ground and analysed for the antioxidant activities. Antioxidant activity for carrot and cucumber methanolic extract are 9.2 and 2.6mg/ml for reducing power method which relates increase in antioxidant effect to increase in absorbance of reacting mixtures while 3.4 and 0.6mg/ml was obtained for aqueous extracts of carrot and cucumber respectively. Total antioxidant capacity was assayed as 12.9 and 10.7mg/ml for methanolic extracts of carrot and cucumber respectively in Phosphomolybdenum method. Highest activity of antioxidant effect was observed in methanolic extract using hydrogen peroxide method. A general inference from these observations was the high antioxidant activity of methanolic extract may be attributable to difference in polarity of both solvents.

Keywords: Antioxidant, Cucumber, carrot, oxidative stress, Phosphomolybdenum.

1. Introduction

Cancer, a disease in which the cell of a tissue undergoes uncontrolled growth (and often rapid proliferation), is one of the major deaths worldwide, it was estimated that between the years 2005 to 2015; around 18 million people will die due to the cancer (Amendeyazdan *et al.*, 2012). Studies reveals that free radical are involved in the initiation and promotion of cancer. Free radicals (any atom or molecule that has single unpaired electrons in an outer shell) are normally produced during metabolic activities in the body, but excessive production of these free radicals can cause oxidative stress (i.e. imbalance between the production of free radicals and the ability of the body to counteract or detoxify their harmful effect through neutralization by antioxidants) and finally, leads to cause of many diseases such as cancer (Taller, 2014). The function of oxidative stress has been shown in different types of cancer like lung and breast cancers. Antioxidant is defined as the molecule capable of showing or preventing the oxidation of other molecules. Oxidation is the chemical reaction that transfers electrons from a substance to an oxidizing agent. Oxidation reaction can produce free radicals which starts chain reaction that damages cells. Antioxidants terminate this chain reaction by removing free radical intermediate, and inhibit other oxidation reaction by being oxidized themselves. As a result of oxidants are often reducing agents such as thiols, ascorbic acid or polyphenols, low levels of antioxidant enzymes cause oxidative stress and many damage and kill cell (Taller, 2014). Antioxidants are compounds that inhibit free radicals, endogenous antioxidants (antioxidant produced by the body) are not enough to inhibit the production of free radicals thus scavenging dietary antioxidants is required. Most food containing antioxidant compound are derived from natural sources especially from plants and marine organism. Plants such as fruits or vegetables are valuable sources of

natural product with biologically active component (Taller, *et al.*, 2012).

Cucumber (*Cucumissatavus* L), a popular vegetable crops which belong to the family Cucurbitaceae like melon, squash and pumpkins is a vegetable very high in water content and very low in calories. Cucumber is more than 90% water (Chang, 2007). It has potential anti-diabetic, lipid lowering and antioxidant activity. Cucumber has a cleansing action within the body by removing accumulated pockets of all waste materials and chemical toxin (El Arab *et al.*, 2013). Tamber, *et al.*, (2011), reported that cucumber have cleansing effect on the bowel and also on digestive acid. It was also found to have other excellent health benefits because it contains rich source of vitamin C, vitamin K, potassium and molybdenum. By consuming cucumber juice regularly, you can reduce the chances of uterine cancer (Johree, *et al.*, 2012).

Carrots are roots plants which belong to the umbelliferae family, named after the umbrella-like flower clusters. However, this same family of plants is also commonly known as the apiaceae family. It has a crunchy texture and a sweet and minty aromatic taste, while the greens are fresh tasting and slightly bitter (Lin and Lucier, 2013). The beta-carotene that is found in carrots was actually named for the carrot itself (Baskar *et al.*, 2012). Carrots are an excellent source of vitamins A (inform of carotenoids). In addition, they are very good source of biotin, vitamin k dietary fiber, molybdenum, potassium, vitamin B6, and vitamin C. They are a good source of manganese, niacin, vitamin B1, phosphorus, foliate, copper, vitamin E, and vitamin B2 (Boardbar, *et al.*, 2011). However, these delicious root vegetables are the source not only of beta-carotene but also of a wide variety of antioxidants and other health-supporting nutrients.

2. Materials and Method

All chemicals used were of analytical grade. Carrots and cucumber were collected along



river Galma, Zaria, samples were sliced, air dried, ground into powder and sieved. 10g of each sample was weighed into separate conical flask containing 100ml methanol, kept for 48hrs with routine shaking after which each sample was then filtered. The filtrates were concentrated to dryness. The same procedure was repeated with distill water to obtain aqueous extract. Antioxidant activities were assayed as described by Jayaprakash, *et al.*, 2011 (Reducing Power method), Prieto *et al.*, (1999) (Phosphomolybdenum method) and Ruch, *et al.*, (2014) (Hydrogen Peroxide method).

3. Result and Discussion

The result obtained showed an activity of 0.6mg/ml for cucumber aqueous extract and 2.6mg/ml for cucumber methanol extract while 3.4mg/ml for carrot aqueous extract and 9.2 for carrot methanol extract in reducing power method. In phosphomolybdenum method, the result obtained were, 7.8mg/ml for cucumber aqueous extract and 10.7mg/ml for cucumber methanol extract while for carrot aqueous and methanol extracts were 12.1mg/ml and 12.9mg/ml. In hydrogen peroxide method, 7.8mg/ml activity was observed for cucumber aqueous extract and 20.6mg/ml for cucumber methanol extract while for carrot aqueous and methanol extracts were 5.6mg/ml and 22.8mg/l as shown in Table 1.

Table 1: Antioxidant activity of cucumber and carrot

Vegetables	Extracts	Concentration (mg/ml)			
		Reducing power method	power	Phosphomolybdenum method	Hydrogen peroxide method
Cucumber	Aqueous	0.6		7.9	7.8
	Methanol	2.6		10.7	20.6
Carrot	Aqueous	3.4		12.1	5.6
	Methanol	9.2		12.9	22.8

4. Conclusion

Increasing interest gained by antioxidants is due to the health benefits provided mainly by natural sourced (exogenous) low molecular weight antioxidants. This consists in preventing the occurrence of oxidative stress related diseases, caused by the attack of free radicals on key bio components like lipids or nucleic acids. Hence

consumption of carrot and cucumber more than other varieties of vegetables are recommended because of their high content of dietary constituent, beneficial health effect and antioxidant activities, especially carrot for fighting against disease and best protection against the development of diseases caused by oxidative stress, such as cancer, coronary heart disease, obesity, type 2 diabetes, hypertension and cataract.



ABSTRACT CCT-: 072

*Shitu, S.¹, Sule, A. M.¹ and Tijjani, M. B.²

¹Department of Basic Research, National Research Institute for Chemical Technology, P.M.B. 1052, Zaria.

²Department of Microbiology, Faculty of Science, Ahmadu Bello University Zaria.

Email: sabiushitu07@gmail.com

A SURVEY OF AFLATOXINS CONTAMINATION IN SORGHUM AND MILLET MARKETED IN ZARIA METROPOLIS

ABSTRACT: Consumption of food contaminated with aflatoxins has caused both chronic and acute aflatoxicosis that has resulted in loss of livestock and human life. The present study aimed at surveying of aflatoxins contamination in sorghum and millet sold in Zaria metropolis. A total of thirty-six samples of millet and sorghum were randomly obtained from six different markets. Aflatoxins were extracted using 80% (v/v) methanol. Enzyme-linked Immunosorbent Assay (ELISA) technique was used in analyzing aflatoxins concentration of the samples. Results show that 33.3% of the entire samples were positive with an aflatoxins level in the range of 0.4 – 52.0 µg/kg. The highest concentration (>10 µg/kg) was found in millets obtained from Zaria, Sabon Gari, Kwangila and Samaru market. However, in sorghum, the highest concentration (>10 µg/kg) was recorded only in Kwangila market. Out of the positive samples 19.4% of them exceeded the SON and NAFDAC Aflatoxins permissible level. The study revealed that the high increasing contamination of the samples can lead to disease and metabolic disorder resulting in poor human and animal health.

Keywords: Aflatoxin, aflatoxicosis, millet, sorghum, Enzyme-linked Immunosorbent Assay (ELISA)

1.0 Introduction

Aflatoxins are potent toxic, carcinogenic, mutagenic, immunosuppressive and teratogenic agents produced as secondary metabolites by *A. flavus* and *A. parasiticus*; in particular, *A. flavus* is common in agriculture (Bennett and Klich, 2003; Krishnamurthy and Shashikala, 2006). These toxins are named after the fungus producing them, e.g. "A" from the genus name *Aspergillus*, "fla" from the species name *flavus* added to toxin to give the name aflatoxin. Among these aflatoxins, the major members are aflatoxins B₁, B₂, G₁, G₂, M₁ and M₂ (Wrather, 2008).

Aflatoxin B₁ is produced most abundantly and is the most toxic followed by G₁, B₂ and G₂. Aflatoxins B₁, B₂, G₁ and G₂ are classified as Group I human carcinogens whereas M₁ is classified as Group 2B probable human carcinogen (Krishnamurthy and Shashikala, 2006).

2.0 Materials and Methods

2.1 Description of the Study Area

Zaria metropolis is located at latitude 11° 07' N and longitude 07°42' E, and is presently one of the most important cities in Northern Nigeria (Ubaet *al.*, 2008). It has a total area of 300 km² and constitutes four major settlements; Zaria City, Tudun Wada, Sabon Gari, and Samaru. As at 2007 Census, Zaria metropolis had a population of 1,018,827 (TWG, 2007).

2.2 Collection of Samples

Thirty-six samples; 18 of each Millet and sorghum were collected from the major grains sellers from six different public markets comprising; Zaria, Tudun Wada, Sabon Gari, Kwangila, Danmagaji and Samaru Markets in Zaria metropolis, in July 2016.

Three vendors were selected at different point in each market and 2 samples (sorghum and

millet). Approximately 100g samples were purchased from each vendor. A total of 36 samples were collected; 18 samples of millet and 18 of sorghum and each was placed separately in clean, sterile container, labeled appropriately and transported immediately to the Laboratory for analyses.

2.3 Detection and Quantification of aflatoxin level in the samples using ELISA

Sample Preparation and Extraction

A representative sample of millet and sorghum was grounded to about 20 mesh sieve size. Fifty gram of the grounded samples was collected into a conical flask and 5.0 g of NaCl was added. The samples were mixed with 100ml of 80% (v/v) methanol and blended at high speed (250RPM) for 3 minutes. The mixture was allowed to settle and filtered. 5ml of the filtrate was mixed thoroughly with 20ml of distilled water and filtered through a glass fiber filter. The optical density (OD) was taken from each micro well and the concentrations were obtained from a graph curve that was obtained from OD and the concentration of the standards (Beacon total aflatoxins ELISA kits user guide 2015).

3.0 Results and Discussion

3.1 Detection of aflatoxins using ELISA Technique.

The aflatoxins concentrations of the various samples of millet and sorghum obtained from the six different markets in Zaria Metropolis used in this study shows values ranges between 0.4 – 52.0 µg/Kg in millet and 3.6 – 11.4 µg/Kg in sorghum, as presented in Tables 1 & 2. Generally, the results of the analyses using ANOVA shows that there were significant differences (*p* value < 0.05) in the level of aflatoxins concentrations present in the samples.



Millet is a major staple food in northern Nigeria. In this study, the highest level of aflatoxins found in millet obtained from Zaria, Sabon Gari, Kwangila and Samaru markets are far beyond the acceptable limit of 10 μ g/kg set by National Agency for food and Drug Administration Control (NAFDAC) and Standard Organization of Nigeria (SON). This could be due to differences in storage conditions between the markets. The concentration of aflatoxins level obtained from this study is not in agreement with the findings of Ezekiel (2014) who reported 0.08-1.40 μ g/kg in millet from Plateau State, Nigeria. The difference in contamination level might be due to the difference in environmental factors (temperature and relative humidity) that favors the growth of aflatoxigenic moulds and also agricultural practices between the two study areas.

Table 1. Aflatoxins Concentrations in Millet from Six Different Markets in Zaria Metropolis

Location	No. of Samples		Concentration (μ g/Kg)
	Analysed	Positive	
Zaria	3	1	52.0
Tundun wada	3	1	5.0
Sabon gari	3	2	23.15
Kwangila	3	2	23.75
Samaru	3	1	39.6
Dan-magaji	3	2	0.4 & 8.0

Table 2. Aflatoxins Concentrations in Sorghum from Six Different Markets in Zaria Metropolis

Location	No. of Samples		Concentration (μ g/Kg)
	Analysed	Positive	
Zaria	3	ND*	0.0
Tundun wada	3	ND	0.0
Sabon gari	3	1	4.3
Kwangila	3	1	11.4
Samaru	3	ND	0.0
Dan-magaji	3	1	3.6

*ND: Not Determined

Sorghum is another staple food and an important starchy food for human and animal consumption in Nigeria. The aflatoxins concentration found in sorghum samples from the study are within the permissible limit standard (<10 μ g/kg) except Sorghum samples obtained from Kwangila market, which exceeded the limit set standard (>10 μ g/kg) by NAFDAC and SON. Though consistent consumption of the aflatoxins contaminated

grains might result in long term accumulation of the toxin, causing disease and metabolic disorder resulting in poor human and animal health. The low level of aflatoxins observed in sorghum might be due to the high phenol and tannin contents present in sorghum which are known to inhibit fungal infestation (U.S. Grain Council, 2008). The finding in this study is similar to the finding of Batagarawa, *et al.* (2015) who reported 1.32 μ g/kg in Sorghum sample in Zaria metropolis.

4.0 Conclusion

The present study revealed that Aflatoxins were found to contaminate the samples in varying degree. Highest concentration occurred in millet samples in the range of 4.2-52.0 μ g/kg, while sorghum samples have least concentration in the range of 3.6-11.4 μ g/kg. This survey also revealed that most of the vendors are not handling the agricultural commodities properly at point of sale and during storage as observed during sampling resulting in contamination of these samples analyzed and poor human and animal health.

Acknowledgement

The authors acknowledged and appreciate the management and staff of National Research Institute for Chemical Technology (NARICT) Zaria, for the opportunity to present this paper. Our gratitude also goes to Mr. Nden Emmanuel N. of NAFDAC Kaduna Area office for his support in getting the ELISA Kit.

References

- Batagarawa, U. S., Dangora, D. B. and Haruna, M. (2015). Aflatoxins Contamination in Some Selected Grains, Feeds and Feed ingredients in Katsina and Zaria metropolis. *Journal of Annals of Experimental Biology* 2015, 3 (3):1-7.
- Beacon total aflatoxins ELISA kits user guide 2015.
- Bennett, J.W. and Klich, M. (2003). Mycotoxins. *Clin. Microbiol. Rev.*, 16: 497 – 516
- U.S. Grain Council, *Sorghum*, 2008, Available at www.grain.org/galleries/default-file/Sorghum.
- TWG (2007). Current population figures for cities, towns and Administrative Divisions of the World. <http://www.worldgazetter.com/home.htm>.
- Uba, S., Adamu, U., Muhammad, S. S., Hamza, A. and Okunola, O. J. (2008). Metals bioavailability in the leachates from dumpsites in Zaria Metropolis, Nigeria. *Journal of Toxicology and Environmental Health Sciences*. 5(7), 131-141.
- Krishnamurthy, Y.L. and Shashikala. J. (2006). Inhibition of aflatoxin B₁ production of *Aspergillus flavus*, isolated from soybean seeds by certain natural plant products. *Letter in Applied Microbiology*, 43(5): 469-474.
- Wrather, J.A. (2008). University of Missouri-Delta Center, Laura, E. Sweets, Plant Pathologist, Commercial Agriculture, University of Missouri. *Aflatoxin in corn*, 573:379-5431.



ABSTRACT CCT-: 021

Yahaya Muhammad Sani* and Abdulmajid Kehinde Hussein
Department of Chemical Engineering, Ahmadu Bello University, 870001 Nigeria.
Email: ayeashah@yahoo.com

**ESTERIFICATION OF CARBOXYLIC ACID WITH ALCOHOL IN
ZnCl₂/UREA DEEP EUTECTIC SOLVENT**

ABSTRACT: Esterification reaction between carboxylic acids and alcohols produces esters and water. The process is a slow equilibrium reaction, which requires the activity of catalyst for the chemical process to reach completion. 1 ml of 98wt% H₂SO₄ was used as a catalyst in the reaction between acetic acid and butyl alcohol at temperatures 80, 100 and 120 °C. 1ml of ZnCl₂/Urea; a green Deep Eutectic Solvent (DES) was also used to catalyze the same reaction at same temperatures which provided a benchmark for juxtaposing both catalysts on the basis of time, temperature, yield and safety. The results showed that at 80 °C, conc. H₂SO₄ could catalyze the reaction while the DES could not. However, at 100 and 120 °C, higher yields; 98 and 99.50% were obtained using the DES at a shorter reaction time. In addition, the DES satisfied the conditions of green chemistry in terms of its recyclability and non-corrosiveness. This implies that the ZnCl₂/Urea DES is a potential substitute as a catalyst in the esterification reaction.

Keywords: Deep Eutectic Solvent, Esterification, Carboxylic Acid

1.0 Introduction

The reaction between carboxylic acids and alcohols to produce esters and water is termed esterification (Sundberg & Carey, 2002). Several methods have been reported on means of synthesizing esters without the use of carboxylic acids and alcohols (Tang, Yuan, Liu, & Lei, 2014). However, these methods have been observed to have one or two limitations (Otera & Nishikido, 2010). This makes the traditional method the most convenient process of obtaining esters. Esterification remains one of the fundamental and valuable organic reactions in synthetic chemistry. This is because the ester products and sometimes, intermediates are valuable chemicals in the cosmetic and pharmaceutical industries (Otera Junzo, 2003). Conversely, the reaction is a slow and equilibrium reaction that requires in most cases, strong mineral acids such as H₂SO₄, *p*-Toluenesulfonic acid and HCl as catalysts (Ishihara, Nakayama, Ohara, & Yamamoto, 2002). These acids have been reportedly toxic, nonrecyclable, dangerous, and environmentally hazardous (Sirsam, Hansora, & Usmani, 2016). Hence, finding new alternatives for catalyzing this reaction becomes imperative. These alternatives must be non-toxic, environmentally benign, cost-effective and recyclable amongst other conditions, in order to satisfy the requirements of a new concept in the field of chemistry termed “green chemistry” (Warner, Cannon, & Dye, 2004).

Deep Eutectic Solvents (DESs) are chemicals composed of a quaternary ammonium mixed with a metal salt or a hydrogen bond donor (HBD) that has the ability to form a complex with the halide anion of the quaternary ammonium salt (Hao & Zhang, 2015). DESs have been used as replacement to many organic solvents and catalysts in various chemical reactions and have proven to satisfy the conditions of green chemistry (Qi *et al.*, 2016). ZnCl₂/Urea is a Type IV DES (Abbott, Capper, Davies, & Rasheed, 2002) capable of replacing the strong mineral acids used in the

traditional esterification reaction due to its ability to produce same hydrogen proton as strong mineral acids do in the reaction. Germani *et al.*, 2012 and Cao *et al.* employed DESs in the traditional esterification procedure. However, these were not without shortcomings like large amount of DES requirement and long reaction time for Germani *et al.* and Cao *et al.* respectively.

One of the most common solvents required in large quantities in the paint, lacquer, coating, and other branches of chemical industry is butyl acetate. Its lower impact on the environment, compared to other aromatics comes in handy towards the modern trend of eliminating volatile solvents. Further, the synthesis of DES is easy, and reasonably inexpensive, energy-saving process with lower investment and operating costs. Consequently, the aim of the present study is to investigate the potentials of ZnCl₂/Urea as a catalyst in the traditional esterification for producing butyl acetate.

2.0 Materials and Methods

All materials employed were obtained from the Departments of Chemistry and Chemical Engineering in Ahmadu Bello University, Zaria without further purification.

Preparation of the DES: The DES was prepared as follows: ZnCl₂ (1 mmol) was mixed with urea (3.5 mmol) and heated at 80 °C in air with stirring until a clear colorless liquid was obtained. Then the mixture was allowed to cool to room temperature before utilization.

Synthesis of n-butyl acetate: Three molar excess of the acetic acid was used to the alcohol (butyl alcohol). Conc. H₂SO₄ was added to act as catalyst at different temperatures of 80, 100 and 120 °C. The DES was also used as catalyst in a fresh mixture of the acetic acid and alcohol at same temperatures with the H₂SO₄ catalyst. After the reactions were completed, separation procedures were carried out in order to isolate



the organic ester. FTIR characterization was carried out on both the synthesized organic esters.

Recycle process of DES: After the reaction was completed, two separate layers were clearly formed, the upper layer being the organic ester was collected in a test tube with the use of a separating funnel while the lower layer consisting of the DES, water, and excess starting acid was extracted with sodium bicarbonate and diethyl ether. The DES was recovered and reused up to three times.

3.0 Results and Discussions

First, the traditional method of catalyzing the esterification reaction was carried out using the strong mineral acid, conc. H₂SO₄. The method

gave good yields as temperature was increased with reaction time reduced. This shows a direct relationship between yield of butyl acetate and temperature (Figure 1) but an inverse one between temperature and reaction time (Figure 2).

The DES was then used in a fresh mixture of the acid and alcohol as a catalyst. At 80 °C, the DES could not catalyze the reaction but at temperatures 100 and 120 °C, higher yields; 98 and 99.50% were obtained. In addition, reaction time significantly reduced as temperature increased. This also shows a direct relationship between yield of the butyl acetate and temperature and an inverse relationship between temperature and reaction time as in the case of the strong mineral acid.

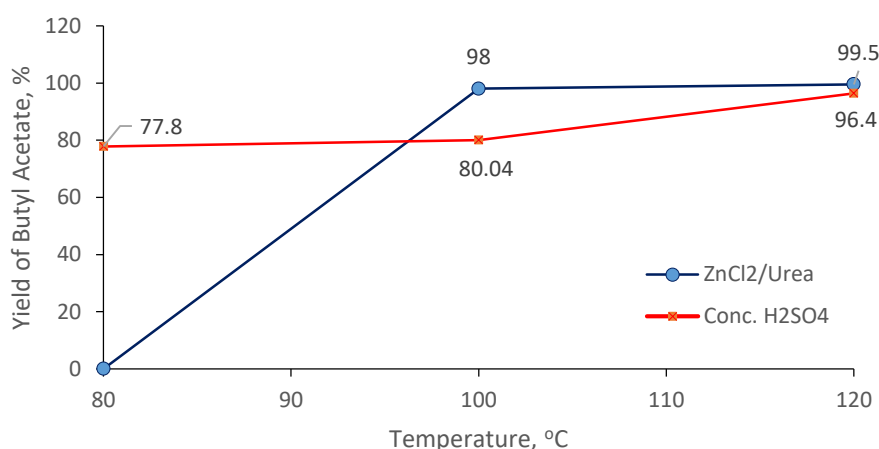


Fig. 1: Relationship between yield of butyl acetate and temperature.

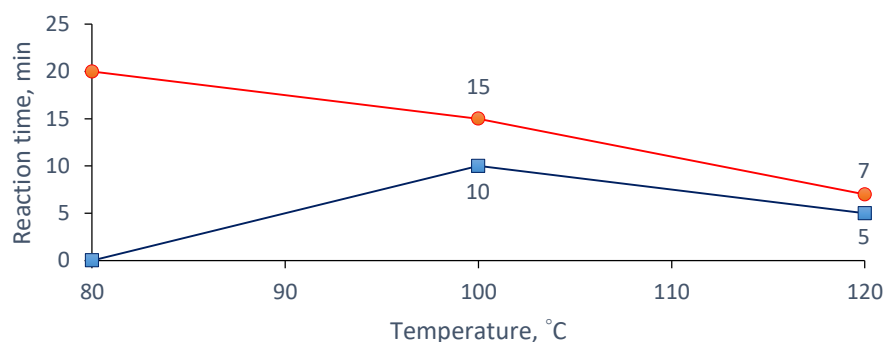


Fig. 2: Relationship between the reaction time for the esterification and temperature.

Table 1. Comparative Assessment of ZnCl₂/Urea DES and 98 wt% H₂SO₄ catalysts

BASIS	ZnCl ₂ /Urea DES	H ₂ SO ₄ catalyst
Temperature	Requires high temperature > 80 °C	Reaction can occur as low as 80 °C
Time	Short Reaction time	Long Reaction time relative to the DES
Yield	Higher yields at temperatures > 80 °C	Less yields at temperatures > 80 °C relative to the DES
Recyclability	Easy separation of products and recyclable	Non-recyclable
Safety	No vapor pressure, non-corrosive and non-flammable	Highly corrosive
Flexibility	Highly tunable	Not tunable

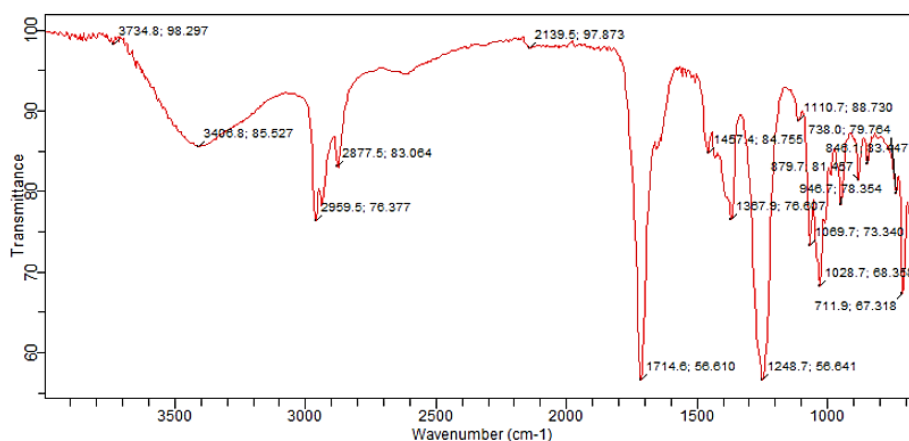


Fig. 3: FTIR of DES-catalyzed butyl acetate.

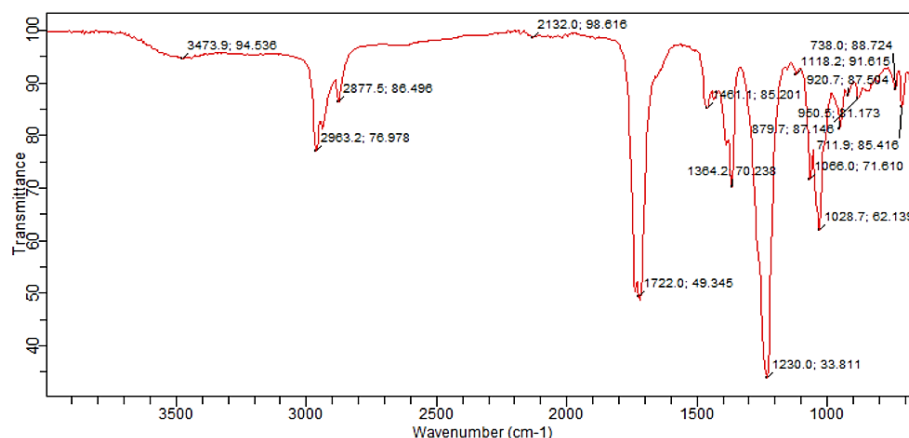


Fig. 4: FTIR of H₂SO₄-catalyzed butyl acetate.

Figures 3 and 4 present the Fourier transform infrared (FTIR) spectroscopy synthesized butyl acetate. The stretches at 2963.2 (H₂SO₄-catalyzed), 2959.5 and 2977.5 cm⁻¹ (DES-catalyzed) indicate all chemical compounds containing -C-C-. Further, the strong peaks observed at 1722.0 cm⁻¹ (H₂SO₄-catalyzed), and 1714.6 cm⁻¹ confirmed the presence of ester-carbonyl group (C=O). Mat-Radzi *et al.* (2005) reported similar finding. The merits of ZnCl₂/Urea DES outweigh those of the H₂SO₄ catalyst (Table 1). Hence, ZnCl₂/Urea DES is a potential substitute as a catalyst in the esterification reaction.

4.0 Conclusion

The study highlighted activity of ZnCl₂/Urea DES as substitute catalyst to sulfuric acid in esterifying acetic acid with butanol for producing butyl acetate. It also emphasized the applicability of ZnCl₂/Urea DES in efficient biphasic reactions as well as its efficiency, recyclability, tenability, easy and reasonably inexpensive preparation protocol.

References

Abbott, A. P., Capper, G., Davies, D. L., & Rasheed, R. K. (2002). Quaternary ammonium zinc or tin-containing ionic liquids: water insensitive, recyclable catalysts for Diels - Alder reactions. <https://doi.org/10.1039/b1084>

Brinchi, L., & Germani, R. (2012). ChemInform Abstract: Novel Brønsted Acidic Deep Eutectic

Solvent as Reaction Media for Esterification of ... *Tetrahedron Letters*, 53(38), 5151-5155. <https://doi.org/10.1016/j.tetlet.2012.07.063>

Ishihara, K., Nakayama, M., Ohara, S., & Yamamoto, H. (2002). Direct ester condensation from a 1 : 1 mixture of carboxylic acids and alcohols catalyzed by hafnium (IV) or zirconium (IV) salts, 58, 8179-8188.

Otera Junzo. (2003). *Junzo Otera Esterification*.

Otera, J., & Nishikido, J. (2010). *Part One Methodology*.

Peng, L., Hao, J., Zhang, Z., & Li-Pong, M. (2015). RSC Advances. <https://doi.org/10.1039/C5RA05746A>

Qi, B., Shang, Y., Huiwen, L., Wenjing, W., Jia, L., Zhiyan, C., ... Zhou, X. (2016). RSC Advances. <https://doi.org/10.1039/C6RA01029F>

Sirsam, R., Hansora, D., & Usmani, G. A. (2016). A Mini-Review on Solid Acid Catalysts for Esterification Reactions. *Journal of The Institution of Engineers (India): Series E*. <https://doi.org/10.1007/s40034-016-0078-4>

Sundberg, R., & Carey, F. (2002). *Advanced Organic Chemistry*.

Tang, S., Yuan, J., Liu, C., & Lei, A. (2014). Direct oxidative esterification of alcohols, 13460-13470. <https://doi.org/10.1039/c4dt01133c>

Warner, J. C., Cannon, A. S., & Dye, K. M. (2004). *Green chemistry*, 24, 775-799. <https://doi.org/10.1016/j.eiar.2004.06.006>



ABSTRACT CCT-: 066

Abidina Bello

National Research Institute for Chemical Technology, Basawa, Zaria

Email: abideenbello45@yahoo.com

ANALYSIS OF ATMOSPHERIC AEROSOLS: AEROSOL OPTICAL DEPTH AND ITS IMPACT ON CLIMATE AND VISIBILITY

ABSTRACT: Eight years (2009-2016) worth of level 2.0 aerosol data was extracted from the Aerosol Robotic Network (AERONET) station, located at Zinder_Airport using the standard algorithm for retrieving AERONET data. The data which consist of aerosol optical depth (AOD), Angstrom exponent (α) and precipitable water (PW) were used to analyze the impact of atmospheric aerosols on climate and visibility in the Sahara Desert. Both statistical methods and Angstrom equations were used in the analysis. The results showed seasonal variation of AOD, Angstrom parameters and precipitable water with lower values during rainy season and higher values during dry season. The AOD values during rainy season decrease more at higher wavelengths, indicating a general reduction in the number of bigger particles, increase in light scattering as well as decrease in atmospheric visibility. The amplitude of the observed high AOD values in dry season is higher (low during rainy season) for longer wavelengths, which shows that coarse particles contribute more to the observed variation as compared to sub-micron particles. Characterization of the aerosol optical depth was done from the obtained values of Angstrom parameters, α and β .

Keywords: Aerosol, AERONET, AOD, Angstrom exponent, Turbidity, Precipitable water

1.0 Introduction

Atmospheric aerosols are tiny particles suspended in the atmosphere in form of fumes, smokes, mineral dusts, sprays, and mists (Vincent 1995). Aerosols affect the earth's radiation budget directly by scattering and absorbing solar and terrestrial radiation (which eventually cause increase or decrease in temperature and atmospheric visibility), and indirectly by modifying the physical and radiative properties of clouds (Charlson et al. 1991). In the course of their collective direct and indirect effects, aerosols are believed to have the potential to cause a climate forcing (IPCC 2001) similar in magnitude, but reversed in sign, to that of greenhouse gases (Jacobson 2001). Zinder_Airport is one of the places where aerosol data is monitored via AERONET observatory. The data used in this work was retrieved from Zinder_Airport AERONET data base using AERONET data retrieval algorithm. Details of the instrumentation, data retrieval algorithm and possible measurement error were discussed by many authors (Holben et al. 2002), (Zhou et al. 2014). AERONET facility provides mixed data of both naturally and artificially generated aerosols. This study, therefore, intends to investigate the impact of these aerosols on climate and atmospheric visibility using statistical method and Angstrom equations.

2.0 Materials and Method

The data retrieved from 2009-2016 were level 2.0 AOD and PW at five spectral wavelengths (440nm, 500nm, 670nm, 870nm and 1020nm) and $\alpha_{440-870}$. The annual mean values and standard deviations were computed and the data are presented graphically in Figures 1-5. The AOD data were then fitted against the wavelength using the second order polynomial fitting algorithm and the generated equations of the curves were compared with the second order Angstrom polynomial equation to obtain the Angstrom coefficients, α_2 , α_1 and β which

are the indices for determining the nature of the aerosol climatic effect and visibility disruption. The Angstrom second order polynomial equation is an extension of the Angstrom equation formulated by Angstrom in 1902:

$$\tau = \beta\lambda^{-\alpha} \quad (1)$$

Equation (1) gives rise to:

$$\ln \tau = -\alpha \ln \lambda + \ln \beta \quad (2)$$

$$\ln \tau = \alpha_2 \ln \lambda^2 + \alpha_1 \ln \lambda + \beta \quad (3)$$

3.0 Results and Discussion

The AOD for the eight years was averaged monthly wise for five different wavelengths and the result is presented in **Figure 1**. The Figure shows that the AOD loading is higher in dry season between March and June due to biomass burning, dust generation and possibly industrial emission from within the Niger Republic and other neighboring countries like Libya via aerosols transportation. α is usually in the range of 0 to 2. Small α to around 0 usually means that the aerosol particles are mainly large with dust particles, while large α to around 2 means aerosol particles are mostly fine mode. $\alpha < 0.6$ indicates the dust aerosol (Dobovik, et al, 2000).

Table 1: Angstrom Parameters generated from the second order polynomial equation

Year	α_2	α_1	β
2009	0.0127	-0.158	1.751023
2010	0.0034	-0.166	1.999106
2011	0.1408	-0.429	1.989931
2012	0.1417	-0.368	1.738808
2013	0.0684	-0.351	1.946241
2014	0.0789	-0.298	1.856884
2015	-0.0520	-0.217	2.090284

Figure 3 indicates that there is dominance of slightly fine particles and very high turbidity. This results in generation of relatively fine aerosol particle which scatter more light coming from the Sun. In other months, the values of α decrease while that of β increase



which signifies prevalence of coarse aerosol particles from the dust as well as low turbidity.

From **Figure 4**, PW is higher between June and September, which is the rainy season and low in other months.

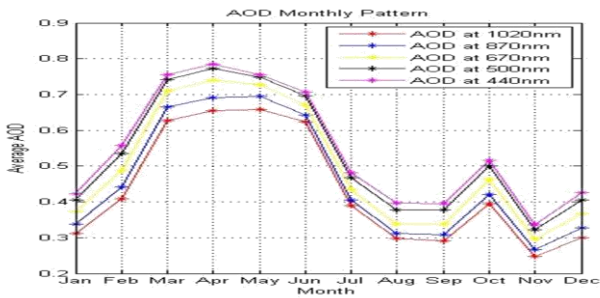


Fig. 1. Average AOD Monthly Pattern from 2009 to 2016 at five different wavelengths

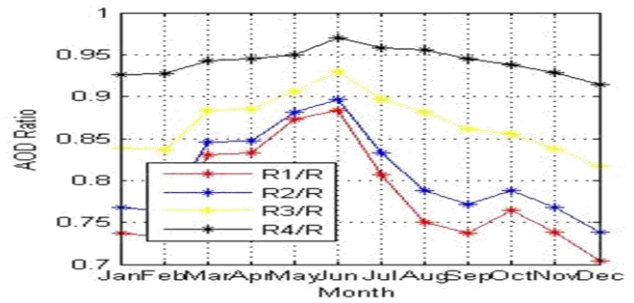


Fig. 2. Average Ratio of Monthly AOD from 2009 to 2016. R=AOD at 1020nm, R1= AOD at 440nm, R2= AOD at 500nm, R3= AOD at 670nm, R4= AOD at 870nm

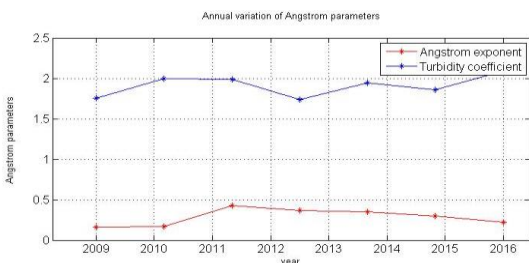


Fig. 3. Pattern of Monthly Variation of α and β from 2009 to 2016 at five different wavelengths

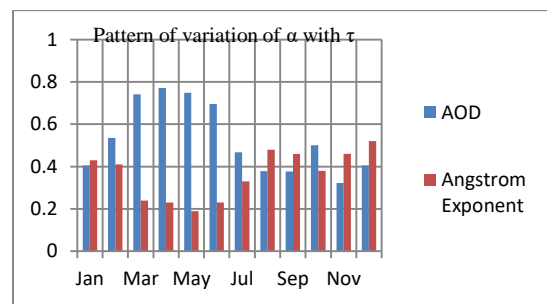


Fig. 5: Pattern of Monthly Variation of α and τ from 2009 to 2016

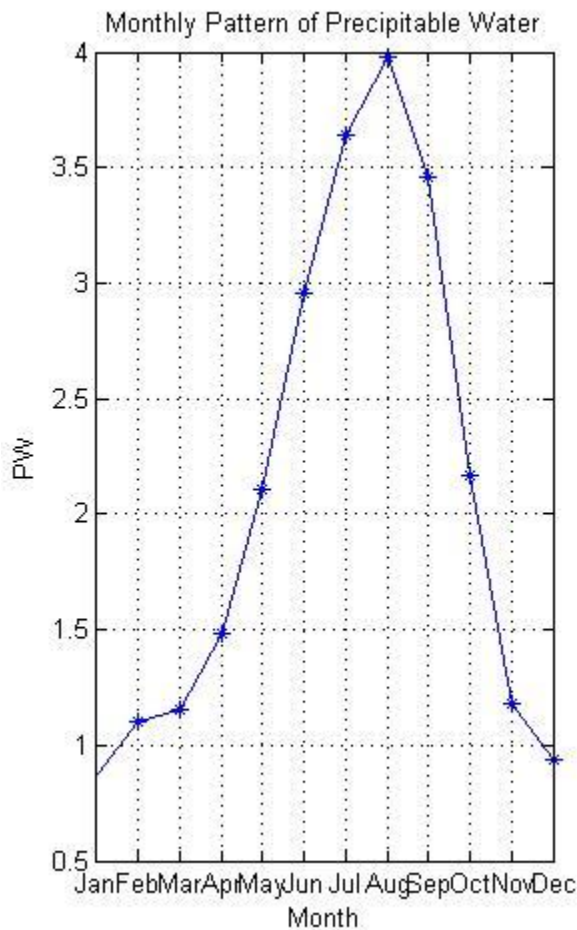
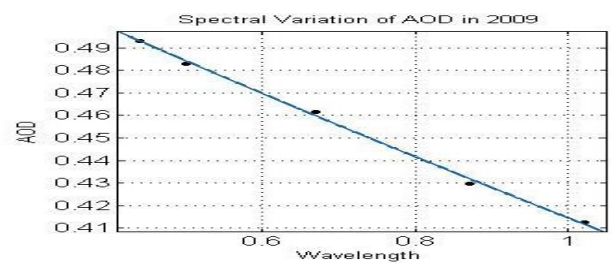
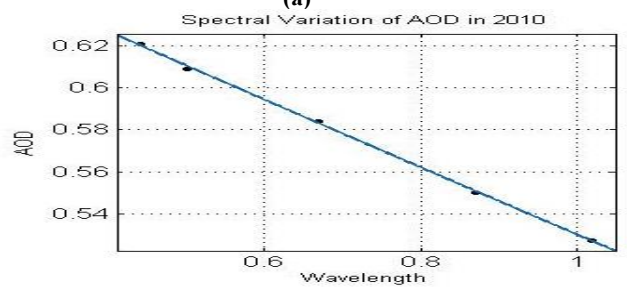


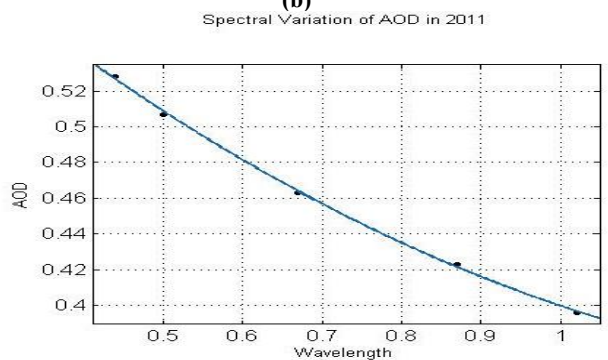
Fig. 4. Monthly Pattern of Average PW from 2009 to 2016 at 500nm



(a)



(b)



(c)

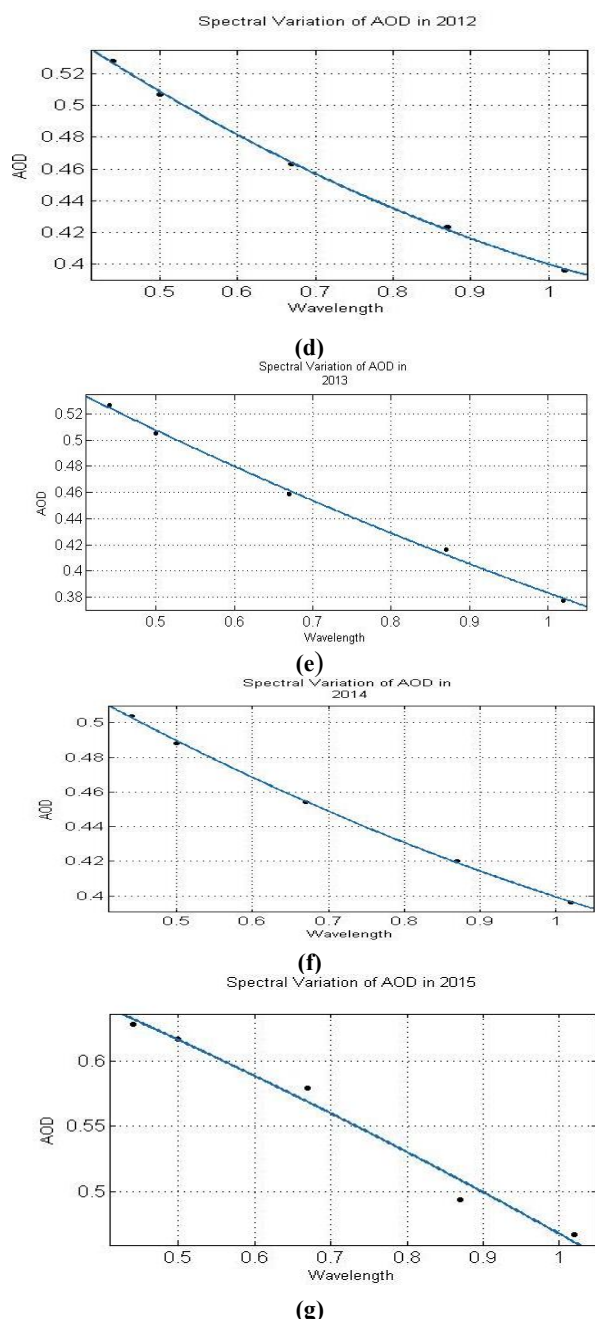


Fig. 6 (a – g). Spectral Variation of AOD from 2009 to 2016 at Five Different Wavelengths

Figure 5 indicates inverse variation of AOD with α . Figure 6 indicates spectral variation of τ with λ . The equation of the second order polynomial curve, $f(x) = ax^2 + bx + c$ provides the parameters α_1 , α_2 and β in equation 3

The Angstrom parameters presented in Table 1 are α_1 , α_2 and β are indices for measuring particle size, multiple aerosol types and visibility respectively. High values of α_1 indicate small particle size and vice versa. Values of $\beta > 0.2$ indicate relatively hazy atmosphere and impaired visibility. High values of α_2 indicate multiple aerosols types and vice versa.

4.0 Conclusion

Aerosols generated in the atmosphere of Zinder are predominantly coarse in nature. Their coarseness makes them absorb more solar radiation than they scatters. The light absorption exhibited by the coarse particles makes the overall temperature to increase, thereby giving the climate of the region its characteristic hotness. It was also established that there exist a fraction of fine particles from anthropogenic sources due to biomass burning, vehicular emission, transported industrial aerosols from neighboring countries which contribute to the haziness of the atmosphere. This fact of multiple aerosol type is observed from the curvature of the graphs of AOD against the wavelength, even though the effect varies annually.

Acknowledgment

I acknowledge the assistance of the principal investigator (PI) of Zinder Airport AERONET site, Niger Republic for providing the data I used in this work.

References

- Akpootu D.O and M. Momoh, The Ångström Exponent and Turbidity of Soot Component in the Radiative Forcing of Urban Aerosols, Nigerian Journal of Basic and Applied Science (March, 2013), 21(1): 70-78.
- Balarabe, M., Abdullah, K. and Nawawi, M. (2016) Seasonal Variations of Aerosol Optical Properties and Identification of Different Aerosol Types Based on AERONET Data over Sub-Sahara West-Africa. Atmospheric and Climate Sciences, 6, 13-28. <http://dx.doi.org/10.4236/acs.2016.61002>.
- Dubovik, O.; Holben, B.; Eck, T.F.; Smirnov, A.; Kaufman, Y.J.; King, M.D.; Tanre, D.; Slutsker, I. Variability of absorption and optical properties of key aerosol types observed in worldwide locations. J. Atmos. Sci. 2002.
- Dubovik, O.; Smirnov, A.; Holben, B.N.; King, M.D.; Kaufman, Y.J.; Eck, T.F.; Slutsker, I. Accuracy assessments of aerosol optical properties retrieved from aerosol robotic network (AERONET) sun and sky radiance measurements. J. Geophys. Res. Atmos. 2000, 105, 9791–9806.
- Smirnov, A., B. N. Holben, Y. Kaufman, O. Dubovik, T. Eck, I. Slutsker, C. Pietras, and R. Halthore (2002), Optical properties of atmospheric aerosol in maritime environments, D J. Atmos. Sci., 59, 4802.
- Vincent, J. H. 1995. Aerosol Science for Industrial Hygienists. Bath, UK: Pergamon.